The feasibility of using sediments from the Theewaterskloof, Greater Brandvlei and Waterzicht Dams as construction materials.

By

Johannes Adolf Dorfling

Thesis presented in fulfilment of the requirement for the degree of Master of Engineering in Civil Engineering in the Faculty of Engineering at Stellenbosch University.

Supervisors: Mrs. Nanine Fouché and Prof. Peter Day

December 2019

Declaration

By submitting this thesis/dissertation[3] electronically, I declare that the entirety of the work contained therein is my own, original work, that I am the sole author thereof (save to the extent explicitly otherwise stated), that reproduction and publication thereof by Stellenbosch University will not infringe any third party rights and that I have not previously in its entirety or in part submitted it for obtaining any qualification."

Signature: ……

Date: ……December 2019…

Abstract

Between 2014 and 2018, the Western Cape experienced the worst drought that the province has faced since 1904. The drought led to numerous water restrictions being applied by municipalities to regulate water use by their respective communities. From the exposed surfaces caused by the receding dam water levels, it was clear that thick layers of sediment have been deposited in the dams over the years, decreasing the storage capacities of these dams. The removal of these reservoir sediments will assist in maintaining optimal water storage capacity.

The aim of this study was to determine the practical and economic feasibility of removing sediments out of the Western Cape's two largest dams namely the Theewaterskloof and Greater Brandvlei Dams as well as the smaller Waterzicht farm dam, and the possible use of these sediments as construction materials such as road building materials, fine aggregates, lightweight aggregates, bricks and landfill clay liners. Field investigations were conducted on the exposed dam surfaces of these three reservoirs. During this fieldwork, zones were demarcated based on sediment type and location and samples were gathered from each zone. Subsequently, laboratory analyses were performed on these samples to determine their engineering and chemical properties.

These properties were used to classify each sample according to the Unified Soil Classification System (USCS) and related to the specific criteria for the various construction materials under investigation. The data from field analyses were used, together with sediment types, to determine the volume of each sediment zone. Where the sediments in a mapped zone were found suitable to be used as construction materials, cost models were prepared based on the type of construction material to be removed to estimate the removal cost per unit volume.

Based on the laboratory results, two cost models for the two zones were calculated. These zones included the poorly graded sands (SP) from zone B5 of the Greater Brandvlei Dam that is suitable for use as fine aggregate and clayey sands (CS) of the Waterzicht Dam that can be used for landfill liners in Class B and Class C type landfills. Three samples from the Theewaterskloof Dam and one sample from the Greater Brandvlei Dam can be used as lower layers of the pavement or in construction of fills, however the low cost, low quality and abundance of such road materials made it not feasible to be recovered for road construction unless such construction occurs adjacent to the sediment zones.

The methods used in the cost models for the removal of sediment from zone B includes dry excavation with and without sheet piling and dredging if the zone is submerged by an increase in dam levels. The removal costs for dry excavation without sheet piling and dredging methods were considered feasible if no more than five sediment removal units are used. For dry excavation to be feasible the minimum proportion of the sediment reserve to be removed ranges from 26% to 100% if one to five excavators are used respectively.

The cost model created for removing clayey sands (CS) from the Waterzicht farm dam estimated that if 100% of the sediment reserve is removed, it will be feasible to use the sediment for compacted clay liners for Class B and Class C landfills if the transport distances are 1 km and 25 km respectively.

From the cost models, it was concluded that the sediments from the Greater Brandvlei Dam and Waterzicht farm dam may be feasibly mined, however the volume estimations indicate that removal of these mapped sediments will result in only a minor increase in storage capacity and will have only a small impact on lessening the effects on future droughts.

Opsomming

Vanaf 2014 tot 2018, het die Weskaap die die ergste droogte ervaar sedert die 1904-droogte. Die droogte het veroorsaak dat daar menige waterbeperkings deur munisipaliteite ingestel is. Die laer damvlakke het dik lae sedimente op die oppervlakkte blootgelê. Dit was duidelik dat hierdie sedimente deur menige jare neergeset is en dat die stoorkapasiteit van die damme verlaag het. Die verwydering van hierdie sedimente sal help met die handhawing van optimale waterbergingskapasiteit van hierdie damme.

Die doel van hierdie studie was om the bepaal of dit prakties en ekonomies lewensvatbaar sal wees om die sedimente van the Weskaapse twee grootste damme genaamd Theewaterskloofdam en die Groot Brandvleidam te verwyder asook die van die kleiner Waterzichtplaasdam. Daar sal ook bepaal word of hierdie sedimente dan gebruik kan word vir konstruksiemateriale.

Die konstruksiemateriale waarvoor sedimente getoets is, sluit in padboumateriaal, fyn aggregate, liggewig-aggregate, bakstene en kleiverseëlings in stortingsterreine. Veldondersoeke is op die blootgestelde damoppervlaktes van hierdie drie damme uitgevoer. Tydens hierdie veldwerk is sones afgebaken op grond van die sedimentstipe en ligging. Monsters uit elke sone is versamel. Vervolgens is laboratoriumontledings op hierdie monsters uitgevoer om hul ingenieursmoontlikhede en chemiese eienskappe te bepaal.

Die data van die veldanalises is saam met die sedimenttipes gebruik om die volume van elke sedimentsone te bepaal. Waar die sedimente in 'n gekarteerde sone geskik gevind is om as konstruksiemateriaal gebruik te word, is daar kostemodelle opgestel volgens die tipe konstruksiemateriaal om te bepaal of die kostes verwant aan die verwydering van die materiale lewensvatbaar sal wees.

Op grond van die laboratoriumresultate is twee kostemodelle vir twee sones bereken. Hierdie sones sluit in die swak gegradeerde sand vanaf sone B5 van die Groot Brandvleidam wat geskik is vir die gebruik as fyn aggregaat en die klei sand van die Waterzichtdam wat gebruik kan word as ‘n kleiverseëling in Klas B en Klas C stortingsterreine. Drie monsters van die Theewaterskloofdam en een monster uit die Groot Brandvleidam kan gebruik word as onderste lae van die sypaadjie of in die konstruksie van vullings, maar die lae koste, lae gehalte en die oorvloed van hierdie tipe padmateriaal maak die ontginning van hierdie materiale nie winsgewend nie, tensy sodanige konstruksie langs die sedimentsones plaasvind.

Die metodes wat gebruik word in die kostemodelle vir die verwydering van sediment uit sone B, sluit droë uitgrawing met en sonder plaatmure en baggering indien die sone onder water is deur 'n toename in damvlakke. Die verwyderingskoste vir droë opgrawings sonder die plaatmure en met baggermetode word as haalbaar beskou as nie meer as vyf sedimentverwydering masjiene gebruik word nie. Vir die uitvoer van droë grawe met behulp van plaatmure, wissel die minimum persentasie van die sedimentreserwe wat verwyder moet word, van 26% tot 100% indien onderskeidelik een tot vyf graafmasjiene gebruik word.

Vanaf die kostemodel wat vir die verwydering van klei sand uit die Waterzichtplaasdam, word dit beraam dat indien 100% van die sedimentreserwe ontgin word, dit die uitvoerbare sediment as klei verseëling vir die stortingsterreine van Klas B en Klas C kan gebruik as die afstande 1 km en 25 km onderskeidelik is.

Uit die kostemodelle is die gevolgtrekking gekom dat die sedimente van die Groot Brandvleidam en die Waterzichtplaasdam moontlik haalbaar ontgin kan word, maar die volume-ramings dui daarop dat die verwydering van hierdie gekarteerde sedimente slegs 'n geringe toename in die bergingskapasiteit sal veroorsaak en slegs 'n klein impak op die vermindering van die gevolge vir toekomstige droogtes.

Acknowledgments

I would like to express my sincere gratitude towards the following persons that aided me during this research project and without whom this project would not have been successfully completed:

- A special thanks to my mother Laura Dorfling for her love, support and financial backing that she provided not only during the period that I worked on my master's degree, but for the entire seven years that I spent completing my tertiary education. During the most recent difficult times that our family had to endure, it was her encouragement that motivated me towards completing my thesis.
- My supervisors Ms Nanine Fouche and Prof Peter Day for their dedication, guidance and editing throughout this project.
- Mr Collin Isaacs, Mr Gavin Williams and Mr Riaan Briedenhann who guided and assisted me with laboratory analyses.
- Julian Spies and Michelle Nortje who provided a helping hand with my laboratory analyses.
- Leendert Dekker, Andries van Wyk, Henré Nortje and Johan Bligenhout that made time to help me during my field investigation on the dams.
- Fanie Visser that helped me during field investigations as well as laboratory analyses.
- The CEO of Van Zyl Mining Frikkie van Zyl for sharing his knowledge about the process and cost associated with small scale mining.
- Lindie Wiehan for information about the legal fees regarding the mining of commodities.
- The plant hiring companies for their quotations regarding machines used in this project.
- The CEO of the NSQ Plant Hire Henré Nortje, who assisted me with information and specification regarding the machinery used in this project.
- The Department of Water and Sanitation (DWS) and the farm owners adjacent to the Theewaterskloof Dam for providing me with access to the dams.
- Mr Livingston-Louw for providing access to his Waterzicht farm dam.
- Ms Christa De Wet for her advice and editing of this project.

Table of contents

List of tables

List of figures:

Chapter 1 : Introduction

1.1 Background and motivation for the study

Between 2014 and 2018, the Western Cape experienced the worst drought that the province has faced since 1904. The drought led to numerous water restrictions being applied by municipalities to regulate the water use by their respective communities. In addition, several alternative sources for water has been investigated such as drilling into aquifers and desalination.

On 29 January 2018, the dam levels for the major dams in the Western Cape Water Supply System (WCWSS) were estimated at 26.3% (see Table 1.1). The Western Cape's largest dam, the Theewaterskloof Dam, was only 13.3% full. The dam levels for the Brandvlei and Kwaggakloof Dams, which together form the province's largest irrigation dam known as the Greater Brandvlei Dam, were recorded as 16.6% and 21.5% respectively (Department of Water and Sanitation, 2018).

Table 1.1 Dam levels for the major dams comprising of the Western Cape Water Supply System (WCWSS, City of Cape Town, 2018)

Major Dams	Storage						
	Capacity	%	%	%	%	%	%
	Ml	29-Jan-18	Previous week	2017	2016	2015	2014
Berg River	130010	53,7	55	49,2	49,9	79	98,5
Steenbras Lower	33517	43,8	45,5	44,6	49,5	53	77,5
Steenbras Upper	31767	85,7	90,2	59,4	76,9	97	99,9
Theewaterskloof	480188	13,3	14,2	34,5	50,9	77,2	89,5
Voëlvlei	164095	18,1	18,6	42	25,7	72,7	83,5
Wemmershoek	58644	52,4	52,3	36,6	56	70,6	84,1
Total stored	898221	236111	244555	354034	425408	682511	802049
% Storage		26,3	27,2	39,4	47,4	76	89,3

The receding water levels in these dams led to large parts of the basins being exposed. The exposed surfaces comprise mostly of thick layers of sediment which were transported by the rivers feeding the dams. As these sediments accumulate in the reservoirs, the dams gradually lose their ability to store water. Beck and Basson (2002) estimated that reservoirs in South Africa lose on average 0.34% of their storage capacity annually due to sedimentation.

To maintain optimal water storage capacity, the removal of these reservoir sediments is required. An increase in the reservoirs' storage capacity will lessen the impacts of a future drought. Dredging is the primary method for sediment removal, but the costs can be exorbitant. However, persistent low dam levels give rise to the possibility of removal of sediments using earthmoving equipment. The value of increased storage capacity combined with the potential use of the sediment for alternative purposes may well justify the cost of removal. Dredged or excavated sediments may be used for construction materials, replacement fill, shoreline stabilisation, agriculture, horticulture and habitat restoration (Paipai, 2003). In the construction sector, the use of these sediments will be dictated by their physical and chemical properties.

1.2 Unique research contribution

In the Western Cape, no studies have been conducted into the possibility of removal of the exposed sediment from the province's major reservoirs to increase their storage capacities. This research project will not only be the first to investigate the possibility of sediment removal from the major reservoirs, but also the first to examine the possibility of using reservoir sediment as construction materials.

Furthermore, this research is unique in the sense that it investigates not only the use of the large government-owned reservoirs for construction materials but also the sediment of smaller private-owned farm dams. Farmers usually excavate the sediment out of their privately-owned dams after the dams have dried out, but these sediments are perceived as waste, and dubious efforts are made put them to beneficial use. Through identifying possible construction uses for these unwanted sediments, the excavation cost of these sediments may be offset by using the material as a building material for own benefit or selling it as a construction material.

1.3 Aims and objectives of the research

This research project aims to determine the practical and economic feasibility of removing sediments out of the Western Cape's two largest dams namely the Theewaterskloof and Greater Brandvlei Dams as well as the smaller Waterzicht farm dam for the possible use of construction materials. The construction materials this study will focus on are road building materials, fine

aggregates, lightweight aggregates, bricks and compacted clay liners for landfills. The objectives of the research include the following:

- Investigating the Western Cape's demand and supply for the selected construction materials.
- Mapping the sediment and geology along the exposed dam surfaces of the Western Cape's two largest reservoirs, the Theewaterskloof Dam and the Greater Brandvlei Dam, and the smaller Waterzicht farm dam.
- Testing the engineering properties of the exposed dam sediments through laboratory analyses. Some of these tests include CBR analyses, sieve analyses, Modified AASTHO compaction tests and uniaxial compression strength tests on stabilised sediments.
- Determining the chemical composition of the fine-grained sediment based on X-ray diffraction (XRD) and X-ray fluorescence (XRF) analyses.
- Determining the potential uses of the sediment as construction materials based on the engineering properties and chemical composition of the sediment located in the three dams.
- Calculating the theoretical amount of sediment that can be removed. With this estimate, the possible increase in reservoirs' capacity after sediment removal will also be known.
- Investigating the costs related to the removal of the sediment suitable for construction use in the three reservoirs.

1.4 Study area

The study area consists of three dams, namely the Theewaterskloof, Greater Brandvlei and Waterzicht Dams (see Figure 1.1). All three reservoirs are in the South Western part of the Western Cape within a radius of 50km of each other. The selection of these dams was based on their size and applicability. The Theewaterskloof and Greater Brandvlei Dams are the two largest dams in the Western Cape and are owned by the Department of Water and Sanitation (DWS). In contrast, the Waterzicht Dam is a small farm dam that was selected due to the more frequent dredging required of farm dams to sustain viable farming.

The regional climate for all three dams is characterised by warm, dry summers and mild, moist winters. The average temperature ranges from 15.6 to 17.6 °C and the average rainfall around Waterizcht area and Theewaterskloof ranges from 770 to 804 mm, while at the Greater Brandvlei Dam it is 400mm (Climate-Data,2019).

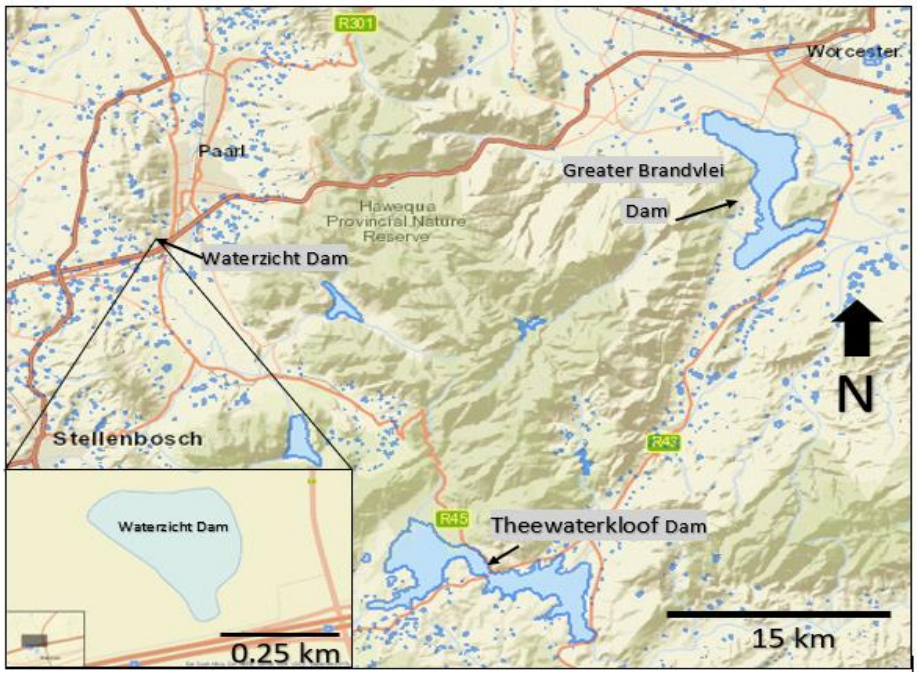

Figure 1.1 Reservoir map indicating the locations of the Theewaterskloof Dam, Greater Brandvlei Dam and Waterzicht Dam. Base map derived from Esri South Africa. Dam locations derived from Department of Rural Development and Land Reform, Chief Directorate: National Geo-Spatial Information.

1.4.1 Theewaterskloof Dam

The Theewaterskloof Dam is an earth-fill dam established in 1978 and located 10km south of Villiersdorp, Western Cape (see Figure 1.2). The dam plays a significant role as a water supplier to the City of Cape Town. With a capacity of 480 million cubic metres, which is equal to about 53% of the total capacity provided to the WCWSS, it is the largest reservoir in the Western Cape (Department of Water and Sanitation,2018).

The mountains of the Hottentots-Holland Nature Reserve serve as the primary catchment area for the dam, with the Riviersonerend River being the dam's main feeder. During the winter rainy season, vast quantities of water run down the Riviersonerend River and the tunnels from the Berg River catchments to feed the Theewaterskloof Dam.

Figure 1.2 Topography map of the Theewaterkloof Dam. Base map derived from Google satellite, contours river and dams derived from Department of Rural Development and Land Reform, Chief Directorate: National Geo-Spatial Information.

The WCWSS connects to the Theewaterskloof Dam through an extensive system of pipelines and tunnels. This system comprises an inter-linked system of six main dams, pipelines, tunnels and distribution networks, and several minor dams, owned and operated by the Department of Water and Sanitation (DWS) and the City of Cape Town. The Department of Water Affairs and Forestry (DWAF,2009) described the water supply within the WCWSS as follows:

- 63% of the water is used for domestic and industrial purposes within the City of Cape Town,
- 5% of water is supplied to the towns of Stellenbosch, Paarl and Wellington, as well as to towns on the West Coast and in the Swartland region,
- 32% is used by irrigation farmers along the Berg, Eerste and Riviersonderend Rivers.

The public can access the Theewaterskloof Dam through Theewater Sports Club for recreational activities.

1.4.2 Greater Brandvlei Dam

The Greater Brandvlei Dam is an earth-fill dam located near Worcester, Western Cape (see Figure 1.3). The dam is situated on a tributary of the Breede River. The construction of the Greater Brandvlei Dam was completed in 1972 through merging the original Brandvlei Dam (constructed in 1949) with the newly built Kwaggaskloof Dam.

The Greater Brandvlei Dam has a capacity of 456 million cubic metres and provides water to various irrigation schemes in the Worcester valley (Department of Water and Sanitation, 2018). During winter rainy season the Smalblaar and Holsloot Rivers fill the Greater Brandvlei Dam. Water is released from the Greater Brandvlei Dam into the Breede River during the summer irrigation periods. The reservoir also provides the locals with recreational activities such as skiing, fishing and camping.

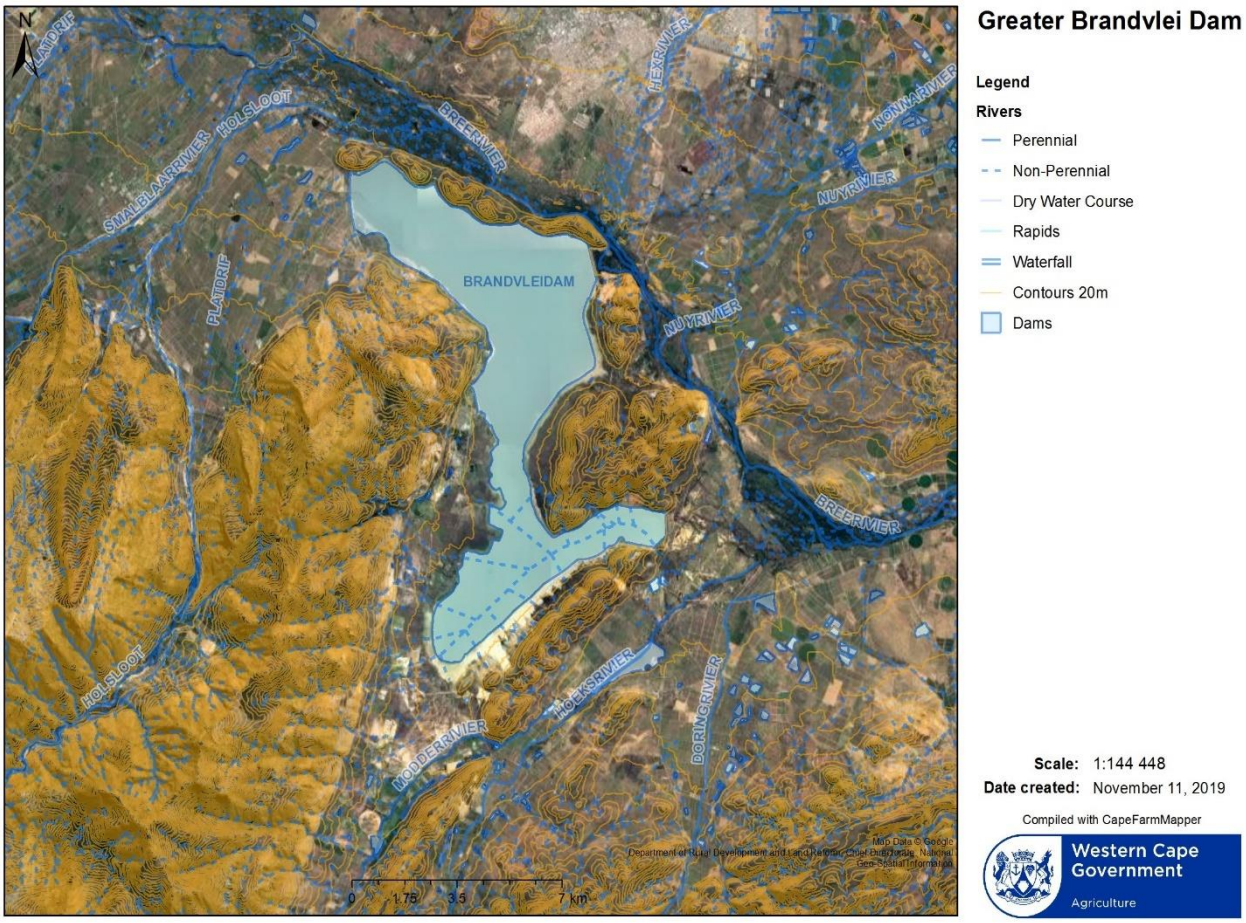

Figure 1.3 Topography map of the Greater Brandvlei Dam. Base map derived from Google satellite, contours, rivers and dams derived from Department of Rural Development and Land Reform, Chief Directorate: National Geo-Spatial Information.

1.4.3 Waterzicht Dam

The Waterzicht Dam, the smallest dam selected for study (estimated during research as about 665 thousand cubic meters), is a privately-owned farm dam located about 5 km outside Klapmuts (see Figure 1.4). The dam was constructed during 1986 and 1987 and is used mainly for the irrigation of fruit crops such as plums, citrus, peaches and olives. Currently, the reservoir is only used for irrigation of citrus as well as recreational purposes. The Waterzicht dam is fed by two small streams which flow from the Rozenmeer Dam, located south of Waterzicht farm, on the opposite side of the N1.

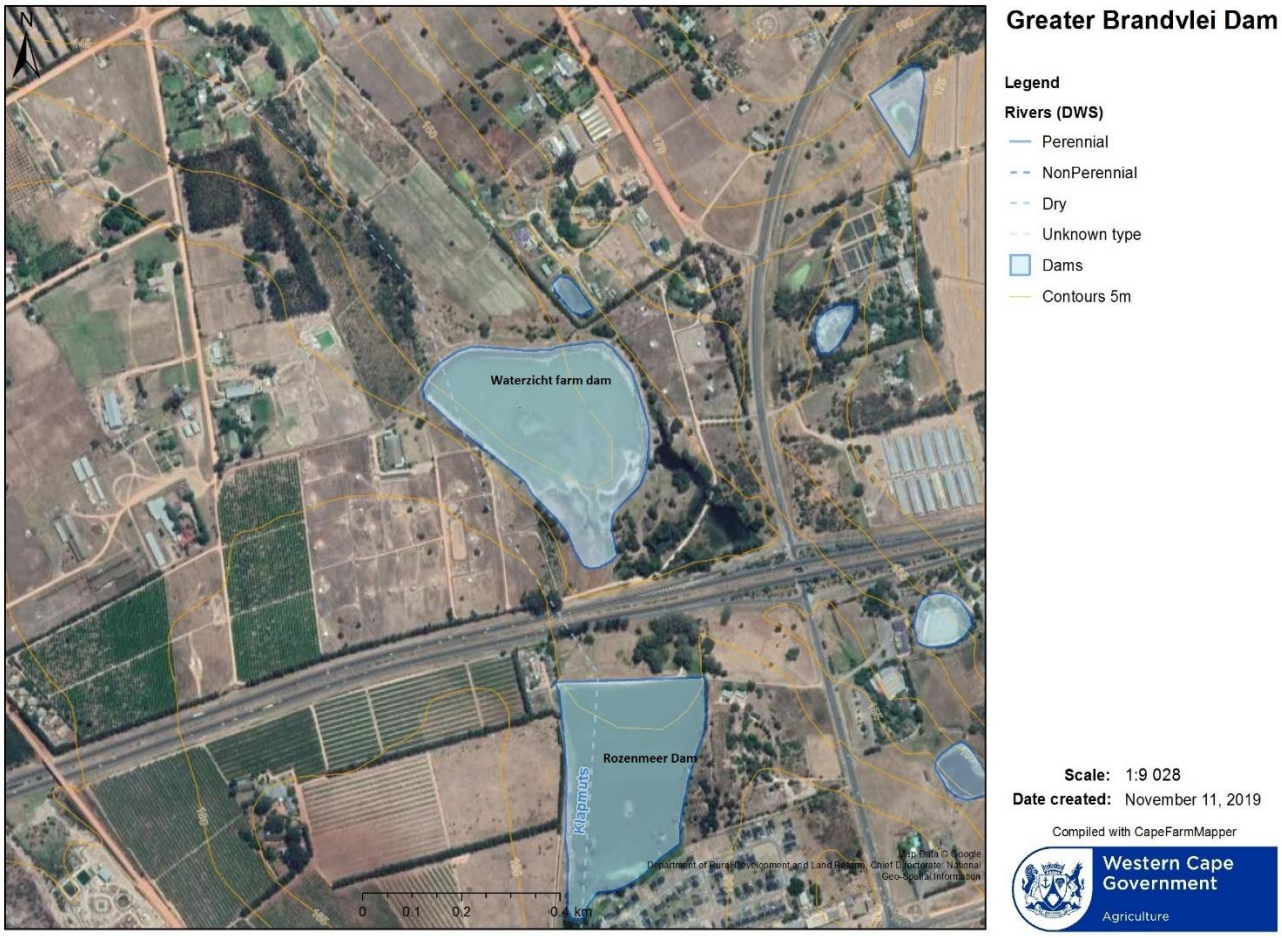

Figure 1.4 Topography map of the Waterzicht farm dam. Base map derived from Google satellite, contours derived from Department of Rural Development and Land Reform, Chief Directorate: National Geo-Spatial Information and rivers and dams derived from Department of Water and Sanitation.

1.5 Limitations

Not all the required methods were applied during field mapping and laboratory analyses, mainly due to inaccessibility, cost of test methods and unavailability of required equipment. Some exposed areas of the Theewaterskloof Dam and Greater Brandvlei Dam were inaccessible for mapping due to access permission and terrain difficulties. Deep bottom sediments of all three reservoirs were also not sampled due it being submerged, and the high costs related to sampling below water. The increase in dam levels during the winter rainfall of 2018, restricted the excavation of numerous test pits spaced at close intervals which will give a more accurate estimate of the volume of exposed sediments. In addition, the water level increase prohibited the resampling of sediments that required more testing. In some instances, the sediment layer was too thick to determine its full thickness.

The testing for the use of sediment for clay bricks was limited due to an insufficient amount of material to construct the mandatory bricks and the unavailability of standard brick kilns. Similarly, no rotary kilns were available for the sintering of clay materials to lightweight aggregates.

However, the accessible areas were successfully mapped, and the available standardised testing equipment was used to obtain the laboratory results from the soil samples obtained from the field visits.

1.6 Overview

The research project consists of six chapters. The first chapter introduces the problems associated with storage loss experienced by the Western Cape's major dams together with the motivation for the utilisation of these sediments for construction materials. The aims of the study and the selected study areas are described in this section.

Chapter 2 consists of an in-depth literature review about the processes and problems of reservoir sedimentation, the different methods of sediment removal, previous uses of reservoir sediment for construction materials, the construction material market of the Western Cape and the regional geology of the three selected dams.

The third chapter explains the methodology used during field mapping and the laboratory analyses of the sampled sediments.

Chapter 4 presents all the results obtained from the field investigation and laboratory analyses. For the field investigation, each dam was divided into separate zones, and the results from the field investigation of each zone are described separately. From the laboratory results, it was determined which sediment samples passed the criteria for which construction materials. The removal costs of the zones that represent the respective sediment samples that passed the specification for certain construction materials were calculated and compared to purchasing or installing costs of conventional construction material. This comparison between the costs of the removal together with volume increase (determined by field investigation) was the main factor to determine if it is feasible to remove sediment to increase reservoir capacity.

The fifth chapter consists of a short conclusion made on the suitability of the utilisation of each reservoir's sediments for construction material together with the feasibility related to the extraction of these sediments.

In Chapter 6 recommendations are made for further research.

Chapter 2 : Literature study

2.1 Reservoir sedimentation

Sediment is a naturally occurring soil or rock material that is broken down by several processes such as erosion and weathering (Corrosionpedia, 2019) and is subsequently transported from the land surface by the action of wind, water or gravity and deposited in another location. This section will discuss the process of reservoir sedimentation including the geometry and patterns caused by sedimentation as well as the negative impacts related to reservoir sedimentation.

2.1.1 Process of reservoir sedimentation

As sediment-bearing water enters a reservoir, a decrease in the flow velocity and transport capacity causes deposition of the sediment load within the reservoir basin (Morris and Fan, 1998). Usually, the coarse proportion of sediment is deposited close to the point where the flowing water enters the reservoir, forming a delta, whereas the fine sediments with lower settling velocities are transported deeper into the reservoir by either stratified or homogenous flow (Van Rijn, 2013). The amount of sediment deposited in a reservoir depends mainly on the sediment type, reservoir shape, the detention storage time and the operating procedures (Van Rijn, 2013). The two most significant contributors to the erosion and subsequent sedimentation in rivers are poorly managed land use and expansion of human impacts onto previously undisturbed areas (Walling, 1999).

Morris and Fan (1998) illustrated the general deposition geometry of sediment in Figure 2.1. The deposition geometry comprises of three zones, namely the top set bed, foreset bed and the bottom set bed.

- The topset bed correlates to the delta deposits of abrupt settling. The delta deposit is mainly coarse-grained but may contain finer sediment such as silt.
- The foreset bed is identified as the part of the transition zone from delta to bottomset bed. The foreset bed is characterised by an increase in downslope angle and a decrease in grain size. A rapid decrease in grain size occurs along with the downstream limit of the delta. This

decrease in grain size may also occur in reservoirs lacking a noticeable delta (Fan and Morris, 1992).

- The bottomset bed is classified as the fine sediment deposition occurring beyond the delta. These sediments dominate the deepest parts of the reservoir. Autochthonous (formed *in situ*) organic matter produced by algae may occur in this zone.

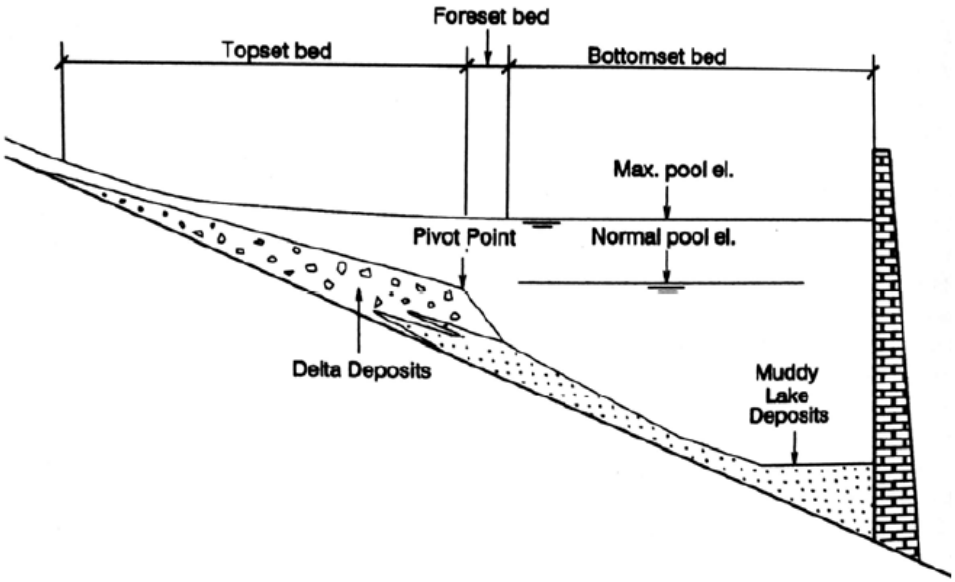

Figure 2.1 Generalised deposition patterns in reservoirs (Morris and Fan, 1998).

In addition, Morris and Fan (1998) characterised four types of deposition patterns that will occur through inflowing sediment (see Figure 2.2).

- **Deltas** deposited to form a bulk of coarse sediment at the inflow of reservoirs.
- The **wedge-shaped** deposits are the thickest at the reservoir base and much thinner upstream. In small dams, wedge-shaped deposits occur when there is a massive influx of fine sediment, whereas large reservoirs may contain this pattern when they operate at low water levels during flood events.
- **Tapering deposits** occur when the thickness of sediment gradually decreases with the downslope of the reservoir. These deposits typically occur in long reservoirs with high dam levels, suggesting continuous deposition of fines along the dam surface.
- **Uniform deposits** are the most unlikely deposits but may occur. This deposit is characterised by a thin load of fine sediment deposited uniformly along the deposition depths. Uniform deposits mainly occur in narrow reservoirs with frequent water level fluctuations.

However, Morris *et al*. (2008) noted that depositional patterns can also be more complicated. Already deposited sediment can be reworked and carried further downstream during a decrease in the hydraulic head or massive floods can transport coarse sediment deeper into the reservoir,

prograde over finer sediment and producing layered deposits. During the period when flood events are absent, only fine sediments and organic material may be present.

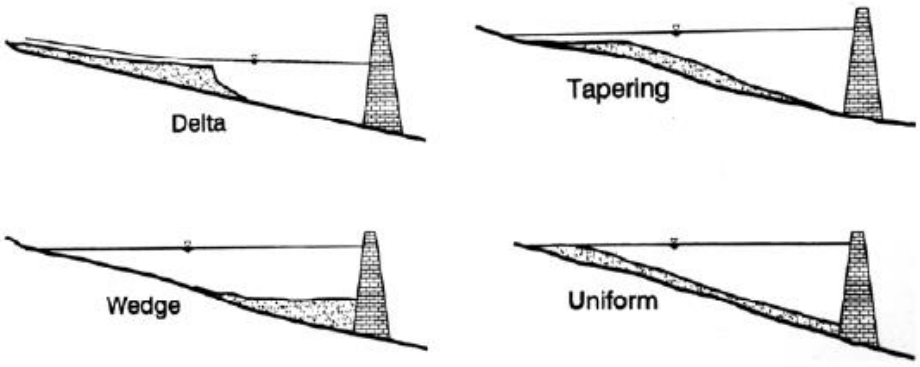

Figure 2.2 The four longitudinal depositional patterns (Morris and Fan, 1998).

Further research by Morris and Fan (1998) describes three processes causing the deposition of sediments in the deepest parts of reservoirs, namely turbidity currents, logarithmic vertical concentration and uniform vertical settling. Turbidity currents are the primary mechanism for depositing sediment at a reservoir's deepest part. These currents are gravity-driven underflows in which the sediments are largely suspended by fluid turbulence. After turbidity currents enter a reservoir, they plunge below the clear water surface due to their higher density and convey the sediment loads to the innermost part of a reservoir where the sediment loads concentrate and settle. The logarithmic vertical concentration profile within a water body enables the focusing of the fine sediment suspension into the nethermost part of the reservoir. In contrast, uniform vertical settling takes place when the sediment suspension is uniformly distributed along the reservoir and settles vertically. Deposition during the latter process will occur directly proportional to water depth.

2.1.2 Negative effects of reservoir sedimentation

Reservoir sedimentation is a major concern and a worldwide problem that affects reservoirs' water storage capacity. White (2001) estimated that large reservoirs lose between 0.5 and 1% of their storage capacity each year. Also, Vorosmarty *et al*. (2003) investigated 633 large and over 44,000 small reservoirs and estimated that more than 28% of the global sediment flux in river basins is trapped in reservoirs. The rate for the total trapping was estimated at 4–5 billion tons per year. The

decrease in reservoir storage can cause numerous complications for water-dependent communities since the core purpose of reservoirs are to store water for irrigation, household consumption, power generations and flood control.

Morris *et al*. (2008) described numerous environmental issues related to the accumulation of reservoir sediment. These issues have an impact not only on the dam ecology but also on upstream and downstream ecosystems. Sediment aggradation which takes place during the formation of the delta at the river mouth may cause the dam shoreline to transgress and cause saturation of vegetative root zones, alter ecological habitats and increase soil salinity. Furthermore, sediment trapping may initiate channel incision downstream of the reservoir, causing the base level of the river to drop, which can activate degradation of tributaries, destabilisation and undercutting of streambanks and sediment depletion of river bars essential for environmental benefits. Besides this, the decrease in sediment transport downstream can also cause a degradation in fish habitats and lead to coastal erosion.

Reservoir sedimentation may also have a severe economic impact. Braune and Looser (1988) estimated that the damage related to sedimentation in South African reservoirs is about 50 million US Dollars per year. Gunatilake and Gopalakrishnan (1999) determined that in 1993 the total sedimentation cost for the Mahaweli reservoir, Sri Lanka, was equal to 838 000 US Dollars. Basson (1996) reported on the direct and indirect economic impact that sedimentation has on dams. The direct economic impact includes the maintenance cost increase for irrigation, remedial works to alleviate sedimentation issues and the additional cost linked to chemical treatment for increased turbidity levels. The indirect economic impact includes agricultural land damage due to aggradation, increase in energy cost due to use of alternative power sources, and remedial cost of infrastructure damages by sediment excess caused by flooding or hydromechanical damages caused by coarse sediment interaction.

2.2 Sediment removal methods

The negative impacts of reservoir sedimentation as discussed in the previous section highlights the importance of efficient sediment management in reservoirs. Sediment removal from reservoirs is an essential component in alleviating the negative impact. The three main methods of sediment removal from reservoirs include dry excavation, dredging and flushing. This section will only focus on the methods of dry excavation and dredging and will include the types of equipment used and

the advantages and disadvantages of each method. The process of flushing was excluded from this section since the aim of this project is to investigate the reuse of sediment; however; flushing does not allow for retainment of sediment.

The low water levels caused by the prolonged drought in the Western Cape create the opportunity for removal of exposed sediments by means of excavation in the dry using conventional earthmoving equipment. For completeness, this research also includes considers the feasibility of dredging of sediments from below the water by means of dredging.

2.2.1 Dry excavation

Dry excavation is the mechanical removal of accumulated sediment from a water body after water is drained or diverted. After excavation, the sediment is hauled to a suitable disposal area by using traditional earthmoving machinery such as dump trucks. The removal of the sediment is completed with conventional earthwork equipment such as hydraulic excavators.

The United States Environmental Protection Agency (US EPA, 2005) described the different equipment for isolating areas which are to be drained and excavated as sheet piling, earthen dams, cofferdams, geotubes, rerouting the water body using temporary dams or pipes, or permanent relocation of the water body. These methods can also be used to prevent the saturation of areas with low water levels efficient for dry excavation area located adjacent to the reservoir.

The process of sheet piling involves the driving of interlocking metal plates into the surface, and thereby isolating the designated area or diverting water flow by splitting the stream down the centre (US EPA, 2005). By splitting the stream down its centre, the one side of the stream can be pumped dry and sediment is excavated. After excavation, the water can be diverted back to the excavated side of the stream and the opposite side may be closed off for dehydration and excavation. Sheet piling is not feasible where bedrock or hard strata are present at or close to the surface (US EPA, 2005). Rerouting a water body using temporary dams and pipes is mainly completed for small streams or ponds, which allows sediments to be exposed for dry excavation. At certain sites with foreseeable seasonal water level variation, dry excavation can be undertaken on a seasonal basis. Due to the high excavation and disposal costs, dry excavation is preferably used for small impoundments rather than large reservoirs (Aras, 2009).

The US EPA (2005) described, where feasible, the following benefits for dry excavation over dredging:

- The operators of excavation machinery and the supervising personnel can observe the operation.
- Dry excavation leads to more effectual removal of contaminated sediments.
- Minimal waterborne contaminants are released when the excavation area has been dewatered.
- Less consideration is required for bottom conditions and sediment characteristics such as grain size and specific gravity.

The main disadvantage associated with dry excavation is the high costs related to water drawdown, transportation cost and suitable disposal area cost (Aras, 2009). However, where sediments are exposed due to seasonal changes or drought the process of dry excavation rates will be greatly reduced. Furthermore, dry excavation may be restricted in certain areas due to difficult terrains. Soft sediment in the dewatered area may not have the required bearing capacity to support the equipment's weight. This may cause a decrease in the precision of the excavation depth (US EPA, 2005). However, this process can easily remove coarser material from the deltas and upper reaches of the reservoirs (Howard, 2000; Annandale *et al*., 2016)

2.2.2.1 Types of dry excavation equipment

In conventional earthwork operations, hydraulic excavators and tractor-loader-backhoes (TLBs) are most commonly used for excavation (see Figure 2.3). The main difference between these machines is the size, weight and capabilities.

A hydraulic excavator consists of a chassis, longarm and tracks. The longarm consists of the boom, which is attached to the chassis and connects to the dipper stick on the other side. The digging bucket is attached to the end of the dipper stick. The boom and chassis can rotate 360 degrees. The weight of excavators used for excavation and loading typically ranges from 20 to 91 tons (One Stop Rent, 2019). Excavators are mainly used on commercial sites where it can carry out numerous tasks including digging holes and trenches, loading, lifting and placement, landscaping and demolition.

They can be fitted with a bucket narrower or wider than the standard bucket for excavation in rock and loading of loose material respectively. Since an excavator moves on tracks, it is slow over large distances but is less prone to becoming bogged down on poor ground than wheeled equipment. Wider "swamp" tracks can be fitted if necessary.

In the case of TLB, the backhoe arrangement is attached to the back end of the tractor and the loader bucket is located at the front of the machine. Therefore, TLBs are used for excavating with the backhoe or loading and lifting with backhoe or loader bucket. The backhoe apparatus is similar to the longarm of an excavator comprising of boom and dipper stick, with the boom supporting the dipper which connects to the bucket. With an average weight of eight tons, backhoes are commonly used on farms and construction sites for light to medium work that requires digging and moving heavy equipment (Leschohier, 2007).

The maximum rotation for the backhoe is 200 degrees to left and right (RME, 2017). TLBs move on wheels which make them mobile at speeds up to 35km/h so they can drive to the site and do not require to be transported with a load bed truck. Their small size and versatility make TLBs popular earthmoving equipment.

The most important factor to consider when comparing excavators with TLBs for a project is described by RME (2017) as site access, capacity, reach, swing and function versatility. The ability to choose the right size machine for the job and production rates for simultaneous digging and loading generally makes an excavator as a better option. The rotation of 360-degree swing of excavator in comparison to the 200-degree swing of a backhoe makes excavators more efficient when loading trucks positioned alongside or behind the excavator. Both machines offer great functional versatility and can be configured with a wide range of attachments to accomplish a broad range of tasks.

Figure 2.3 A) hydraulic excavator B) TLB (The Constructor, 2007)

2.2.2 Dredging

2.2.2.1 Background

The Oxford Living Dictionary (2019) describes dredging as clearing the bed of (a harbour, river, or other areas of water) by scooping out mud, weeds, and rubbish with a dredge. The removal of sediment through dredging may be undertaken for several reasons including waterway creation and maintenance, excavation, reclamation, ecosystem maintenance and the gathering of construction materials (GeoForm International, 2019).

The process of dredging is undertaken in three different stages (see Figure 2.4) which must be repeated until the target amount of sediments is dredged (Thorn, 1975). The **first stage** includes the excavation of sediments by hydraulic and/or mechanical cutter (Antipov *et al*., 2006; Du and Li, 2010). Different types of dredging equipment can be selected for excavation depending on sediment

depths and types, but similar extraction methods, whether by suction, bucket or grab, are be required for all kinds of dredging (Fujimoto and Tadasu, 1998).

The **second stage** of dredging consists of the transportation of the excavated sediments. Sediments are transferred by suction pipes, conveyor belts, buckets or the grabs into hopper bags or pipelines, which are then used to transport the dredged sediment to the designated disposal or stockpile site.

The **third stage** includes the disposal of the sediment at the selected site. The most economically feasible and widely used method for disposing of dredged sediment is employing open water disposal through the opening of the bottom gate of the hopper barge (Krishnappan,1975). The method of open disposal may, however, be prohibited when handling contaminated or very fine-grained sediment (Krizek *et al*., 1975). Remedial approaches that can be used on contaminated sediments before disposal include physical separation processes, washing, thermal extraction, bioremediation and containment (Mulligan *et al*., 2001). An alternative technique to the open disposal method that is widely used, is pumping the dredged sediment ashore (Welte, 1975). Additional methods include agitation dumping, side casting, dumping in rehandling basins and sump rehandling (Manap and Voulvoulis, 2015).

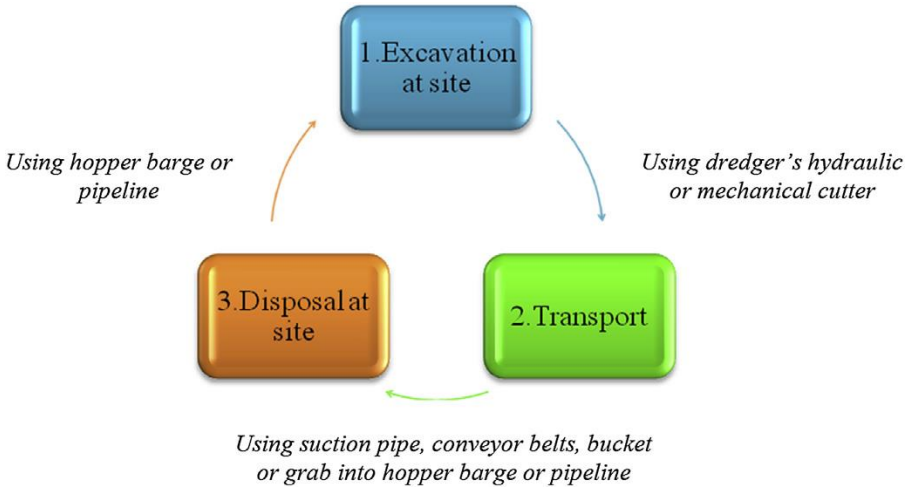

Figure 2.4 Stages of dredging (Highley et al., 2007; Verbeek, 1984)

The benefits of dredging compared to dry excavation include that dredging is normally more affordable than dry excavation for large projects (Annandale *et al*., 2016), higher production rates and the ability to dredge without interfering with the impoundment process (Aras, 2009). Through dredging, the negative economic and environmental impact of sediments can be lessened. However,

dredging also poses disadvantages, mainly associated with contamination and economic difficulties of dredging.

The leaching and dispersion of toxic contaminants such as polychlorinated biphenyls (PCBs) and heavy metals in sediments through dredging can contribute to severe health issues for humans including nausea, headaches, dizziness, loss of balance, neurological problems, eye and skin irritation and cancers (Schantz *et al*., 2001). Also, the dispersion of contaminants during dredging may influence ecosystems since it causes bioaccumulation in the food chain (De Nobili *et al*., 2002).

Even though dredging is mainly more economical than dry excavation for large projects, the cost related to dredging is generally extortionate. A study by Annandale *et al*. (2016) estimated that at the time dredging would cost more than 3 US dollars per m^3 sediment removed. This estimation excluded the cost related to engineering and permitting fees and the cost related to pumping distances exceeding 2 kilometres.

The grain size of the sediment also plays a vital role in the cost-effectiveness of dredging.
The coarser the sediment, the costlier the dredging operation, since more energy is required for the transport of coarser particles. Besides, dredging pumps will be more susceptible to abrasion from coarser material than the pumping of uniform fine-grained sediment (Annandale *et al*., 2016).

2.2.2.2 Types of dredging equipment

A study by Elzinga (2017) listed the seven most important pieces of dredging equipment suitable for reservoir sedimentation as suction dredge, cutter suction dredge, grab dredge, backhoe dredge, submersible dredge, water injection dredge and syphon dredge. These methods are described in more detail below except for the water injection dredge since this method does not remove the sediment, which is objective of this study, but rather conveys sediments to deeper portions of the reservoir.

Suction dredge

A suction dredge is a ponton coupled by a pump and long suction pipe. For the dredging of sediments, the pump is carried down to the reservoir bottom, where it will be turned on and will subsequently suck up the water and surrounding loose material. Large quantities of sediment can be obtained through this process. The most suitable materials to be collected by a suction dredge are mainly sands and silts. For material containing debris, a suction dredge will be far less efficient,

since the coarse material will block and obstruct the flow path of sediment to the suction mouth (Elzinga, 2017). A deep suction dredge can reach maximum depths of 155 m (IADC Dredging, 2014).

The Cutter Suction Dredge (CSD)

The Cutter Suction Dredge (CSD) is a standard suction dredge with a cutter header applied to the front of the dredger. The purpose of the installed cutter is to cut into compacted soil, which the ordinary suction dredge is unable to attain, thereby fragmenting the soil to make it more attainable for the suction dredge. A wide variety of soils can be dredged by a CSD; however, debris material such large rocks and tree stumps can cause damage to the cutter head or clog the suction pipe and should, therefore, be avoided when dredging with a CSD.

CSDs used for dredging reservoirs are usually of a size that can be transported by truck or train. The maximum depths of dredging will vary with the type CSD being used. Small CSD dredgers can dredge in less than 2 metres depth, whereas the biggest CSDs can reach depths of more than 35 metres (IADC Dredging, 2014)

Grab dredge

The Grab dredge is used worldwide due to its simplicity. It consists of a floating stationary crane with a grab attached to it. The size of the grab can vary from 1 m^3 to 200 m^3 (Elzinga, 2017). Dredging using a grab dredge comprises of the repeated process of excavating the submerged sediment, bringing the sediment up and depositing it into a hopper or transport barge until the required amount of sediment is dredged.

The grab dredge is a piece of very versatile dredging equipment. The type of grab used depends on the sediment type and site environmental conditions, e.g. a flat grab clamshell is used for muddy sediment, while a grab clamshell with teeth is used for sand and clay. Unlike the suction dredge and CDS, the grab dredge can be particularly useful in areas where depth is inconsistent or where large materials such as boulders and tree stumps are present. Depths of up to 200 m can be reached, with the only limiting factor being the length of cable available (Elizinga, 2017).

Backhoe Dredge

A backhoe dredge consists of an excavator mounted on a pontoon. The excavator can be directly installed or can be a standard excavator attached to the raft. The latter makes the backhoe dredge a very versatile dredging method since it can function on water or land.

The process of dredging is very similar to that of the cyclic method of grab dredging. The bucket gets lowered into the sediments, where it is filled, retracted and lifted to the surface, and the sediment is deposited into a hopper or transport barge. In addition, the backhoe dredge is also very similar to the grab dredge regarding the flexibility of dredging different sediment types, since the applicable bucket can be attached for the type of sediment (from clays to boulders) that needs to be dredged.

Advantages of backhoe dredging over grab dredge include the better precision of dredging, absence of anchor wires, the lack of required auxiliary equipment and the faster cycle time of dredging (IADC Dredging, 2014). However, small backhoe dredges will become inappropriate for depths exceeding 10 m, in comparison to the deep depths of grab dredges (Elizinga, 2017).

Submersible dredge pump

The submersible dredge pump is an enhanced version of a suction dredger. Since the dredge pump is submersible it can be lowered to more efficient depths, where it can be operated from further. If the pump is lowered close to the material that needs to be dredged, an increase in the attained solids can be achieved, thereby increasing suction efficiency (Vlasblom, 2004). Submersible pumps are very versatile since they can be mounted to booms of excavators or CSDs or released into the water through cables.

The advantages of using a submersible pump include the ability to dredge at deep depths and areas that are difficult to access as well as the pump's incessant dredging ability. In addition, if the distance of dredged sediment from designated deposition is not too far, it can be directly transported through the suction pump. The depth that submersible pumps can be lowered into water is limited by the maximum availability of the total head.

Syphon dredge

The syphon dredging method makes use of the difference between the hydraulic head of the reservoir and the river downstream of the reservoir. The available head allows the dredging of the dam sediment.

The advantage of using a syphon pump is the low operating cost in relation to other methods. However, the disadvantages of syphon dredging include that this method is only applicable very close to reservoirs and its incapability of dredging coarse materials such as gravel or densely

compacted material. The reason for a syphon dredge to be applied at reservoirs is because it is an environment with an efficient head difference and short required pipe lengths.

The achievable dredging depths are related to the available head; therefore, a large available head will contribute to dredging at deeper levels.

2.3 Sediments as construction materials

The recycling of sediments as construction materials will not only reduce environmental effects but also presents an opportunity to make the removal process more economically feasible. No studies have yet been conducted in South Africa on the possible reuse of reservoir sediments as construction materials. However, internationally a wide variety of studies have investigated the use of reservoir sediment for the variety of construction material.

This section focuses on previous investigations conducted on the possible use of sediment for pavement material, natural aggerate for concrete and mortar and plaster, lightweight aggregates for concrete, bricks and landfill clay liner.

2.3.1 Road construction material

The use of sediment can serve as an innovative sediment management solution by using the sediment in the lower layers of the roadways or pavements. The suitability of the sediment as a road construction material depends on the sediment's mineral composition, availability and geotechnical properties (Saussaye *et al*., 2017; Achour *et al*., 2014). However, the fine sediments associated with dredging the deeper portions of the dam are more difficult to be used in road construction due to high moisture content, the possible presence of pollutants and organic matter and poor mechanical properties (Zentar *et al*., 2009). Therefore, additional sediment treatment is usually required before these sediments can be used as road construction materials. No studies were found where untreated sediments were used as road material.

Miraoui *et al*. (2011) investigated the use of dredged sediment treated with steel slag to produce potential road construction material. They found that the dredged sediment from the Dunkerque Harbour in France required the addition of steel slag to comply with the mechanical and physical

properties for road materials. Two types of steel slags, a slag with low lime content of about 6.6 % and residue with higher lime contents of 13.9%, were used in this study.

Achour *et al*. (2014) studied the use of fine-grained sediments (mainly silt) that were dredged from the harbour of Dunkirk as road subbase materials. The study concluded that the fine dredged sediment had an inadequate bearing capacity, primarily due to the high organic content and grain size distribution. However, treatment of the fine sediments by addition of courser dredged sediment (66% of mixture), lime (1% of mixture) and cement (6% of mixture), enhanced the material to road construction material standards.

Tribout *et al*., (2011) researched the applicability of contaminated sediment treated by the Novosol® process for road construction materials based on the sediment's mechanical and leaching properties. The Novosol® process (developed by the Solvay Company) stabilises heavy metals by introducing phosphates and causes the degradation of organics through calcination at temperatures of 700°C. The results concluded that sediments treated with Novosol® could be used as an economically viable aggregate in road construction.

Maherzi *et al*. (2018) focused on the beneficial reuse of marine-dredged sediments from Brest Harbour (Bretagne, France) in road construction. This study reported good strength results for a Mix12C2 formulation, which contains in volume ratio, 30% sand (as granular corrector) and 70% sediment, treated with 3% lime and 15% binder C2. These results passed the requirements for road subbase material.

2.3.2 Natural aggregate for conventional concrete and mortar

Natural aggregates such as crushed stone, gravels or sands are used with a binding material (e.g. cement) to produce composite materials such as concrete or mortar. For concrete, the right type and quality of the aggregate are vital, since the fine and coarse aggregates generally make up 60% to 75% of the concrete's volume (about 80% of the mass). In addition, the aggregates are responsible for the concrete's strength, volumetric stability, durability and thermal properties (Alexander, 2014).

Natural aggregates are divided into coarse and fine aggregates based on their grain sizes. The coarse aggregates consist of a material with grain sizes greater than 5 mm, whereas in fine aggregates at

least 90% of the content must be smaller than 5mm and should contain no more than 5 % dust according to SANS (South Africa Nation Standard) 3001-AG1 (2014). Both coarse and fine aggregates are used for the mixing of concrete, whereas only fine natural aggregates are used for the making of mortar and plaster.

Junakova *et al*. (2015) researched the feasibility of using the sediment of the Klusov reservoir, Slovakia, for an aggregate and cement replacement in concrete. Coarse-grained sediments were reprocessed as a partial natural aggregate and the fine-grained sediments as a cement replacement in the concrete. The results of the study indicated that the compressive strength of a specimen where coarse-grained sediments replaced 20 % by weight of the reference aggregate was similar to the sample containing only reference aggregate. Specimens that were made with fine-grained sediment as a cement replacement, at a 40:60 sediment/cement weight ratio, achieved compressive strength that was 35% lower than that of the reference concrete. However, the flexural strengths of the concrete specimen prepared with sediment replacement were higher in comparison to the reference specimen at all ages of curing. Also, all the concrete samples passed the freeze-thaw specifications.

Cho (2013) researched the effect that fine sediments (mainly silt) that attach to mined river sands have on the properties of concrete. The study indicated that a decrease in durability occurs when the fine aggregate contains more than 5% silt. Furthermore, the compressive strength stays relatively constant for samples containing 1-5% of silt, an increase in the silt content to 7%-9% decreases the compression strength by 4-3 MPa.

Millrath *et al*. (2001) investigated the use of untreated and treated marine dredged sediments of Port of New York and New Jersey as a constituent of concrete. The sediments were treated with CUT powder (Columbia University Treatment) and Echo chemical. The research concluded that concrete made with 20% untreated dredged sediment behaves similarly to conventional concrete in the sense that it displays a strong inverse relationship between the strength and water-cement ratio. However, the traditional concrete formed without dredged sediment (treated or untreated) produced the highest strength.

Benzerzour (2018) studied mortar made from heat-treated dredged sediments from Grand Port Maritime de Dunkerque, located in northern France. The mortar was made through substituting an

ideal portion of cement with sediments that were calcination-treated at 750 °C. The mortar specimens produced from the treated sediment had similar or improved mechanical properties. The compressive strength of mortar containing 10% treated sediments substituting for cement was 10% higher than the standard reference mortar.

2.3.3 Natural lightweight aggregates for concrete

Most lightweight aggregates are produced from sintering materials such as clay, shale or slate at high temperatures between 1100 and 1300°C (Riley, 1951). However, blast furnace slag, natural pumice and perlite can be used as substitutes. These lightweight aggregates are mainly used in the production of lightweight concrete. Lightweight concrete has numerous benefits over conventional concrete including cost-effectiveness due to the reduction of the required reinforcement, improved thermal properties, improved fire resistance and savings in transport cost (Mineral Products Association, 2019).

Numerous studies have investigated the possibility of using fine reservoir sediment for the manufacturing of lightweight concrete. Wang *et al*. (2010) investigated the dredged sediment of seven reservoirs in southern Taiwan for the use of aggregates for high-performance lightweight aggregate concrete. The study concluded that the lightweight aggregates produced by dredged silt from all the southern Taiwan reservoirs were suitable for lightweight aggregate.

Research by Chen *et al*. 2011, Hung and Hwang (2007) and Hwang *et al*. (2012) focused on the usability of the dredged sediment (inorganic clays of low to medium plasticity) of the Shihmen Reservoir, northern Taiwan. Chen *et al*. (2011) determined that the Shihmen Reservoir sediment passed engineering requirements to be used as aggregate for lightweight concrete. Hung and Hwang (2007) focused their study on the qualitative and quantitative chemical analysis of the dredged sediment and sintered lightweight aggregates. The results indicated that the chemical composition fell in Riley's (1951) required 'area of bloating'. In this area of bloating, if a clay is sintered at temperatures ranging from 1100°C to 1300°C, the material will form a viscous glassy phase and produce gas compounds which will lead to expansion of the material. Expansion of the clay material is important because it increases the porosity of the material to give it a lower density.

Hwang *et al*. (2012) studied reservoir sediment mixed with municipal solid waste incinerator (MSWI) furnace fly ash to produce self-consolidating lightweight aggregates. The test results indicated that the aggregate presents a good quality if the fly ash composition is less than 30% of the aggregate.

2.3.4 Brick making material

Bricks have been used as a building material over the centuries and are still used today mainly for wall construction. Bricks can be classified in numerous ways, depending on their shape, use, manufacturing method and the type of raw materials. Common types of bricks in construction include fired clay bricks, sand-lime bricks, concrete bricks, fly ash bricks and refractory bricks.

Numerous scholars have investigated reservoir sediment as an alternative source for brick-making material. Research by Cheng *et al*. (2014) concluded that the production of non-sintered cured bricks from reservoir sediment and construction waste from hydroelectric plants can produce suitable bricks together with improving environmental protection, recycling and energy conservation. Torres *et al*. (2009) evaluated the inclusion of river silt from the Aveiro lagoon, Portugal, as the raw material in the production of bricks sintered at 950-1100 °C. The study concluded that bricks produced with 5% of river silt would achieve the same properties as standard industrial bricks.

Hamer and Karius (2001) researched the possibility of brick manufacture using contaminated Bremen harbour sediments as an alternative to landfill disposal. The study determined that brick manufacturing will be a better option than the construction of new landfill with dewatering facilities due to the municipality of Bremen's limited area for future urban development and prohibition of natural resource depletion. The study concluded that the sediment produced bricks which met the appropriate industry standards and that no negative environmental impacts will occur during the life cycle of bricks.

Mezencevova *et al*. (2012) studied the viability of the production of fired bricks from sediments dredged from the Savannah Harbour (USA). For bricks, the raw material was selected as 100% dredged sediment (80% clay/silt sediment and 20% sand sediment) or as a 50% sediment and 50% natural brick-making clay. The bricks were fired at temperatures between 900 and 1000 °C. The mechanical and physical properties of the produced bricks complied with a suitable standard for

building brick. However, the bricks manufactured using dredged sediment -natural clay mixture had improved properties in comparison to bricks produced solely by dredged sediment.

2.3.5 Landfill clay liner

All municipal waste landfills must be appropriately sealed to prohibit possible leaching and contamination into the surrounding natural environment. The most commonly used materials for sealing landfills are compacted clay liners (CCLs) and geosynthetic clay liners (GCLs). GCLs consist of a layer of clay (typically bentonite) combined one or more layers of geotextile. Properties of clay liners are low permeability, high adsorption value and resistance to erosion and different chemicals (Koś and Zawisza, 2016).

Koś and Zawisza (2016) and Maher *et al*. (2013) investigated the use of fine reservoir sediments for the sealing of landfills. The study by Koś and Zawisza (2016) concluded that bottom sediments (predominantly silt) of the Rzeszowski Reservoir (southern Poland) might be used for compacted clay liners in landfills, although it is recommended to increase the clay content for a more appropriate permeability coefficient. Maher *et al*. (2013) found that dredged clay from Newark Bay, in northeast New Jersey (USA), can be used as a more economically viable option for capping sanitary landfills than traditionally mined material.

2.4 Western Cape's construction material market

As mentioned in Section 1.2 there is no available research on the utilisation of reservoir sediment in South Africa. However, the terrestrial mining of sediment for construction materials occurs throughout South Africa. This section will describe the current South African construction market, the Western Cape construction sector and the supply and demand for construction materials in the Western Cape.

2.4.1 South Africa's construction sector.

The construction sector is the part of the economy that includes the designing, building, maintenance and demolition of buildings and infrastructure (Chun *et al*., 2015). In South Africa, the construction industry makes up more than 50% of the total national capital investments and contributes about 4% of the country's GDP (gross domestic product) (Construction Industry Development Board, 2018). In 2019, the construction sector is estimated to experience an increase of 1.9% in the GFCF (gross fixed capital formation), which is the net increase in physical assets within the measurement period (Budget Review, 2018).

It is important to note that the performance of South Africa's construction sector is related to the state of the economy, which is currently under pressure due to numerous difficulties facing the country. These pressures include the threat of rising interest rates in advanced economies (Construction Industry Development Board, 2018), the awarding of contracts to sometimes poorly skilled black-owned businesses due to black empowerment (Price Waterhouse Coopers, 2017), reduction of qualified skills (Pillay & Mafini, 2017) and high operation costs related to corruption and fraudulent practices (Bowen *et al*., 2007). If these problems are not mitigated, the construction sector will be impacted heavily with the rest of the South African sectors.

2.4.2 Supply and demand for construction materials in the Western Cape

The Western Cape's construction sector is currently experiencing flat growth due to passive housing prices. Previously, it was the province's top growth sector, with about 3% growth per year from 2012 until 2016 (Western Cape Government Provincial Treasury, 2018). However, the report forecasts an increased growth of 2.4% between 2018 and 2022 (*Quantec Research, 2018*). This section will investigate the market for the construction material under investigation for this research.

2.4.2.1 Road construction materials

The demand for road construction material is related to the provincial and national government's expenditure on transportation infrastructure. Transportation infrastructure includes design, planning, construction and maintenance. The Western Cape Government Provincial Treasury (2018) has estimated that the expenditure on transport infrastructure will decrease by 2.6% from 2018/19

to 2019/20 with but will increase with 4.9% from 2019/20 to 2020/21. Therefore, the demand for road materials will slightly increase until 2021.

The subbase used in road construction is usually made of crushed stone or natural gravel. Gravels are obtained from various sources including ferricretes and terrace gravels (Hill *et al*.,1992). Pedocretes, which include ferricretes and calcretes, are produced by pedogenesis accompanied by fluctuations in the water table and are used as subgrade for pavements and as a gravel wearing course on unsealed roads (Netterberg, 1998). Terrace gravels, on the other hand, are mainly used for subgrade and subbase or an alternative source for building sand (Roberts, 2001).

The supply of gravel is widespread over the Western Province and exploited locally. Ferricretes form numerous small resource fields, rarely exceeding 2km² in area extent, throughout much of the Western Cape Province except for the Great Karoo. The terrace gravels associated with the Berg River are prominent between Paarl and Saron. Five years ago, there were sixteen working pits and two hundred abandoned pits, with the majority being concentrated near urban areas Cole *et al*. (2014).

2.4.2.2 Natural fine aggregates

Natural fine aggregates are widely used in construction in concrete, mortar and plaster. Thus, the demand for fine aggregates will increase with the growth of the construction sector. The low value and heavyweight of the material mean that transportation costs can make up a significant proportion of the final price the customer pays. As a result, there is a demand for aggregate sources within a radius of less than 100 km of the development site (Pienaar, 2017).

In the Western Cape, the supply of fine aggregates for concrete, mortar and plaster are mainly extracted in the Greater Cape Town area. However, these sands are located all over the Western Cape, except in areas underlain by Karoo Supergroup sedimentary rocks and dolerite between Laingsburg, Beaufort West and Murraysburg (Ngcofe and Cole, 2014). In the Greater Cape Town area, mortar and sands are mined from hairpin parabolic dunes of the Holocene Witzand Formation in the Philippi and Macassar areas (Ngcofe and Cole, 2014). Southwest of Malmesbury and northwest of Darling, concrete sand is attained from hillwash deposits (Cole *et al*., 2014). In the

Saldanha and Vredenburg urban area, colluvial and hillwash sands are mined for concrete, mortar and plaster. In the southern part of the province, east of Port Beaufort, vast resources of mortar and plaster grade building sand are mined from Cenozoic dunes of Strandveld and Wankoe Formations parallel to the coast (Roberts *et al*., 2006). In addition, concrete grade sands are mined from hillwash, colluvial and alluvial sediments located in the same area.

Building sand resources in the northern and eastern parts of the Western Cape include concrete, mortar and plaster sand from colluvial deposits north of Vredenburg, mortar sand in the Vredenburg Urban area and mortar- and plaster-grade building sand in the Port Beaufort - Mossel Bay – George - Knysna area (Ngcofe and Cole, 2014).

The natural fine aggregates have historically been very abundant and cheap in the Greater Cape Town area but have become more limited since the start of the twenty-first century (Cole & Viljoen, 2001). The sources have not only become more depleted but also inaccessible due to environmental concerns or alternative land use (Alexander and Mindess, 2005). A rough estimation by Ngcofe and Cole (2014) suggests that the building sand resources of the Greater Cape Town area will probably be depleted within the next 20 years. Cole and Viljoen (2001) recommended that crushed sand from the Table Mountain Group sandstone will be the best suitable replacement for building sand.

2.4.2.3 Lightweight aggregates

The demand for lightweight concrete is increasing due to the numerous benefits it has over conventional concrete. Lighter concrete applies lower dead loads than for conventional concrete, thereby decreasing the required reinforcement. The lighter loads also mean trucks can carry larger volumes of aggregate, thereby increasing fuel efficiency and reducing the environmental impact (Subramani and Suresh, 2015). Furthermore, lightweight aggregates also improved the thermal properties and fire resistance of the concrete (Mineral Products Association, 2019). The positive impact offsets the environmental impact caused by lightweight aggregate manufacturing. The emission of greenhouse gasses produced by the sintering of raw material such as shale, clay or slate is relatively low since these materials consist mainly of silica (Subramani and Suresh, 2015). Also, the energy of the rotary kiln to produce lightweight aggregates (3 GJ per ton) from raw material is significantly less than to produce cement (5.5 GJ ton), thus also using less fuel (Subramani and Suresh, 2015).

The supply of lightweight concrete in South Africa is relatively low, with only a few companies selling concretes mixed with vermiculite, perlite or chemical foam (The Concrete Institute, 2018). However, there is an abundant source of raw materials for lightweight aggregates throughout South Africa in the form of expansive clays. The primary sources for raw materials for lightweight aggregates are expansive clays (see Figure 2.5), vermiculite and perlite (Mueller *et al*., 2008). In the Western Cape, expansive clays are mainly derived from argillaceous rock units particularly those of the Karoo Supergroup (Diop *et al*., 2011). These clays are mainly weathered from shales and mudrocks of the Dwyka, Ecca and Beaufort Groups. An alternative source that can be used is expansive aggregates from LECA, Europe's largest producer of lightweight expansive clay aggregates. The company imports its aggregates to South Africa mainly for horticultural use. Cured LECA aggregates will contribute to high strength lightweight concrete (Mahdy, 2016). However, the high costs related to the large quantities of LECA aggregates required to manufacture concrete will contribute to this process being exorbitant.

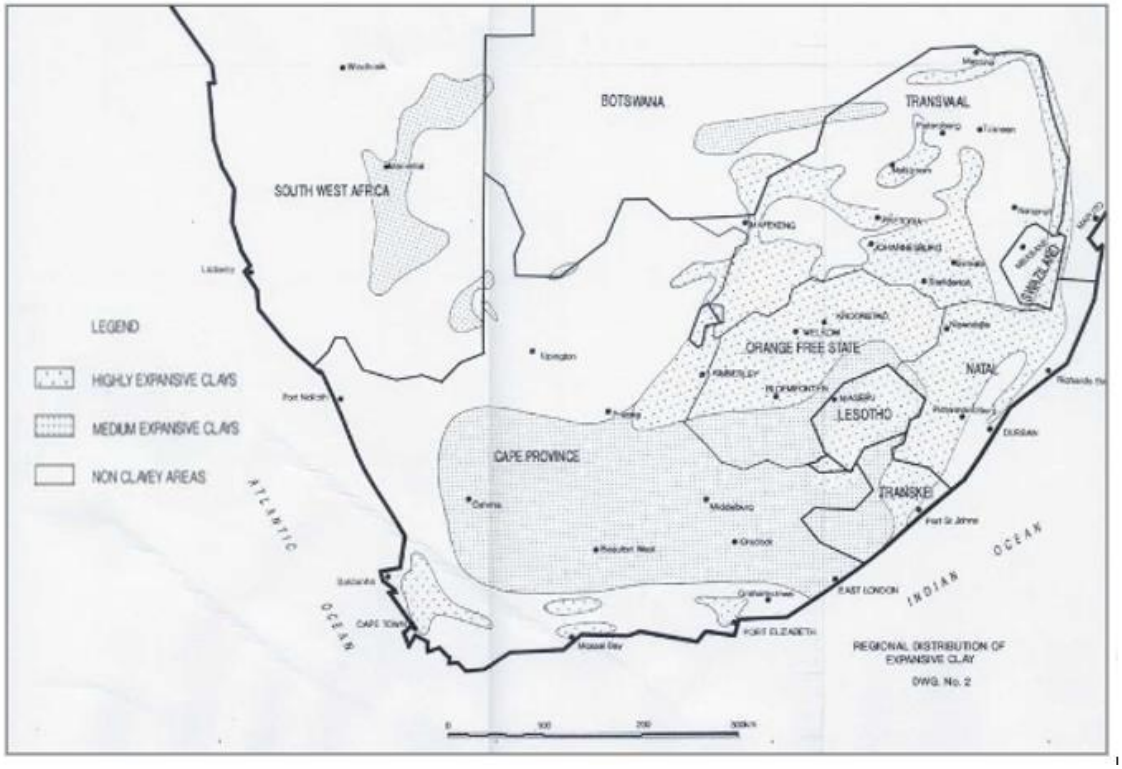

Figure 2.5 Distribution of expansive clays in South Africa (Department of Public Works, 2006).

2.4.2.4 Brick Clay

The demand for conventional clay brick manufacturing might gradually decrease with an increase in demand for a more sustainable building environment. However, out of about 3.6 billion bricks manufactured in South Africa annually, approximately 45% are made from clay, with cement bricks and other materials representing 45% and 10% respectively of the total number of bricks (Clay Brick Association of South Africa, 2016). The popularity of clay bricks is mainly due to their aesthetic and durability benefits.

An environmentally friendly method of producing fired bricks is using a VSBK (vertical shaft brick kiln, see Figure 2.6). A standard VSBK consists out of two vertical shafts and stationary fire with conveyor belts moving the bricks. The kiln operates like a counter-current heat exchanger, with the heat transmission occurring between the air moving upwards and the bricks moving downwards. The bricks are fired inside the shaft with fixed dimensions and within a short time period of about 24 to 28 hours. Fuel can be added to a VSBK in two forms namely internal fuel and external fuel. The internal fuel is added to the clay prior to moulding and may consist of coal powder, fly ash and bagasse. The external fuel is added with brick batches from the top of the shaft and can only consist of the coal.

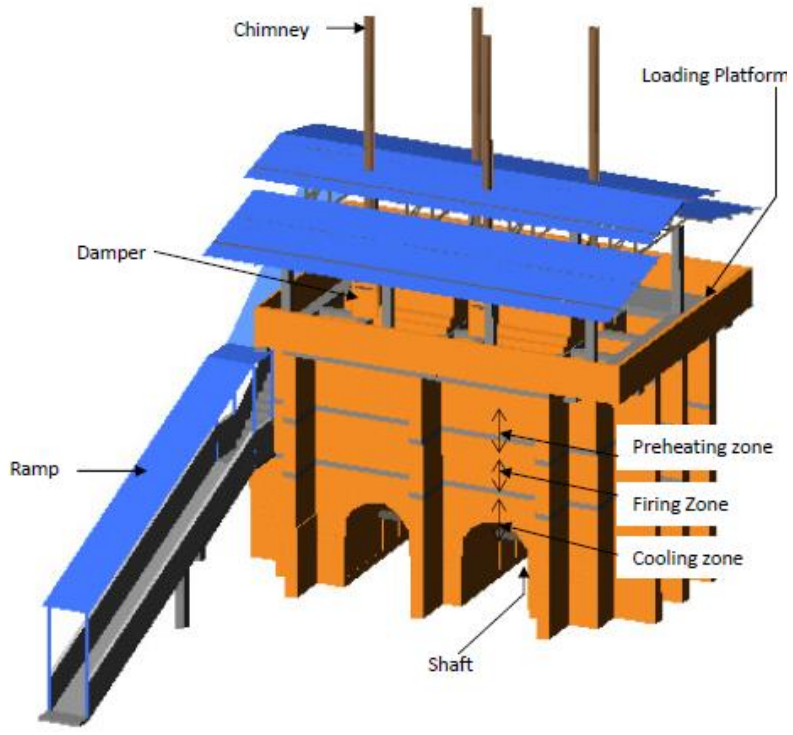

Figure 2.6 VSBK technology model (Prajapati and Maity, 2010).

There are numerous suppliers and manufacturers of clay bricks in the Western Cape such as Corobrik, Cabrico, Apollo Brick, De Hoop Brickfields and Boland Bricks. Corobrick is one of the largest

clay brick suppliers in the Western Cape with branches in George, Phesantekraal, Stellenbosch and Vredenburg.

Suitable clay sources for brick manufacturing are also widely spread over the province. These sources include residual clay of the Malmesbury Group shale near Cape Town, Ceres and Hopefield (Cole, 2003); the Gifberg Group schist near Klawer (Cole, 2013); the Saasveld Formation schist and phyllite in the George area (Roberts *et al*., 2008) and of the Kirkwood Formation mudstone near Oudtshoorn and Swellendam (Cole *et al*., 2014).

The Greater Cape Town area also has resources of high plasticity. Plastic clays are used as strengthening and plasticising additives in the manufacturing of clay bricks (Cole, 2003). The two most abundant resources in the Cape Town area are Camphill Village and an area northeast of Philadelphia, with smaller deposits between Kraaifontein and Klapmuts. Ngcofe and Cole (2014) estimated that the depletion of plastic clays in the Western Cape would take longer than 50 years.

2.4.2.5 Clay liner for landfills

The sealing of landfills is required to prevent the leaching of contaminants that may be harmful to the environment and human health. The most commonly used materials for sealing landfills are compacted clay liners (CCLs) and geosynthetic clay liners (GCLs), mainly due to their low hydraulic conductivity (Shankar and Mater, 2017). CCLs are the oldest and most widely used in landfills. However, in recent years, the demand has increased for GCLs as an alternative to CCLs in the sealing of waste containment facilities because they have very low hydraulic conductivity and have a relatively low cost (Nafati *et al*., 2012).

In the Western Cape, it is estimated that most landfills will have reached their storage capacity in less than five years (Palm, 2017). The closure of landfills will increase the demand for CGLs and CCLs, due to the obligation for the capping of old landfills as well as for the construction of new landfills.

CCL's are typically produced from clays on-site or from clays close to the source that pass the conductivity and swelling requirements after compaction. GCLs are comprised of a thin layer of sodium, or calcium bentonite (clay produced by the alteration of volcanic ash and that are primarily composed of smectite) bonded to a layer or layers of geosynthetic, normally geotextile or geomembrane (Nafati *et al*., 2012). The biggest suppliers of GCLs in the Western Cape include Fibertex SA and Kaytech. Bentonite deposits are associated with the Kirkwood Formation located

in five rift-related basins in the Cape Fold Belt, namely the Robertson Basin, Swellendam Basin, Heidelberg – Riversdale Basin, the Mossel Bay Basin and Plettenberg Bay Basin (Cole *et al*., 2014). Only the bentonite of the Heidelberg – Riversdale Basin is currently being mined (Department of Mineral Resources, 2018).

2.5 Regional geology

The understanding of the regional geology of reservoirs plays an essential role in determining the sediment type and as well as residual soil in the reservoir. This section will focus on the regional geology as well as the geological history of each of the three study areas.

2.5.1 Regional geology of Theewaterskloof and Greater Brandvlei Dams

Both the Theewaterskloof and the Greater Brandvlei Dam are situated in the Hottentots-Holland Mountains. These mountains comprise 500 to 330 Ma old Cape Supergroup sedimentary units which form part of the Cape Fold Belt (Thaum and Johnson, 2006). The Cape Supergroup sediments were deposited in a passive margin basin along the Southern part of Gondwana (Thaum and Johnson, 2006). The subsequent cape orogeny or folding (230 to 278 Ma) caused uplift and deformation of the Cape Supergroup, pre-Cape rocks and units of the younger Karoo Supergroup to form the Cape Fold Belt (Hälbich *et al*.,1983).

The extent of the Cape Fold Belt stretches from Stellenbosch to the north of Van Rhynsdorp and east to Great Fish River mouth. The Cape Supergroup consists of three subdivisions named the Table Mountain, Bokkeveld and Witteberg Groups.

2.5.1.1 Theewaterskloof Dam

The geology surrounding as well as underlying the Theewaterskloof Dam is dominated by the Ceres Subgroup of the Bokkeveld Group (see Figure 2.7). The stratigraphy of the Bokkeveld Group presents a diagnostic upward-coarsening cycle of silts to sandstones (Theron, 1972). In the Ceres Subgroup, three upward-coarsening sequences can be recognised namely the Gydo and Gamka Formations (lower cycle), Voorstehoek and Hex River Formations (middle cycle) and the Tra-Tra and Boplaas Formations (upper cycle). The Gydo, Voorstehoek and Tra-Tra Formations consist of siltstones and mudstones whereas the Gamka, Hex River and Boplaas Formations include arenites and feldspathic wackes (Thaum and Johnson, 2006). The bedrock of the reservoir consists predominantly of Gydo

formation, with the younger formations of the Ceres subgroup (Gamka to Tra-Tra) all exposed adjacent to the southern part of the eastern flank of the dam.

The steep surrounding mountains, bordering on the northern and western parts of the Theewaterskloof Dam consist of sandstones of the Skurweberg formation of the Table Mountain Group whereas the Eastern part of the Dam is adjacent to the flat laying Rietvlei Formation.

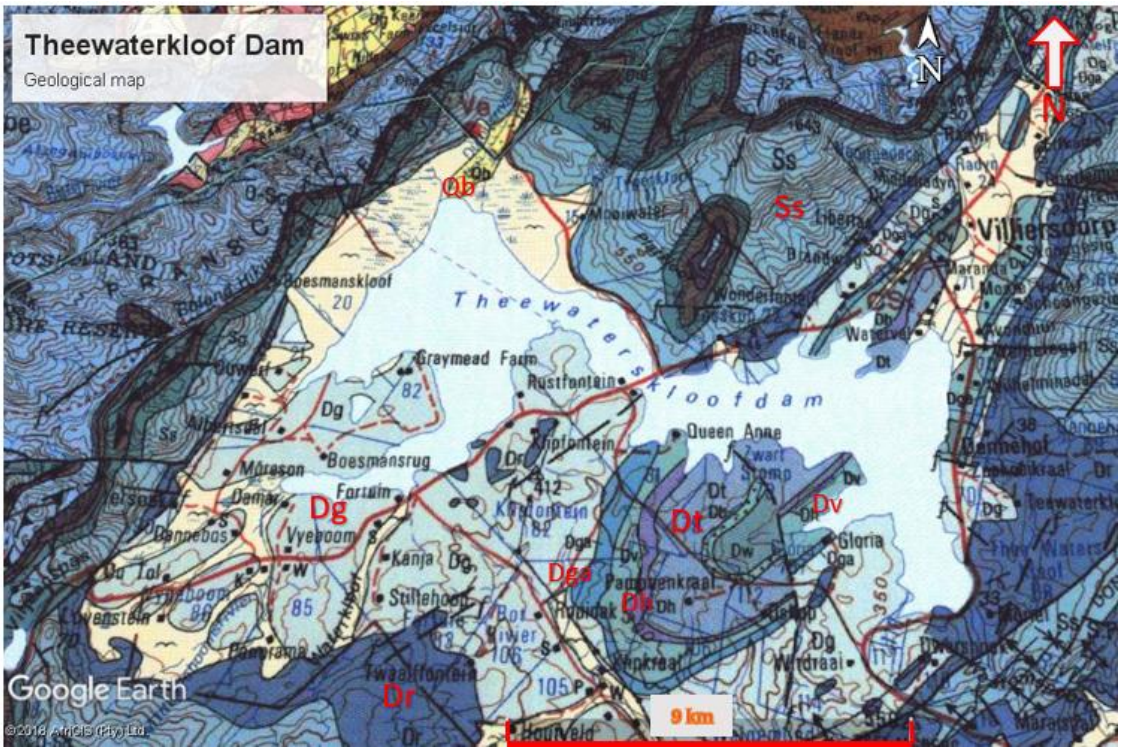

Figure 2.7 Geological map of the bordering mountains and base rocks of Theewaterskloof Dam. Derived from 1: 250 000 geological sheet 3319 Worcester (Council for Geoscience, 1997). Formations: Dt- Tra-Tra, Dh- Hex River, Dv- Voorstehoek, Dga- Gamka, Dg-Gydo, Dr- Rietvlei Ss-Skurweberg, Qb-brackish calcareous soil.

2.5.1.2 Greater Brandvlei Dam

The mountains bordering the west side of the dam comprise sedimentary strata of the Table Mountain Group whereas the Witteberg Group forms the adjacent northern and eastern hills of the dam basin (see Figure 2.8). The base of the Greater Brandvlei Dam consists of alluvium of the Cenozoic age.

The sedimentary units of the Table Mountain group consist mostly of sandstones of the Nardouw Subgroup and Peninsula Formation. Shales of the Cederberg formation are also present. The

bedding of these Cape Supergroup mountains facing the dam consist dips at approximately 30° to the north-west (see Figure 2.8).

The adjacent hills on the northern to eastern sides of the dam basin are dominated by the Devonian age Witteberg Group (Boucot *et al*., 1983). The main rock types of the Witteberg Group include the white quartzites of the Witpoort Sandstone and Blinkstone Formations as well as carbonaceous and micaceous shales of Swartruggens Formation and Wagens Drift Formation. The beds strike E-W and dip at about 50° to the north (Brink, 1984).

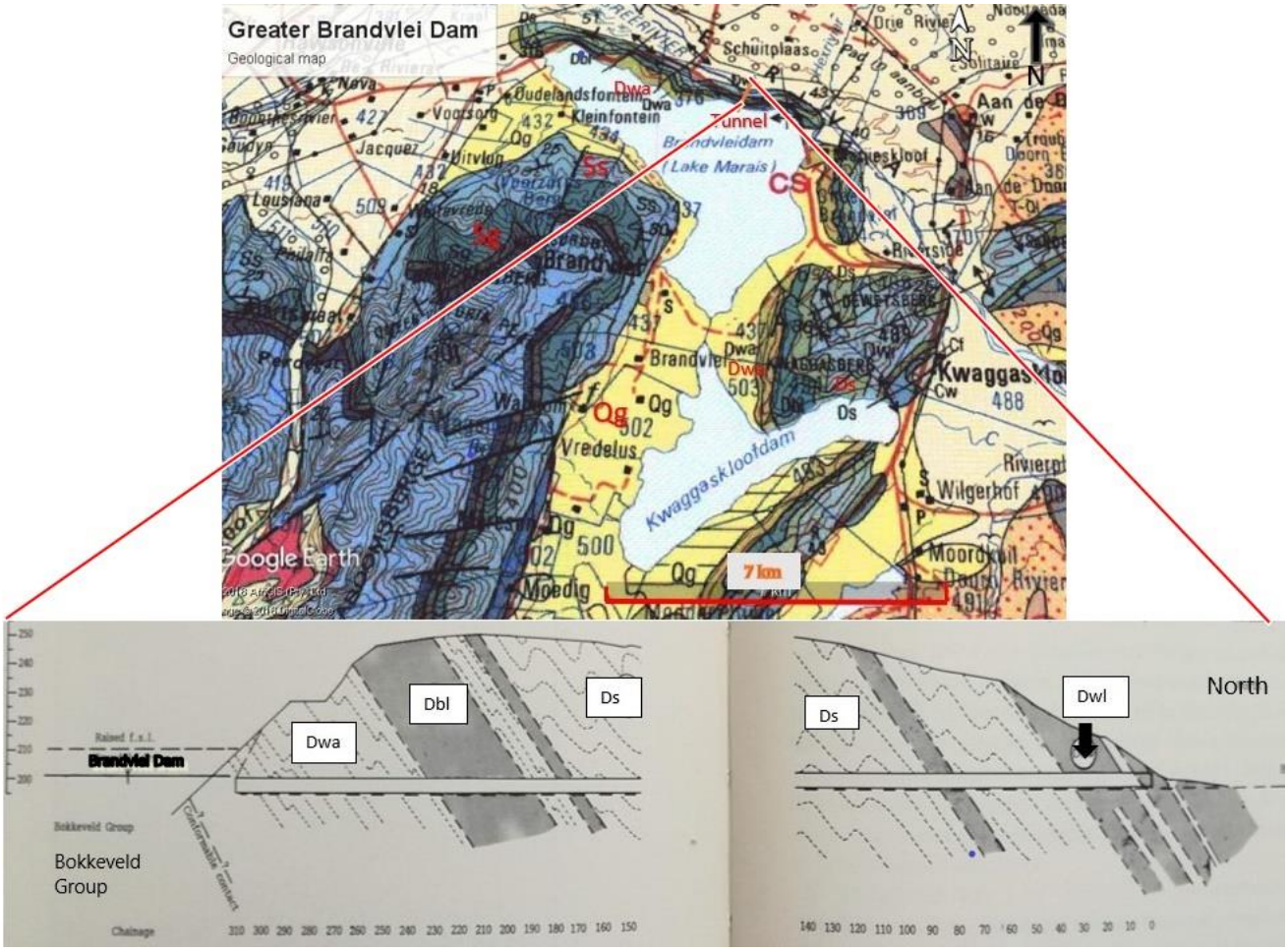

Figure 2.8 Top: The geological map of the Greater Brandvlei Dam. Derived from 1: 250 000 geological sheet 3319 Worcester (Council for Geoscience, 1997). Bottom: Cross-Section of the dam wall. After Brink (1984). Symbols: Qg-sandy loam, SS- Skurweberg, Sg-Nardow, Dwa-Wagen Drift, Dbl-Blinkberg Dwl-Witpoort, Ds -Swart Ruggens

2.5.2 Regional geology of Waterzicht Dam

Klapmuts is situated in the low relief hills of the Cape Winelands and is covered by Quaternary alluvium which is underlain by the northern part of the Stellenbosch Batholith and is surrounded by Malmesbury Group (Resource Management Services, 2015). The Stellenbosch Batholith forms part of the Phase 1 magmatism group of the Cape Granite Suite (Scheepers and Schoch, 2006). The 515 to 556 Ma old Cape Granite Suite (Frimmel, 2000) intruded into the Neoproterozoic metasedimentary rock, mainly Malmesbury Group rocks which formed during the formation of Pan-African Saldanian Belt (Scholtz, 1946). The Malmesbury Group sediments were deposited during the enlargement of the Adamastor Ocean through continuous rifting and separation of the Kalahari and Rio De La Plata Cratons 900 – 700 Ma (Siegfried, 1993). The subsequent Neoproterozoic Pan-African orogenesis, which led to the formation of Gondwana, caused the closure of the Adamastor Ocean and the deformation of the Malmesbury Group sediments (Gresse *et al*. 2006).

Von Veh and Wolter (1983) divided the Malmesbury Group into three domains, namely the Tygerberg terrane (southwestern), Swartland terrane (central) and Boland terrane (northeastern) (see Figure 2.9). The Klapmuts area is surrounded by the sedimentary and metamorphic rocks belonging to the Tygerberg Formation. The Tygerberg terrain is separated from Swartland terrane by the Colenso Fault and the stratigraphy is characterised by alternations of greywacke, phyllitic shale and siltstone, quartzite and minor occurrences of thin limestone and conglomerate beds (Gresse *et al*., 2006).

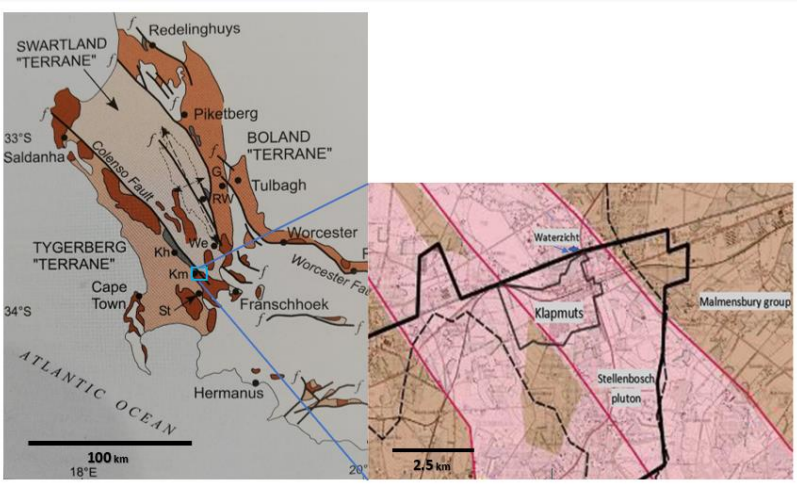

Figure 2.9 Left: Distribution of Malmesbury Group and Cape granite suite. Fr- Franschhoek G-Gouda, Kh- Klipheuwel, Km- Klapmuts, RW- Riebeek West, ST- Stellenbosch, We-Wellington. Derived from Gresse et al. (2006). Right: Geology of Klapmuts area. Derived from Cape Winelands Professional Practices in Association (2016)

2.6 Synthesis

The literature study concluded that based on the adverse effects of reservoir sedimentation, sediment control and removal in reservoirs are essential. Dredging or dry excavation are the two main methods of removing sediment from reservoirs. However, the costs related to sediment removal techniques are high and contamination of the sediments may have a negative effect on the surrounding environment. Various authors have concluded that the problems arising with sediment removal may be mitigated through the utilisation of dredged sediments for construction materials. The primary uses of these sediments include subgrade layers in road construction, manufacture of standard as well as lightweight concrete, bricks and clay liners for landfills. In the Western Cape, the demand for these materials will increase with the forecast recovery in the construction sector, the rise in sustainable building requirements, landfill closures and construction of new landfills, and shortages of material supply close to the construction site.

The findings during the literature study provide information about the importance of utilising reservoir sediment as construction materials. The sediment of the Theewaterskloof, Greater Brandvlei and Waterzicht Dams will be investigated by field investigation, followed by soil classification to determine the applicable analyses required, since different sediment types may be used for different construction materials. The cost of dredging of sediments below the water level will be compared with the cost of excavation in the dry will be compared to assess which method is more feasible. Cost models will be prepared based on the most suitable method of sediment removal for the zones where sediments are suitable for use as construction materials. The removal costs of the sediment will be compared to the costs procuring similar materials conventional sources close to the investigated reservoirs.

Chapter 3 : Methodology

This research project was divided into two stages. First, field investigation and mapping were conducted on the sediments exposed by the drought in the Theewaterskloof and the Waterzicht Dams during May 2018, thereafter the field investigation of the Greater Brandvlei Dam was conducted during July 2018. Laboratory analyses were conducted on the samples taken from these reservoirs.

From the results of this investigation and testing, the volume of each type of sediment (based on the Unified Soil Classification System) in each mapped zone was estimated. The laboratory results of each sample were related to specific criteria for the different material applications to determine the suitability of these sediments as construction materials. Where sediment was found suitable, cost models were prepared to estimate the removal cost per unit volume. The removal costs were used to determine if it will be feasible to remove the various types of sediment. It is important to note that specific tests were, in most cases, only conducted once due to the cost of these tests.

3.1 Field investigation

The Theewaterskloof and Greater Brandvlei Dams were selected based on their size, being the largest two reservoirs in the Western Cape. The Waterzicht dam chosen to investigate the feasibility of removing sediment from smaller farm dams. Before the field analysis at the selected reservoirs, a thorough desk study was completed on the geology of the areas, the occurrence of sediments and the accessibility of the exposed surface areas. The field investigation comprised of a site walkover, the excavation of test holes, dynamic cone penetrometer (DCP) testing and GPS surveying. The accessible areas of the exposed dam surfaces were divided into zones based on farm boundaries or the natural separation with rivers or hilly terrains. Figure 3.1 illustrates the nine zones that were mapped during field investigation for the Theewaterskloof Dam, which was further subdivided into subzones (see numerals in Figure 3.1) based on terrain and sediment occurrence. The Greater Brandvlei Dam was dived into seven zones (see Figure 3.2.), whereas the Waterzicht Dam was only divided into three subzones during the field investigation. The codes used for the zones mapped at Theewaterskloof are abbreviations of the farm names adjacent to the respective zones, whereas

the zone codes for Greater Brandvlei Dam and Waterzicht Dams start with B or WZ respectively followed by a number indicating the order in which they mapped.

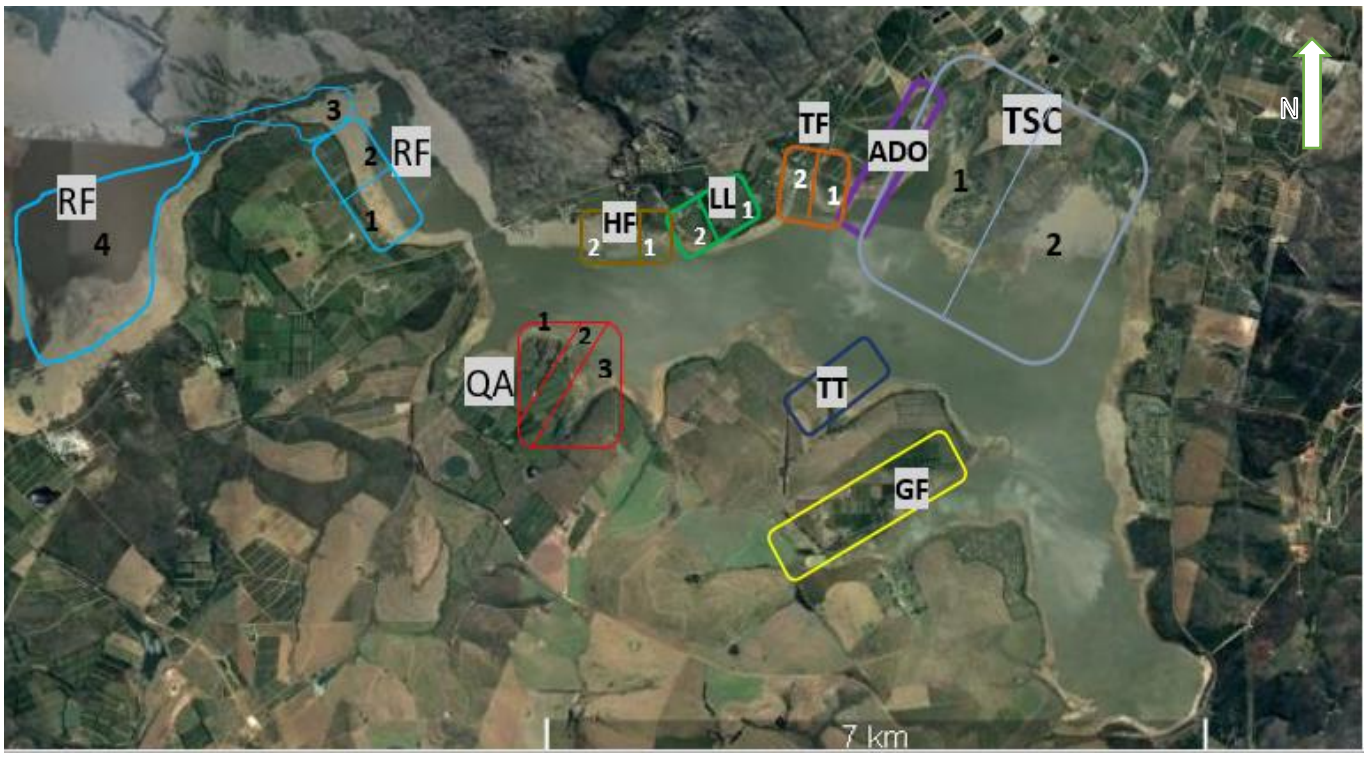

Figure 3.1 Map of the Theewaterskloof Dam indicating the main zones (letter codes and colour borders) and respective subzones (indicated by the number in each zone) under investigation.

Figure 3.2 Map of Greater Brandvlei Dam indicating the main zones under investigation.

Figure 3.3 Map of Waterzicht Dam indicating the main zones under investigation.

3.1.1 Site walkover

Before any field testing was conducted, a walkover of each zone on the dam surface was undertaken. During the walkover, special attention was given to the sediment type, surrounding geology, vegetation and occurrence of remnants of farm infrastructure. The observed sediment type was classified based on grain size and colour, with more detailed classification conducted during soil profiling.

3.1.2 Test pitting and soil profiling

38 test holes were excavated in straight lines in the exposed sediments, at irregular intervals (ranging from 5 to 150 m), from the water line to the high water mark (see Figure 3.4 A). The depth of the test holes ranged from 0.2 to 0.5 m. A more accurate method of test pitting for the estimation of total sediment volume would have been obtained if test pits were scattered across the sediment zone in a grid pattern. However, as mentioned in Section 1.5, the increasing water levels in the reservoirs during the period of research restricted excavation of test holes to only 38 holes.

A hand auger was used from within the test holes to investigate the soil profile at greater depths where the bedrock was not intersected (see Figure 3.4 B). Each layer of sediment excavated with the hand auger was described. The hand auger used has a length of 1.93 m, with the bucket and

bucket blades of the auger having a length and diameter of 0.19 m and 0.09 m respectively. The description of the *in-situ* soil layers was based on the MCCSSO method described by Jennings *et al*. (1973). The MCCSSO method describes each layer of soil based on the moisture condition, colour, consistency, structure, soil type and origin of the soil.

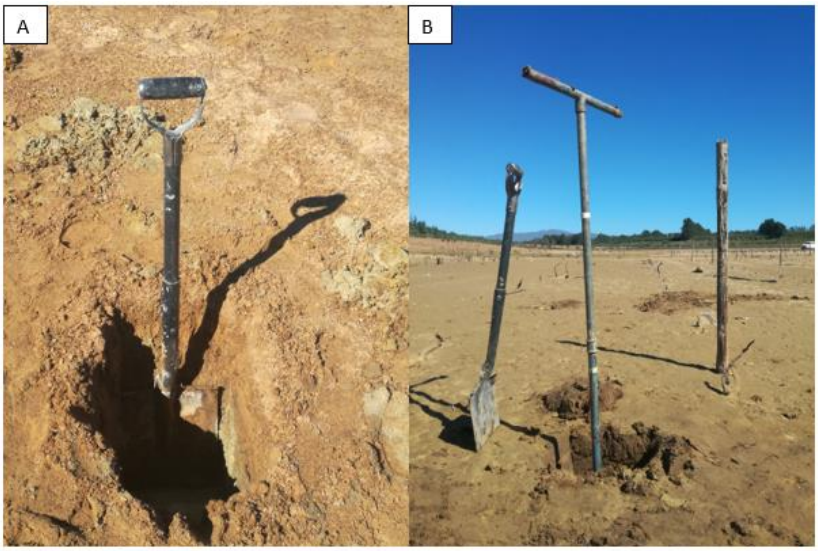

Figure 3.4 A) Excavation of the soil profile at zone TT. B) Hand auger drilling at zone QA

3.1.3 Dynamic cone penetrometer (DCP) testing

DCP testing was conducted next to the test holes as well as upslope where no test holes were excavated. GPS points marked the locations where DCPs were undertaken (see Chapter 4). The DCP testing was conducted on the exposed surface to determine the depths of different layers and their corresponding DCP numbers (DN) based on the standards described by method ST6 in the Technical Methods for Highways (THM6, 1984). The standardised DCP configuration with 2 m length that was used in the DCP analysis is illustrated in Figure 3.5. To determine the DN value, the penetration was recorded every five blows, except where the soil was very stiff where the penetration was recorded at every ten blows. The *in situ* CBR (California Bearing Ratio) values were calculated from the DN values based on Equation 1 and Equation 2 from Kleyn (1984). These *in situ* CBR values will give an indication whether the sediment is able to carry conventional machinery such as tipper trucks that will need to access the zone if dry excavation is to be commenced and if treatment of soil will be required.

$$IF\ DN\ >\ 2mm/blow\quad CBR\ =\ 410\ x\ DN^{-1.27} \qquad \textit{Equation 1}$$

$$IF\ DN \leq 2mm/blow \quad CBR = (66.66\ x\ DN^2) - (330\ x\ DN) + 563.33 \qquad \textit{Equation 2}$$

In addition, where the bedrock could not be measured through auger drilling or DCP analysis, the DCP rod was inserted in the auger hole, and the weight dropped until stiffer strata were reached. Important to note that no DCP analyses were done in zones QA, TT and GF since the DCP equipment was unavailable at the time of the investigation.

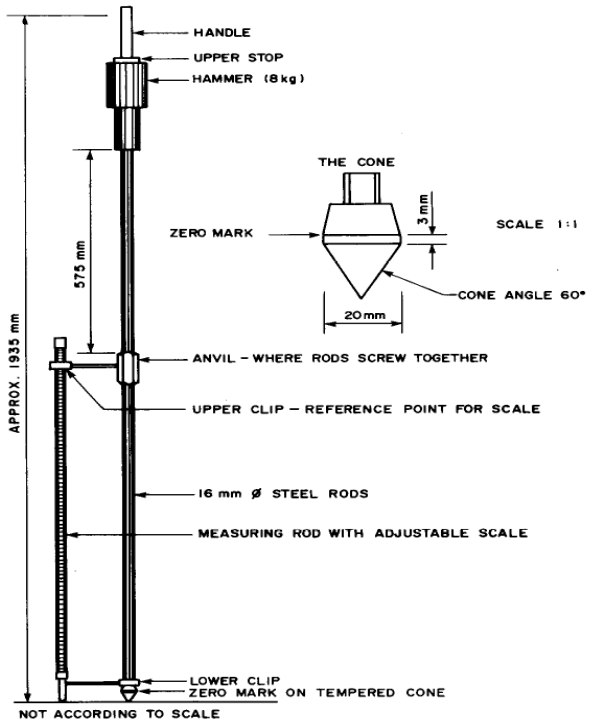

Figure 3.5 Standardised DCP configuration (TMH, 1984)

3.1.4 GPS surveying

GPS surveying was undertaken using a Trimble CS3 GPS to record the locations of test holes were excavated, sampling points and DCP tests, and the position of the water's edge at the time of the fieldwork (see Figure 3.6). The slope gradients of the exposed surfaces were calculated, through the use of the elevation rise and slope run (distance over which elevation increases) deduced from the GPS measurements (see Figure 3.7). However, no elevations could be obtained for zones QA, TT and GF since the GPS equipment was unavailable at the time of the investigation.

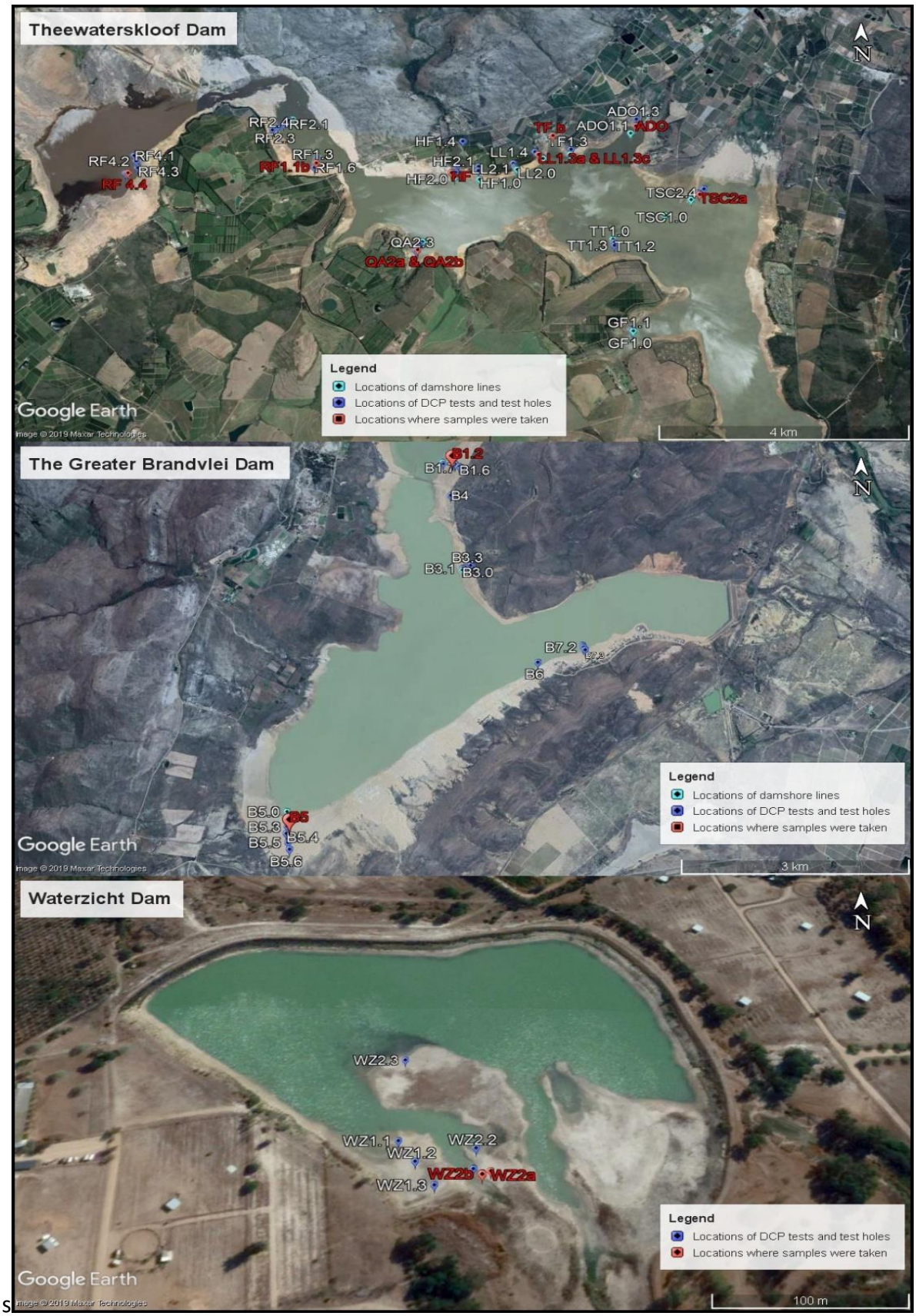

Figure 3.6 Maps of Theewaterskloof Dam (Top), Greater Brandvlei Dam (Middle) and Waterzicht Dam (Bottom) indicating the locations of GPS points indicating DCP, test holes and sampling locations. Important to note, that not all GPS points could be retained on these figures due to the inability to indicate each individual point in a clustered zone of the point on the current map scales. Enlarge images of the different parts of these dams with all the respective GPS points are provided in Chapter 4.

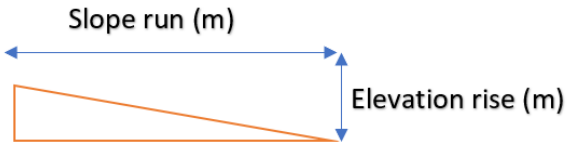

$$\text{Slope gradient} = \frac{\text{Elevation rise}}{\text{Slope run}}$$

Figure 3.7 Illustration indicating the calculation of the slope gradient from slope run and elevation rise.

3.1.5 Sediment sampling

Most of the samples were taken with a shovel, and only a few samples collected with the hand auger. Bulk samples, ranging in weight from 50 to 70 kg, were taken from the main sediment layers occurring within the selected zones (see Figure 3.8) and smaller samples ranging from 1 to 5 kg in weight were taken both from main and lesser sediment layers as well as from residual soil layers. The larger bulk samples were for tests that required larger quantities of material such as California Bearing Ratio (CBR) tests and tests for soluble deleterious impurities, whereas the smaller samples were used for index type tests.

Figure 3.8 One large sample split between two large bags.

Maps for each reservoir, indicating the surface sediment and geology, were constructed in Google Earth based on the data from the site walkovers and soil profiles from test holes. The GPS points for test holes, DCP tests, water's edge and points for gradient calculations were added to the soil and geology maps. In addition, Google SketchUp (version 8) was used to construct 2D columns of the soil profiles based on the test hole data and GPS measurements.

3.2 Laboratory analysis

The separation of the soil samples for laboratory testing was completed in two stages (see Figure 3.9). Firstly, the samples were separated into coarse-grained (50% of grains > 0.075mm) and fine-grained (50% of grains ≤ 0.075mm) materials. After the initial separation based on dominant grain size, the samples that consisted predominantly of coarse-grained material were separated based on their suitability for road materials and fine aggregate. The fine-grained materials were selected for testing for lightweight aggregates, clay bricks and landfill liners based on their plasticity properties. The detailed methodology of laboratory analyses is described in more detail in the following sections.

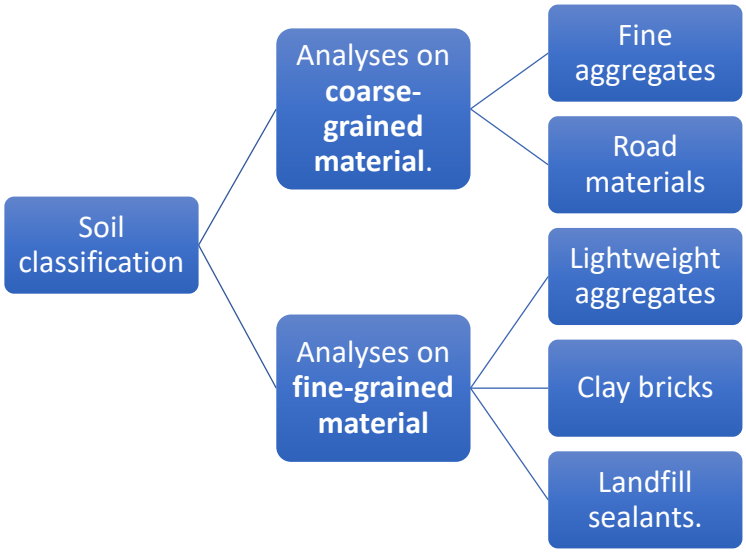

Figure 3.9 Flow diagram for the separation of samples for testing.

3.2.1 Soil classification

The classification of soils was based on the Unified Soil Classification System (USCS) shown in Figure 3.10 and described in Standard D 2487 of ASTM (2006). The USCS categorises soils based on the particle size distribution and Atterberg limits, which were determined using the methods described in TMH1 (1986). The particle size distribution was estimated through wet sieving of 500g sediment through sieves with opening sizes of 13.2mm, 4.75mm, 2mm and 0.425 mm, with the distribution of particles with sizes smaller than 0.425 mm determined through an additional 100g of sample

sieved through the 0.212mm, 0.15mm and 0.075mm sieves. The mass of soil retained on each sieve was determined and taken as a percentage of the entire soil mass. For samples that were tested to contain less than 5% fines the grading characteristics were estimated by means of the uniformity coefficient (Cu) and curvature coefficient (Cc). The calculations for the uniformity coefficient (Cu) and curvature coefficient (Cc) require the particle sizes D10, D30 and D60, which represent the particle diameter corresponding to a certain percentage finer than the given particle value. For example, D10 means 10% are of particles are finer and 90% of the particles are larger than D10 size. The D10, D30 and D60 sizes for the samples containing less than 5% fines were plotted on the particle-size distribution curves. A uniformity coefficient (Cu) value greater than 6 categorizes the samples as well graded. For a Cu value of less than 6, the sample is categorized as poorly graded or uniformly graded. In addition, the curvature coefficient (Cc) must range between 1 and 3 for the sample to classify as well graded.

UNIFIED SOIL CLASSIFICATION AND SYMBOL CHART

COARSE-GRAINED SOILS (more than 50% of material is larger than No. 200 sieve size.)			
GRAVELS More than 50% of coarse fraction larger than No. 4 sieve size	Clean Gravels (Less than 5% fines)	GW	Well-graded gravels, gravel-sand mixtures, little or no fines
		GP	Poorly-graded gravels, gravel-sand mixtures, little or no fines
	Gravels with fines (More than 12% fines)	GM	Silty gravels, gravel-sand-silt mixtures
		GC	Clayey gravels, gravel-sand-clay mixtures
SANDS 50% or more of coarse fraction smaller than No. 4 sieve size	Clean Sands (Less than 5% fines)	SW	Well-graded sands, gravelly sands, little or no fines
		SP	Poorly graded sands, gravelly sands, little or no fines
	Sands with fines (More than 12% fines)	SM	Silty sands, sand-silt mixtures
		SC	Clayey sands, sand-clay mixtures
FINE-GRAINED SOILS (50% or more of material is smaller than No. 200 sieve size.)			
SILTS AND CLAYS Liquid limit less than 50%		ML	Inorganic silts and very fine sands, rock flour, silty of clayey fine sands or clayey silts with slight plasticity
		CL	Inorganic clays of low to medium plasticity, gravelly clays, sandy clays, silty clays, lean clays
		OL	Organic silts and organic silty clays of low plasticity
SILTS AND CLAYS Liquid limit 50% or greater		MH	Inorganic silts, micaceous or diatomaceous fine sandy or silty soils, elastic silts
		CH	Inorganic clays of high plasticity, fat clays
		OH	Organic clays of medium to high plasticity, organic silts
HIGHLY ORGANIC SOILS		PT	Peat and other highly organic soils

LABORATORY CLASSIFICATION CRITERIA

GW	$C_u = \frac{D_{60}}{D_{10}}$ greater than 4; $C_c = \frac{D_{30}}{D_{10} \times D_{60}}$ between 1 and 3	
GP	Not meeting all gradation requirements for GW	
GM	Atterberg limits below "A" line or P.I. less than 4	Above "A" line with P.I. between 4 and 7 are borderline cases requiring use of dual symbols
GC	Atterberg limits above "A" line with P.I. greater than 7	
SW	$C_u = \frac{D_{60}}{D_{10}}$ greater than 4; $C_c = \frac{D_{30}}{D_{10} \times D_{60}}$ between 1 and 3	
SP	Not meeting all gradation requirements for GW	
SM	Atterberg limits below "A" line or P.I. less than 4	Limits plotting in shaded zone with P.I. between 4 and 7 are borderline cases requiring use of dual symbols.
SC	Atterberg limits above "A" line with P.I. greater than 7	

Determine percentages of sand and gravel from grain-size curve. Depending on percentage of fines (fraction smaller than No. 200 sieve size), coarse-grained soils are classified as follows:

Less than 5 percent ..... GW, GP, SW, SP
More than 12 percent ..... GM, GC, SM, SC
5 to 12 percent ..... Borderline cases requiring dual symbols

PLASTICITY CHART

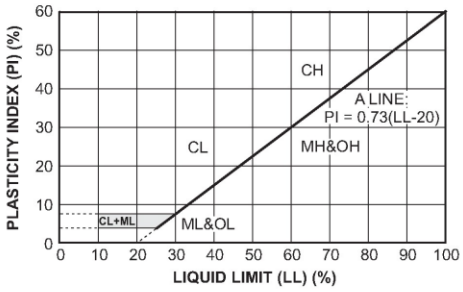

Figure 3.10 Unified Soil Classification System

A Bouyoucos hydrometer and cylinder were used on a 100g sample (passing the 0.075mm sieve) to estimate the percentage of particles smaller than 0.05 mm and 0.005mm (the clay and silt size fractions). This process included the addition of 5 ml of sodium silicate and sodium oxalate solutions as dispersion agents to a mixture of 400 ml of distilled water and the 100g soil sample. The mixture stood for two hours before it was vigorously stirred for 10 minutes. The suspension was added to the Bouyoucos cylinder and filled with distilled water (see Figure 3.11).

Figure 3.11 The determination of the grain size distribution in soils by means of a hydrometer

The hydrometer was inserted into the solution after it was rapidly inverted. Respective readings were taken 40 seconds and 1 hour after the sample was inverted. The values obtained from the hydrometer readings were inserted into Equation 3 and Equation 4 to estimate the percentage passing the 0.05mm and 0.005mm sieves.

$$P_2 = \frac{Sf(100 - F)}{Sm}$$ *Equation 3*

$$P_3 = \frac{Sf(F - C)}{Sm}$$ *Equation 4*

$P_2 = Percent\ passing\ the\ 0.05mm\ sieve$

$P_3 = Percent\ passing\ the\ 0.005mm\ sieve$

Sm = percentage soil mortar in the total sample (determined in Method A1)

Sf = percentage soil fines in the total sample (determined in Method A1)

F = 40 − second hydrometer reading

C = 1 − hour hydrometer reading

The Atterberg Limits are the collective name for the liquid limit (LL), plastic limit (PL) and shrinkage limit (SL). These limits are determined from the fraction of a respective sample that passes the 0,425 mm sieve. Furthermore, these limits were only calculated for samples where the fine-grained fraction possessed plasticity (able to deform without rupture/breaking under external force when moist).

The fine fractions of the sample under investigation were mixed with distilled water until a stiff consistency was achieved and transferred to the Casagrande Apparatus. Small amounts distilled water were added and the sample transferred to the Casagrande cup and a groove formed down the middle of the specimen using the grooving tool before commencing the test. The test was repeated until the consistency was achieved which allows the soil faces on either side of the groove to connect after 25 taps in the Casagrande apparatus (see Figure 3.12).

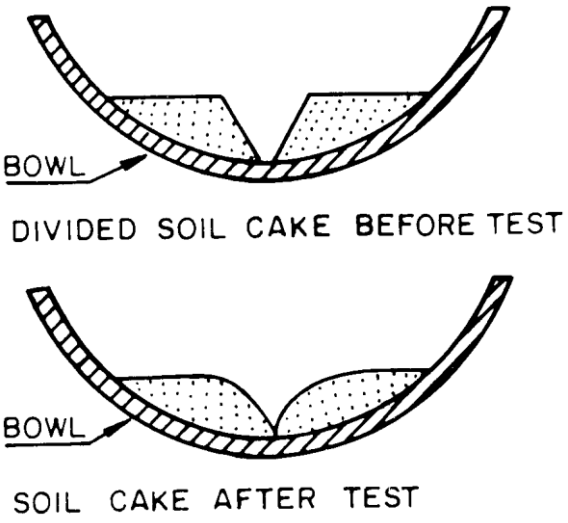

Figure 3.12 Illustration of the linking of the two bottom parts of the separate soil faces that must occur after 25 taps with the liquid limit device.

Once the specimen displayed adequate consistency after 25 taps, a piece of the sample was placed into a container, weighed and inserted directly into the drying oven directly. The change in weight

and the weight of the sample after drying was used in Equation 5 to calculate the moisture content at the liquid limit:

$$LL = \frac{Moist\ sample - Oven - dried\ sample}{Oven - dried\ sample}\ x\ (\frac{Number\ of\ taps}{25})^{0.12} \quad \textit{Equation 5}$$

From the remaining soil in the Casagrande Apparatus, a piece was selected and rolled by hand until cracks formed and it became too brittle to form a 3 mm diameter thread. The crumbled piece was weighed and subsequently placed in the oven. As for the liquid limit, change in weight and the weight of the sample after drying was used in Equation 6 to calculate the moisture content at the plastic limit. The plasticity index (PI) was calculated by subtracting the PL from LL (see Equation 7).

$$PL = \frac{Moist\ sample - Oven - dried\ sample}{Oven - dried\ sample} \quad \textit{Equation 6}$$

$$PI = LL - PL \quad \textit{Equation 7}$$

For the linear shrinkage (LS), the saturated sample was placed into a small mould with a length of 150 mm and inserted into the oven for 24 hours. The length of the oven-dried sample was measured and incorporated into Equation 8 to calculate the linear shrinkage.

$$LS = \frac{Length\ of\ moist\ sample - Length\ of\ ovendried\ sample}{Length\ of\ moist\ sample} \quad \textit{Equation 8}$$

3.2.2 Coarse-grained material

3.2.2.1 Road construction materials

Nine samples, classified as coarse-grained materials, were selected for testing their suitability as road construction material and fine aggregate for concrete. Potential road building materials were classified according to Colto (1998, see Table 3.1) and the Technical Recommendations for Highways

(TRH14, 1985 see Table 3.2). The difference between the Colto (1998) and TRH14 (1985) classifications is that the THR14 (1985) are recommendations that are widely used in South Africa, while the COLTO (1998) document is the official specification. The engineering properties that this classification requires are the particle size distribution, Atterberg limits, California Bearing Ratio (CBR), percentage swell at maximum dry density (MDD) and the grading modulus.

Table 3.1 Criteria for the natural material to be used in road layers, derived from Colto (1998).

	Natural gravel, or natural gravel & boulders which may need crushing			Natural material (soil, sand or gravel)		
	G4	**G5**	**G6**	**G7**	**G8**	**G9**
Grading modulus	-	2.5 ≥ GM ≥ 1.5	2.6 ≥ GM ≥ 1.2	2.7 ≥ GM ≥ 0.75	2.7 ≥ GM ≥ 0.75	2.7 ≥ GM ≥ 0.75
Atterberg limits	a) All materials except calcrete **LL ≤ 25, PI ≤ 6, LS ≤ 3%**	All materials except calcrete. **LL ≤ 30, PI ≤ 10, LS ≤ 5%.**	All materials except calcrete: **PI ≤ 12** or a value equal to **2 times the GM plus 10**, whichever is the higher value. **LS ≤ 5%.**	All materials except calcrete: The **PI ≤ 12** or a value **equal to 3 times the GM plus 10**, whichever is the higher value.	All materials except calcrete: The **PI ≤ 12** or a value **equal to 3 times the GM plus 10**, whichever is the higher value.	The **PI ≤ 12** or a value equal to **3 times the GM plus 10**, whichever is the higher value.
Strenght (CBR)	CBR at **98%** of modified AASHTO denisty **≥ 80%**	CBR at **95%** of modified AASHTO density **≥ 45%**	CBR at **95%** of modified AASHTO denisty **≥ 25%**	CBR at **93%** of modified AASHTO density **≥ 15%**	CBR at **93%** of modified AASHTO density **≥ 10%**	CBR at **93%** of modified AASHTO **≥7%**
Swell	Swell at 100% modified AASHTO density **≤ 0.2%** for all materials except calcrete	Swell at 100% modified AASHTO density **≤ 0.5%**	Swell at 100% modified AASHTO density **≤ 1.0%**	Swell at 100% modified AASHTO density **≤1.5%**	Swell at 100% modified AASHTO density **≤1.5%**	Swell at 100% modified AASHTO density **≤1.5%**

Table 3.2 Recommendations for the natural material to be used in road layers, derived from THR14 (1985)

Property	**Material type**				
	G6	**G7**	**G8**	**G9**	**G10**
Minimum CBR AT 93% Mod.AASHTO density	25	15			
Minimum CBR at in-situ desinty (usually minimum 90% MDD)	-	-	10	7	3
Maximum swell at 100% Mod.AASHTO density	1	1,5	1,5	1,5	1,5
Grading modulus	1,2	-	-	-	-
Atterberg limits	PI=12 or 3*GM^2 + 10	PI=12 or 3*GM^2 + 10	-	-	-

The maximum dry density (MDD) and optimum moisture content (OMC) were obtained for the Modified AASHTO compaction effort (55 blows with a 4.536 kg tamper on five layers of soil) using the method described in Method A7 of standard THM1 (1986). Each sample was divided into at least four samples of 7 kg each. The 7kg samples were compacted at different moisture contents, with

the intervals ranging between 2 and 3 %. The dry density value of each compacted 7kg sample was plotted against the respective moisture content. The peak of the dry density - moisture content curve indicates the MDD and the OMC of the sample on the y-and x-axes respectively (see Figure 3.13). If no peak is noted, more samples should be compacted until a peak in curvature is observed.

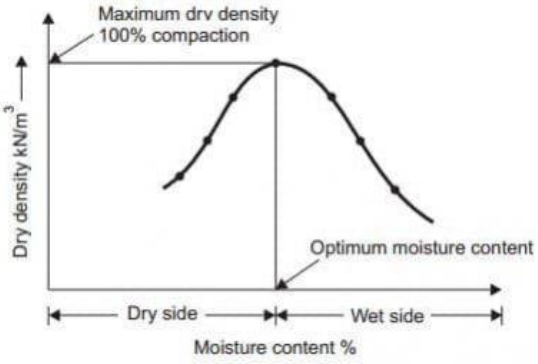

Figure 3.13 The estimation of the maximum dry density and optimum moisture content (Anupoju, 2019)

The CBR values and swelling were determined based on Method A8 of THM1 (1986). Preparation of the samples for CBR analysis included mixing water into the samples to achieve their respective OMCs. Each sample was compacted in three different moulds at:

- 55 blows with 4.536 kg tamper (457,2 mm drop) on five layers of soil
- 25 blows per layer with a 4.536 kg (457,2 mm drop) tamper on five layers of soil
- 55 blows per layer with a 2,495 kg (304,8 mm drop) tamper on three layers of soil

The dry density of each of the three compacted specimens was calculated. To obtain the swelling of each specimen, a perforated plate with an adjustable stern was placed on top of a filter paper on the surface of the material and a 4,536 kg surcharge weight placed carefully on top of the plate. A tripod with a dial gauge was placed carefully on top of the stern and an initial reading was taken from which the swelling was to be determined. After four days of soaking, a final reading was taken and used to calculate the swelling in the sample in each mould. The soaked specimens were placed in an automatic CBR press (see Figure 3.14) which was set as described in TMH1 (1986). The load readings were recorded at each 0,635 mm increment until the plunger had penetrated the sample to a depth of 9.53 mm. The CBR results for the three compacted specimens of each sample were plotted on a CBR versus depth of penetration plot. Where a concave upward shape was detected at the initial stage, the straight line succeeding the concave part of the curve was extended downwards until it intersects the abscissa (see Figure 3.15). This point of intersection is then taken as the zero-

depth of penetration. Using this new zero, the load is taken at 2.54 mm penetration for each specimen. The CBR values for each specimen were obtained through Equation 9.

$$CBR\ value\ (\%) = \frac{Load\ (kN)\ at\ 2.54\ mm\ penetration}{13.344} x\ 100.$$

Equation 9

For each sample, the dry density of the sample was determined and a graph was plotted of CBR against dry density. From this graph, the CBR values were obtained at 98%, 95%, 93% and 90% MDD.

Figure 3.14 Automatic CBR press

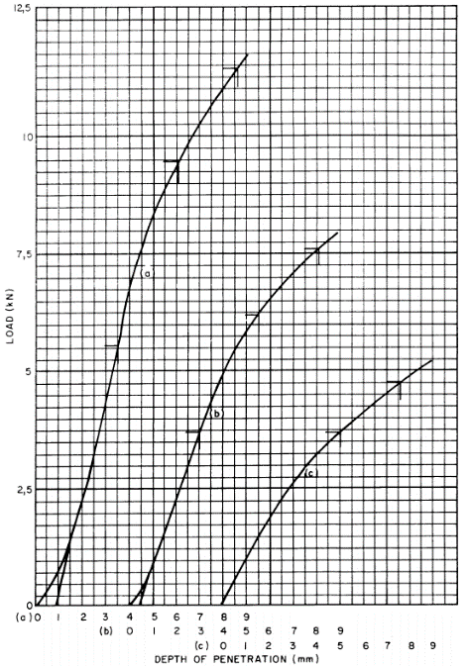

Figure 3.15 Example of the corrections that were applied to initial concave parts of the load against penetration curves

The grading modulus calculation was based on code SANS 3001-PR5 (SANS 3001-PR5:2011). This formula uses the particle size distribution results of each sample. Equation 10 was used for the calculations of the grading modulus (P=percent passing):

$$GM = \frac{(300 - (P_{2\ mm} + P_{0.425\ mm} + P_{0.075\ mm}))}{100}$$

Equation 10

3.2.2.2 Natural fine aggregates

The testing for natural fine aggregates for concrete was based on the criteria described in SANS 1083 (SANS 1083:2017). Natural fine aggregates for mortar and plaster was tested according to the requirements specified in SANS 1090 (SANS 1090:2009, see Table 3.3). Figure 3.16 describes the process of assessing the suitability of the sediments for use as fine aggregates.

Table 3.3 Criteria from SANS 1083(2017) and SANS 1090 (2009)

Natural fine aggregate criteria -SANS 1083 (2017)& SANS 1090 (2009)			
Property	**Concrete**	**Mortar**	**Plaster**
Grading, mass percentage that passes sieves of sizes (µm):			
5000	92-100		
4750	90-100	100	100
2360		90-100	90-10
1180		70-100	70-0
600		40-100	40-10
300		5-85	5-0
150	5-25	5-35	5-90
Dust content max % (<0,075mm)	5%	12.5%	7.5
Methylene blue adsorption value, max %	0.7		
Clay content % (<5µm)	5	2	
Chloride content-max mass %:			
Concrete for prestressing:	0.01	-	
Normal reinforced concrete	0.03	-	
Non-reinforced concrete	0.03	-	
Fineness Modulus	1.2-3.5	-	
Organic impurities	The colour of the liquid above the fine aggregate shall not be darker		
Presence of sugar	Free from sugar	-	
Soluble deleterious impurities	The strength of specimens made with the fine aggregate shall be at least 85 % of that of the specimens made		
Drying shrinkage of mix, % max	-	0.12	0.1

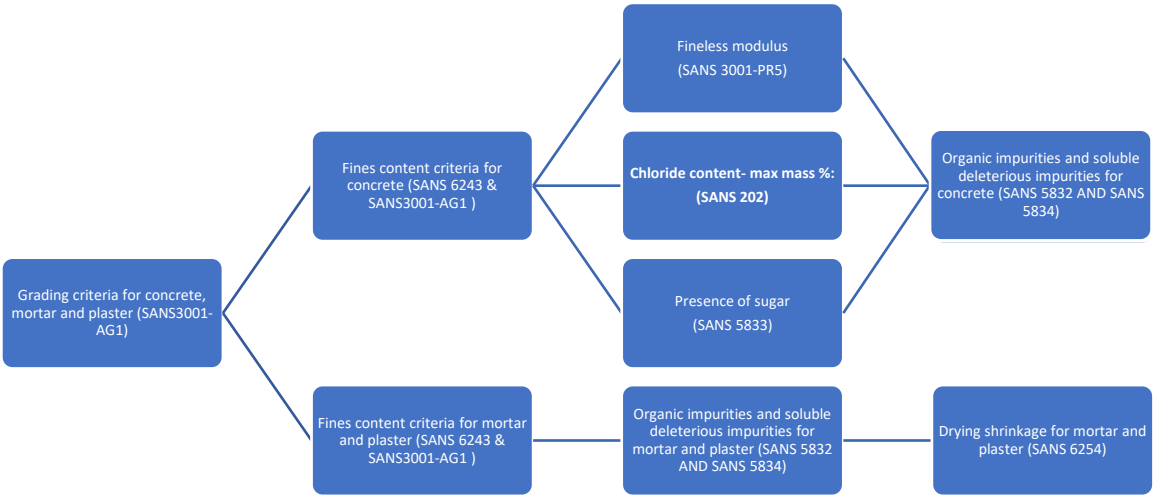

Figure 3.16 Flow diagram representing the order of the properties that were tested during laboratory analyses for fine-grained aggregates

Both the SANS 1083 and SANS 1090 standards require wet sieving to be completed according to SANS 3001-AG1 (SANS 3001-AG1:2014). From the nine selected coarse-grained samples, only the samples that passed the grading requirements for concrete, mortar and plaster sand were considered for further testing. If the dust content (particles size smaller than 0.075mm) failed the allowable maximum of each requirement (5% for concrete,12.5% for mortar and 7.5% for plaster), the methylene blue adsorption value was calculated based on SANS 6243 (SANS 6243:2008, see Figure 3.17). The methylene blue adsorption value indicates the clay content of the fines of an aggregate containing deleterious swelling clay minerals.

For the calculation of methylene blue adsorption, approximately 5 g of the material that passed the 0.075 mm sieve, was boiled in hydrogen peroxide for 30 minutes. The treatment with hydrogen peroxide is only required if organic impurity contents fail the criteria of SANS 1083 and SANS 1090. However, no examination on organic impurities of samples was completed at that stage (test scheduled near the end of the test sequence, see Figure 3.16) and, since the treatment process of the 5 g sample was less expensive than an organic impurity test, the conservative approach was to assume that the samples contained organic impurities.

The test was completed by titrating 0.5 mℓ (1 mℓ at later stages of analysis) of indicator solution (0,1 g of methylene blue dissolved in 100 mℓ distilled water) into a solution consisting of 30 mℓ distilled water and 1 g treated sediment. After each titration of the indicator solution into solution

with sediment, the contents were stirred for 1 minute, followed by removal of a drop of sediment solution which was then placed on the white filter paper. This process was repeated until either a definite blue halo was observed or more than 15 mℓ of indicator solution was used (for a mass of 1g, indicator exceeding 7mℓ exceeds the limitations reference criteria). If the methylene blue adsorption value of the sample exceeds 0.7, the utilisation of the sample is dependent on the clay content (< 0.005 mm) of the sample, which should not exceed 5% for concrete and 2% for mortar and plaster. If the clay content of a sample exceeds these allowable contents, the sample was discarded, and no further tests relating to fine aggregates were carried out on the sample.

Figure 3.17 Methylene blue solution on the right and indicator solution of the left.

The samples that passed the grading requirement for concrete, were tested for the fineness modulus based on the method described in SANS 3001-PR5 (SANS 3001-PR5:2011), the chlorite content based on the method described in SANS 202 (SANS 202:2006), the sugar presence based on the method described in SANS 5833 (SANS 5833:2006), the organic impurities based on the method described in SANS 5832 (SANS 5832:2006), and the soluble deleterious impurities based on SANS 5834 (SANS 5834:2006). The samples that passed the grading requirements for mortar and plaster also underwent the test for organic impurities and soluble deleterious substances as well as the estimation of initial drying shrinkage based on SANS 6254 (SANS 6254:2006). The fineness modulus was determined based on the sieve results conducted in accordance with SANS 3001-AG1.

3.2.3 Fine-grained material

The composition of the fine sediments (silts and clays) was determined through semi-quantitative X-ray diffraction (XRD) and X-ray fluorescence (XRF) analyses. The XRD analyses indicate the type and quantity of minerals present in the sample, whereas the XRF analysis determines the type and quantity of the major oxide elements present in each sample. Preparation of the samples for both

XRD and XRF analyses includes the milling of the samples to a particle size less than 70µm using a swing mill.

The equipment that was used to complete XRD analysis was a Panalytical Empyrean X-ray Diffractometer (see Figure 3.18) equipped with a copper side window tube, an anode consisting of Rh and a W cathode (filament), and an X Celerator detector. In addition, the whole-rock major element compositions were determined by XRF spectrometry on a Panalytical Axios Wavelength Dispersive spectrometer.

Figure 3.18 Panalytical Empyrean X-ray Diffractometer

3.2.3.1 Analyses for lightweight aggregates

The use of the sediments as lightweight aggregates is based on the particle size distribution, Atterberg limits and mineral composition of the samples. The major minerals obtained in the samples through XRD analysis were compared to the distinctive minerals in lightweight aggregates according to research by Rattanachan and Lorprayoon (2005, see Table 3.4). The major oxides were plotted on the tertiary diagram to determine if the sample composition plots in Riley's (1951) "area of bloating" (see Figure 3.19). This area indicates sufficient bloating characteristics that mineral must experience when sintered at high temperatures (1100 to 1300°C). for the production of lightweight aggregates. The three main constituents on the ternary graph are SiO_2, Al_2O_3 and the third constituent being a flux of major elements (CaO, MgO, FeO, Fe_2O_3 K_2O and Na_2O).

Table 3.4 Mineral composition for lightweight aggregates (Rattanachan and Lorprayoon, 2005)

Mineral composition for LWAs (Rattanachan & Lorprayoon, 2005)
Main minerals
Kaolinite
Smectite
Illite
Chlorite
Varying concentrations:
Quartz
Feldspars
Carbonates
Iron oxides
Hydroxides
Minor amounts
Sulfides
Organice matter

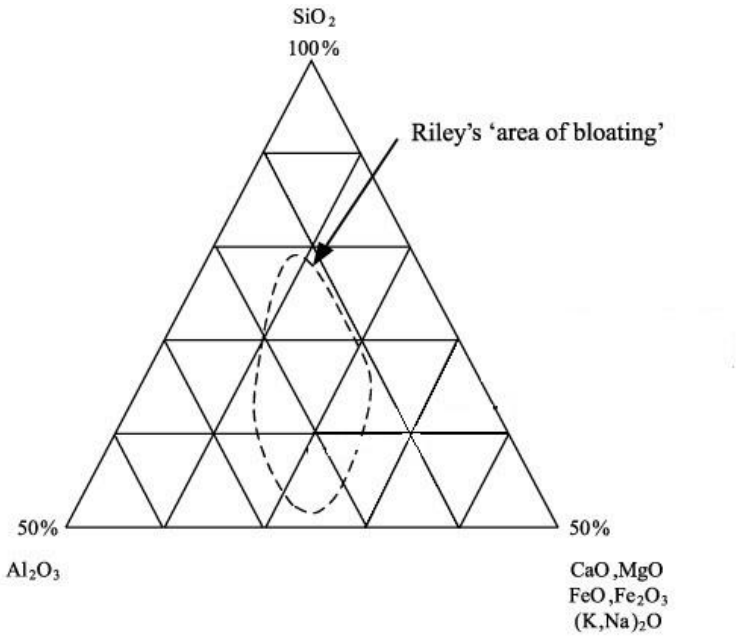

Figure 3.19 Ternary diagram indicating Riley's (1951) "area of bloating".

3.2.3.2 Analyses for clay bricks

The fine-grained sediment samples were investigated to be used as raw material for the manufacturing of fired and unfired bricks. No bricks were fired, but the chemical and physical properties of the sample were related to the suitable soil properties for producing VSBK (Vertical Shaft Brick Kiln) bricks, described by Prajapati and Maity (2010, see Table 3.5). The properties

related in the latter criteria were attained from the particle size distributions, Atterberg limits and XRF analysis undertaken on the respective samples. The percentage of a sample that is smaller than 0.002 mm was obtained through interpolation of the particle size distribution curves. In addition, the mineral compositions of the samples determined through XRD analysis were related to that of the brick clays in the Western Cape, namely Malmesbury clays (see Table 3.6, Heckroodt 1980).

Table 3.5 The recommendation for chemical and physical properties for VSBK bricks. Derived from Prajapati and Maity (2010). Abbreviation: PSD-particle size distribution.

Chemical properties	
Test parameters on dry basis (% by mass)	**Percentage (%)**
Loss of ignition	3,2
Silica as SiO2	60
Iron as Fe2O3	>3
Alumina as Al2O3	23
Sodium as Na2O	0,1
Potassium as K2O	2,76
Calcium as Cao	Trace
Magnesium as MgO	1,2
Organic Carbon as C	0,8
Physical properties	
Elements	**Percentage (%)**
PSD of 0,063-2 mm	20 - 45
PSD of 0,02-0,063 mm	25 - 45
PSD of <0,02 mm	20 - 35
Liquid limit	25 - 38
Plasticity index	7 to 16
Volumetric shrinkage	15 - 25

The investigation of unfired bricks included the manual production of bricks and examining the bricks after they were air-dried, as well as testing their compressive strengths. Only three clay bricks were manufactured by manual compaction of clay material, close to optimum moisture content, into moulds with dimensions 220mm length x 110mm breadth x 70mm height. The bricks were air-dried for two weeks before Uniaxial Compression Strength testing (UCS). The automatic CBR press was set to the UCS option and the load application rate was set to 150 kN per minute. The recorded failure load of each brick was recorded (in Newton) and divided by the area of brick (mm^2) on which the force was exerted. The average compression strength was recorded and related to the typical compression strengths (1 to 4 MPa) described by Sutton *et al*. (2011). In addition, the dried unfired bricks were investigated for cracks and shrinkage. It is important to note that the preparations and

testing methods of samples were adjusted due to limitations associated with these tests (see Section 1.5).

Table 3.6 Mineral composition of the brick clays in the Western Cape (Heckroodt, 1980)

Malmesbury Clay (Heckroodt,1980):
Main minerals
Kaolinite
Quartz
Illite
Varying concentrations:
Iron oxides
Hydroxides

3.2.3.3 Analyses for landfill liners

The criteria used for testing the clay as a liner (see Table 3.7) were based on the requirements of the Department of Water Affairs and Forestry (DWAF, 1998), which was updated in the Government Gazette (2013) to accommodate geosynthetic clay liners (GCL) as an replacement option for compacted clay liners (CCL). The required soil properties for the determination of its suitability as a clay liner include the particle size distribution, Atterberg limits, mineral composition and permeability coefficient (k value).

The permeability coefficient was determined at 95% of the Modified AASHTO MDD through the falling head method described in ASTM D5084 (ASTM D5084:2010) using the MDD and OMC for the sample previously determined using method A7 from THM1 (see Section 3.2.2.1). The approach of trial and error was used by changing the number of blows and a number of soil layers during compaction until a dry density of about 95% of the MMD was achieved.

The mould containing the sample compacted to about 95% MDD was encapsulated with a permeameter which connects to a standpipe with a cross-sectional area of 1.86×10^{-5} m^2 (see Figure 3.20). The standpipe provides the water head and allows the measuring of the volume of water passing through the sample. Water is transferred from standpipe to specimen, but measurements were only taken after the specimen was fully saturated. After saturation, three readings were taken at 100 to 170-second intervals, together with the respective head loss over these intervals. At each of the time intervals, the permeability coefficient was determined, and the average of these three

values was correlated with the landfill criteria (see Table 3.7). The formula for determining the permeability coefficient through the failing head method is given in Equation 11:

$$k = \frac{a * L}{A * \Delta t} * \ln(\frac{\Delta h1}{\Delta h2})$$

Equation 11

$k = Permeability\ coefficient\ (m.s^{-1})$

$a = Cross - sectional\ area\ of\ standpipe\ (m^2)$

$L = Length\ of\ specimen$ (m)

$A = Cross - sectional\ area\ of\ specimen\ (m^2)$

$\Delta t = Interval\ of\ time\ (s)$

$\Delta h1 = Head\ loss\ over\ specimen\ at\ t_1 (m)$

$\Delta h2 = Head\ loss\ over\ specimen\ at\ t_2 (m)$

Table 3.7 Clay liner criteria for landfill types based on DWAF (1998) and updated by Government Gazette (2013)

Criteria (DWAF,1998 and Government Gazette, 2013)			
Maximum particle size	25 mm		
Plasticity Index (PI)	Minimum 10 and a maximum that will not result in excessive desiccation cracking		
	Maximum k value (m.s-1)	Thickness of compaction clay layer (0.6m)	Type of waste
Landfill types:			
Class A	1 x10-9	0.6	Hazardous
Class B	1 x 10-8	0.6	Municipal
Class C	1 x 10-8	0.3	Post-Consumer packaging and tyres
Class D	-	-	Inert, builders rubble

Figure 3.20 Specimen connected to standpipe during falling head permeability test

3.3 Sediment volume estimations and cost models related to sediment removal.

This section describes the methods applied to estimate the volume of each zone mapped during field investigation. For the zones where sediment passed the criteria to be utilized as a construction material, cost models were created in Excel to calculate the cost for the removal of the sediment in these zones. The cost of removal was calculated as a cost per m^3 for the use of road materials and fine aggregates, cost per brick for fired and unfired bricks, cost per kg for lightweight aggregates and cost to cover m^2 area for landfill clay liners. These costs per specified unit were related to the costs per specified unit of conventional construction materials to determine if it will be feasible to mine these sediments for the respective construction materials.

3.3.1 Volume estimations

Data obtained during mapping of the dam sediment, including the sediment layer thickness and the soil types based on the USCS classification, were used together with the area measurement tool in Google Earth to calculate the volume of each type of sediment occurring on the mapped surfaces. The calculation of the volume for each zone or subzone was completed through multiplying the average depth of the sediment layers obtained from the soil profiles in each zone with the total area of the zone which was measured in Google Earth (see Equation 12).

Where the full depth of the sediment layer was not measurable, due to the sediment layer being too deep to measure with the field equipment or due to the occurrence of a shallow water table, the maximum measurable depths were used for calculating the *average depth* used in Equation 12. The percentage storage increase of a reservoir if sediment in a zone or subzone is to be removed was calculated through dividing the '*sediment volume of the zone*' by the '*total capacity of the reservoir*' and multiplying the result by 100 (see Equation 13).

$$Sediment\ \ volume\ =\ Average\ depth\ \ x\ Surface\ area \qquad \textit{Equation 12}$$

$$Dam\ storage\ increase\ if\ \ sediment\ is\ removed\ (\%) = \frac{Sediment\ volume\ of\ \ zone}{Total\ capacity\ of\ \ the\ \ reservoir}\ x\ 100 \qquad \textit{Equation 13}$$

3.3.2 Cost models: Coarse-grained material to be mined as road materials and fine aggregates.

The costs models related to coarse-grained material to be mined as road materials and fine aggregates were designed to calculate the removal costs per m^3 if different proportions of the sediment reserves in the respective zones are to be mined.

For the design of the cost models related to mining sediment from the two large reservoirs, Theewaterskloof Dam and Greater Brandvlei Dam, there were two sediment removal methods considered namely dry excavation and dredging. In addition, the cost model was designed to include dry excavation with the aid of sheet piling and without sheet piling. The addition of sheet piling with

dry excavation was included since it will the prohibition of raising dam water from entering the mining area. Dry exaction without sheet piling will therefore only be commenced when sediment remains dry.

For dry excavation, 20-ton excavators and tipper trucks with 16 m^3 capacity were selected due to their capability of removing large amounts of sediment. For dredging, an 8-ton amphibious excavator that is attachable to pontoons and with a cutter suction pump (Bell200 pump) with a 200 m long depositing pipe connected to the excavator's arm, was used. For the excavation of Waterzicht Dam, only dry excavation was considered due to dredging machinery being too expensive to be used on such a small area as well as being more facile to prohibit water level increase.

The prices associated with these methods were obtained from civil plant hire companies, dredging companies, and a piling company in the greater Cape Town area (see Appendix A). Additional costs, such as legal fees and infrastructure costs, were applicable to both methods. All the rates obtained for the respective machinery were received as "wet" rates, meaning that the fuel was included in the hourly rate. It should be noted that these hourly rates will fluctuate as they are subject to the change in fuel prices. However, the prices received were not altered during the duration of this research project to avoid intricacy.

The gathered prices and properties for all the applicable methods were entered in a costs model to calculate the '*cost per m^3 sediment removal*' of each zone (where sediment was determined suitable to be utilised for road materials and fine aggregates).

Figure 3.21 illustrates the Excel template used for calculating the removal costs per m^3 of the sediment reserve for the respective methods. The blue cells indicate where values should be added. In the top cells, the machinery type to be used to remove sediment, the respective zone from which the sediment is under investigation and the calculated volume of sediment in this zone must be inserted. In addition, the template requires the percentage of sediment to be removed, the number of units, costs per day for the machinery, the rate of sediment removal and establishment, infrastructure, labour and establishment costs to be manually inserted.

After all the latter values are inserted, the '*number of days required to remove sediment' is calculated* (see Equation 14) based on the '*volume of sediment to be mined'*. '*The total cost of sediment removal'* is then calculated by multiplying the machinery costs per day with the '*number of days required to remove sediment*' (see Equation 15). The '*total project cost'* is calculated by

adding the *'total cost of sediment removal'*, *'establishment costs'*, *'maintenance'* (5% of the total cost of sediment removal), *'infrastructure'*, *'legal'*, *'labour costs'* and *'additional cost'* together (see Equation 16).

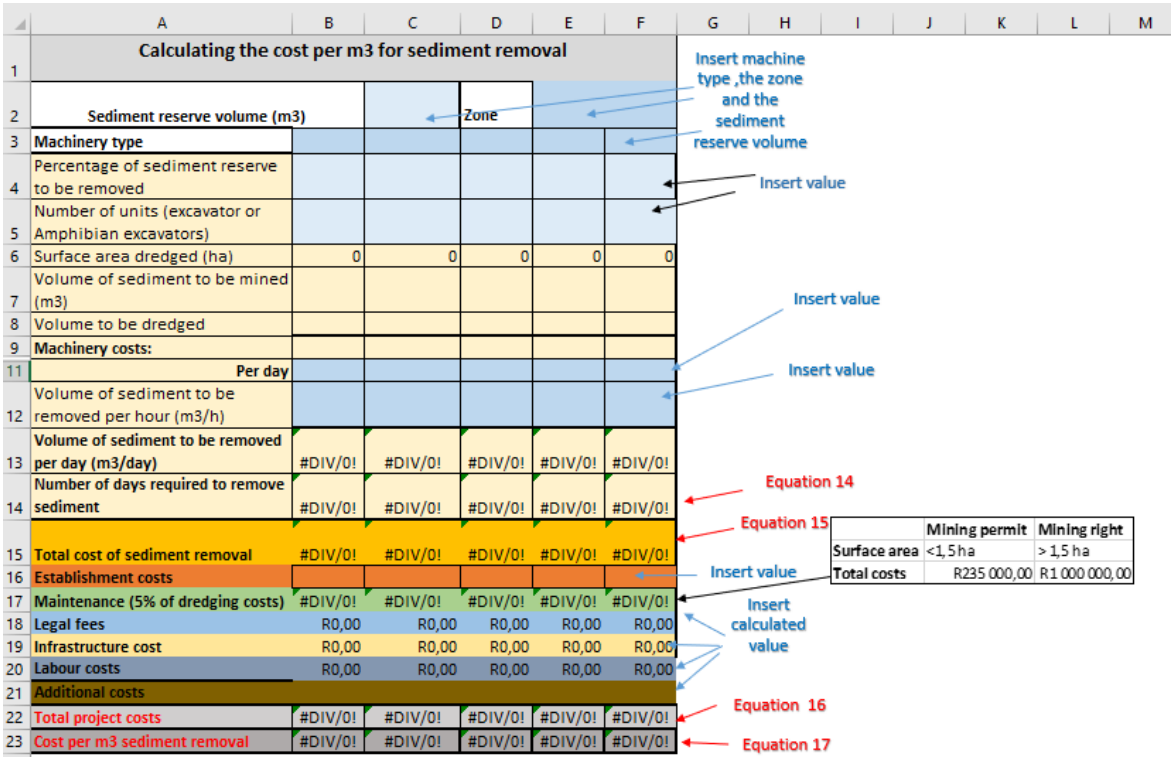

Figure 3.21 Template for calculating the cost per m³ of sediment removal.

$$Number\ of\ days\ required\ to\ remove\ sediment\ = \frac{Unit\ cost\ per\ day\ \mathbf{x}\ number\ of\ units}{Removal\ rate\ per\ day} \qquad \textit{Equation 14}$$

$$Total\ cost\ of\ sediment\ removal = (Unit\ cost\ per\ day \times Number\ of\ units \times Number\ operating\ days\ until\ sediment\ is\ removed) \qquad \textit{Equation 15}$$

$$Total\ project\ costs = Sediment\ excavation\ and\ transport\ costs + E\text{stablishment costs} + Additional\ costs + Legal\ costs + Maintenace + Infrastructure\ costs \qquad \textit{Equation 16}$$

$$Cost\ of\ m^3 sediment\ removal\ = \frac{Total\ cost\ related\ to\ sediment\ removal}{Total\ volume\ to\ be\ removed} \qquad \textit{Equation 17}$$

The infrastructure costs will include the sum of invoices received for portable toilets, screens, office containers and storage containers (see Appendix A). The legal fees depend on the size of the surface

area; mining permits are issued for surface areas smaller than 1.5 ha and will cost about R235 000 and mining rights are issued for surface areas larger than 1.5 ha and will cost about R1000 000. The '*additional costs'* refer to the extra fees related to a specified method of sediment removal. For dry excavation, the '*additional costs'* will include road construction and sheet piling to permit saturation of the dry surface. A*dditional costs related to* dredging of saturated sediment may include small dam construction for the water being pumped out with sediment as was dehydration treatment of sediment.

Subsequently, the '*cost of removal of 1m^3 sediment'* resource was estimated by dividing the '*total project costs related to sediment removal'* by the '*total volume of sediment be removed*' (see Equation 17).

For the removal costs to be feasible it should be equal or less than the selected reference cost, which was based on the average cost related to the average purchasing price of the construction material under investigation from nearby suppliers. The results generated in cost model in Figure 3.21 was used to plot the removal costs (per m^3) against the percentage of the sediment volume that is to be removed for each of specified number of sediment removal units selected (excavators or amphibian excavators). From these graphs, the range for which the sediment removal is to be feasible was derived by observing where the removal costs plots under the reference costs.

3.3.3 Cost model: Fine-grained material to be mined as raw material for lightweight aggregates

Where sediments can be used to manufacture lightweight aggregates (LWA), the '*manufacturing costs per kg* of *LWA'* will be calculated and compared to the selling price of alternative lightweight aggregates as well as conventional concrete aggregates.

To estimate the '*manufacturing costs per kg'*, the *'total project costs'* related to producing of the LWAs (legal fees, excavation, sintering, labour, infrastructure costs etc.) was divided by '*weight of the sediment to be excavated'* (see Equation 18). The '*weight of the sediment to be excavated'* was calculated by multiplying the '*volume of the sediment to be excavated'* with an '*average density value for lightweight aggregates'* (see Equation 19). It is important to note that the calculated '*weight of sediment to be excavated'* will be an approximate value since the volume of sediment will expand after being sintered.

$$Manufacturing\ costs\ per\ kg\ \text{of}\ LWA = \frac{Total\ project\ costs}{Weight\ of\ the\ sediment\ to\ be\ excavated\ (kg)}$$

Equation 18

$$Weight\ of\ the\ sediment\ to\ be\ excavated\ (\text{kg}) = Volume\ of\ the\ sediment\ to\ be\ excavated\ \text{x}\ The\ average\ density\ of\ lightweight\ aggregate$$

Equation 19

3.3.4 Cost model: Fine-grained material to be mined as raw material for bricks

In the case where sediment is suitable to be used in the manufacturing of clay bricks, the '*costs to manufacture one clay brick'* (fired or unfired) is compared to the average purchase costs of one brick. For the calculation of the '*costs to manufacture one clay brick',* the *total project costs* (legal fees, excavation, production, labour and firing costs) is divided by the *number of bricks to be manufactured* to calculate the costs per brick (see Equation 20). The '*total number of bricks to be manufactured*' in the previous equation is estimated by dividing the '*volume of sediment to be excavated* by the *volume of a single brick'* (see Equation 21).

$$Costs\ to\ manufacture\ one\ clay\ brick\ = \frac{Total\ project\ costs}{Number\ of\ bricks\ to\ be\ manufactured}$$

Equation 20

$$Number\ of\ bricks\ to\ manufactured\ = \frac{Volume\ of\ sediment\ to\ be\ excavated}{Volume\ of\ a\ single\ brick}$$

Equation 21

3.3.5 Cost model: Fine-grained material to be mined to produce landfill liners

In the case where sediment is to be used for landfill liners, the clay-rich material will not be mined to be sold as profit, but rather be used by the company with the mine permit/right to produce its own clay liners, since there is currently no market for compacted clay liner (CCL) materials. The cost related to mining and hailing 1 m^2 of CCL will be compared to the costs per 1 m^2 for geosynthetic clay liners (GCLs) within the Western Cape.

In Excel a template was created (see Figure 3.22) to calculate the '*total project costs*' of the mining of the sediment (see Equation 22), the '*costs per 1 m^3 sediment removal and transport*' (see Equation 23) and '*cost to cover 1 m^2 with CCL*' (see Equation 24). To calculate the '*cost to cover 1 m^2 with CCL*', the '*volume of material required to cover 1 m^2* 'was estimated by Equation 25. The '*volume of material required to cover 1 m^2*' needs to comply to the thickness of the respective landfill design for which the material is suitable, therefore the design thickness is used plus a 1/6th of the respective material to compensate for the thickness loss during compaction of the material.

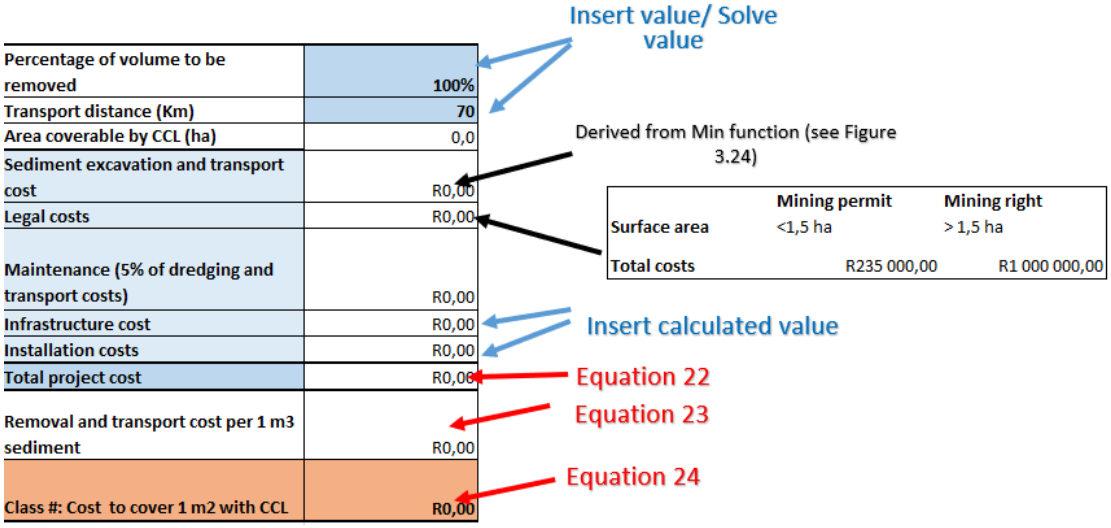

Figure 3.22 Excel template for calculating the cost to cover 1 m^2 area with CCL for a designed landfill

$$Total\ project\ costs\ (CCL) = Legal\ costs\ +\ Sediment\ excavation\ and\ transport\ costs + Maintenace + Infrastructure\ costs + CCL\ installation\ costs$$

Equation 22

$$Removal\ and\ transport\ Costs\ per\ 1m^3\ sediment = \frac{Total\ project\ costs}{Total\ sediment\ volume\ x\ percentage\ sediment\ to\ be\ removed}$$

Equation 23

$$Cost\ to\ cover\ 1\ m^2\ with\ CCL = Volume\ of\ material\ required\ to\ cover\ 1m^2\ x\ Costs\ per\ 1m^3\ sediment\ removal\ and\ transport$$

Equation 24

$$Volume\ of\ material\ required\ to\ cover\ 1m^2 = (Required\ landfill\ type\ thickness + Additional\ material\ for\ compaction\ compensation)\ x\ 1m^2$$

Equation 25

The '*sediment excavation and transport cost*' related to using sediment for landfill liners will differ based on the travel distance from the reservoir to the areas where the CCLs are to be installed. As distance for the sediment transportation varies from the reservoir, the number of trucks required to achieve the most economically viable '*total project costs*' will also differ. Therefore, different scenarios were created to represent the different numbers of trucks used to transport and deposit sediment. In addition, the feasibility of removing sediment depends on the proportion of the total sediment volume that is to be removed, since it influences the number of days required to remove the sediment. The number of days to remove and transport sediment plays a significant role since the machines and labour are paid per day. However, a shorter duration of excavation and transport of sediment does not necessarily mean the project cost will be more economical because to achieve a shorter period of excavation and transport of sediment, more machinery is required to work per day which means higher fees per day. Therefore, the aim of the feasibility model was to use variation in the number of trucks, travelling distances and proportion of sediment volume to be mined to indicate which will be the most feasible option in comparison with GCL.

When adding a value in the '*transport distance*' cell in the Excel template (see Figure 3.22), Excel will calculate the '*total sediment excavation and transport costs*' for the use of one, two and three trucks based on the number of cycles that can be completed in one day (see Figure 3.23). Each cycle

consists out of the duration it takes for the truck to be loaded by an excavator, the time the truck takes to transport the sediment to the site where CCLs are to be installed, the depositing time of the sediment and the travel time to return to the excavator. The average speed at which the travel time was calculated was 50 km/hour (see Table 3.8) for parameters used in the Excel template. After the '*transport distance'* cell value was entered, the '*total travel time'* is calculated (see Equation 26) for each truck. The '*travel time'* is then added to *'time finished loading'* and '*depositing time'* (15 mins) to calculate '*time truck takes to complete cycle'* (see Equation 27). The '*time truck takes to be loaded with excavator*' was calculated as 19 mins by dividing the 16 m^3 capacity of the truck into the sediment removal rate of the excavator 50m^3/h (see Table 3.8).

The calculations for the "*time finished loading*" for the subsequent cycles depend on the number of trucks being used to transport sediment. If only one truck is being used, the truck can be reloaded immediately, but if more than one truck is being used it is possible that the returning truck is not able to be loaded since the excavator is occupied with another truck.

Therefore, an IF function was coded into the Excel template to calculate the "*time finished loading"* for the cycles succeeding "cycle 1". If the '*time truck takes to complete cycle'* is longer than '*time finished loading'* of the last truck at the excavator, the '*time finished loading'* for the truck that completed the cycle will be calculated by adding the time a truck takes to be loaded by the excavator to the '*time truck takes to complete cycle'*. However, if the '*time truck takes to complete cycle'* occurs before '*time finished loading'* of the previous tipper truck at the excavator is completed, the '*time finished loading'* for the truck is calculated by adding the time a truck takes to be loaded by the excavator to the '*time finished loading'* of the previous truck.

This process is repeated until '*time truck takes to complete cycle'* exceeds 540 minutes (9 hours). The cells containing values exceeding 540 minutes will be assigned a "Completed" value and will turn red, whereas the cells below or equal to 540 will be assigned an "Incomplete" value and will stay white. In the cells assigned to '*total cycles completed per day,'* a COUNTIF function is encoded to count the total "Incomplete" values for each scenario.

From the '*total cycles completed per day'* cells, the '*total volume of sediment deposited per day*' is calculated (based on the premise that each truck will transport 16m^3, see Equation 28). The '*days required for removal of sediment'* is estimated by dividing the volume of the sediment to be mined by the '*total volume of sediment deposited per day'* (see Equation 29).

The 'sediment excavation and transport costs per day' were calculated by adding the 'truck rate per day' multiplied by the 'number of trucks' to the 'excavator rate per day' and to the personnel rate per day (see Equation 30). Lastly, the 'total sediment excavation and transport costs' for each scenario are calculated by multiplying the 'sediment excavation and transport costs per day' with the 'days required for removal of sediment' (see Equation 31). The minimum '*total excavation and transport cost'* value from the different scenarios is then taken to represent the 'excavation and transport cost' value when calculating '*the total project cost'* for the inserted distance.

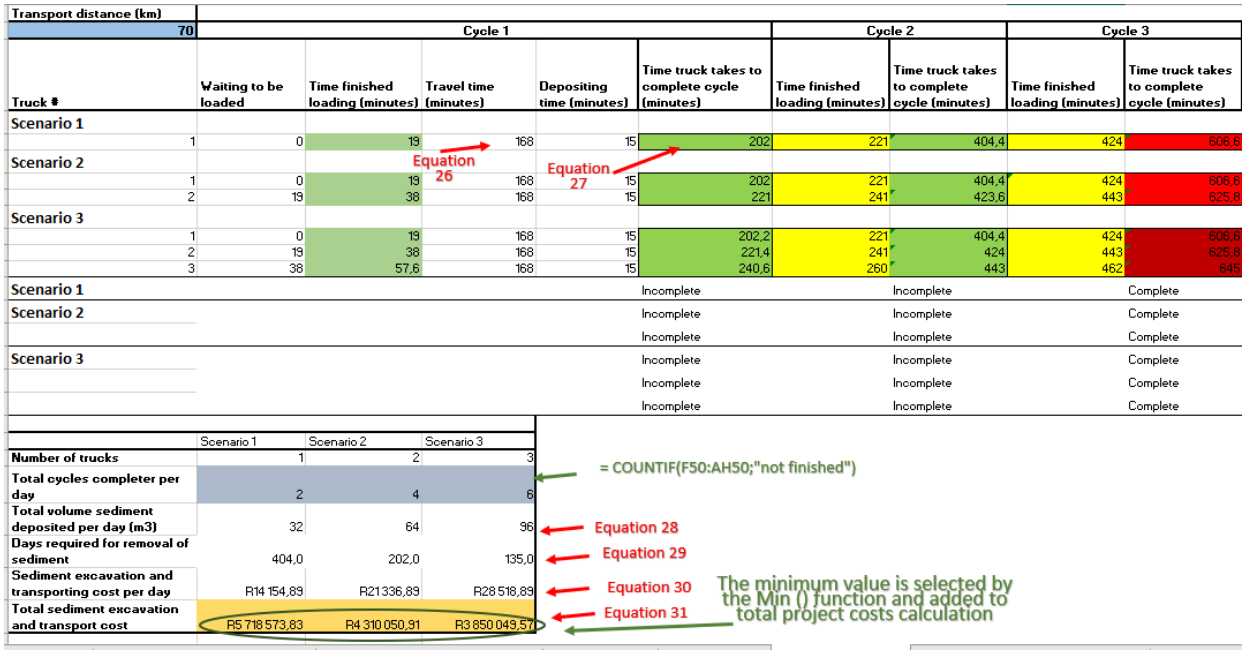

Figure 3.23 Estimating the total excavation and transport cost for each scenario by adding the total trips per day manually.

$$Travel\ time\ per\ truck\ = \frac{Distance\ travelled\ by\ truck}{Average\ speed\ of\ truck} x60$$ *Equation 26*

$$Time\ truck\ takes\ to\ complete\ cycle = Time\ finished\ loading\ + time\ travelled\ + depositing\ time$$ *Equation 27*

$$Total\ volume\ sediment\ deposited\ per\ day = Total\ cycles\ finished\ per\ day\ x\ tipper\ truck\ capacity$$ *Equation 28*

$$Days\ required\ for\ removal\ of\ sediment = \frac{Volume\ of\ sediment\ reserve\ x\ percentage\ to\ be\ mined}{Total\ volume\ sediment\ deposited\ per\ day}$$

Equation 29

$$Sediment\ excavation\ and\ transport\ cost\ per\ day = Tipper\ truck\ rate\ per\ day\ x\ number\ of\ trucks + Excavator\ rate\ per\ day + Personnel\ rate\ per\ day$$

Equation 30

$$Total\ sediment\ excavation\ and\ transport\ cost = Sediment\ excavation\ and\ transport\ cost\ per\ day\ x\ Days\ required\ for\ removal\ of\ sediment$$

Equation 31

Table 3.8 Parameters used during the design of the costs models.

Parameters	
Average travel time of tipper truck (**km/h**)	50
Rate of removal with hydraulic Excavator, 0.5m^3 bucket, Sand/Soil (**m3/hour**)-Metvin (2012)	50
Rate of sediment removal with Bell 200 pump (**m3/hour**)- Bovu Pumps (2008)	250
Tipper truck carrying capacity (**m^3**)	16
Time truck takes to be loaded with the excavator (**minutes**)	19

From Appendix A the legal costs (dependent if permit or mining right is required) and the infrastructure costs (the type of infrastructure required based on reservoir size and construction material type to be mined) were derived.

For the project to remain feasible the calculated cost per m^2 must not exceed a reference value which was selected based on the average price for GCL liners in the Western Cape. The Excel Solver

function was used within the cost model to determine the minimum proportion of the sediment reserve that can be removed for the project to be feasible over 5km, 10 km, 20 km, 50 km and 100 km for Class B and Class C landfills respectively (Figure 3.24). In addition, the Solver function was used to calculate the maximum transport distances for each truck for which the project will remain feasible for each landfill type

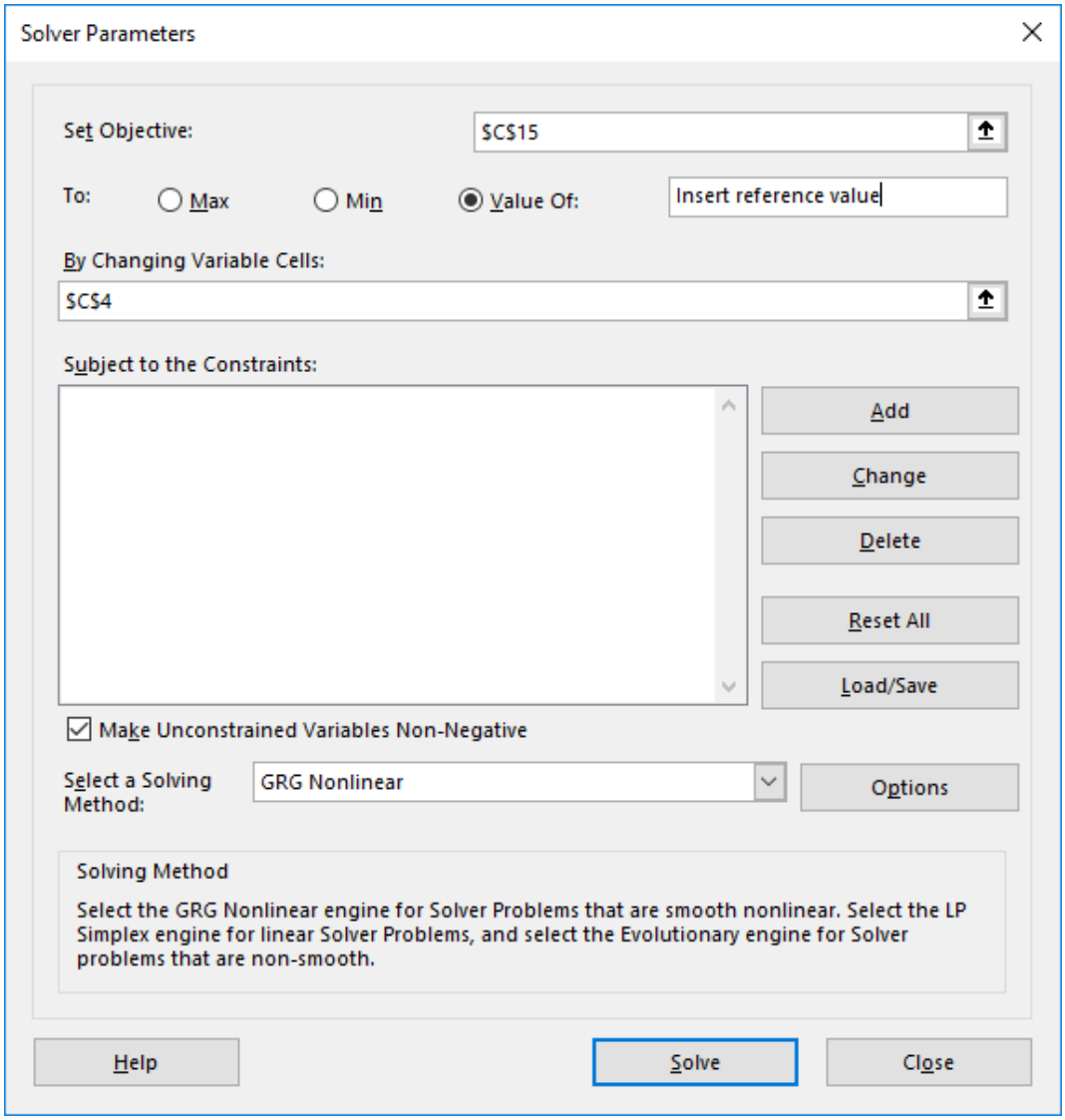

Figure 3.24 Excel Solver function used to determine the variables that will result in the cost per m² to be the same as the reference value.

Chapter 4 : Results

This chapter presents the results obtained during field investigation on the exposed surfaces of the Theewaterskloof, Greater Brandvlei and Waterzicht Dams together with the laboratory test results on sediment samples from these dams. The results of the field investigations are subdivided into three sections consisting of the field data of each zone which include sedimentary maps, soil profiles of dam surfaces and DCP results. The test pit profiles and DCP numbers against depth graphs are located in Appendix B and C respectively.

The laboratory analyses were divided into the soil classification of sampled material, the test results for coarse-grained materials for road materials and as fine aggregate and the test results for fine-grained material for lightweight aggregates, clay bricks and clay liners.

Using the field data, together with the sediment types (classified according to the Unified Soil Classification System, USCS) from laboratory analyses, the volume of the respective sediment type was determined at each mapped zone. Based on the laboratory results, cost models were designed in Microsoft Excel to determine the feasibility regarding the mining of sediment. The costs per m^3 were calculated in these models and were related to the purchasing price or installation price of the respective construction material per specified unit to estimate if the sediment is feasible to mine.

4.1 Field investigation

4.1.1 Theewaterskloof Dam

Ten zones were mapped during the field investigation and were further subdivided into subzones based on terrain and sediment occurrence (see Figure 4.1). The data collected during field analyses of each zone is explained in detail in the succeeding subsections. The dominant sediment type occurring throughout the investigated areas of the Theewaterskloof Dam was described as slightly moist, dark brown to yellowish-brown, loose, intact, medium-grained sand (0.4-0.6mm sized grains) of alluvial origin. The medium-grained sand was mainly observed to have deposited in a tapering pattern, with the sediment thickness gradually decreasing from dam bank to shoreline.

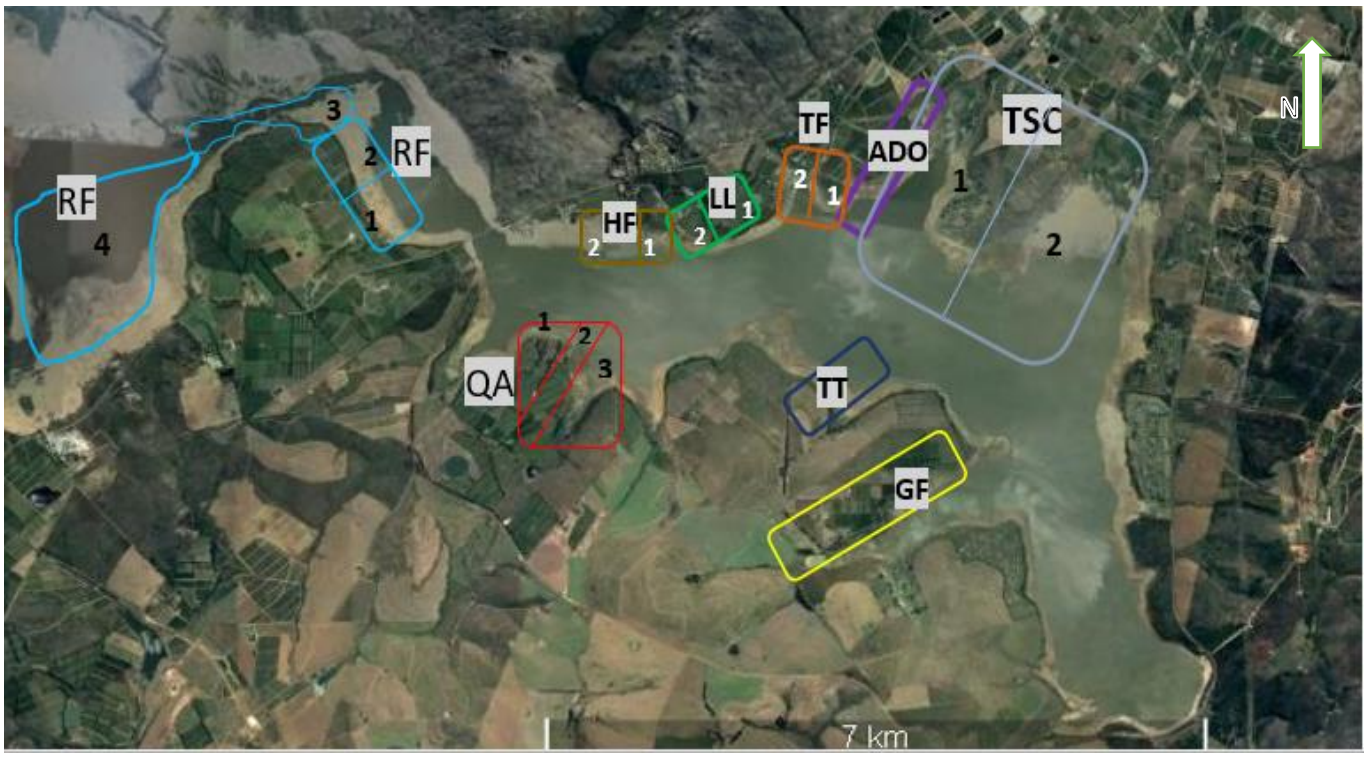

Figure 4.1 Map of the Theewaterskloof Dam indicating the main zones (letter codes and colour borders) and respective subzones (indicated by the number in each zone) under investigation.

4.1.1.1 Zone RF

Zone RF was subdivided into four subzones namely, RF1, RF2, RF3 and RF4. The soil and geology types of the exposed areas were identified through fieldwork and are illustrated in Figure 4.2. Subzone RF3 was discarded for research since sediment is mainly absent in this area with sandstone dominating the exposed parts in this subzone.

The distance from the water's edge (shoreline) to the high-water mark (dam bank) for the exposed areas of subzone RF1 and RF2 ranges from 300m to 500m and 450m to 650m for subzone RF4. From Google Earth, the total areas were derived for subzones RF1 and RF2 as 623,066m^2 and for subzone RF4 as 419,486m^2. GPS measurements calculated a moderate slope gradient of 5.5% for subzones RF1 and RF2 while subzone RF4 remain flat.

The sediment layer exposed within the subzones RF1, RF2 and RF4 consists out of a slightly moist, dark brown, loose, intact, medium-grained sand of alluvial origin. This sediment surface extends from the reservoir shoreline to between 200m and 350m upslope where the bedrock, varying between sandstone, shale and conglomerate appears on the surface. Most of this bedrock is covered with coarse gravel (10mm in diameter) with aeolian dunes and sandstone boulders (up to 2m) also present.

Minor amounts of pebbles and organic material are present on the exposed surface at subzone RF1. However, an abrupt increase in pebbles and organic matter, mainly tree stumps, was observed on the sediment surface of subzone RF2. In addition, traces of parallel planted tree lines were observed as low tree trunks emerging just above the surface at the border between subzones RF1 and RF2.

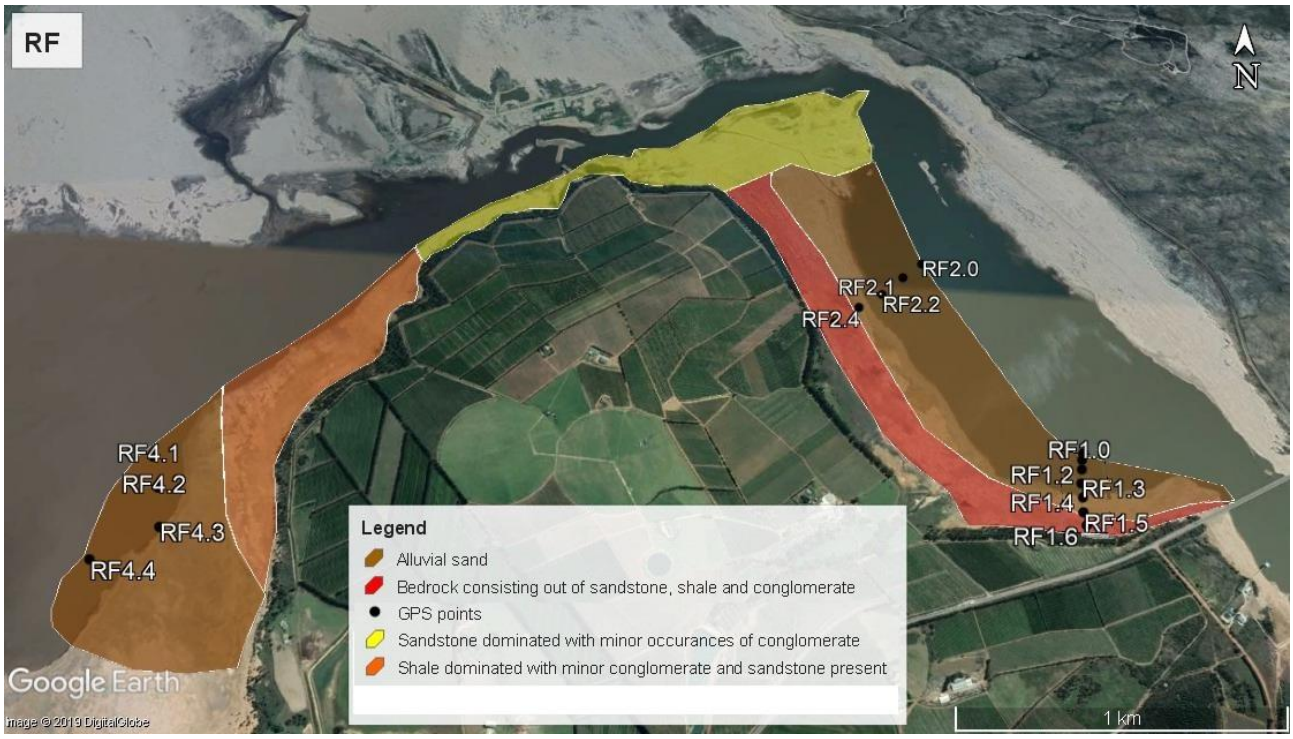

Figure 4.2 Map of the geology and soil types of zone RF

Soil profiles were constructed using data from test pits, DCP analyses and GPS measurements for samples RF1.1 to RF1.4 (see Figure 4.3) and RF2.1 and RF2.2 (see Figure 4.4). Hole RF1.1 was dug about 27m from the dam shore, with slightly brown sand present to 0.5 m where the water table was reached, which made it difficult to measure the depth of the sediment. However, the depth of the sediment layer to bedrock was observed at 0.5m, 0.3m and 1.4m at RF1.2, RF1.3 and RF1.4 respectively. The distance from the dam shoreline (point RF1.0) to the dam bank (RF1.6) was measured as 264m and the elevation increase over this distance was about 14.5m. Samples were taken for laboratory analyses for construction materials at this subzone due to the thickness of the sediment layers.

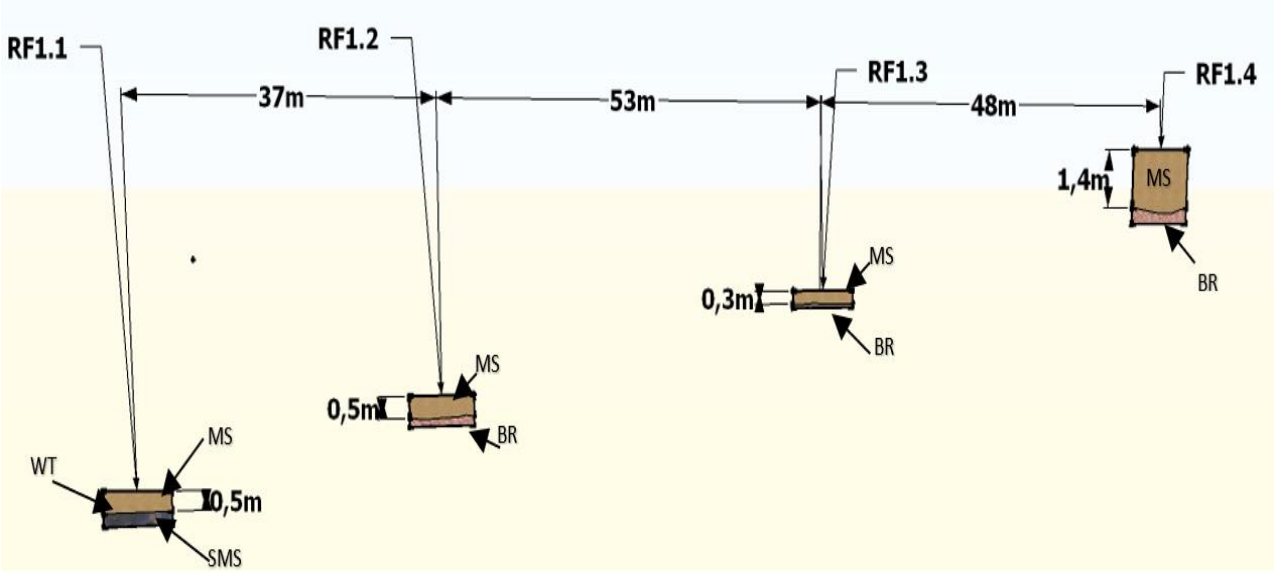

Figure 4.3 Soil profile along points RF1.1 to RF1.4. Annotations: Ms-Medium-grained sand, SMS-saturated medium-grained sand, BR-bedrock, WT- Water table.

At subzone RF2, two test holes were dug at GPS points RF2.1 and RF2.2 respectively. Point RF2.1 consisted of dark brown medium-grained sand present up to 0.5 m when pebble-rich bedrock was reached. RF2.2 consisted of the same medium-grained sand with the colour changing from dark brown to light brown at 0.25m. With the DCP rod, the hard stratum was reached at a depth of 1.25 m. These two test holes corresponded roughly to test holes RF1.2 and RF1.4. Samples were taken at GPS points RF1.1 and RF1.3 for laboratory analysis.

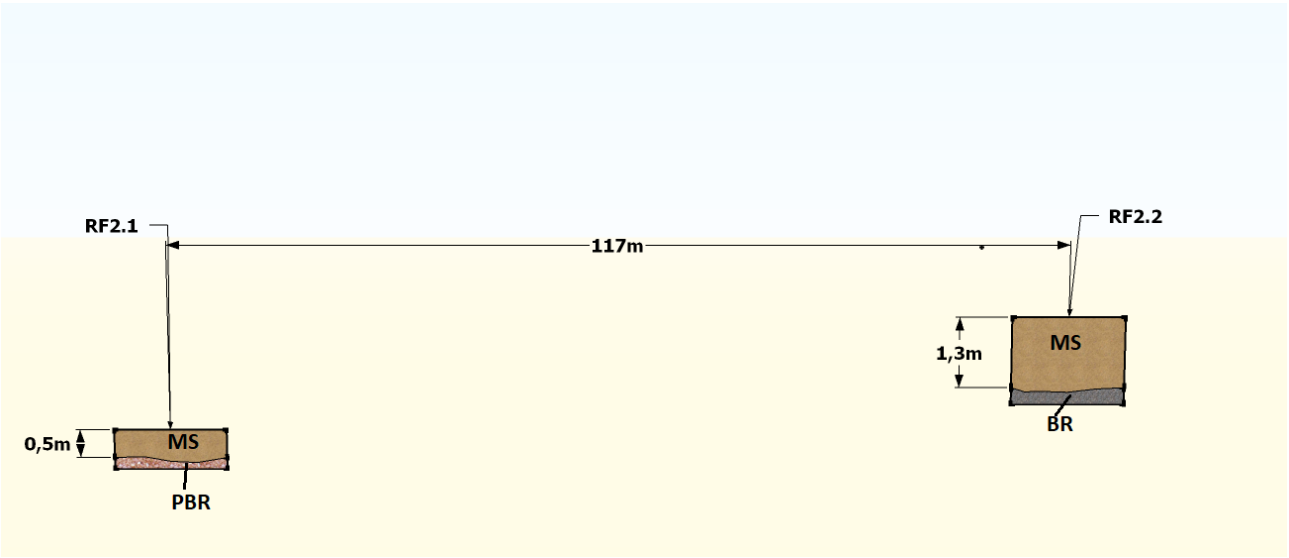

Figure 4.4 Soil profile along points RF2.1 and RF2.2. Annotations: Ms-Medium-grained sand, BR- bedrock, PBR- pebble rich bedrock.

Figure 4.5 indicates the *in situ* CBR results derived from the DCP for subzones RF1 and RF2. The results for RF1.1 display a low *in situ* CBR value of 1% from the surface to 0.7m depth, from where it increases to 10% at 0.82m depth. This abrupt increase is attributed to a denser underlying layer.

CBR results for RF1.2, RF2.2 and RF2.3 indicated an *in situ* CBR value varying between 1.5% and 2.5% to a depth of 0.4 to 0.6m, from where the CBR value gradually increased to about 40% at 1 m depth. The gradual increase in CBR values with depth indicates a homogenous sediment layer. However, the CBR results for RF1.3 and RF1.5 abruptly increased from about 8% at 0.1m to 0.3m to 70% or more at about at 0.3 m depth, which was maximum penetration depth. These high *in situ* CBR values for RF1.3 and RF1.5 were obtained due to the shallow bedrock.

The low CBR values of 1 to 10% for most of the GPS points suggest that if dry excavation is commenced, heavy machinery should not travel over the sediment surface. It is recommended that sediment excavation is initiated at the top of the slope where the bedrock is shallow, thereby exposing bedrock which will serve as a more stable foundation for the heavy equipment. If the sediment downslope must be accessed first, treatment of the sediment surface by compaction or covering it with a subbase material will be required to create a path for heavy vehicles.

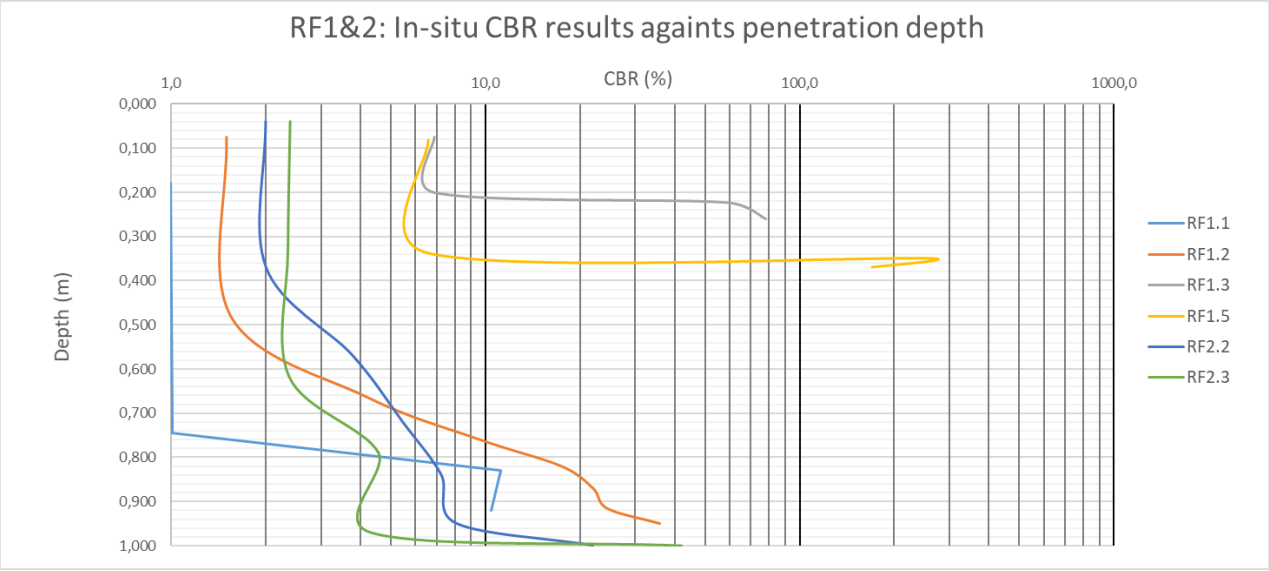

Figure 4.5 In situ CBR results for subzones RF1 and RF2.

Subzone RF3 consisted of steep slopes of mainly massive sandstone exposures, with a minor occurrence of conglomerates. For study purposes, exposed sediment in this subgroup is present in insignificant amounts. The geology and soil types of subzone RF4 are present in Figure 4.2 The

distance from the shoreline to the dam bank of the exposed surface range between 240 m and 650 m.

The dominant bedrock type in subzone RF4 was a reddish shale with weathered sandstones and conglomerates in the northern parts of this zone. This shale-dominated bedrock is covered sparsely with pebbles on the northern side of the exposure. The southern part of the mapped surface was flat and dominated by dark medium-grained sand. Minor amounts of pebbles and tree branches covered the surface.

Four test holes were excavated together with four DCP analyses and GPS measurements. The test hole at point RF4.1 consisted of medium-grained sand with the colour changing from dark brown to brownish-yellow sand at 0.4m. With the DCP, the sand was determined to be relatively loose until a stiffer stratum was reached at 0.95 m. Hole RF 4.2 exposed brown medium-grained sand to a depth of 0.5m, where the stiffer stratum was exposed as a slightly moist, grey, very stiff, mottled with red strips residual soil (weathered bedrock). The residual soil is possibly the remnant of weathered bedrock material.

At hole RF4.3 the sand layer decreased in thickness to 0.15m covering the very stiff mottled residual soil. Figure 4.6 illustrates the thinning of the medium-grained sand layer from GPS point RF4.1 to GPS point RF4.3. The decrease in sediment thickness corresponds to the increase in distance from the dam shoreline. In hole RF4.4, which was closer to the dam shoreline, the sand colour varied between dark brown and light brown throughout the hole. From the DCP testing, the sediment layer was found to be about 0.7 m deep until a stiffer stratum was reached (weathered bedrock).

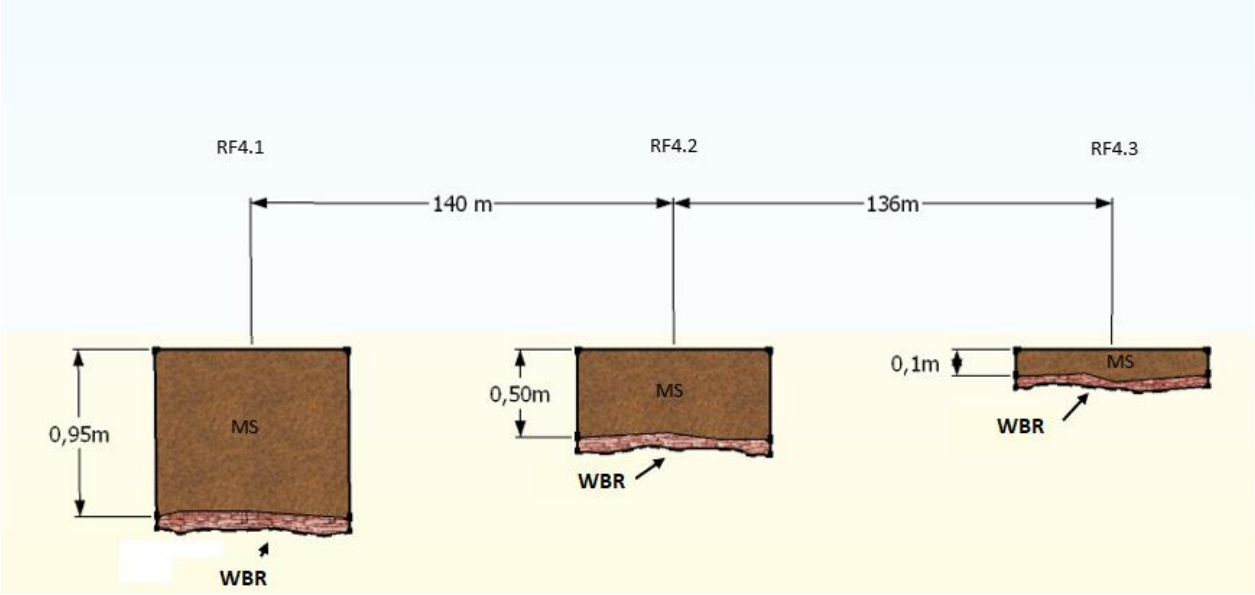

Figure 4.6 The soil profiles for GPS points RF4.1, RF4.2 and RF4.3. Abbreviations: MS-medium-grained sand, WBR-weathered bedrock

Figure 4.7 indicates the *in situ* CBR results over depth for the four soil profiles investigated at subgroup RF4. The *in situ* CBR results for point RF4.1 stayed below 10% to a depth of 0.87m was the CBR value increased with increasing depth to 22% at 1 m. The *in situ* CBR results for points RF4.2 and RF4.4 indicated similar patterns with constant low CBR values of about 5% up to a depth of about 0.7 m. From 0.7m to 1 m depth, these CBR values ranged between 10 and 30 %. RF4.4 experienced a sharp drop to 10 % at 0.84 m followed by a sharp increase to about 30%. This drop may be contributed to heterogeneities in the weathered bedrock.

Point RF4.3 experienced a rapid increase in CBR values at 0.3m depth and reached maximum penetration depth at 0.3m at CBR values of 25%. These *in situ* CBR patterns for the four points indicate an increase in CBR values along the increasing distance from the dam shoreline. The low CBR values at point RF4.1 were caused by the higher moisture content at this point, whereas the shallow residual soil beneath sediment layer at RF4.4 was directly responsible for the rapid increase in CBR values with depth.

The low CBR values of 1 to 10% for most of the samples to depths to 0.7 m suggest the treatment of the sediment surface by compaction or the addition of a subbase material is required for creating a pathway for heavy vehicles if dry excavation is used.

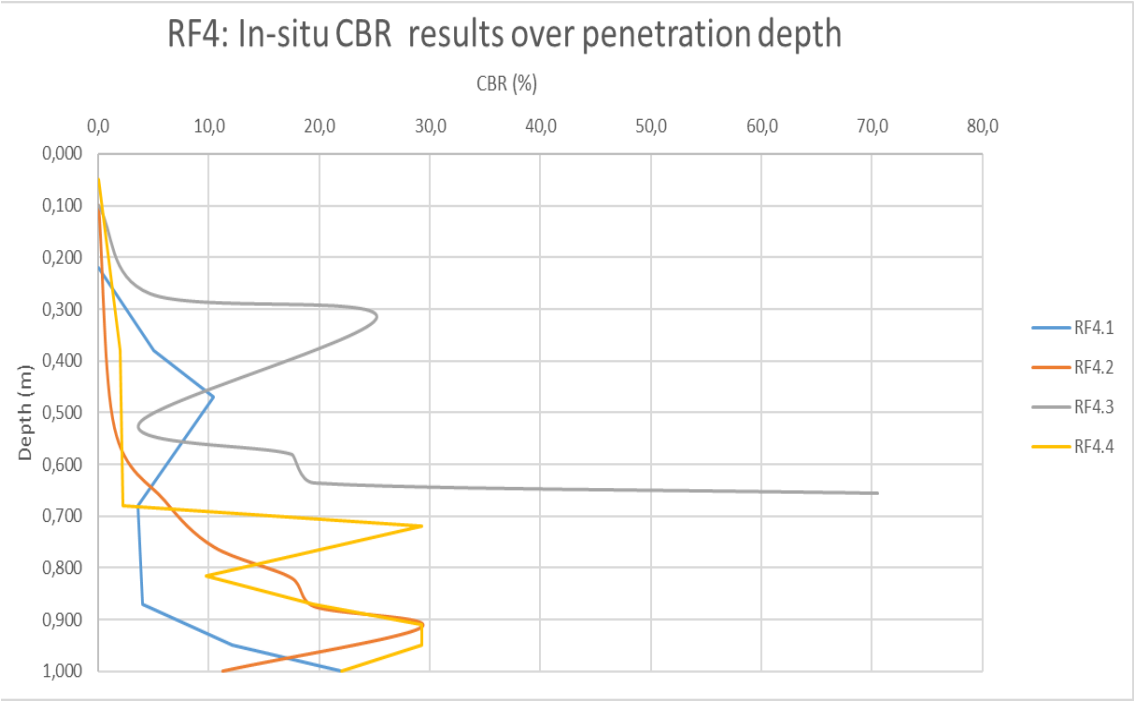

Figure 4.7 CBR against penetration depth for subzone RF4.

4.1.1.2 Zone QA

The geology and soil type of zone QA are illustrated in Figure 4.8. The exposed dam surface at zone QA consisted mainly of slopes coated with reddish gravel. The slopes were dominated by greyish shales, with sediment deposits only occurring in subzone QA2, which was observed as a flat surface between two steeper slopes (QA1 and QA3) facing each other, representing a small valley. Subzone QA2 was characterized by a light brown surface, the appearance of mud cracks, an increase in organic material, the presence of old vineyard remnants and the absence of the reddish-orange gravel observed on the slopes of QA1 and QA2 (see Figure 4.22 A). The exposed area of the silt surface was about 500 m in length. The area of the silt surface was calculated as 75,779 m^2 in Google Earth. Samples were taken for laboratory analyses for construction materials at this subzone due to the volume of the sediment layers observed in the field.

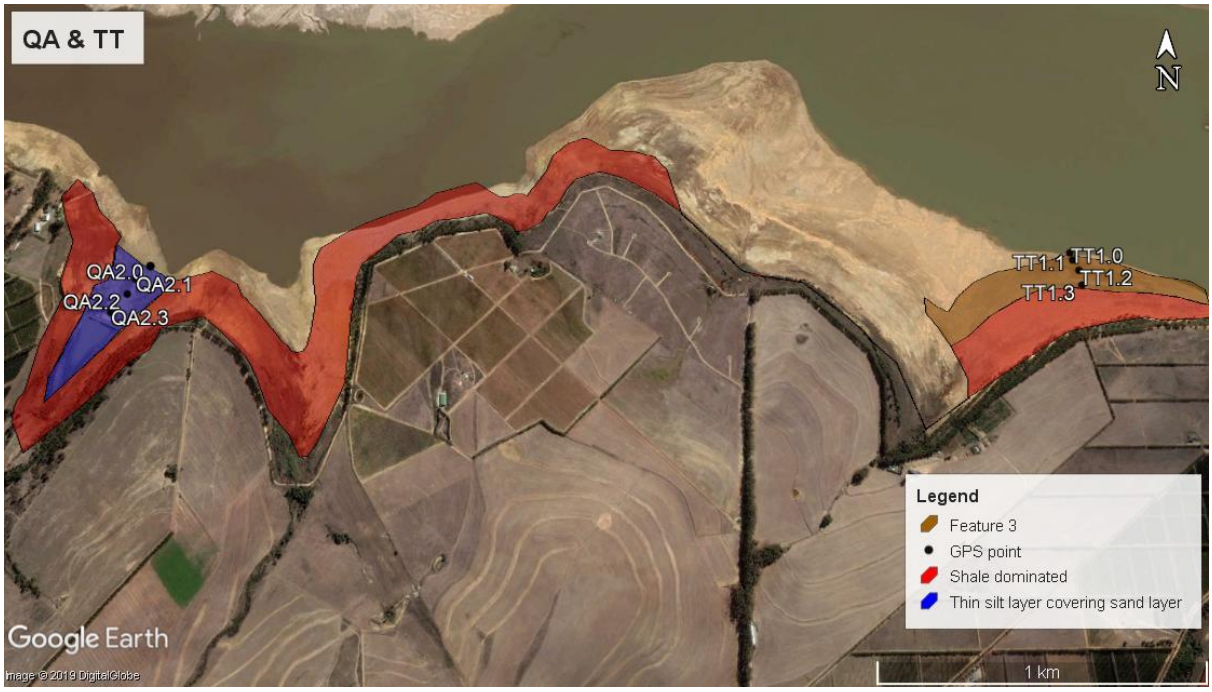

Figure 4.8 Map of the geology and soil types identified for zones QA, TT and GF.

Figure 4.9 illustrates the soil profiles of test holes QA2.1, QA2.2 and QA2.3. From the test holes, two sediment types were observed. In the top 0.10 to 0.16m of the soil profiles the sediment layer was described as slightly moist, light brown, firm, intact, silt (chalky feel on teeth) of alluvial origin. Underneath the silt layer, a dark brown medium-grained sand layer rich in organic matter was observed. With an auger drill, the water table was reached at depths of 0.6m, 1.2m and 1 m at GPS points QA2.1, QA2.2 and QA2.3 respectively. The saturated sand below the water table changed

colour from dark brown to light grey. The presence of a water table prohibited the measurement of the depth to bedrock.

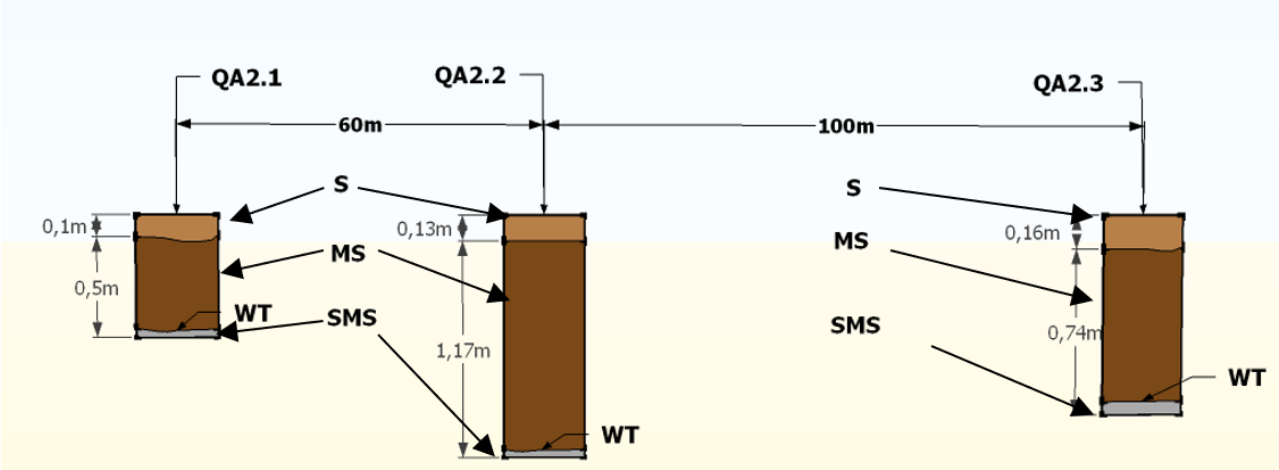

Figure 4.9 Soil profile of test holes QA2.1, QA2.2 and QA2.3. Abbreviations: S-Silt, MS-medium-grained sand, SMS- saturated medium-grained sand

The occurrence of silty material overlying the alluvial sand may be explained by a previous inflow of water followed by a dam level rise at the valley located in subzone QA2. Initially, the inflow caused the coarser sediment to deposit in the valley, and with subsequent dam levels, the shoreline transgressed causing the whole area of QA to be submerged by fine-grained sediments settling to the bottom of the valley, forming the thin silty layer. An alternative model for the thin silt layer covering sands might be explained by the presence of the remnants of vineyards in the area, suggesting humans have deposited the underlying sand for agricultural use before the construction of the Theewaterskloof Dam.

No DCP tests were conducted in this zone due to the DCP equipment not being available during the time of the field investigation of this zone. However, a weak bearing capacity in the silty surface was observed during the field investigation. Hence no heavy machinery would be able to move on this surface. Conventional earth moving machines will be required to excavate sediment from the shale-dominated bedrock adjacent to the silt and sand deposits.

4.1.1.3 Zone TT

The geology and soil type identified during fieldwork for zone TT is illustrated in Figure 4.8. At subzone TT1 the exposed surface was measured as about 268 m from the dam shoreline to the dam bank and consisted of a gentle slope. A flat occurring medium-grained sand was observed from the shoreline to about 115m towards the dam bank, where the surface steepens and change from being sediment dominated to bedrock dominated . The area of sediment surface was calculated in Google

Earth to be 105,182m^2. The sediment and bedrock surfaces are sparsely covered with a thin layer of gravel reddish-brown gravels occurring in layers parallel to the dam shoreline

At the test holes TT1.1, TT1.2 and TT1.3, the thickness of an alluvial light brown sand was measured as 0.45m, 0.15m and 0.2m respectively to rigid weathered bedrock. Aeolian sand dunes and trees were present 20m from the dam bank.

No soil profiles were designed due to appropriate GPS equipment being unavailable to determine elevations during this period of fieldwork. In addition, no DCP tests were conducted in this zone due to the DCP equipment not being available during the time of the field investigation of this zone.

At subzone TT2, the steep slopes were covered with layers of pebbles (10 to 120 mm in grain size), with shale and sandstone being exposed at upper parts of the slopes. This was not applicable for research investigation since no sediment was exposed

4.1.1.4 Zone GF

The exposed surface of zone GF was estimated as 320m from the shoreline to the dam bank and comprise of an area of 54,496m^2. The area consisted of a shallow dipping slope consisting of bedrock with alluvial medium-grained sand occurring parallel to the dam shoreline (Figure 4.10). The upper slope surface was dominated by vegetation and coarse gravel which was absent on the light brown alluvial sand surface. A thin silt (0.05m thick) layer covered the alluvial sand, with sporadic occurrences of shrinkage cracks.

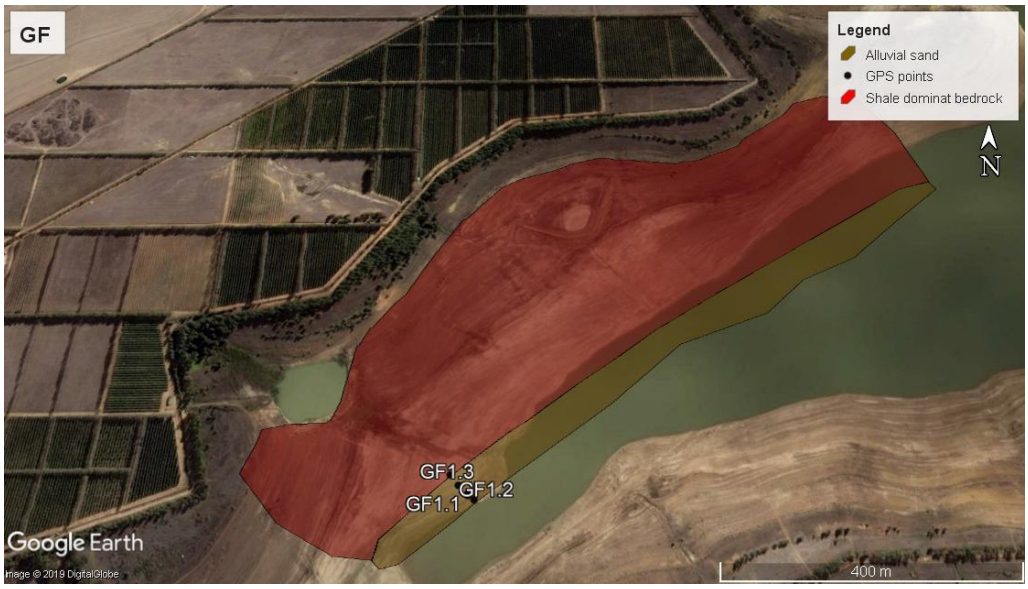

Figure 4.10 Map of the geology and soil types identified for zone GF.

At the three test holes, the sediment was described as light brown medium-grained sand. At hole GF1.1 the maximum measurable depth was estimated as 0.7m since the water table was pierced at this depth. At holes, GF1.2 and GF1.3, the thickness of the sediment layer to the stiff weathered bedrock ranged from 0.15 m to 0.25m respectively (see Figure 4.22 B). The thin layer of sediment occurring in this zone makes it unsuitable to test its engineering properties for the utilisation of construction materials.

Similar to zone TT, no soil profiles or DCP analyses were performed in this zone due to the unavailability of the appropriate GPS and DCP equipment during this period of fieldwork.

4.1.1.5 Zone TSC

The geology and soil type of the exposed reservoir surface at Zone TSC are illustrated in Figure 4.11. The surface of subzone TSC 1 was characterised by sandstone boulders (up to 0.8m in diameter) and bedrock and the remnants of foundations of houses. No applicable sediment deposits were observed for sampling in this subzone. GPS point TSC1.0 indicated the furthest point of the exposed surface.

At subzone TSC 2 the exposed area was flat with intact vineyard remnants visible throughout the area (see Figure 4.22 C). The length of the alluvial sand surface was measured to be about 1500m with and area of 1,612,925m^2 measured in Google Earth. This area was situated at the mouths of the Spreeudrifspruit and Elands Rivers. An old elevated road, located approximated 60m from the dam shoreline, runs parallel with the dam shoreline, through the flat area. Boulders occur sporadically on the dark brown surface of the exposed sand surface. A shallow slope gradient of 0.3% was calculated from GPS measurements.

Figure 3.11 represents a soil profile from GPS points TSC2.1 to TSC2.3, which was constructed from the test holes data, DCP results and GPS measurements. The aerial extent was mapped by means of in-field observations together with Google Earth imagery, however, only a few test holes were excavated due to inaccessibility due to the lack of roads on the low load-bearing sediment plain.The surface elevation from test hole TSC2.1 to TSC2.3 increase about 1 m. The alteration in surface elevation was analogous with the sediment thickness. Hole TSC2.1 was dug at the southern part of the crossing road. The hole was dug to a depth of 0.65 m where yellow weathered bedrock was reached. The hole exposed medium-grained sand that presented a colour change from dark brown to yellow-brown at depth 0.2 m.

Holes TSC2.2 and TSC2.3 were excavated north of the road. At hole TSC2.2, a dark medium-grained sand was observed to 0.3m, where a cobble rich bedrock was observed. At hole TSC2.3, dark brown medium-grained sand was observed to 0.5 m, where the colour changed to yellowish-brown sand and an increase in moisture content was experienced to a depth of 0.9 m. With the DCP rod, the stiffer strata were measured at 1.2 m. Samples were taken for laboratory analyses for construction materials at this subzone due to the sufficient volume of the sediment layers observed in the field.

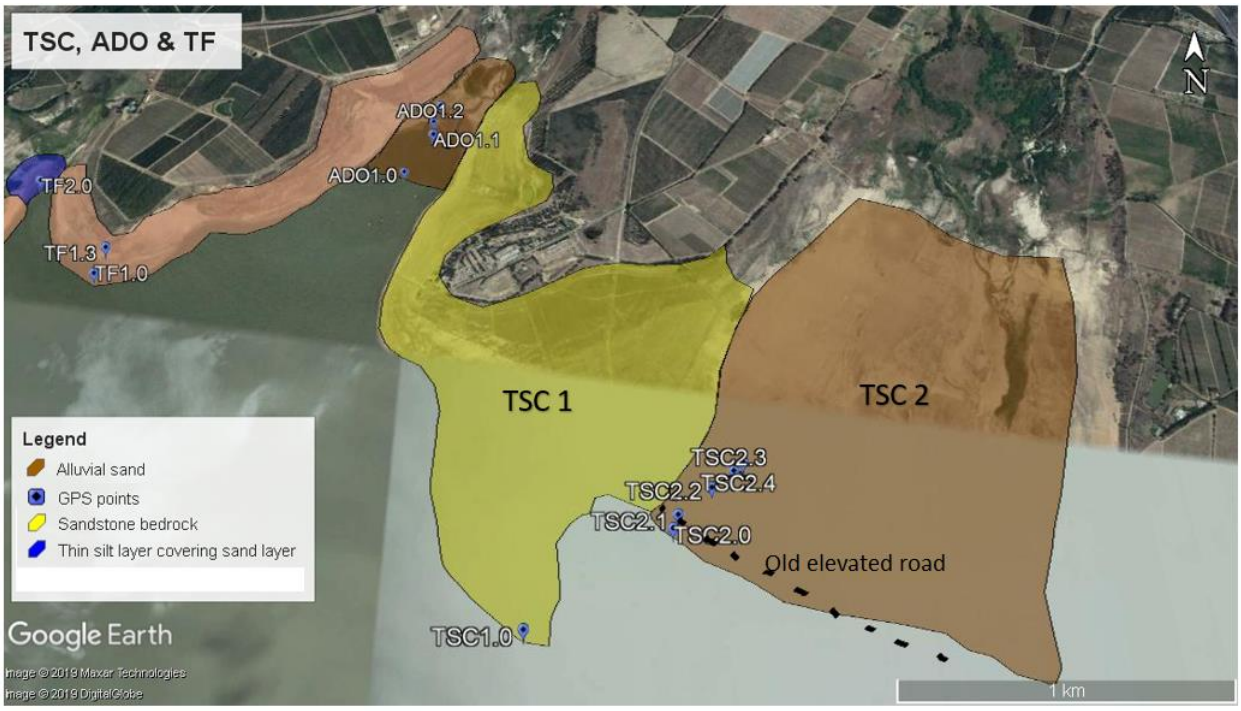

Figure 4.11 Map indicating soil type and geology for zones TSC, ADO and TF.

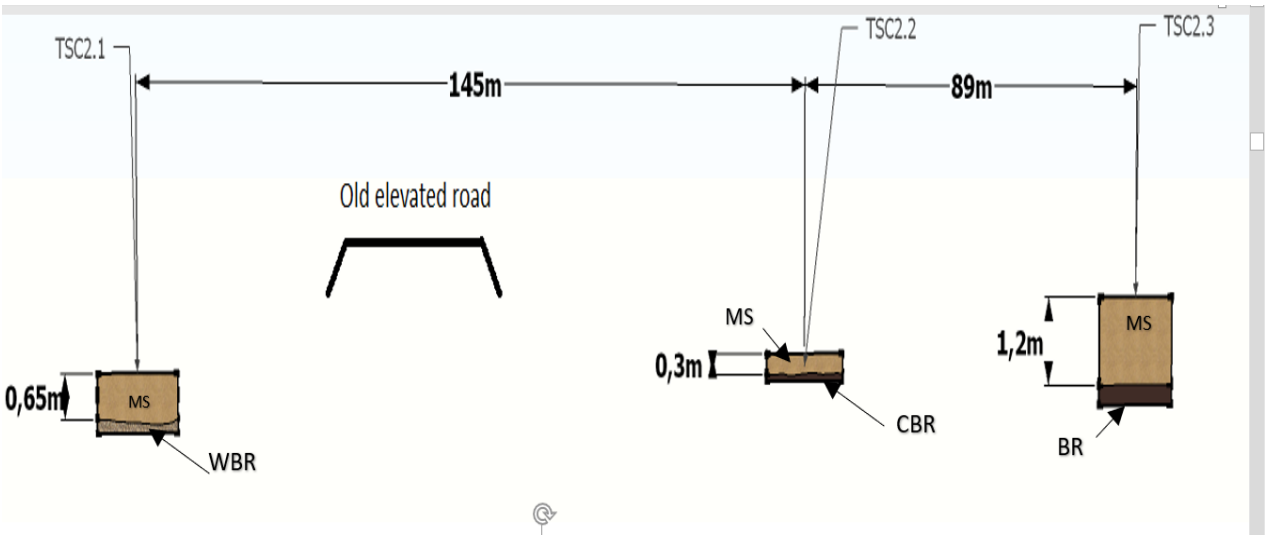

Figure 4.12 Soil profiles for GPS points TSC2.1 to TSC2.3. Abbreviations: MS-medium-grained sand, WBR-weathered bedrock, CBR-cobble rich bedrock, BR- bedrock.

Figure 4.13 indicates the *in situ* CBR analysis over depth for the four soil profiles ranging from TSC2.1 to TSC2.4. TSC 2.1 presented CBR values of 5 to 15% from 0.15 m to about 0.6 m deep. The maximum penetration depth was reached at 0.65m, where CBR values reach 300%. The CBR values at point TSC2.2 ranged from 2.5% to 9.1% from depths 0.1m to 0.48 m, with the maximum penetration depth reached at a 0.49m depth, where CBR values of 170% were recorded. The maximum penetration depths encountered at TSC2.1 and TSC2.2 is an indication of shallow bedrock at these two points.

At point TSC2.3, the CBR values increased from 2% at 0.4m to 29% at 0.65 m depth, from where it gradually decreased to 13% at 0.95m. The CBR values for TSC2.4 gradually increased from 3% at 0.32m to 20% at 0.87m. From 0.87m to 0.89m depth, CBR values rapidly increased from 20% to 300% where maximum penetration depth is reached.

The rapid increases in CBR values correspond to the depths of the bedrocks. If dry excavation is to be undertaken, only minor treatment will be required to the sediment surface if the operation starts where the bedrock (*in situ* CBR of 120%) is shallow. The shallow bedrock will be easily exposed through excavation at points TSC2.1 and TSC2.2 which will allow heavy machinery to move sufficiently on the exposed bedrock. Otherwise, compaction and the addition of a subbase will be required to accommodate heavy machinery on the sediment surface.

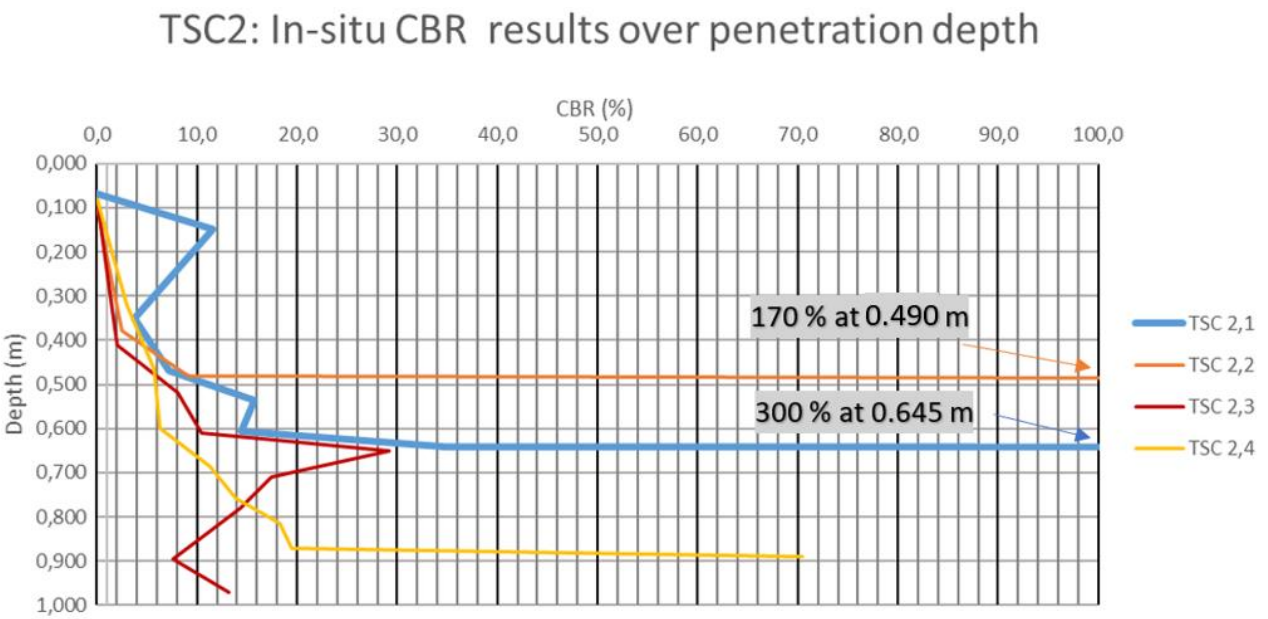

Figure 4.13 In situ CBR analysis over the depth for subzone TSC 2.

4.1.1.6 Zone ADO

The surface of zone ADO was dominated with dark brown medium-grained sand, with the length of the mapped exposure measured at about 600m and consists of sediment covering an area of 158,652m^2 (see Figure 4.11). The exposed sand surface was relatively flat, with scrubland increasing inland. This zone was situated at the mouth of a tributary. A shallow stream was observed flowing into the Theewaterskloof Dam. A shallow slope gradient of 0.3% was calculated from GPS measurements.

Three auger holes were drilled at the point ADO1.1, ADO1.2 and ADO1.3. No bedrock was found. The water table was observed at 0.4m, 1.4 m and 1.55m respectively (see Figure 4.14). The DCP rod was extended into an auger hole to determine the depth of bedrock. Bedrock was absent with the depth of loose material exceeding 1.5 m at each auger hole. The elevation increased about 0.9m from ADO1.1 to ADO1.3. Samples were taken for laboratory analyses for construction materials at this subzone due to the ample volume of the sediment layers observed in the field.

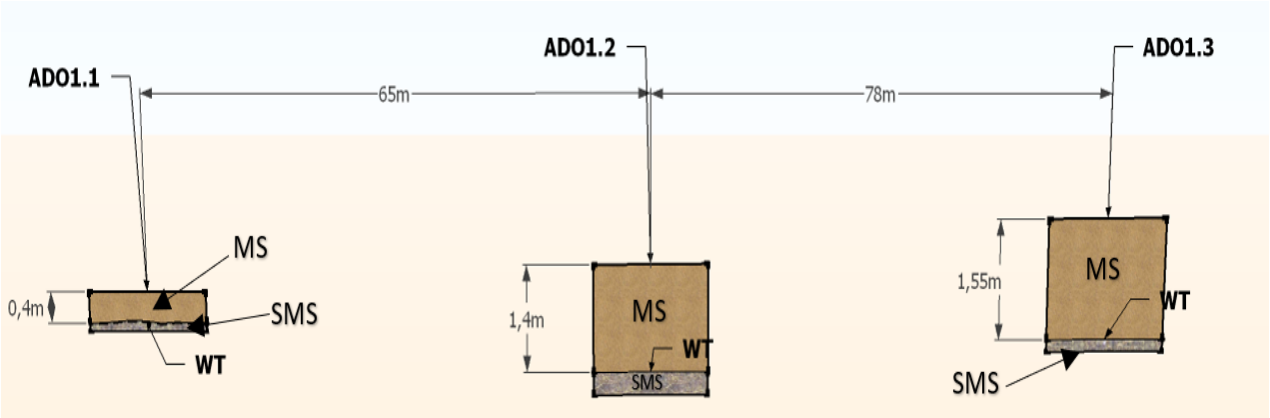

Figure 4.14 Soil profile for GPS points ADO1.1 to ADO1.3. Abbreviations: MS-medium-grained sand, SMS-saturated medium-grained sand.

In situ DCP results at GPS points ADO1.1 and ADO1.3 showed relatively low *in situ* CBR values of around 2% up to a depth of 1m, except for ADO1.1 experiencing a rapid increase to 6% from 0.9 to 1m (see Figure 3.13). This rapid increase of the *in situ* CBR values at point ADO1.1 can be contributed to a more competent sediment layer. The CBR value increase is still too low at 1 m to suggest a transition into bedrock. The overall low *in situ* CBR values obtained at ADO1.1 and ADO1.3 may be due to the sediment being deposited at the tributary mouth. The frequent turbulence due to constant inflow into the reservoir through this zone disturbs the sands and deny them to densify through self-weight causing the sediments to be loose and thereby obtaining low *in situ* CBR values.

The significantly low values *in situ* CBR and the deep bedrock observed at ADO1.1 indicated that dry excavation of this area will be very challenging. Extensive treatment of the soil surface together with adding a subbase is required to improve the stability of these soils to accommodate heavy machinery if dry excavation is undertaken. However, remnants of roads exposed by the droughts in this area can be used for limited access for heavy machinery.

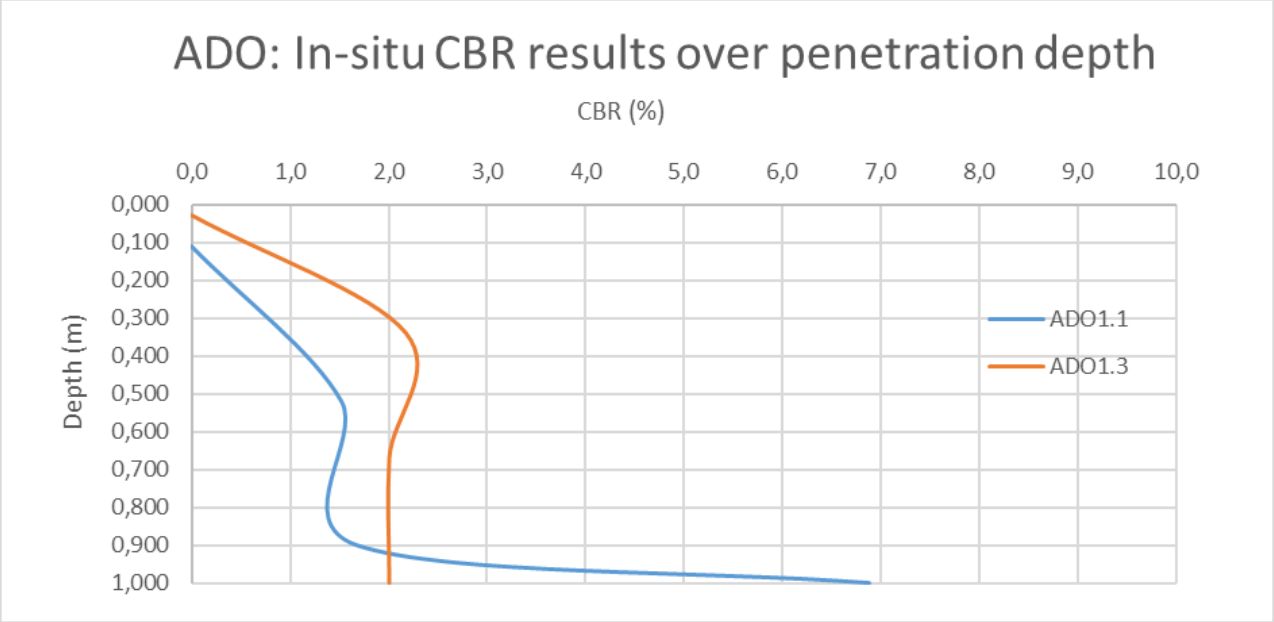

Figure 4.15 In situ CBR against penetration depth for zone ADO.

4.1.1.7 Zones TF, LL and HF

The exposed surface area through zones TF, LL and HF consisted predominately of conglomerate slopes with alluvial sediment deposits present at low lying subzones TF2 and HF2 (see Figure 4.16).

The conglomerate was covered with a thin yellow wacke (sandstone of which the mud matrix in which the grains are embedded amounts to between 15 and 75% of the mass) coating. In subzone TF1 the conglomerate bedrock extended a distance of 170 m from the shoreline to the dam bank and was covered with reddish-yellow gravel.

Figure 4.16 Geology and soil type map of zones TF, LL and HF.

A silt layer was located at subzone TF2, the mouth of a small tributary. This zone was characterised by the presence of shrinkage cracks, remnants of grapevines and sparse vegetation. The silt surface extends from shoreline to dam bank is about 170m with the area calculated as 31,285m^2.

The soil profile was determined by a test hole followed by applying a hand auger at GPS point TF2.3 (see Figure 4.17). The top 0.15 m was described as slightly moist, dark brown, firm, intact, silt (chalky feel on teeth) of alluvial origin, followed by a dark brown, medium-grained sand. The water table was observed at 1.28 m and prohibited the measurement of the depth of the bedrock.

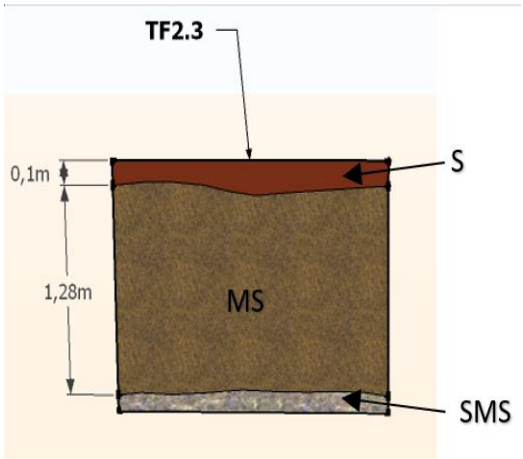

Figure 4.17 Soil profile for GPS point TF2.3. Abbreviations: S- Silt, MS- medium-grained sand and SMS-saturated medium-grained sand.

Unlike the conglomerate slopes of subzone TF1, the reddish gravel cover was absent on the surface zone LL to HF. At zone LL, the exposed area of the conglomerate dominated slopes were measured at about 207m from the dam shoreline to the dam bank. The remnants of a tar road and subbase running in the northeast-southwest direction were observed. Also, a few occurrences of *in situ* tree trunks were scattered over this area. Shallow to moderate slope gradient of 6.2% was calculated.

The only reservoir sediment was located adjacent to the dam shoreline at point LL1.1. A test hole at LL1.1 exposed a top layer (0.1m thick) of fine-grained (particle size ranging from 0.06 to 0.2mm) sand, followed by a 0.35m thick medium-grained sand which exhibited a change in colour from dark brown to light yellow at depth of 0.25m. Below the medium-grained sand, a bedrock was observed which prohibited further excavation.

Figure 4.19 indicates similar CBR patterns for LL1.2, LL1.3 and LL1.4 and similar patterns for LL1.1 and TF1. The similar CBR pattern for LL1.2, LL1.3 and LL1.4 indicated a sharp increase in maximum CBR values in the range of 40 to 60% followed by a sharp decrease.

A test hole was dug into the stiff surface at point LL1.3 to locate the cause of the abrupt decrease in the DCP penetration resistance. The sequence from top to bottom of the hole consisted of 0.10 m yellow weathered wackes, 0.22m layer of red to yellowish, loose, intact, medium to coarse-grained gravel with minor amounts of silt which overlaid a weathered red shale.

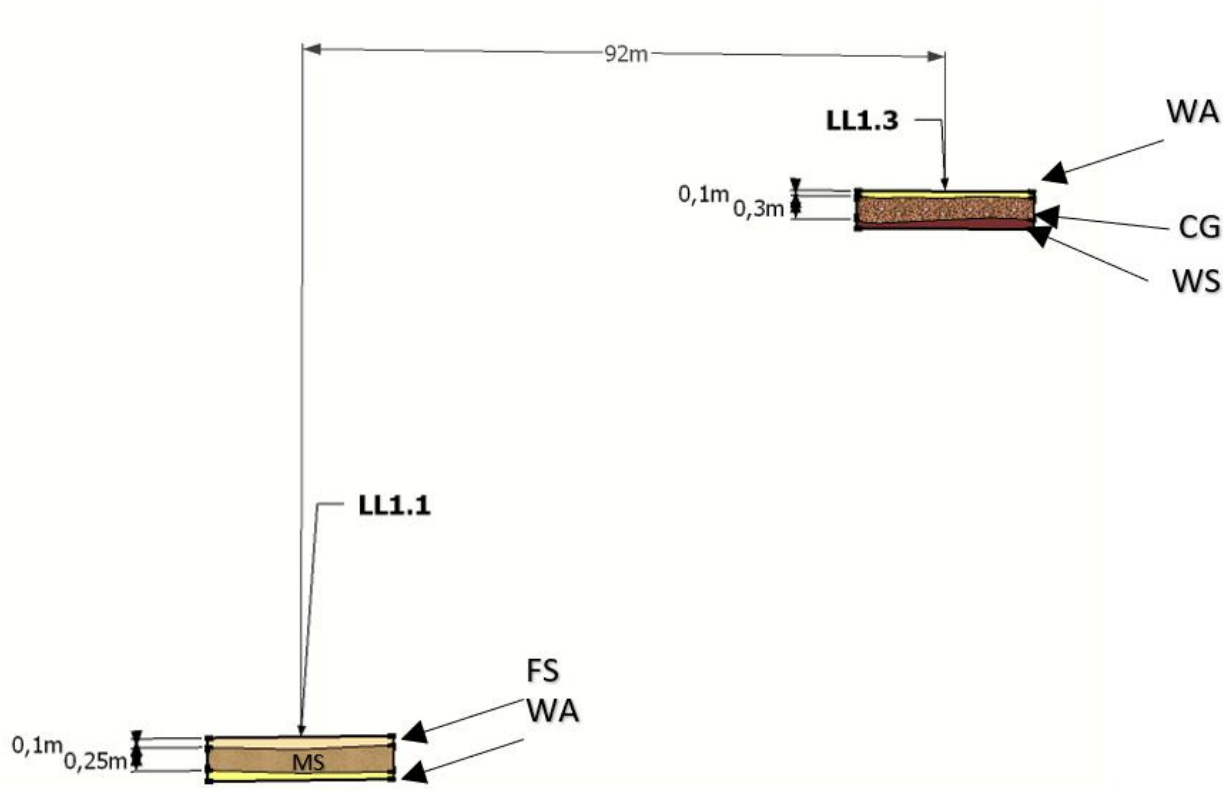

Figure 4.18 Soil profile for GPS points LL1.1 and LL1.3. Abbreviations: FS- fine-grained sand, MS-medium-grained sand, WA- wacke, CG-Coarse-grained gravel, WS-Weathered shale.

The sequence of LL1.3 was observed upslope in the form of an unweathered sedimentary rock sequence consisting of 0.1 m thick fine yellow wacke with black subangular grains (3-5mm), a 0.6 m thick reddish and yellow conglomerate with subrounded grains (5-15mm) and reddish shale at the bottom of the exposure (Figure 4.22 D). This sequence was observed on the slopes from zone TF to zone HF.

The sharp increase in the *in situ* CBR values indicated the residual gravel layer (derived from weathered conglomerate) with the subsequent decrease in CBR values indicating the weathered shale layer. Points LL1.1 and TF1.3 reached maximum penetration depths at 0.45m and 0.7m respectively, which is an indication that the stratum is very competent and was most likely an unweathered conglomerate bedrock. The deeper maximum penetration at point LL1.1 was due to the sediment layer occurring up to a depth of 0.5m. The thin layer of sediment occurring in the zone results in it not being suitable to be tested whether it can be used as construction materials.

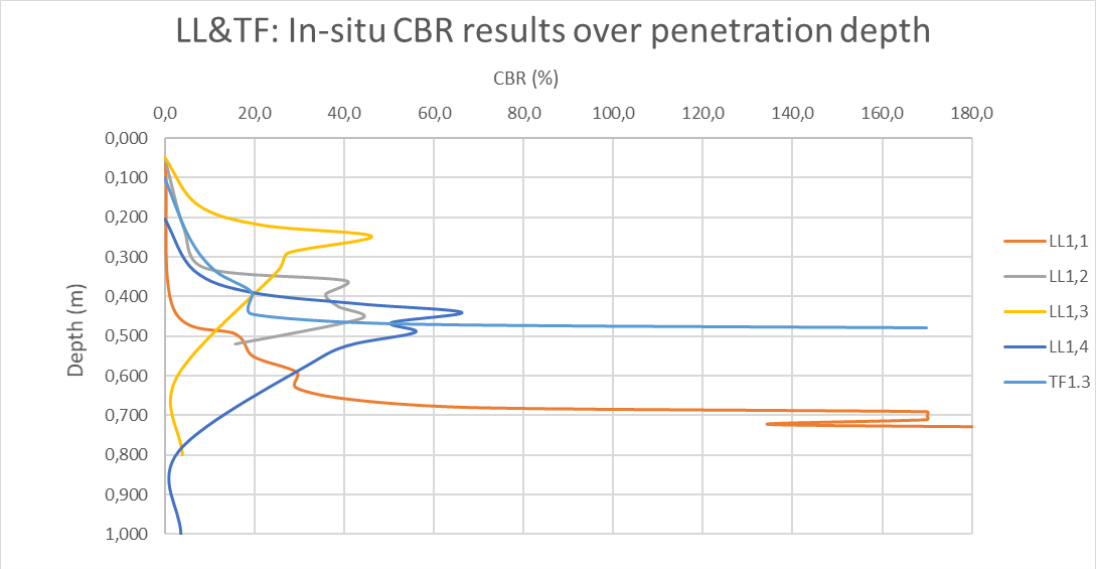

Figure 4.19 In situ CBR against penetration depth for zones TF and LL

At subzone HF1 the exposed surface flattened out and was covered with sandstone boulders. The conglomerate covered by yellow wacke was exposed near the dam bank. This area was insufficient for the aim of this project since no prominent evidence of sediment accumulation was present. A shallow slope gradient of 1.2 % was calculated from GPS measurements.

Subzone HF2 was located at the mouth of a small river. Shrubland and trees were covering most of the dry river upslope with the vegetation gradually becoming sparser closer to the river mouth. The surface was dominated by an alluvial sand surface, which extended 360m from the dam shoreline to where river vegetation ends with the area of this surface calculated as 253,164m^2. No flowing water was observed in this tributary and a remnant of an old road structure crosscut the alluvial sand parallel to the dam shoreline. The flat surface from the road to dam shoreline was approximately 170m and had a white appearance due to a coating of quartz and sandstone fragments. Samples were taken for laboratory analyses for construction materials at this subzone due to the applicable thickness of the sediment layers.

Test holes were excavated at points HF2.1 and HF2.2 followed by auger drilling and DCP analysis. With the DCP rod, the total depth of loose material at holes HF2.1 and HF 2.2 was estimated as 1.03 m and 1.3m respectively (see Figure 4.20). Samples were taken for laboratory analyses for construction materials at this subzone due to the applicable volume of the sediment layers observed in the field.

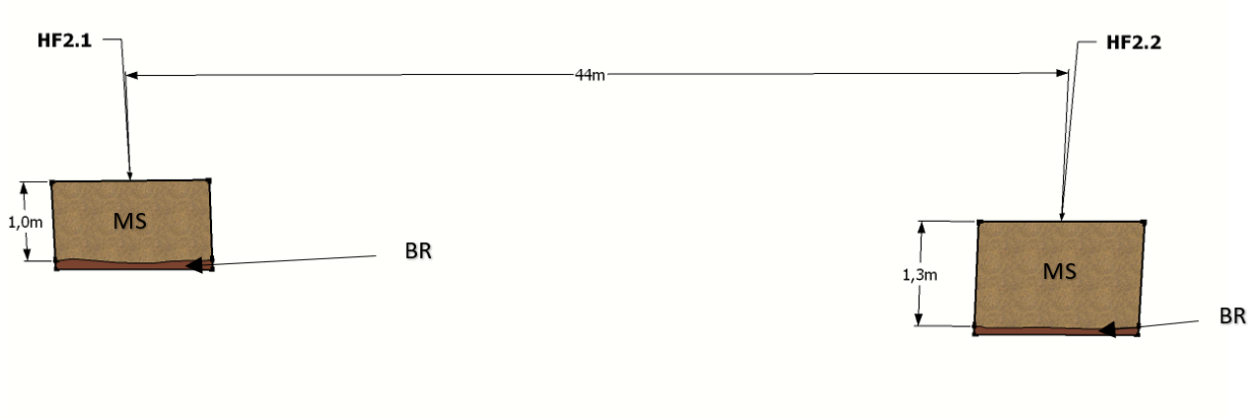

Figure 4.20 Soli profile of points HF2.1 and HF2.2. Abbreviations: Ms-medium-grained sand and BR- bedrock.

Figure 4.21 represents the *in situ* CBR values calculated at GPS points HF2.1, HF2.2 and HF2.3. The *in situ* CBR values were obtained throughout the depth were significantly low, with maximum values ranging from 0.9 to 4.2% at depths ranging from 0.45 to 0.65m. Similar to zone ADO, the low CBR values may be caused by the position of the sediment strata being located at the mouth of a tributary, which suggest a lesser number of fines and an increase in moisture content which will allow for lower CBR values.

Extensive treatment of sediment surface with stabilisers and subbase material will be required due to the significant low *in situ* CBR values obtained through the strata if dry excavation is commenced.

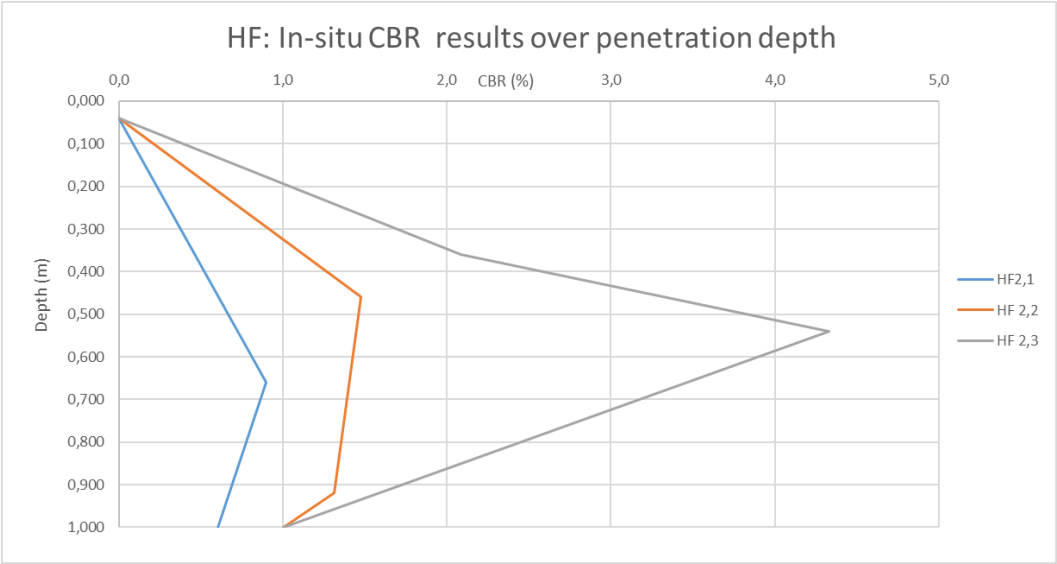

Figure 4.21 In situ CBR results against penetration depths for subzone HF.

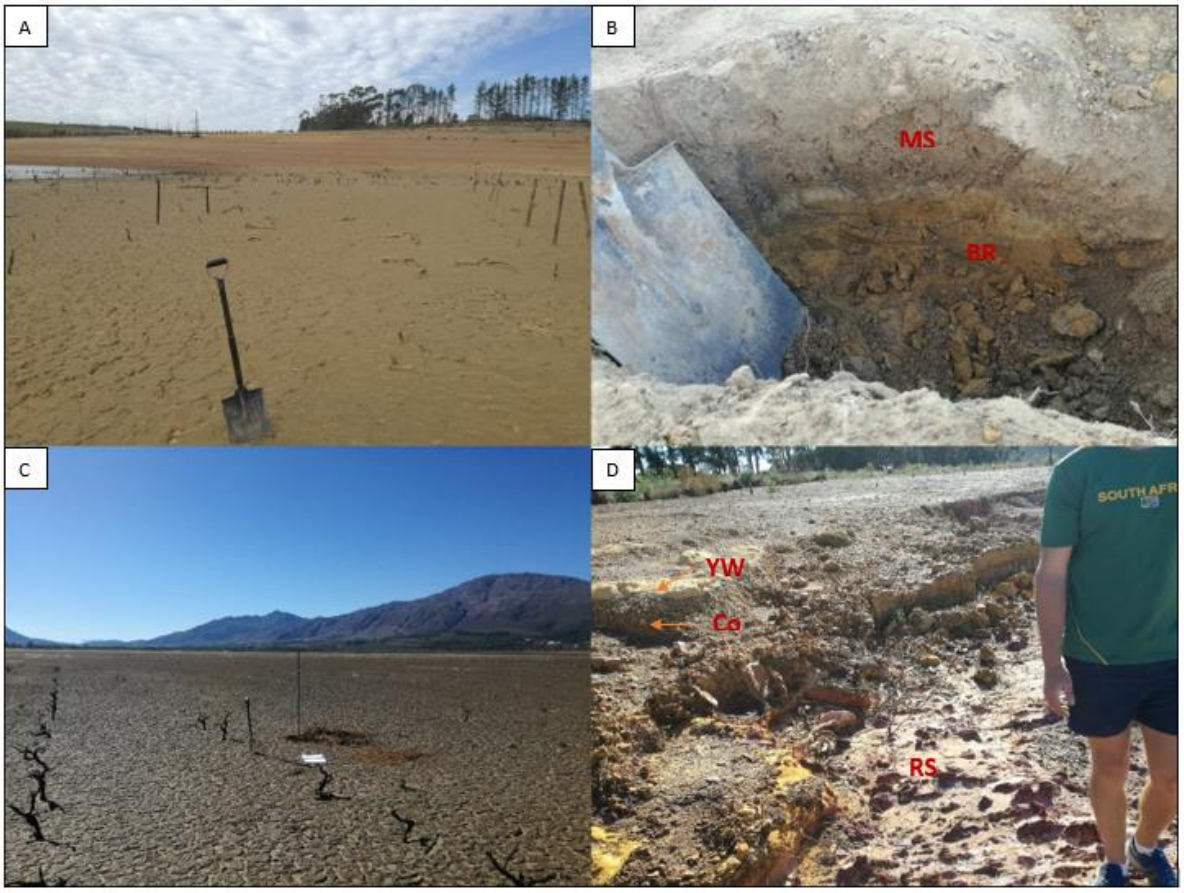

Figure 4.22 A) Flat laying brown sediment surface with remnant poles of old vineyards at subzone QA2. B) Test hole at GF1., indicating shallow sediment layer covering a stiff weathered bedrock. C) The large flat surface of the medium-grained sands and residual grape vines at subzone TSC2.D) Bedrock sequence of yellow wacke, covering conglomerate layer which in turns cover reddish shales. Abbreviation: Ms- medium-grained sand, BR-bedrock, Co-conglomerate, RS- red shales, YW-yellow wacke.

4.1.1 Greater Brandvlei Dam

Figure 4.23 illustrates the seven zones that were mapped during field investigation. The results of the field investigation of seven zones indicate only adequate sediment thickness for testing in zones B1 and B5. The surfaces of zones B2, B3, B4, B6 and B7 consisted out of *in situ* rock exposures, shallow sediment layers (less than 0.1m) and boulders. Shale was the dominant bedrock in the latter zones (Figure 4.24). The only alternative *in situ* surface to the shale bedrock was sandstone occurring at zone B6. The shale and sandstone exposure are weathered close to the dam shore and un-weathered closer to the dam bank. In addition, Zone B4 was the only zone were vegetation (mainly grass) was observed on the exposed surface.

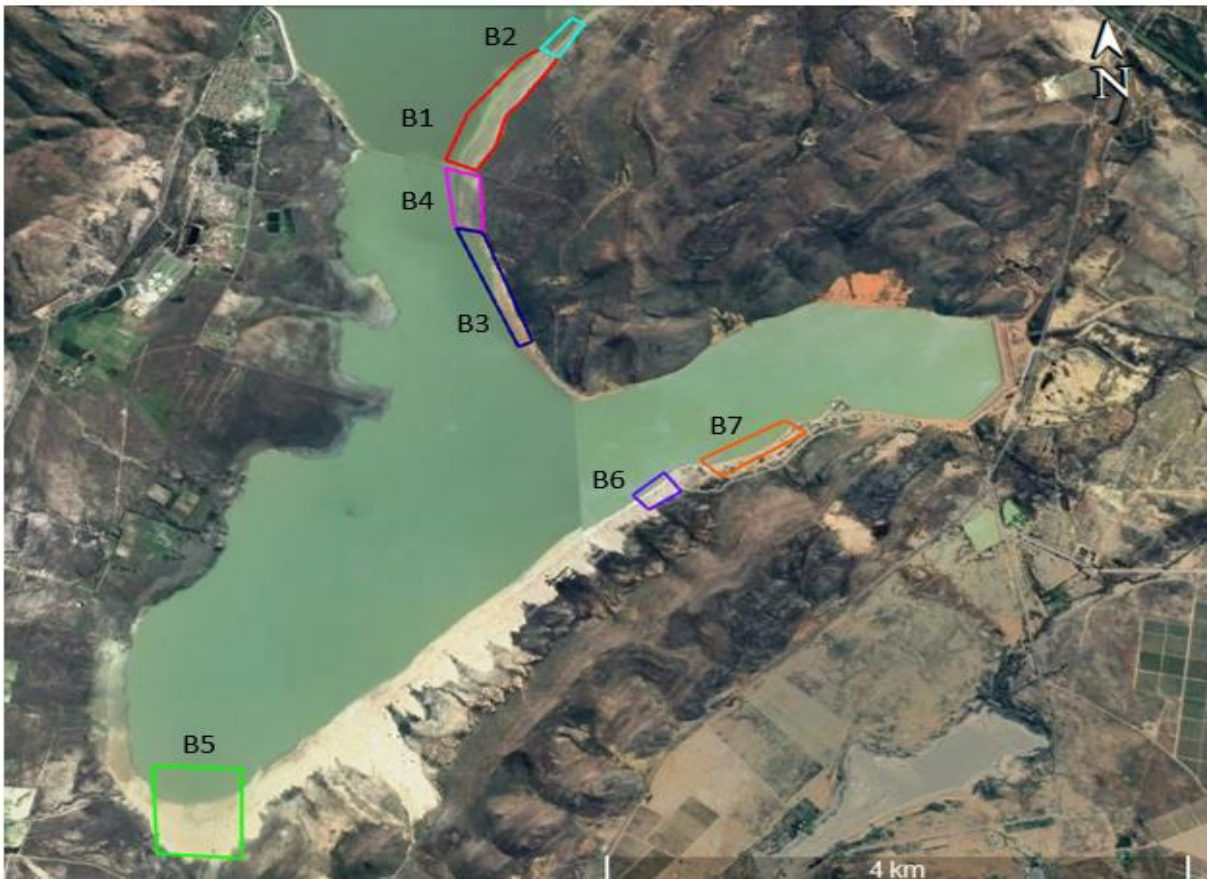

Figure 4.23 Map of Greater Brandvlei Dam with the indicated zones that were under investigation.

Figure 4.24 Map indicating the geology and soil type together with GPS points of the Greater Brandvlei Dam.

4.1.2.1 Zone B1

The extent of the exposed dam surface from the dam shore to the dam bank was measured as about 300m (see Figure 4.25). The zone was relatively flat with a slope gradient of 1.59% calculated from GPS measurements.

The bedrock was exposed near the dam shoreline, with coarse-grained reddish-brown sediment appearing at B1.2, thickening closer to the dam bank and disappearing at B1.5. The coarse-grained sediment layer was roughly 60m wide and 1300m in length. Figure 4.26 illustrates the results obtained from the test holes at points B1.2, B1.3 and B1.4. The surface elevation increased from B1.2 to B1.4 with 0.7m. The deposition pattern of the sediment in zone B1 is most similar to a deltaic pattern since the bulk of coarse sediment occurs near the inflow with little to no sediment occurring downslope.

The sediment layer at these three holes was described as a slightly moist, reddish-brown, very loose, intact, coarse-grained sand to fine-grained gravel (0.7-5mm) of alluvial origin. A thin horizontal layer (0.1m thick) was observed cutting through the coarse-grained sand in profiles B1.2 and B1.3 at depths of 0.14m and 0.2m respectively, whereas hole B1.4 consisted only out of coarse-grained sand to fine-grained gravel. The thin cross-cutting layer was described as moist, light brown, very loose, intact structure, fine-grained sand (0.06 to 0.2 mm) of alluvial origin. At hole B1.3, below the thin sediment layer, a coarse-sand to a fine gravel layer was observed in a cross-lamination formation (see Figure 4.31 A). A water table was pierced in holes B1.2, B1.3 and B1.4 at depths of 0.65m, 0.9m, and 0.6m respectively.

Samples were taken for laboratory analyses for construction materials at this subzone due to the suitable volume of sediment layers observed in the field.

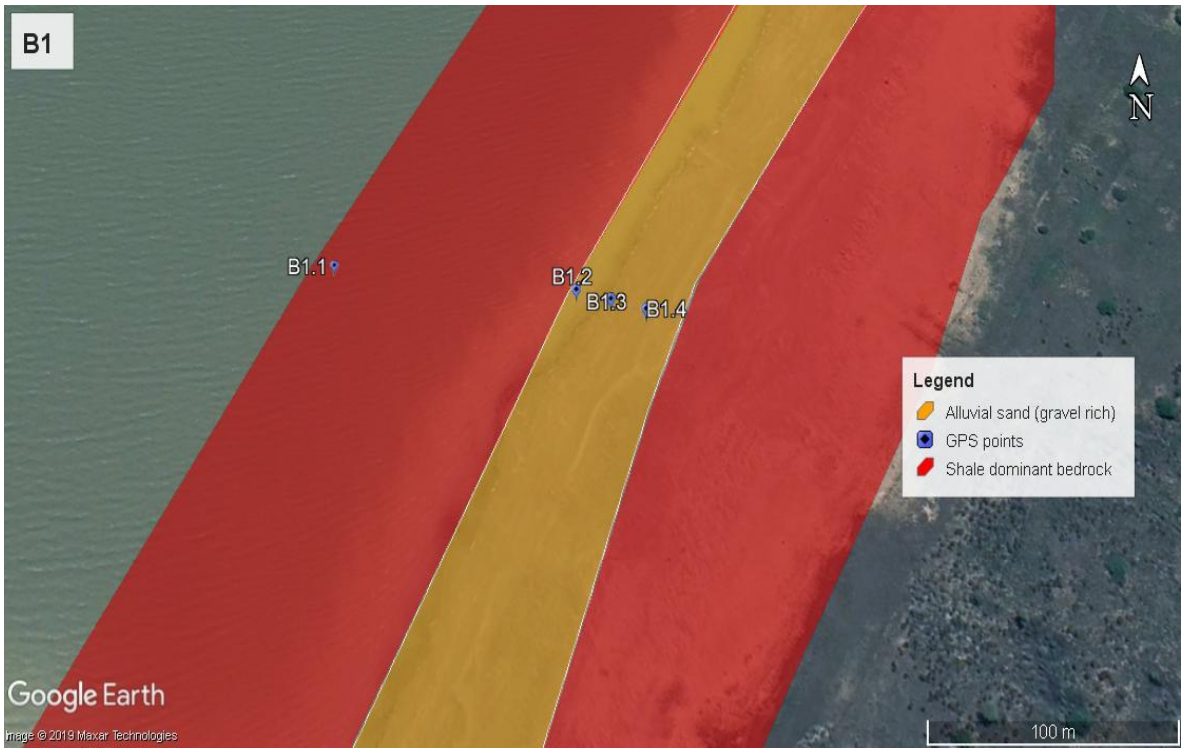

Figure 4.25 Sediment and Geology map of Zone B1.

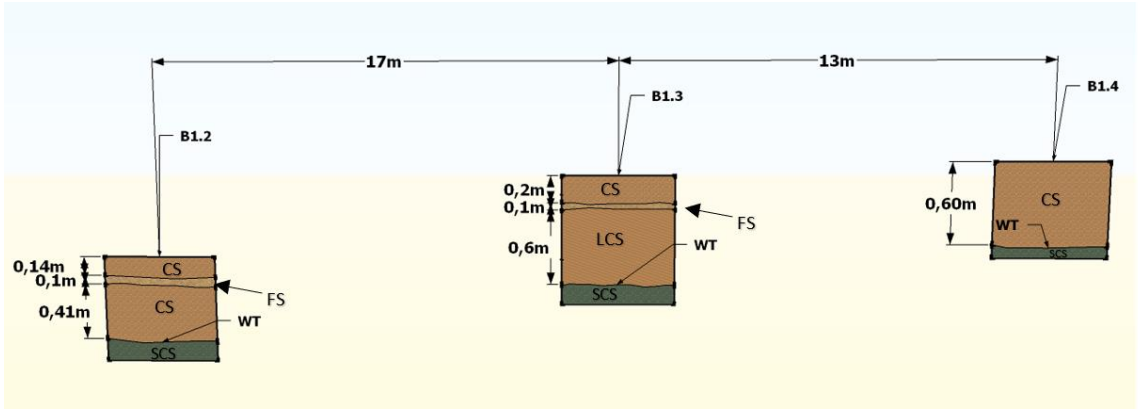

Figure 4.26 Soil profile columns of test holes B1.2 and B1.3. CS- Coarse-grained sand to fine-grained gravel, FS- fine-grained sand, LCS-cross laminated sand, SCS- saturated coarse-grained sand and WT-water table.

Figure 4.27 illustrates the *in situ* CBR results for subzone B1. The loose surface cover resulted in the initial CBR values starting from 0.2m to 0.4m.

The *in situ* CBR results indicated two patterns. The first pattern was at B1.1, which indicated bedrock, with high CBR values (>100%) at about 0.3m depth where maximum penetration depth was reached. The second pattern indicated a uniform layer of low CBR values for B1.2 to B1.4. The

CBR values for B1.2 increased to 6% at 0.6m and decreased to 2% at 1m, whereas B1.3 and B1.4 reached maximum CBR values of 8% at 0.8m and decreased to 6% at 1 m.

If dry excavation is commenced, the alluvial sand would be accessed through the competent bedrock (*in situ* value of 170 %) surrounding it. A dozer can be used to move the alluvial sand onto a heap which will expose more competent bedrock and will improve the ease of sediment removal.

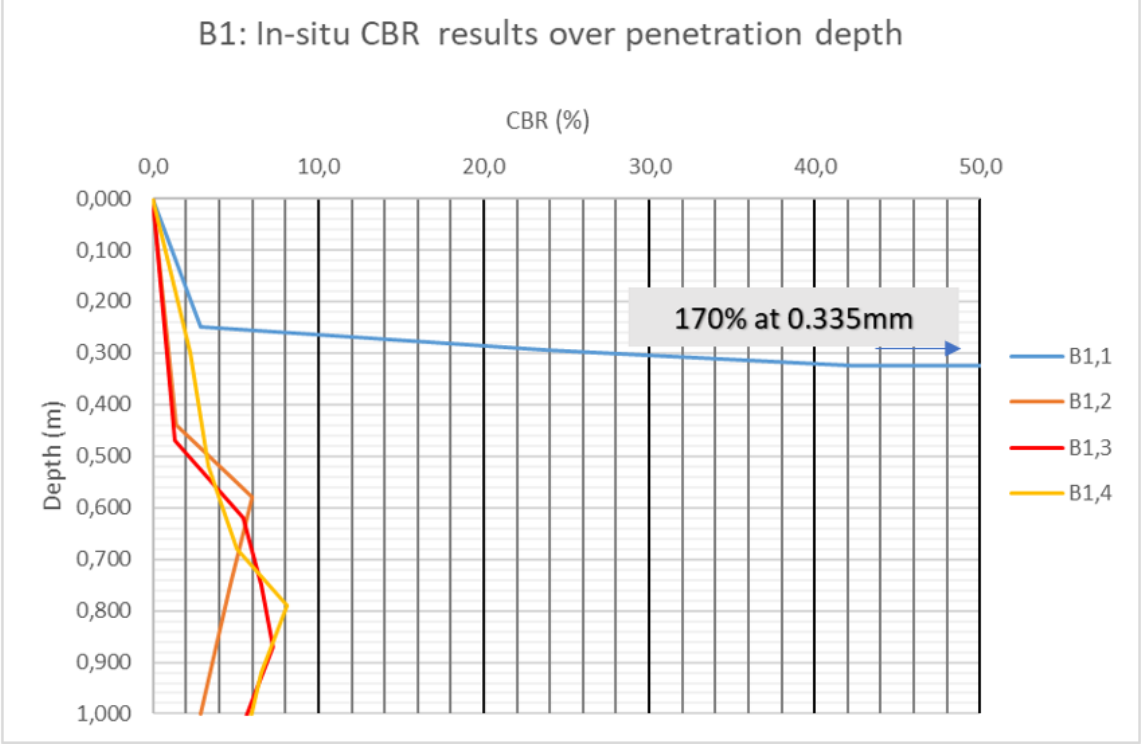

Figure 4.27 In situ CBR results for zone B1.

4.1.2.2 Zone B5

The exposed dam surface at zone B5 consisted mainly of dark brown alluvial sand (see Figure 4.28). The spread from the dam shore to the dam bank was measured as about 580m. The total area for the zone was estimated as 343,490m^2. A very shallow slope gradient of 1.02% was calculated from the GPS measurement for the exposed surface. Fine reddish-brown gravel (2 to 10mm grain size) covered the surface near the riverbank but gradually disappeared towards the dam shoreline (see Figure 4.31 B).

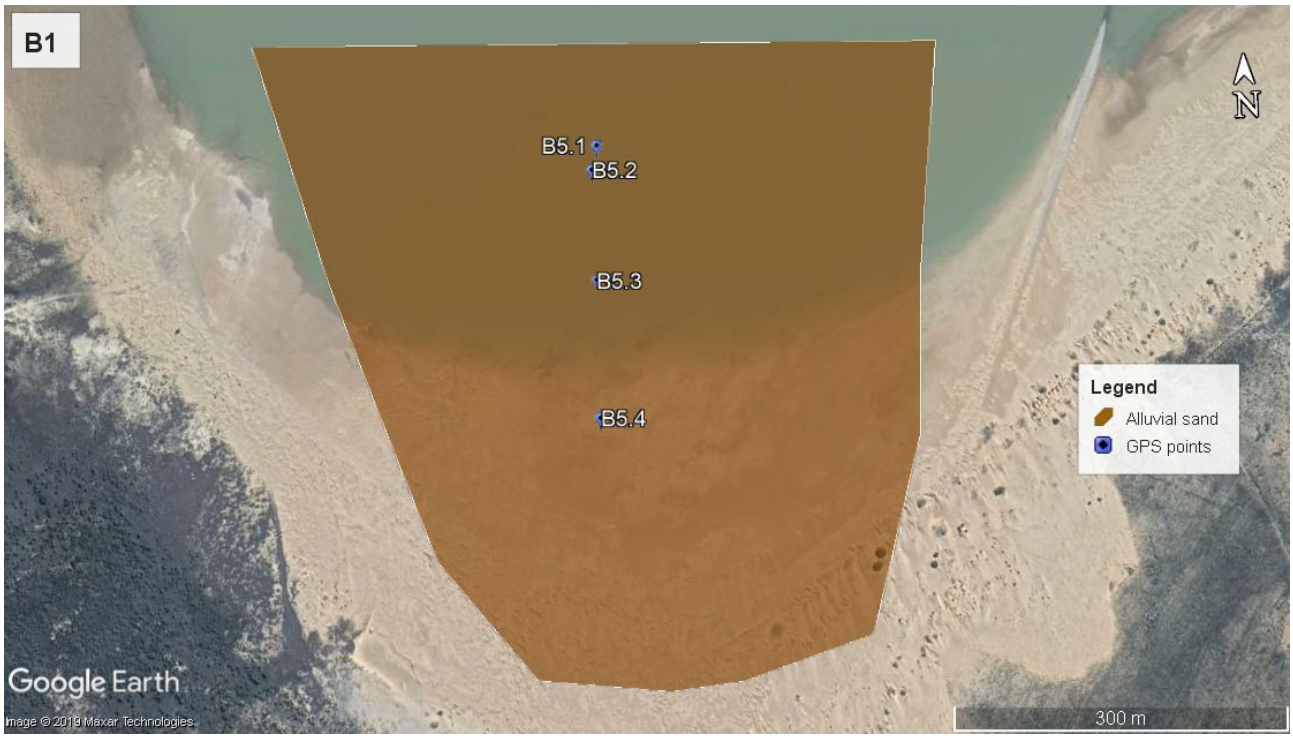

Figure 4.28 The mapped sediment area for zone B5.

Figure 4.29 indicates the constructed soil profiles which were based on data from the test pit data, hand auger excavation and DCP analysis at the four GPS points. The sediment layer occurring homogenously throughout the soil profiles was described as a light brown, slightly moist, very loose fine to medium to coarse-grained sand (1-2 mm) and fine gravel (2.5-5mm) of an alluvial origin. The depth of the water table increased from 0.4m from B5.1 to 0.6m at B5.4. With the use of DCP, it was determined that the medium-grained sand exceeds the depth of 1.5m at each GPS point. The sediment thickness could not be obtained due to lack of appropriate equipment, however, the decrease of slope towards the dam shoreline can be analogous with gradual sediment thickness decline indicating a tapering deposition pattern.

Samples were taken for laboratory analyses for construction materials at this subzone due to the suitable volume of the sediment layers observed in the field.

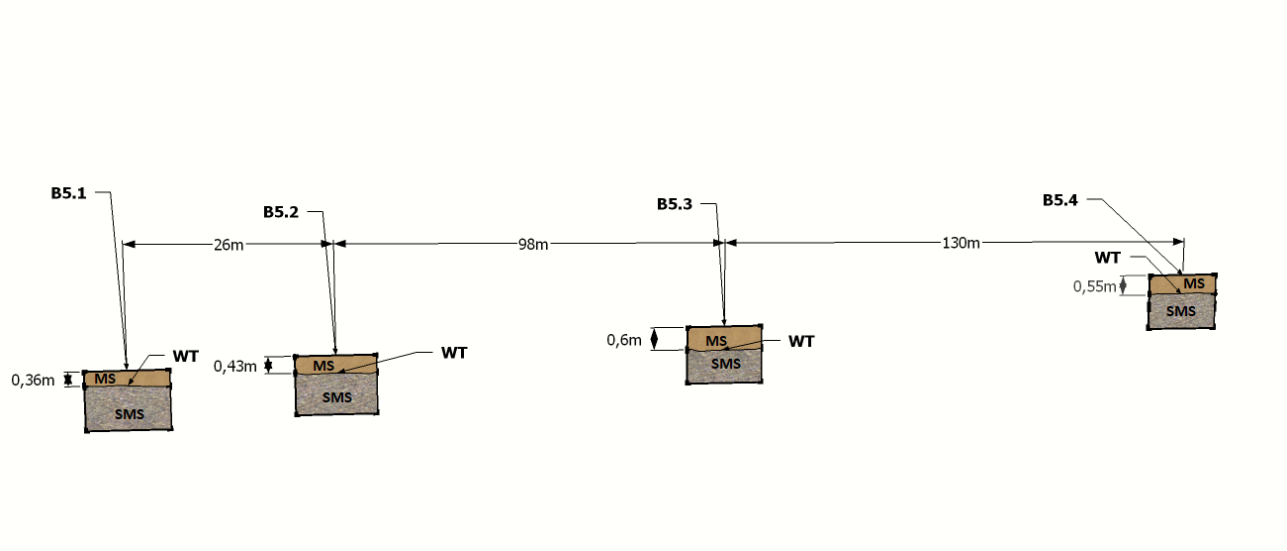

Figure 4.29 Soil profiles from GPS points B5.1 to B5.4. Abbreviations: Ms-medium-grained sand and SMS-saturated medium-grained sand

Figure 4.30 illustrates the *in situ* CBR values over DCP penetration depth for zone B5. The *in situ* CBR results at points B5.1 and B5.2 increased to 3% at 0.3m. From this depth, the CBR values for B5.1 increased to 11% at 0.75m depth before decreasing to 5% at 1 m depth. The *in situ* CBR values for B5.2 increased slowly up to a depth of 0.55m where it rapidly increased to 12% to 22% at depths of 0.6 to 0.95 m. The latter range indicated layers of higher and lower strength. At point B5.3, the *in-situ* results indicated a gradual increase from 2.5% to 14.5% with increasing soil depth. The gradual increase of *in situ* CBR values of the three points indicated the increase of density with depth.

The sediment surface where heavy machinery is to move should be treated by compaction and covered with subbase material to improve the low *in situ* CBR values. The depth of the bedrock should also be estimated.

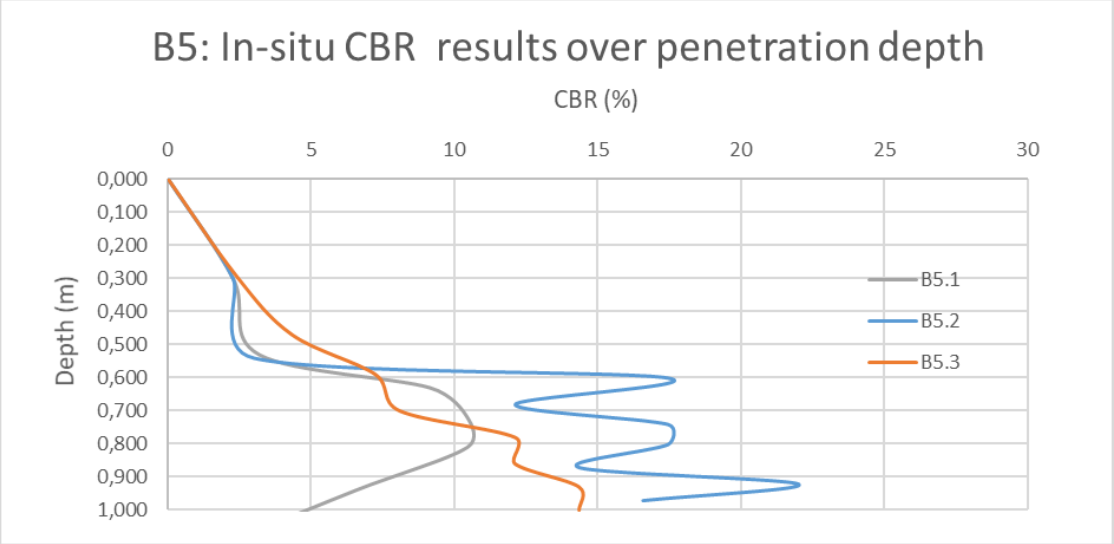

Figure 4.30 In situ CBR over depth results for zone B5.

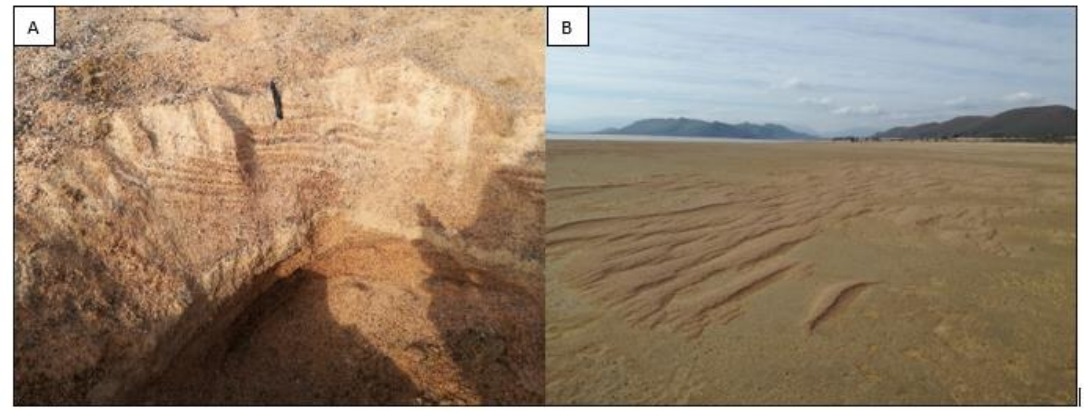

Figure 4.31 A) Cross-laminations observed in test hole B1.3. B) Flat laying sand surface covered by sporadic occurrences of fine-grained gravel at zone B5.

4.1.2 Waterzicht

The exposed surface at the Waterzicht Dam consisted mainly of silt banks overlaying organic-rich alluvial sands (see Figure 4.32). The exposed surface was located at the inflow of the dam and was measured as about 180 m in length and 33,778m^2 in area. The occurrence of the thick sediment layers at the inflow of dam is diagnostic for delta depositional pattern.

Prominent mud cracks were observed on the surface throughout the exposed area (see Figure 4.33 A) with vegetation present on the outer parts of the surface adjacent to the dam bank.

The silt banks were elevated 0.4 to 1 m above the medium-grained sands (see Figure 4.33 B). The properties of the silt were observed to be slightly moist, grey in colour with orange mottled textures, stiff, very fine-grained (grains felt on nails) with isolated coarser grains (0.5-1.5mm) also present,

intact structure and of alluvial origin. The sand underlying the silt was described as dark in colour, moist to slightly moist, loose, medium-grained (0.3-0.6mm) and of alluvial origin. During fieldwork only test holes were excavated at GPS points WZ1.1, WZ1.2, WZ1.3 and WZ2.1. In contrast, only DCP testing was done at GPS points WZ2.2 and WZ2.1.

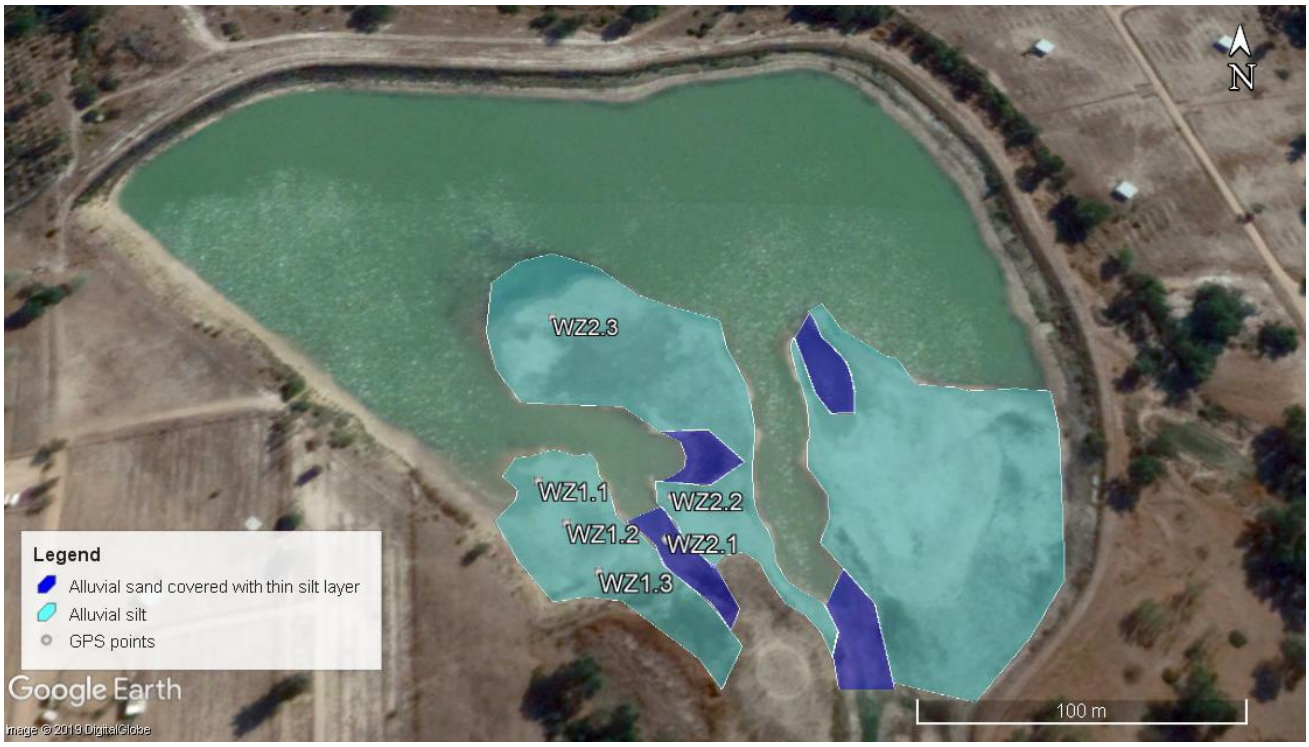

Figure 4.32 Map indicating the geology and soil type of the exposed surface of the Waterzicht Dam.

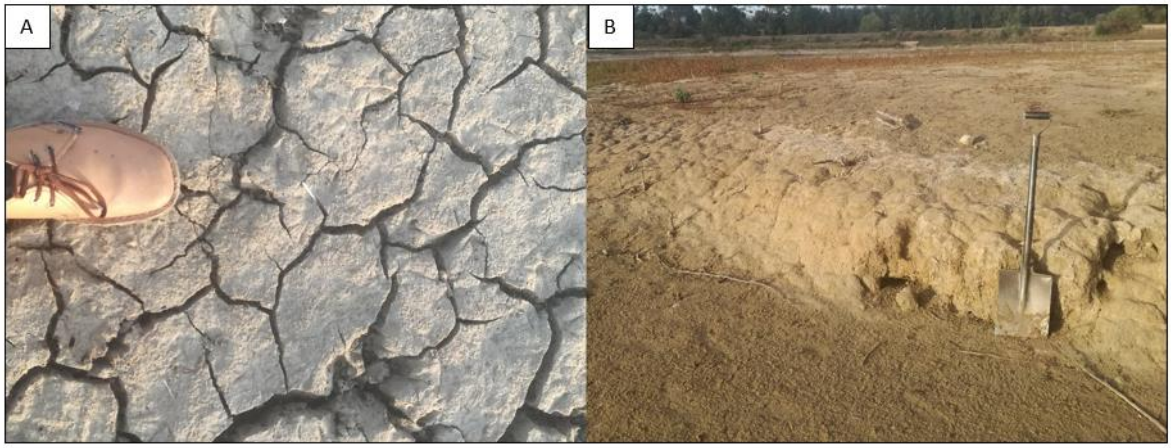

Figure 4.33 A) Prominent shrinkage cracks observed on the silt surface at point WZ1.2, B) Stiff silt banks overlying medium-grained sands.

At the three test holes excavated at GPS points WZ1.1, WZ1.2 and WZ1.3 a thin brown sand layer (0.05 to 0.15m thick) was observed covering the very stiff silt layer (see Figure 4.34). The stiffness

of the silt layer restricted the penetration of the auger during the excavation of the test hole beyond about 0.3 m for these three test holes. The covering sand layer was too thin to be considered as sediment reserve for testing for construction materials or be included in volume estimations.

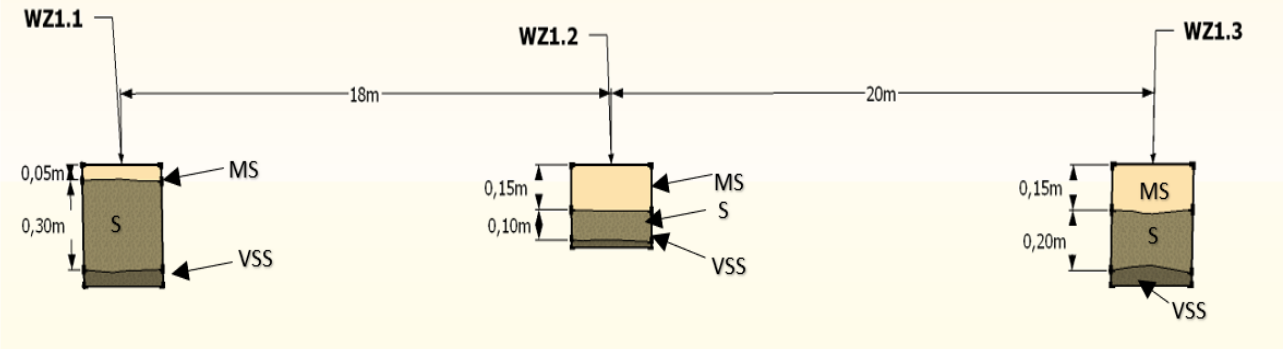

Figure 4.34 Soil profiles for GPS points WZ1.1, WZ1.2 and WZ1.3. Abbreviations: MS-medium grained sand, S-silt, VSS-very stiff silt.

Figure 4.35 illustrates the soil profile of the test hole at point WZ2.1. The first 0.25 m of excavation consists of moist grey silt. Medium-gained sand was observed from a depth of 0.25m downwards. This layer of sand experienced a colour change from dark grey to light grey at 0.4 m. The depth of the colour change corresponds with the depth of the water table. The water table prohibited the estimation of the depth of the sand layer. Samples were taken for laboratory analyses for construction materials at this subzone due to the suitable volume of the sediment layers observed in the field.

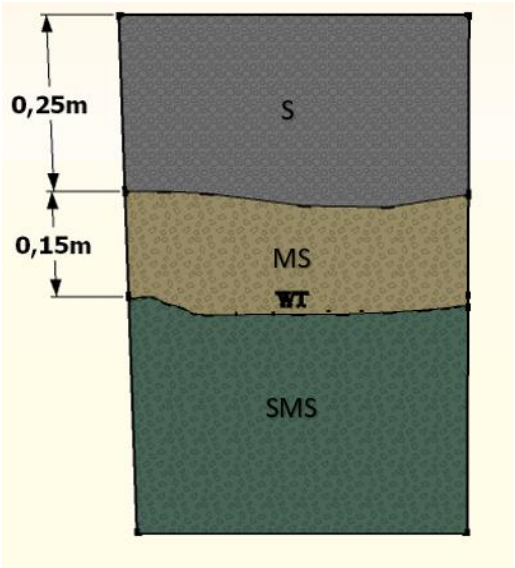

Figure 4.35 Soil profile at GPS point WZ2.1. Abbreviation: S- silt, Ms-medium-grained sand, SMS-saturated medium-grained sand, BR- bedrock and WT-water table

Figure 4.36 illustrates the *in situ* CBR values over-penetration depth. At point WZ2.2 the CBR values increased rapidly to 29% at 0.6m. With further depth increase in depth, the CBR values rapidly decreased to about 1% at 1m. This rapid decrease was due to the transition of the stiff silt layer to loose medium grain sand. At point WZ2.3 the CBR values experienced two sequences consisting of a rapid increase followed by a decrease with increasing depth. The first sequence occurred at depths of 0.2m to 0.67m, where the CBR values increase rapidly up to 27% where it consolidates for 0.2m before decreasing to 12%-14%. In the second sequence, the CBR value increased to 38% at 0.97 m before decreasing to 19% at 1m. The pattern of CBR values of the first sequence at point WZ2.3 may be an indication of sand lenses within the silt layer which will allow for lower densities. The decrease in the *in situ* CBR values for the second sequence may indicate the transition from silt into the underlying sand layer since the surface elevation at point WZ2.3 was about 0.3m higher than point WZ2.2, which means the depth of the underlying sand layer will be deeper by 0.3m at WZ2.3.

The sediment in the dam was inaccessible by vehicle during the time of the investigation. Therefore, a road should be constructed towards the exposed sediment if they are to be removed by dry excavation. It is preferred that machinery remains on the bedrock located at the dam base due to irregularities in the *in situ* CBR values caused by stiff silt banks and loose sandy materials. However, this bedrock should be first exposed and subsequent DCP testing should be done to determine if the rock is capable of carrying heavy machinery.

The occurrence of the stiff silty banks overlying alluvial sands at the inlet of the dam may be described as the transgression of the dam shoreline. The coarser alluvial sand was first deposited at the inlet as delta sediment. As the dam level increased, these deltaic sediments became submerged. When the dam was full or close to full, the transportation energy decreased at the inlet. The decrease in transport energy caused coarser-grained material to deposit upstream and fine-grained sediments to deposit at the bottom of the reservoir, thereby covering the sandy banks.

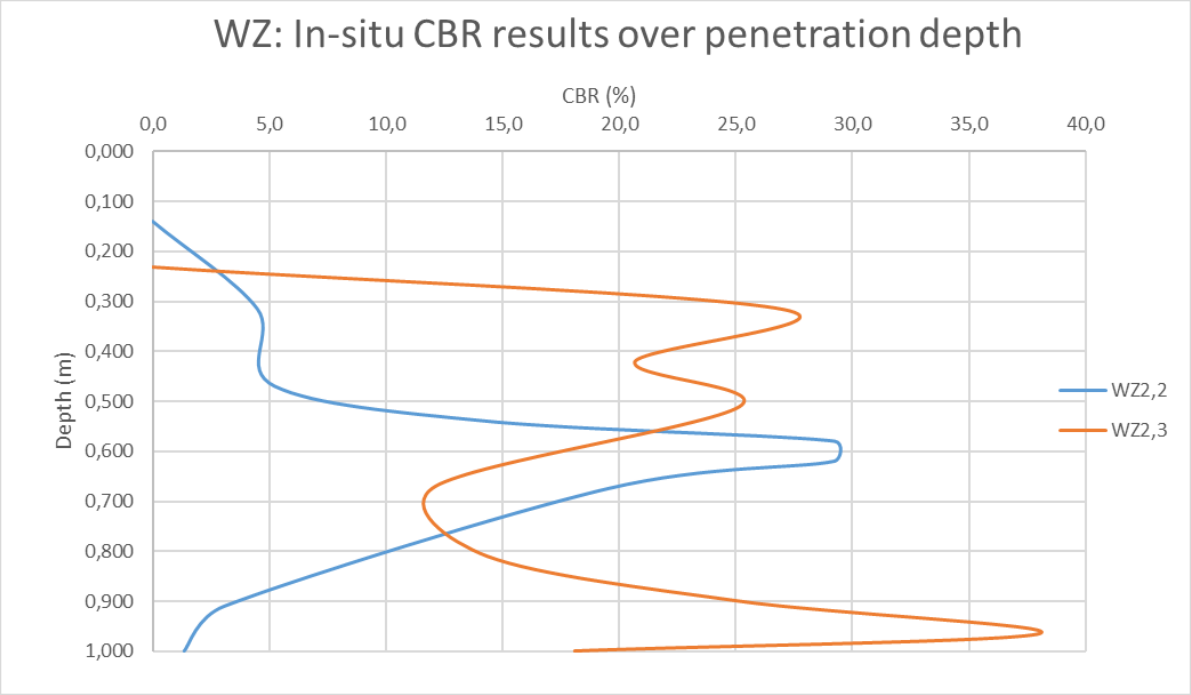

Figure 4.36 The in situ CBR values with increasing depth for zone WZ.

4.2 Laboratory results

4.2.1 Soil classification

The locations where samples were taken for laboratory analysis together with these samples' respective particle size distribution curves are presented in Figure 4.37 for the Theewaterskloof Dam, Figure 4.38 for Brandvlei Dam and Figure 4.39 for Waterzicht Dam.

From all three dams only three sediment samples, QA2a; WZ2a and RF1.3a, and the residual material from sample LL1.3c show any significant plasticity (see Table 4.1). The majority of these samples are at relatively low plasticity (below 8%), with only sample WZ2a presenting high plasticity of 26.8%.

Table 4.2 contains all the soil classification results using the USCS criteria and the data from the particle distribution graphs and Atterberg limits. The resulting classification indicates the dominance of silty sand (SM) in the Theewaterskloof Dam with the only exceptions being sample QA2a which is classified as lean clay (CL) and sample LL1.3c which can be described as a poorly sorted sand and silty sand (SP and SM). The uniformity of sample LL1.3c is indicated by a coefficient of curvature (Cz) below 1. Both samples of the Greater Brandvlei Dam (B1.2 and B5) consisted of poorly graded sands

or gravelly sands with little to no fines (SP). The uniform grading of B1.2 and B5 are indicated by uniform coefficients (Cu) and coefficients of curvature (Cz) less than 4 and 1 respectively. Classification of the samples of the Waterzicht Dam indicates clayey sands (CS) for WZ2a and silty sands (SM) for WZ2b.

Based on the UCSC, the subsequent laboratory tests were divided into separate tests for coarse-grained and fine-grained material reflecting the different uses to which the materials could be put. The sediments grouped under coarse-grained sediment included the silty sands and poorly sorted sands, whereas the sediments grouped under fine-grained material consisted out of clayey sands and lean clays.

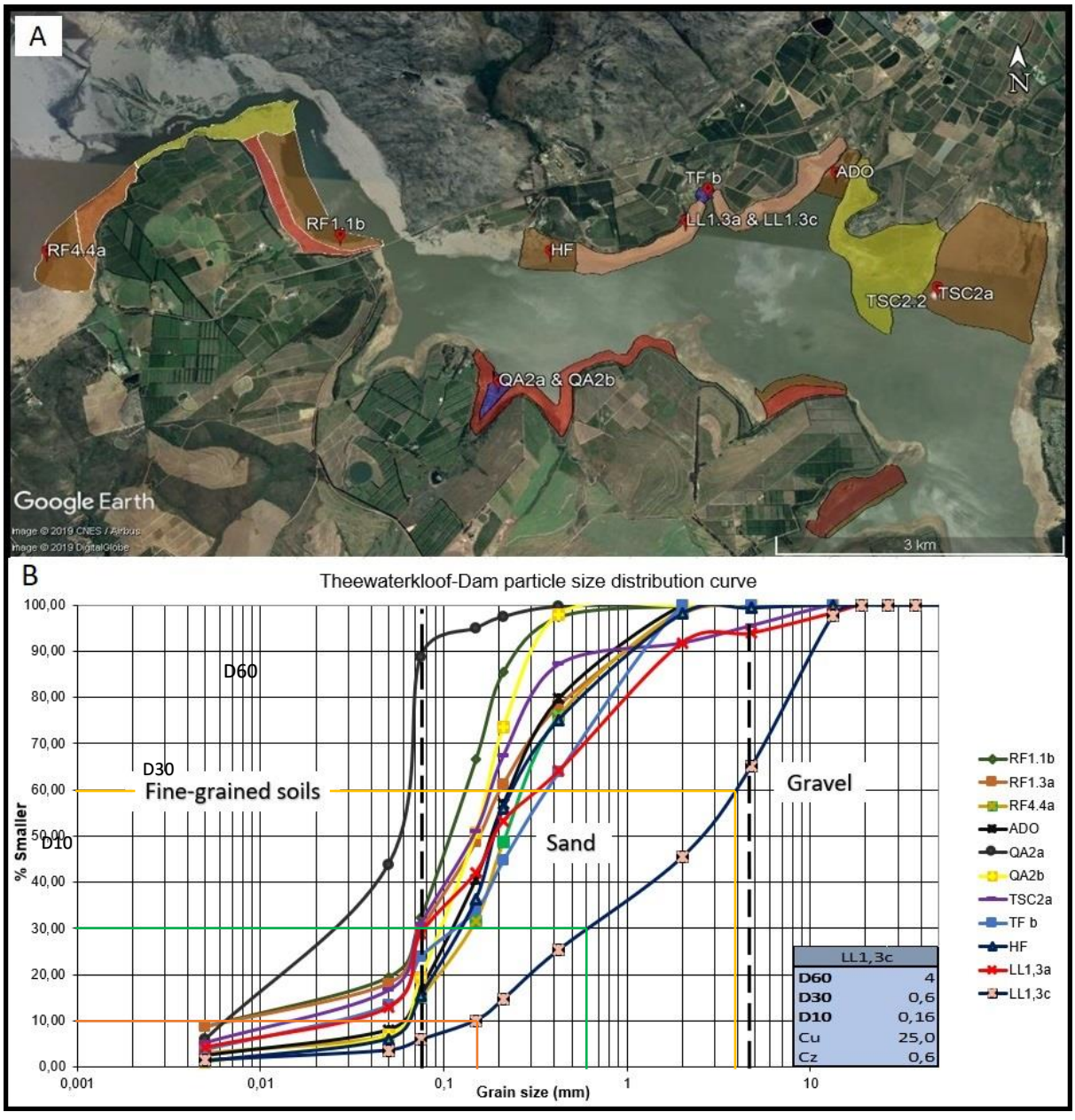

Figure 4.37 A) Sediment and geological map with sample data points of Theewaterskloof Dam. B) Particle size distribution curve of the samples taken at A).

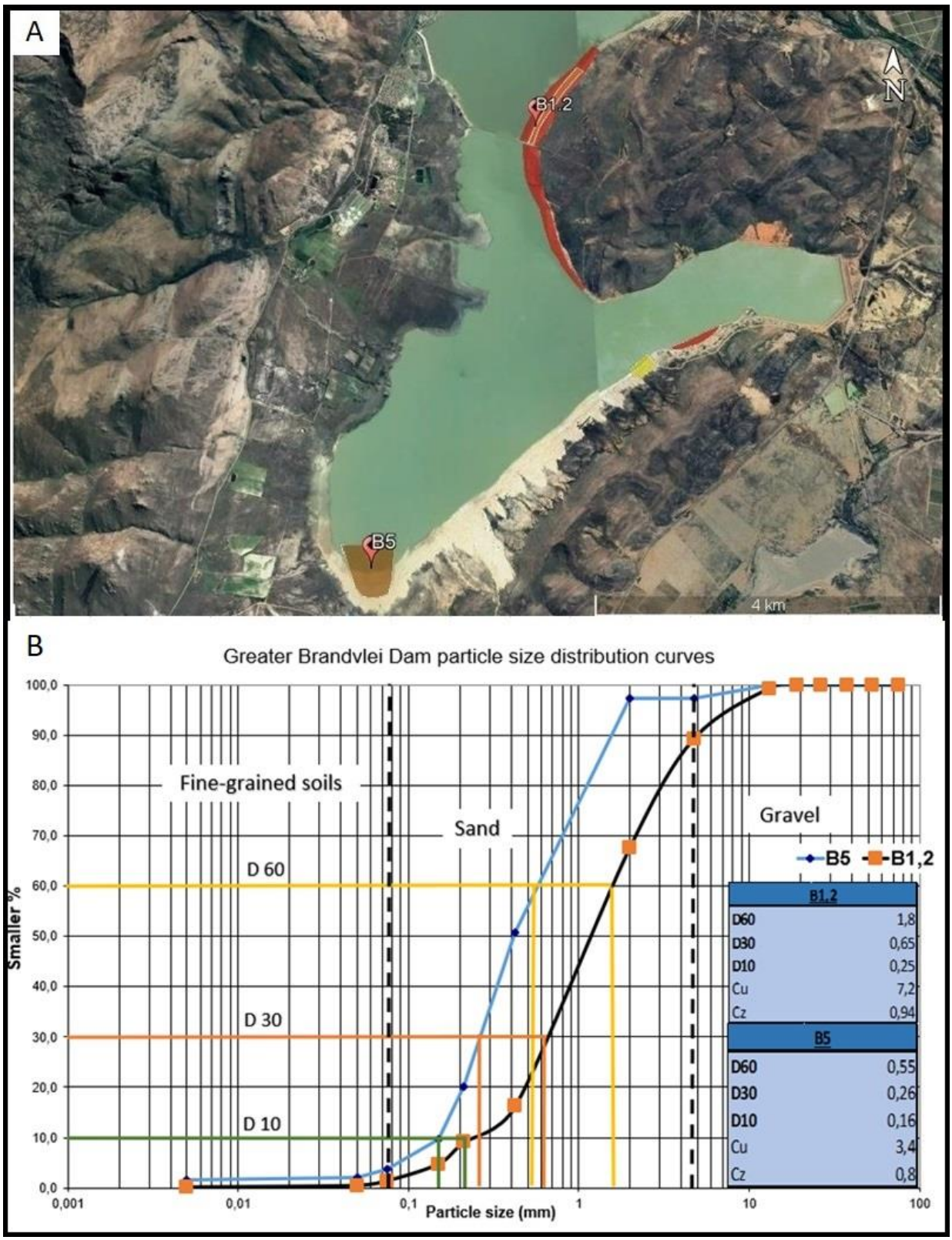

Figure 4.38 A) Sediment and geological map with sample data points of Greater Brandvlei Dam. B) Particle size distribution curve of the samples taken at A).

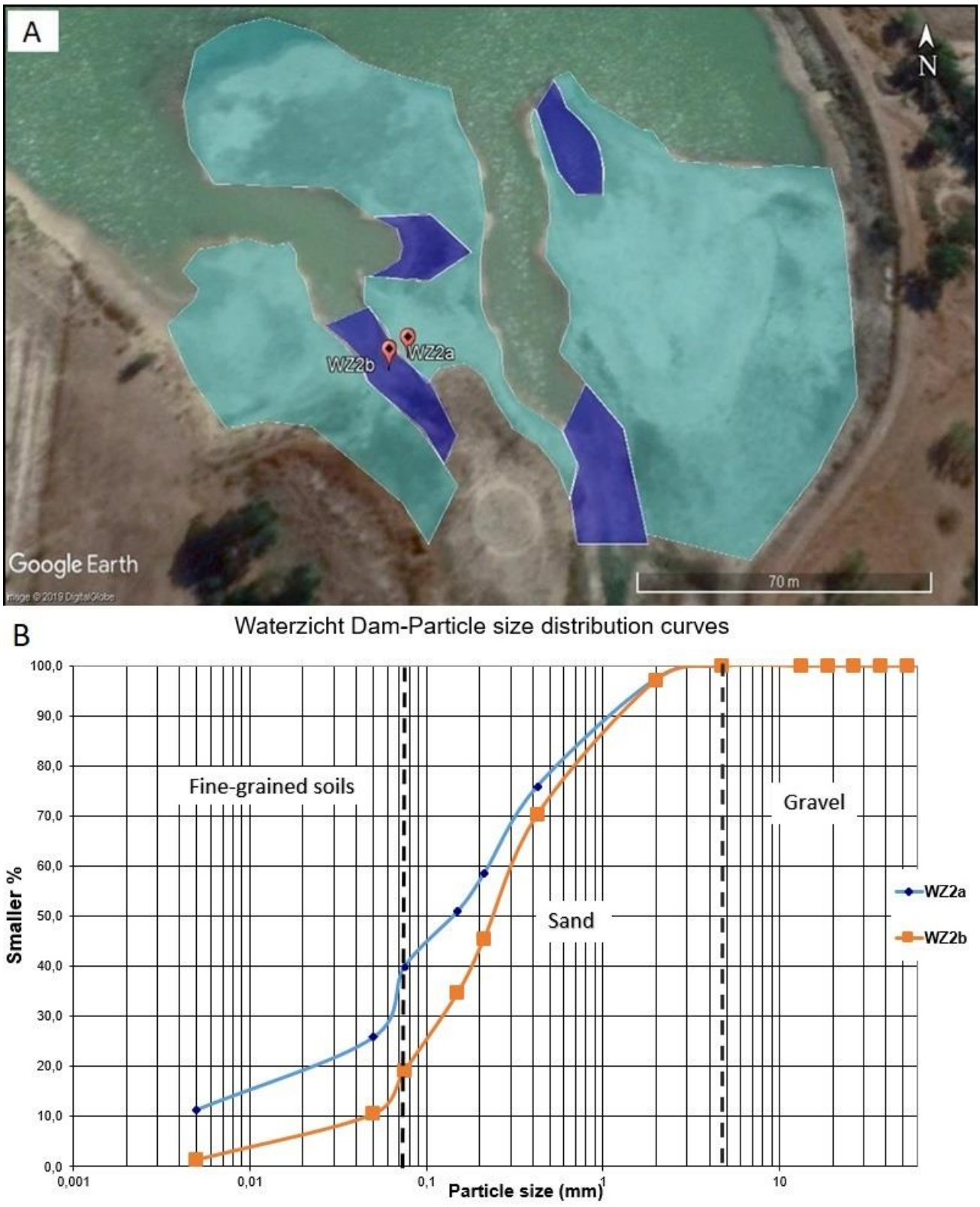

Figure 4.39 A) Sediment and geological map with sample data points of Waterzicht Dam. B) Particle size distribution curve of the samples taken at A).

.

Table 4.1 Atterberg limits for the samples that presented plastic properties

Atterberg limits				
	Sediment			Residual material
Sample #	**Wz2a**	**RF 1,3a**	**QA2a**	**LL1,3A**
Liquid limit	38,7	16,0	33,3	20,9
Linear shrinkage	4,0	1,3	4,0	3,3
Plasticity Index	26,8	3,7	7,6	5,2

Table 4.2 Classification of soil type of the samples taken for the three selected dams based on ASTM (2006).

Theewaterkloof Dam	
Sample #	**Soil type**
RF1,1b	SM
RF1,3a	SM
RF4,4a	SM
ADO	SM
QA2a	**CL**
QA2b	SM
TSC2a	SM
TF B	SM
HF	SM
Weathered Bedrock:	
Ll1,3a	SM
LL1,3c	**SM & SP**

Greater Brandvlei Dam	
Sample #	**Soil type**
B 1,2	SP
B 5	SP
Waterzicht	
Sample #	**Soil type**
WZ2a	SC
WZ2b	SM
Group Symbol	**Classification**
SM	**Silty sands**, sand-silt mixtures
SP	**Poorly graded sands** and gravelly sands, little or no fines
SC	**Clayey sands,** sand-clay mixtures
CL	**Lean clays**, gravelly clays, sandy clays, silty clays, Inorganic clays of low to medium plasticity

4.2.2 Coarse-grained material

The nine samples that were classified as sands (grain size dominant 0.075 to 4.25 mm) were selected for testing for road materials and fine natural aggregates in concrete, mortar and plaster. These samples include QA2b, RF1.1b, RF4.4, TSC2a, ADO and HF from Theewaterskloof Dam, WZ2b from Waterzicht and B1.2 and B5 from Greater Brandvlei Dam.

4.2.2.1 Road materials

For the CBR values, the maximum dry density (MDD) and optimum moisture content (OMC) were determined for each of the selected samples. These results were derived (at peak dry density levels) from the dry density against moisture curves plotted in Figure 4.40 and Figure 4.41. The six samples from Theewaterskloof showed MDDs ranging from 1725 $kg.m^{-3}$ to 1940 $kg.m^{-3}$ and OMC values ranging from 8.5% to 13.5%. The two samples of Greater Brandvlei Dam, B1.2 and B5, display MDD of 1772 $kg.m^{-3}$ at 7% OMC and 1645 $kg.m^{-3}$ at 10.7% OMC, with sample WZ2b from Waterzicht having an MDD of 1827 $kg.m^{-3}$ at 8.5 % OMC.

The CBRs, CBR swell and grading modules of each of the nine samples were compared to the criteria of Colto (1998) and THR14(1985, see Table 4.3). Only two samples passed the requirements of Colto (1998) to be used as road materials - sample B5 classified as G8 material with sample ADO classified as a G9 material. According to the recommendations from THR14 (1985) sample B5 passed as a G10 material, sample RF1.1b passed as G9 material and samples QA2b and ADO passed as G10 materials (generally used as fills). According to Colto (1998), sample RF1.1b obtained sufficient CBR values to classify as G9 material, but the grading modulus was too low.

A CBR value was estimated for each sample at 90%, 93%, 95% and 98% MDD (see Appendix B). The overall resulting CBR values were low with an average of 9.3% obtained at 98% MDD, 6.3% obtained at 95% MDD, 4.0% obtained at 93% MDD and 2.9 at 90% MDD. No swelling occurred in the samples and a grading modulus ranged from 0.71 to 2.15.

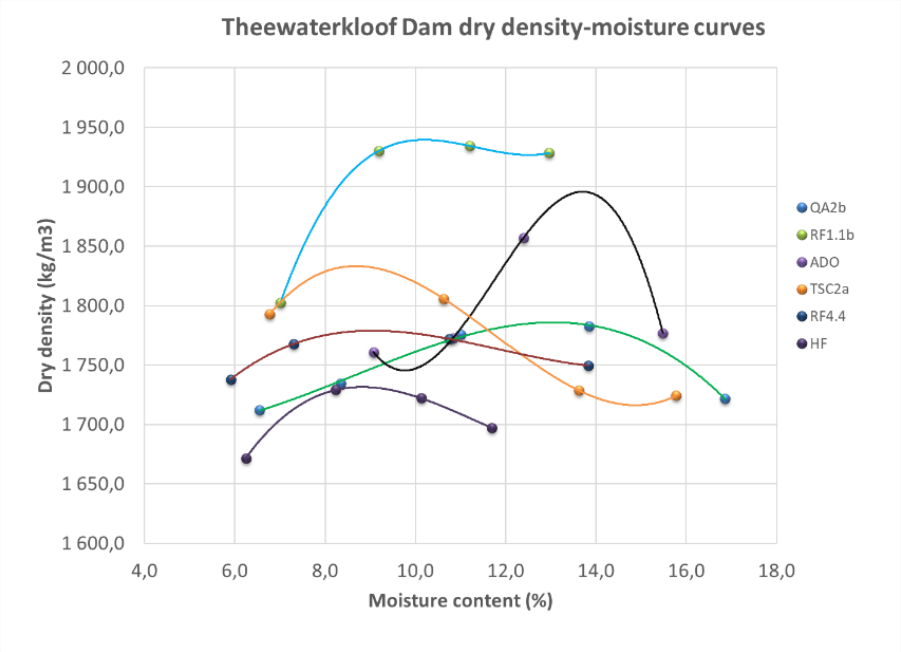

Figure 4.40 Dry density over moisture curve for the Theewaterskloof Dam samples.

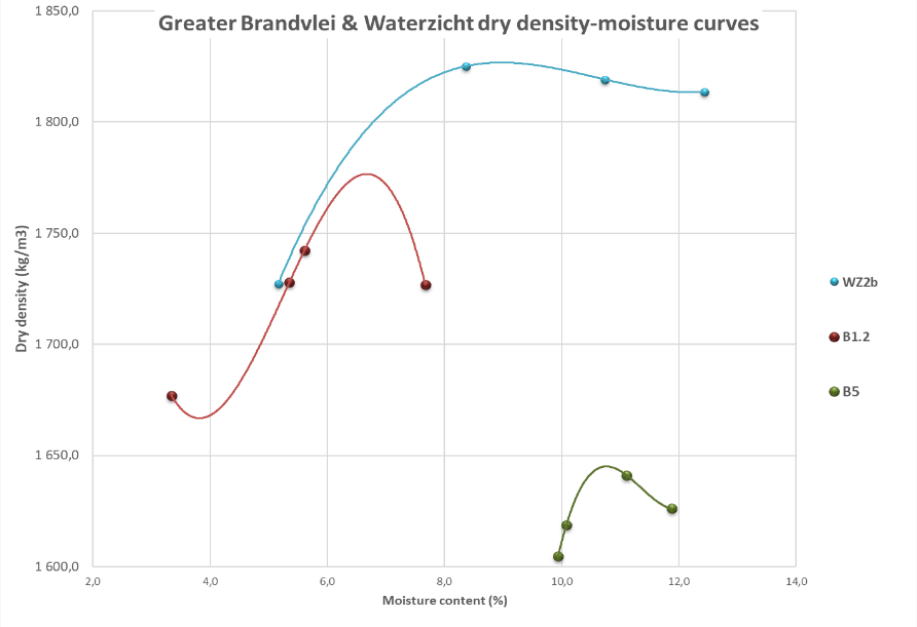

Figure 4.41 Dry density against moisture curve for the Greater Brandvlei and Waterzicht Dam samples.

Table 4.3 Road material classification of the coarse-grained sediment sample as road construction materials based on Colto (1998)

Sample	CBR (%) at 98% MDD	CBR (%) at 95% MDD	CBR (%) at 93% MDD	CBR (%) at 90% MDD	Swell	Grading modulus	Road material classification- Colto (1998)	Road material classification- THR14 (1985)
RF1,1b	6,4	7	7,6	7,8	none	0,71	-	G9
RF4,4	7,2	2	0,8	0,05	none	1,10	-	-
QA2b	6,5	5,5	4,8	4,2	none	0,83	-	G10
TSC2a	22,5	17	3	0,05	none	0,90	-	-
ADO	6,4	6,4	7	6	none	1,04	G9	G10
HF	3,9	0,1	0,05	0,05	none	1,11	-	-
WZ2b	8,5	0,5	0,2	0,05	none	1,13	-	-
B1,2	11,5	6	1	0,5	none	2,15	-	-
B5	11	12,6	11,8	7,4	none	1,48	G8	G8
Average	9,3	6,3	4,0	2,9	1,2			

4.2.2.2 Natural aggregates for concrete, mortar and plaster

The process used for the testing of sediment for natural aggregates was completed in the form of an elimination testing approach based on the criteria for fine aggregates described in SANS 1083 (2017). This method of testing means that a sample must first pass the criteria for an initial test before it can be subjected to further tests. The sequence of the properties that were tested during the elimination analysis approach is illustrated in Figure 3.16 (flow diagram) in Section 3.2.2.

Figure 4.42 illustrates that sample B5 passed the grading criteria and subsequent tests for concrete and mortar, except for the organic impurity test. The failing of the organic impurity test requires the sample to pass the test for soluble deleterious impurities, which sample B5 passed. Sample RF4.4a passed the grading criteria for concrete but failed at the subsequent criteria for percentage dust contents, methylene blue adsorption value as well as percentage clay content.

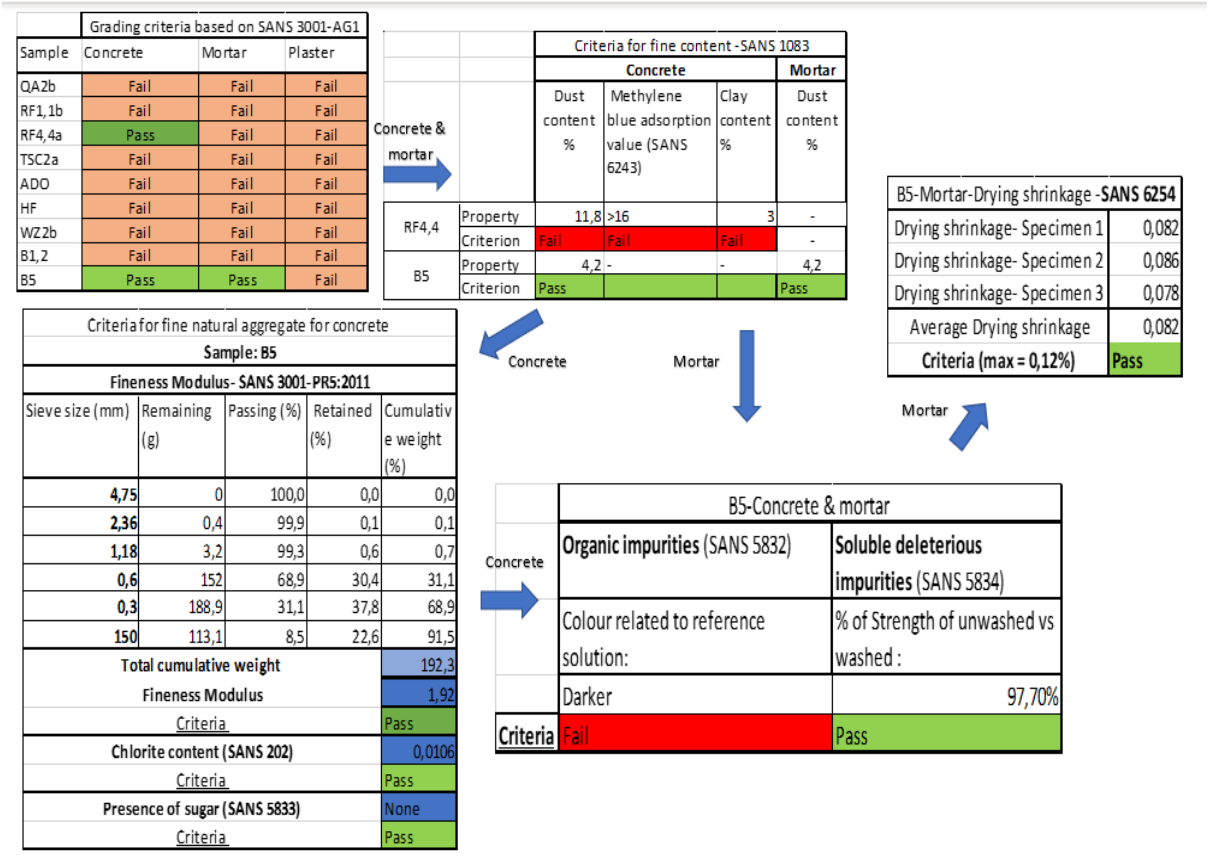

Figure 4.42 The testing procedure flow path for the testing of fine aggregates for concrete, mortar and plaster.

4.2.3 Fine-grained material

Based on the USCS, only sample QA2a classified as fine-grained soil (50% or more passing through the 75µm sieve). However, due to sample WZ2a's high plasticity (26.8) and a moderate fines content (40% of sample passed through the 75µm sieve), the sample was rather analysed for fine-grained construction materials than coarse-grained.

In addition to PI value and grain size, the chemical composition of fine-grained materials plays a significant role in its utilisation in construction. The mineral composition and the major oxides contents were determined through XRD and XRF analyses respectively (Table 4.4 and Table 4.5).

Table 4.4 XRD results for samples QA2a and WZ2a

Sample	Quartz	K-feldspar /Rutile	Plagioclase	Clinochlore	Mica	Kaolinite
QA2a	63%	4%	8%	10%	15%	
WZ2a	85%	5%				10%

Table 4.5 XRF results for samples QA2a and WZ2a

Sample name	Al2O3	CaO	Cr2O3	Fe2O3	K2O	MgO	MnO	Na2O	P2O5	SiO2	TiO2	L.O.I.	Sum Of Conc.
	(%)	(%)	(%)	(%)	(%)	(%)	(%)	(%)	(%)	(%)	(%)	**(%)**	(%)
QA2a	8,29	0,11	bdl	3,63	1,17	0,29	0,02	0,40	0,07	80,01	0,72	5,18	99,89
WZ2a	8,44	0,10	bdl	1,81	1,36	0,24	bdl	0,13	0,01	84,31	0,32	3,25	99,97

4.2.3.1 Lightweight Aggregates

The testing of samples QA2a and WZ2a for lightweight aggregates (LWAs) was based only on the chemical composition of the samples. Table 4.6 indicates which of the minerals and elements that are essential to produce LWAs (Rattanachan and Lorprayoon, 2005) is present in samples QA2a and WZ2a. Both samples failed the criteria due to the absence of major clay minerals in each sample with quartz being the dominant mineral in both samples. Furthermore, the major oxides in Table 4.5 plotted outside Riley's (1951) area of bloating in a ternary diagram (see Figure 4.43). This indicates that the minerals present in these sediments do not possess the required expansive characteristics for LWAs if sintered under temperatures 1100 to 1300°C. If no bloating occurs to the sediment when sintered, the density of will not decrease to the suitable levels required to be used as lightweight aggregate.

Table 4.6 Relating the mineral compositions of samples QA2a and WZ2a with the required mineral compositions described by Rattanachan and Lorprayoon (2005)

Mineral composition for LWA (Rattanachan & Lorprayoon, 2005)	**Sample QA2a**	**Sample WZ2a**
Main minerals		
Kaolinite	-	Present
Smectite	-	-
Illite	-	-
Chlorite	Present	-
Varying concentrations:		
Quartz	Present	-
Feldspars	Present	Present
Carbonates	-	-
Iron oxides	-	-
Hydroxides	-	-
Minor amounts		
Sulphides	-	-
Organic matter	Present	Present
Criteria	Fail	Fail

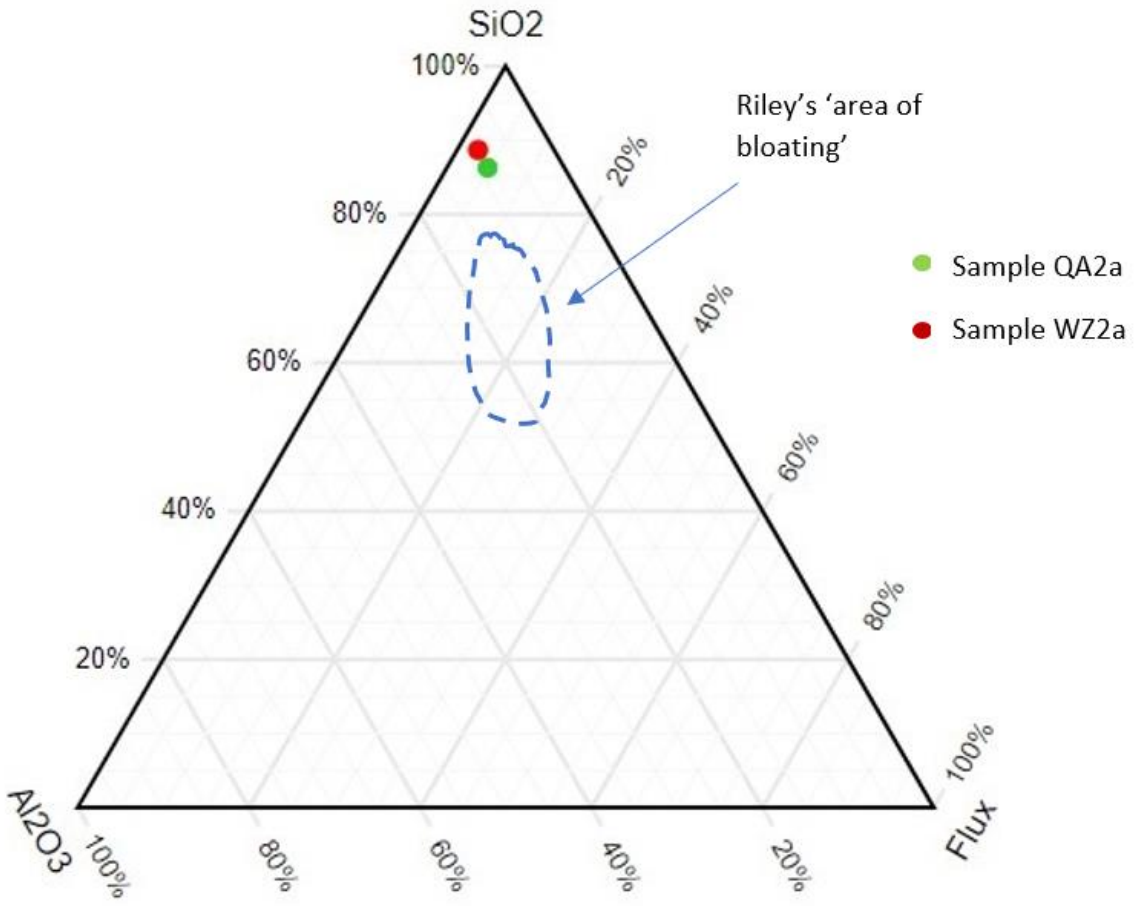

Figure 4.43 Samples QA2a and WZ2a plotting outside Riley's (1951) area of bloating on a ternary diagram.

4.2.3.2 Clay Bricks

The fine-grained samples (QA2a and WZ2a) were analysed to determine if they can be used as a raw material to manufacture VSBK (vertical shaft brick kiln) bricks, normally fired clay bricks and unfired bricks.

To determine if the samples were suitable for the manufacturing of VSBK bricks, the chemical and physical properties for sample WZ2a were related to the properties recommended for VSBK bricks by Prajapati and Maity (2010, see Table 4.7). Most of the chemical and physical properties for sample QA2b and WZ2a failed to meet the recommendations described by Prajapati and Maity (2010). Sample QA2a passed the recommended Fe_2O_3 content, particle soil distribution (PSD) between 0,02-0,063 mm, liquid limit (LL) and plasticity index (PI) whereas sample WZ2a met the recommended loss of ignition value, Na_2O content, particle soil distribution (PSD) between 0,02-0,063 mm and liquid limit. No testing was completed to determine the organic carbon and

volumetric shrinkage in the two samples since the results of these test would have a trivial impact when concluding if samples are suitable as raw materials for bricks. With the majority of the recommendations not reached by sample QA2a and WZ2a, these samples were not considered to be utilised as raw material for VSBK manufacturing.

Table 4.7 The suitable soil properties for manufacturing VSBK bricks VSBK (Prajapati and Maity, 2010). Green indicates a property passed the criterion and red indicates the property failed specific criteria.

Recommended properties for soil to be manufactured as VSBK bricks			
Chemical properties			
	Criteria	**QA2a**	**WZ2a**
Test parameters on dry basis (% by mass)	**Percentage (%)**		
Loss of ignition	3,2	**5,18**	**3,25**
Silica as SiO2	60	**80,01**	**84,31**
Iron as Fe2O3	>3	**3,63**	**1,81**
Alumina as Al2O3	23	**8,29**	**8,44**
Sodium as Na2O	0,1	**0,40**	**0,13**
Potassium as K2O	2,76	**1,17**	**1,36**
Calcium as Cao	Trace	**0,11**	**0,10**
Magnesium as MgO	1,2	**0,29**	**0,24**
Organic Carbon as C	0,8	-	-
Physical properties			
	Criteria	**QA2a**	**WZ2a**
Test parameters on dry basis (% by mass)	**Percentage (%)**		
PSD of 0,063-2 mm	20 - 45	**55**	**62,4**
PSD of 0,02-0,063 mm	25 - 45	**29**	**20,0**
PSD of <0,02 mm	20 - 35	**16**	**15,0**
Liquid limit	25 - 38	**33,3**	**38,7**
Plasticity index	7 to 16	**7,6**	**26,8**
Volumetric shrinkage	15 - 25	**-**	-

To determine if samples QA2a and WZ2a can be used as raw materials for typically fired bricks manufactured in the Western Cape, the mineralogy of the samples was related to the composition of the brick clay deposits, namely Malmesbury clays (Heckroodt,1980).

Table 4.8 lists the minerals that form part of the three deposits and indicates which of these minerals are present in samples QA2a and WZ2a. From the XRD results, QA2a consists of none of the main minerals required for the sediment to classify as a Malmesbury clay deposit except for quartz (63%) which is required in Malmesbury clays. Similarly, sample WZ2a contains mainly quartz (85%), with the small amounts of kaolinite (10%) present, however no illite in the sample not being efficient to be classified as the main mineral. The two samples were discarded based on the absence of the required main minerals described by Heckroodt (1980).

Table 4.8 Correlating the mineralogy of samples QA2a and WZ2a with the mineralogy of the three common brick clays situated in the Western Cape.

Malmesbury Clay (Heckroodt,1980):	Sample QA2a	Sample WZ2a
Main minerals		
Kaolinite	Absent	Present
Quartz	Present	Present
Illite	Absent	Absent
Varying concentrations:		
Iron oxides	Present	Present
Hydroxides	Absent	Absent
Criteria	Fail	Fail

Based on the mineralogy, plasticity and sediment origin (horizontal deposit with no relict structures at the river mouth), sample WZ2a relates mainly to that of sedimentary ball clay (Orris, 1998). However, for the sample to classify as ball clay, the kaolinite percentage must be higher. An increase in kaolinite content of clayey sands may be achieved through the removal of coarser sand grains (predominantly quartz) through screening. However, in brick manufacturing in the Western Cape, ball clay is mainly added to Malmesbury clays to improve extrudability of the brick clay (Cole *et al*., 2014). Based on the abundant resources of good quality brick clays in the Western Cape (twenty-two working pits), the absence of essential minerals associated with brick clay and a low deposit volume in Waterzicht Dam makes it unfeasible to mine these clayey sands for fired clay bricks. The focus should instead be placed on the utilisation of these clayey sands for unfired and non-loadbearing walls, such as internal wall construction.

During the process of moulding soil samples for the manufacturing of unfired brick, sample QA2a was discarded due to the sample lacking the plasticity for efficient moulding. From sample WZ2a, three clay bricks were manually compacted and air-dried for two weeks. Unconfined compression tests resulted in an average of 1.5 MPa for the three manufactured bricks (see Table 4.9). The compression strengths of these bricks fall in the range for typical properties of unfired clay bricks (1 to 4 MPa). However, after air drying, numerous cracks were observed in the bricks (see Figure 4.44), which will make bricks unsuitable as a construction material, since these cracks will be prone to deterioration. A moisture increase of 1 to 6% in unfired bricks caused the compressive strength of the bricks to decrease by approximately 50% (Heath *et al*., 2009).

Table 4.9 The failure loads of three unfired, manual compacted bricks

Brick dimensions		
L (mm)	220	
B (mm)	110	
Area (mm^2)	24200	
Unconfined compression test		
Sample	**Failure load(kN)**	**Compression strength (MPa)**
WZ2a,1	41,44	1,71
WZ2a,2	37,55	1,55
WZ2a,3	29,64	1,22
Average:		1,50

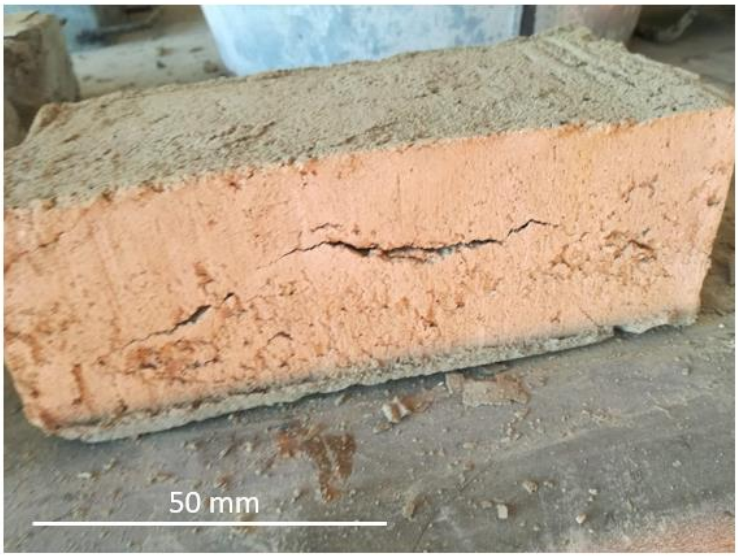

Figure 4.44 Cracks in manual compacted clay brick

4.2.3.3 Landfill clay liners

Table 4.10 shows the measured PI values and the maximum particle size of samples QA2a and WZ2a, together with comments on their properties based on the criterion described by DWAF (1998) as well as the updates to this criterion recorded in the Government Gazette (2013). Sample QA2a passed the maximum particle size criteria but failed the plasticity criteria due to the sample's PI being below the required value of 10 and therefore no further testing was completed on the sample. In comparison, sample WZ2a passed both the maximum particle size and plasticity criteria and therefore further testing for the permeability coefficient (k) was required. Two falling head tests

were completed, and the average k value was calculated from these tests and related to the maximum k value of the three different landfill types described by Government Gazette (2013). The average k value obtained from sample WZ2a passed the criteria for a clay liner design for Class B (for municipal waste) and Class C landfills (for tires and consumer packaging) but were too high for Class A landfill (hazardous waste). The liner design for Class B and C landfill are illustrated in Figure 4.45.

The measured PI and maximum particle size of samples QA2a and WZ2a, together with pass-fail comments regarding these properties based on the criterion described by DWAF (1998).

Table 4.10 Correlating the plasticity index and maximum particle size of samples QA2b and WZ2b with the requirements of DWAF (1998) for landfill liners.

	Plasticity Index (PI)	Criteria (=>10)	Maximum particle size (mm)	Criteria (=<25 mm)
QA2a	7,6	**Fail**	0,425	**Pass**
WZ2a	26,8	**Pass**	4,75	**Pass**

Table 4.11 The permeability coefficient (k) of on sample WZ2b based on the falling head test and the relation of k to the criteria of different landfill classes based on DWAF (1998).

Calculation of the permeability coefficient (k) of sample WZ2b and relation to the different class landfill criteria based on DWAF (1998)			
	95% MDD		
a (m^2)	0,0000186		
L (m)	0,13		
A (m^2)	0,24		
Δt (s)	136,17	106,98	170,8
h1 (m)	0,315	0,285	0,26
h2 (m)	0,285	0,26	0,225
k (m/s)	7,5E-09	8,8E-09	8,7E-09
Average: k (m/s)	8,3E-09		
Clay liner criteria (DWAF,1998 and Government Gazette, 2013)			
Class A	**Class B**	**Class C**	
Fail	**Pass**	**Pass**	

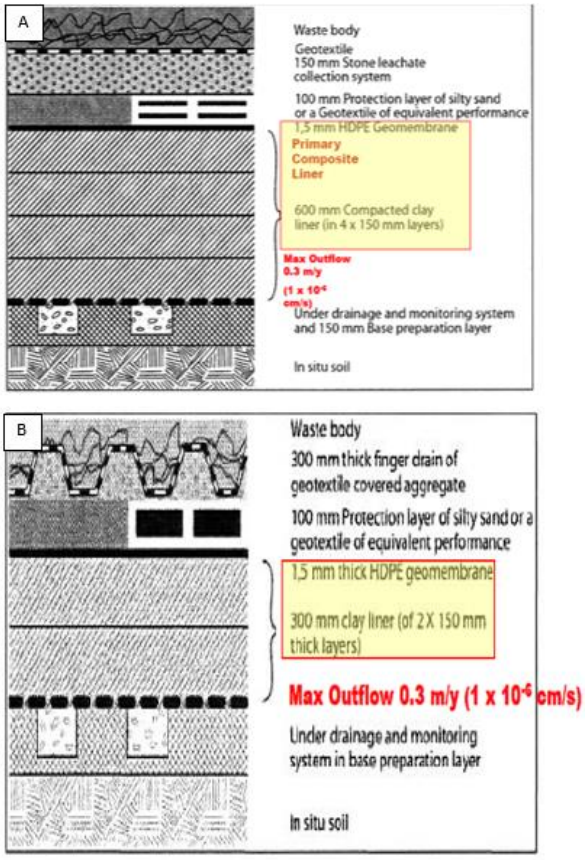

Figure 4.45 Liner designs for A) class B landfill and B) class C landfill medium and large general landfill profile with significant leachate content which needs to be managed (Government Gazette,2013).

4.3 Cost model for sediment removal

4.3.1 Sediment volume calculations

The average depth and total zone area estimated in Sections 4.1.1 to 4.1.3 were used to roughly estimate the dry sediment volume located at each analysed zone (see Table 4.12). It is important to note that the depth of the water table was inserted into the calculation of average depth since the water table prohibited the calculation of exact layer depth.

The sediment volume for Theewaterskloof Dam was estimated at 2,623,009 m^3, with silty sands (SM) making out 2,613,158m^3 and lean clays (CL) only representing 9,851m^3 of the total mapped area. The storage capacity of the reservoir will only increase with 0,55% if all the mapped sediment is to be removed.

The Greater Brandvlei Dam recorded a volume of 593,470 m^3 of poorly graded sand (SP), from which zone B5 consisted of 515,235m^3 poorly graded sand (SP) and B1 only of 78,235m^3 poorly graded

sand (SP). The storage capacity of the Greater Brandvlei Dam will increase with 0.13% if all the mapped sediment is removed. It is important to note that the field investigation of the Greater Brandvlei Dam was commenced two months after the field investigation of Theewaterskloof Dam and Waterzicht Dam. During this period rainfall occurred and dam levels increased, therefore less sediment was exposed at Greater Brandvlei Dam in comparison to the time the Theewaterskloof and Waterzicht Dams were investigated.

The sediment volume of the smaller Waterzicht Dam consists of a total volume of 16,438 m^3 of which 12,910m^3 is clayey sand (SC) and 3,528m^3 is silty sand (SM). A storage increases of 2.47% can be achieved if the mapped sediment is removed.

Table 4.12 Volume estimates for the sediment in the analyses exposed surfaces

Theewaterskloof Dam				
Silty sands (SM)	Area (m^2)	Average depth (m)	Volume (m^3)	Dam storage increase if sediment removed (%)
Zone RF (RF1 to RF2)	623066	0,5	311533	0,06%
Zone RF (Shoreline to RF4,3)	183052	0,7	128136,4	0,03%
Zone RF (RF4,3 to dam bank)	236434	0,1	23643,4	0,00%
Zone QA	75779	1,3	98513	0,02%
Zone TT	105182	0,27	28399	0,01%
Zone GF	54496	0,2	10899	0,00%
Zone TSC	1612925	0,9	1451633	0,30%
Zone ADO	158652	1,5	237978	0,05%
Zone TF	31285	1	31285	0,01%
Zone HF	253164	1,15	291139	0,06%
Total volume (m^3)			**2613158**	**0,54%**
Lean clays (CL)				
Zone QA	75779	0,13	9851	0,00%
Total volume (m^3)			**9851**	**0,00%**
Total reservoir volume (m^3)			**2623009**	
Total dam storage increase if sediment removed				**0,55%**
Greater Brandvlei Dam				
Poorly graded sand (SP)	Area (m^2)	Average depth (m)	Volume (m^3)	
Zone B1	104313	0,75	78235	0,02%
Zone B5	343490	1,5	515235	0,11%
Total volume (m^3)			**593470**	0,13%
Total reservoir volume (m^3)			**593470**	
Dam storage increase if sediment removed				**0,13%**
Waterzicht Dam				
Clayey sand (SC)	Area (m^2)	Average depth (m)	Volume (m^3)	
Zone WZ	16138	0,8	12910,4	1,94%
Total volume (m^3)			**12910**	1,94%
Silty sands (SM)				
Zone WZ	17640	0,2	3528	0,53%
Total volume (m^3)			**3528**	0,53%
Total reservoir volume (m^3)			**16438**	
Dam storage increase if sediment removed				**2,47%**

4.3.2 Cost models

After the laboratory analyses on the different sediment samples from the three dams were completed, it was concluded that only four samples passed the requirement to be used as construction materials.

Three samples from Theewaterskloof Dam (representing silty sands in zone RF1, zone QA2 and zone ADO) could be classified as G9 and G10 road material and one sample from Greater Brandvlei Dam (representing zone B5) could be classified as G8 road material. The removal of these sediments were not considered to be feasible due to the low quality, major availability and low costs of G8, G9 and G10 materials together with low *in situ* CBR values obtained in these sediment zones (which will require expensive stabilisation if dry excavation is commenced to improve the bearing capacity of the ground) and the minor increase in storage capacity that will be achieved if these sediment zones are removed.

From the Greater Brandvlei Dam, the sample from zone B5 also passed the requirements to be used as a fine aggregate in concrete and mortar. With the absence of significant building sand suppliers in the Worcester area together with the forecast suggesting the construction sector to slightly increase in coming years, the utilisation of the sediments located in zone B5 was considered. A cost model was formulated to determine the removal cost per m^3 sediment and relate it to average costs of conventional fine aggregate R300 per m^3 if it is to be delivered in the Worcester area to determine if the project will be feasible.

The clayey sands from the Waterzicht Dam passed the requirement for clay liners used in Class B and C landfills. The fact that numerous of the Western Cape's landfills face closure due to these landfills reaching their maximum capacity in the coming years, means that the demand for landfill liners will increase due to the requirement for the capping of these landfills and creating bottom linings for new landfills that will need to be constructed. A cost model to determine the removal and transportation costs (costs per m^2) of clayey sands from the Waterzicht Dam for using these CCLs in the area surrounding Klapmuts was formulated. These costs will vary based on the hauling distances to sites and the proportion of the sediment reserve to be removed. Contrary to removal costs for zone B5, the cost model will determine which travelling distances and which proportions

of the sediment reserve should be mined to make the project feasible by keeping total removal and transportation costs at or below R53 per m^2.

No material passed the requirements to be utilised as raw materials for LWAs and clay bricks, hence no cost models were formulated for these materials.

4.3.2.1 Zone B5

Cost models were constructed to estimate the removal costs per specified unit of the poorly graded sand in zone B5. To remove sediment from zone B5, three methods may be considered, namely dry excavation with the aid of sheet piling, dry excavation without sheet piling and dredging. Dry excavation method includes 20-ton excavator(s) and tipper trucks with 16 m^3 capacity (at excavator: a truck ratio of 1:2). For dry excavation to be effective, removal of sediment should only be done in times when water levels are low. However, for the removal of sediments to be undertaken without interruptions due to increase in water levels, the mining site can be kept dry with the aid of sheet piling that block or convey water away from the operation site.

For dredging, an 8-ton amphibious excavator that is attachable to pontoons and with a cutter suction pump (Bell 200) with a 200 m long depositing pipe connected to the excavator's arm, was used. Dredging was selected in the case that the zone will be fully submerged

From quotes received from the industrial sand provider companies closest to Worcester, the purchasing costs together with delivery costs of building sand to be used in concrete and mortar is equal to about R300 per m^3. The latter amount was used as the reference value to indicate at which of the calculated removal costs will the different removal methods be feasible to be used as fine-grained aggregates in the surrounding Worcester area.

From the results of the cost models, five graphs were plotted (each representing a different number of sediment removal units) illustrating the removal costs per m^3 for the respective removal methods against the percentage of the sediment reserve in zone B5 to be removed (see Figure 4.46). Throughout these graphs, the removal costs for dry excavation without sheet piles and dredging were observed to remain below the reference costs of R300 per m^3 and will, therefore, be classified as feasible if five units are the maximum and regardless the removal percentage of the sediment reserve. However, the method of dry excavation with sheet piling will exceed the reference costs in all five graphs. If one, two, three, four and five sediment removal units are used the minimum percentages of the sediment reserve to be removed to remain feasible are 26%, 34%, 39%, 55% and 100% respectively.

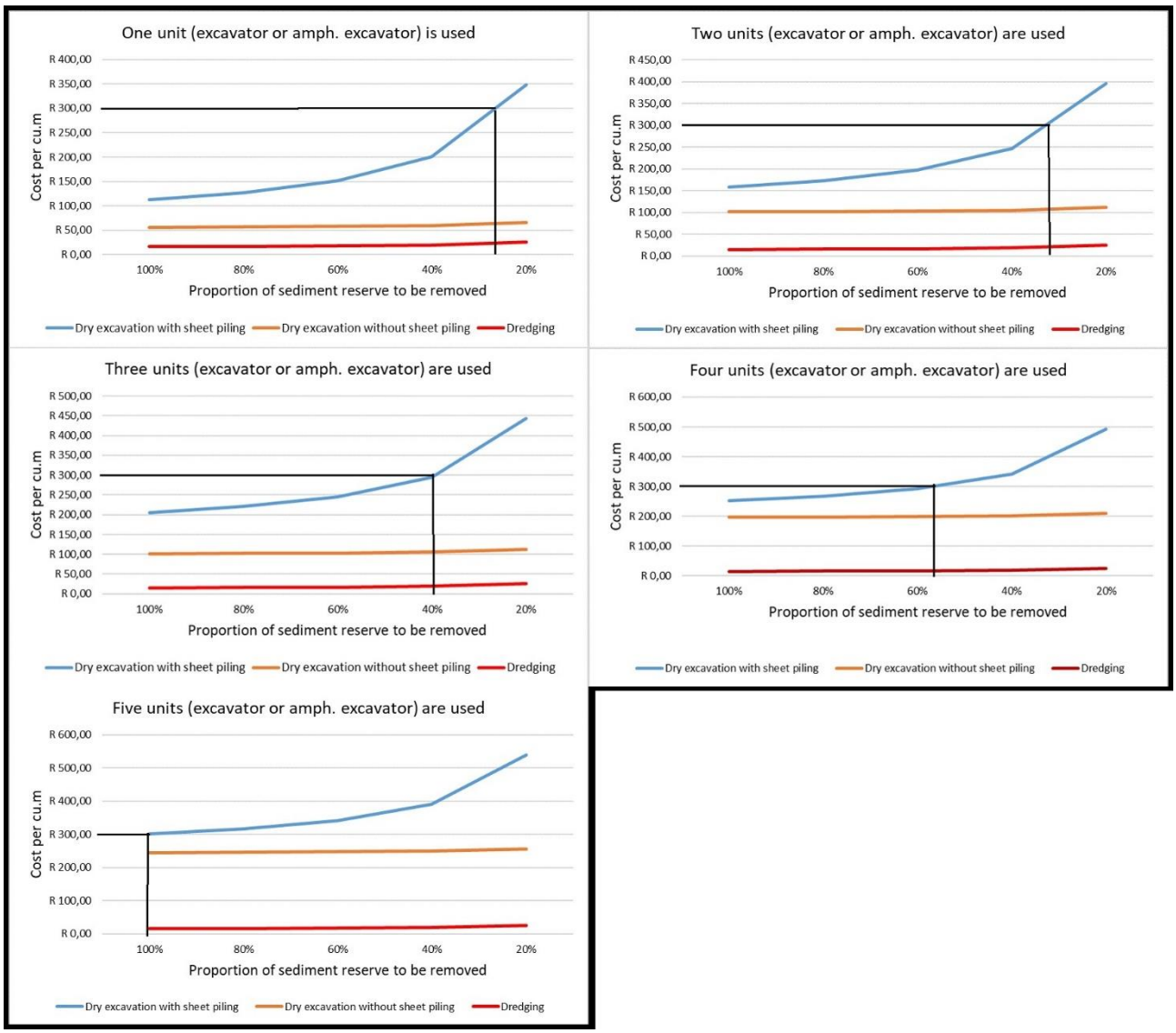

Figure 4.46 The removal costs per m³ against the percentage of B5 zone to be removed with dry excavation (with and without sheet piling) and dredging graphs for the respective number of units used.

From the data in Figure 4.46 the removal costs for dry excavation (with and without sheet piling) increase as the number of units used for sediment removal increase and the percentage of the sediment reserve to be mined decrease. The minimum values for dry excavation with the use of sheet piling and without the use of sheet piling are R112 and R55 respectively if 100% sediment of zone B5 is to be removed with one excavator. If dry excavation with and without sheet piling is undertaken to remove 20% of the sediment reserve with five excavators, the costs will be around R540 and R250 respectively. The addition of pilling to dry excavation will cause the removal cost to double. This is due to the exorbitant costs of R29 155 000 assigned to the installation of sheet piling.

For dredging the removal costs range varies little with the number of amphibian excavators used and the change of proportion of sediment to be removed. The minimum costs (R15.46 per m³)

related to dredging is when three or four amphibian excavators are used to remove 100% of the sediment reserve and the maximum removal costs (R25.94 per m^3) was calculated if five amphibian excavators are used to remove 20% of the sediment reserve.

From the cost models, it is evident that the method of dredging will be most cost-effective. The main reason for this is due to the higher sediment removal rate of the dredging equipment (250 m^3/h, see Table 3.8). The shorter the duration until the specified sediment proportion is removed the more economical the project will be since the hiring days of units will decrease.

The mining of the sediment in zone B5 will, however, only increase the capacity of the Greater Brandvlei Dam with 0.11%.

4.3.2.2 Waterzicht Dam

For the removal of the clayey sands in Waterzicht Dam, dry excavation with an excavator and tipper trucks was the only method considered since it will be too expensive to use dredging equipment on such a small area.

In Excel, a cost model was designed to estimate the removal and transport costs of 1 m^2 of CCL for both Class B and Class C landfills. The calculation consists of three main variables, namely the total volume of sediment to be removed, the transport distance from the dam to where clay liners are to be installed and the number tipper trucks used to transport the material. For the material to be feasible for use as clay liner, the cost per m^2 must be equal or less than the average material costs obtained for GCLs which is about R53 per m^2.

Table 4.13 indicates the results of the cost model which designed to estimate the amount (in percentage) of the clayey sands reserve from Waterzicht Dam to be mined to achieve R53 per m^2 over five different travel distances to Class B landfills. No values were obtained to be less or equal to the reference amount of R53 per m^2 and therefore these sediments cannot be feasibly mined and hauled for distances over 5 km.

Table 4.13 The minimum proportion of sediment reserve to be removed for respective distances to achieve a feasible removal and transportation costs of Class B landfill liners.

Minimum percentage of sediment volume to be removed	**100%**	**100%**	**100%**	**100%**	**100%**
Transport distance (km)	**5**	**10**	**20**	**50**	**100**
Area coverable by CCL (ha)	1,8	1,8	1,8	1,8	1,8
Number of tipper trucks	**3**	**3**	**3**	**3**	**2**
Number of days for sediment to be removed					
Sediment excavation and transport cost	R741 491,03	R941 123,23	R1 283 349,86	R2 310 029,74	R5 760 814,91
Legal costs	R235 000,00	R235 000,00	R235 000,00	R235 000,00	R235 000,00
Maintenance (5% of dredging and transport costs)	R37 074,55	R47 056,16	R64 167,49	R115 501,49	R288 040,75
Infrastructure cost	R98 000,00	R98 000,00	R98 000,00	R98 000,00	R98 000,00
Total project cost	R1 111 565,58	R1 321 179,39	R1 680 517,35	R2 758 531,23	R6 381 855,66
Removal cost per 1 m3 sediment	R86,10	R102,33	R130,17	R213,67	R494,32
Class B: Cost to cover 1 m2 with CCL	**R60,27**	**R71,63**	**R91,12**	**R149,57**	**R346,02**

Similarly, Table 4.14 comprises of the minimum proportions of the clayey sands reserve from Waterzicht Dam to be mined for the similar five travel distances to Class C landfill. These results show that for transport distances of 5 to 20 km, the minimum proportions that the sediment reserve can be mined range from 29% to 57% respectively. From 50 km to 100 km, the clayey sands of Waterzicht cannot be feasibly mined.

Table 4.14 The minimum proportion of sediment reserve to be removed for respective distances to achieve a feasible removal and transportation costs of Class C landfill liners.

Minimum percentage of sediment volume to be removed	**29%**	**36%**	**57%**	**100%**	**100%**
Transport distance (km)	**5**	**10**	**20**	**50**	**100**
Area coverable by CCL (ha)	0,5	0,7	1,1	1,8	1,8
Number of tipper trucks	**3**	**3**	**3**	**3**	**3**
Number of days for sediment to be removed	32	25	18	10	4
Sediment excavation and transport cost	R228 151,09	R342 226,63	R741 491,03	R2 310 029,74	R5 760 814,91
Legal costs	R235 000,00	R235 000,00	R235 000,00	R235 000,00	R235 000,00
Maintenance (5% of dredging and transport costs)	R11 407,55	R17 111,33	R37 074,55	R115 501,49	R288 040,75
Infrastructure cost	R98 000,00	R98 000,00	R98 000,00	R98 000,00	R98 000,00
Total project cost	R572 558,64	R692 337,96	R1 111 565,58	R2 758 531,23	R6 381 855,66
Removal cost per 1 m3 sediment	R151,36	R151,06	R151,05	R213,67	R494,32
Class C: Cost to cover 1 m2 with CCL	**R52,98**	**R52,87**	**R52,87**	**R74,78**	**R173,01**

In Table 4.15, the maximum travel distances were calculated through Excel Solver for which sediment removal and transport is to remain feasible. If the mapped sandy clay (SC) is to be fully mined from Waterzicht Dam as clay liner materials for Class B landfills, the maximum transport distance will be 1 km. In contrast, if the mapped sandy clay (SC) is to be fully mined as clay liner materials for Class C landfills, the maximum transport distance will be 25 km.

From the cost models for the Waterzicht Dam, the most economical results are obtained when hauling distances decrease, the material to be removed increase and three tipper trucks are hauling the sediment to the landfill sites.

Table 4.15 The maximum transportation distances for sediment to be used for clay liners in Class B and Class C landfills.

	Class B: Maximum transport distance to for CCL to be feasible	**Class C: Maximum transport distance to for CCL to be feasible**
Percentage of sediment to be removed in zone	100%	100%
Transport distance (km)	**1**	**25**
Class B: Cost to cover 1 m2 with CCL	**R52,15**	R105,73
Class C: Cost to cover 1 m2 with CCL	R26,08	**R52,87**

Chapter 5 : Conclusions and Recommendations

5.1 Conclusions

This study was commenced to investigate the feasibility of removing sediments out of the Western Cape's two largest dams namely the Theewaterkloof and Greater Brandvlei Dams as well as the smaller Waterzicht farm dam to increase the storage capacity of these reservoirs. The feasibility of removing sediment from these reservoirs was based on the sediments' capability to be used as construction materials. Laboratory analyses were conducted on samples derived from these three reservoirs to determine the engineering and chemical properties of these sediments. These properties were correlated with requirements for five types of construction materials, namely road materials, fine aggregates for concrete and mortar, lightweight aggregates, the raw material for clay bricks and clay liners. Each sediment sample represented a zone of sedimentation in each reservoir which was mapped during field analyses. Through calculating the volume of mapped sediment in each zone, the possible storage increases if these sediments were removed was also determined. During the time of field investigation, not all exposed sediments could be mapped due to accessibility issues related to these areas. However, the mapped area still represents a large area of the reservoir and the increase won't be significantly higher if the sediment from restricted areas is also removed.

5.1.1 Theewaterkloof Dam

Based on field and laboratory analyses, the Theewaterkloof Dam sediment consists mainly of silty sands (SM). From the volume estimation, the storage capacity of the Theewaterkloof Dam will only increase by about 0.54%, if all the mapped sediments are removed.

From the laboratory analyses, one sample (ADO) from Theewaterkloof Dam passed the requirements for G9 road materials according to the Colto (1998) specification. Whereas sample RF1.1b passed for G9 material and samples TSC2a and ADO passed the recommendations for G10

materials. The low quality of these sediments together with the low costs and abundance of similar quality materials made it not feasible to be mined to be used for road materials unless road construction occurs adjacent to the sediment zones.

It was concluded that the removal of the mapped sediments from the Theewaterkloof Dam will not be feasible, due to a minor increase in storage capacity from removing these sediments, the sediments only being suitable for low-quality road materials and the exorbitant costs related to sediment removal methods.

5.1.2 Greater Brandvlei Dam.

The Greater Brandvlei Dam is predominantly filled with poorly graded sands (SP) and the removal of these sediments will only contribute to an increase of 0.13% in the capacity of the dam. Sample B5 from Greater Brandvlei Dam passed the requirements for G8 materials (according to Colto, 1998 and THR14, 1985) and fine aggregates to be used in concrete and mortar. Similarly, to G9 and G10 materials, the low quality of these sediments together with the low costs and abundance of similar quality materials contribute to the removal of these materials not being feasible unless it is mined for road construction adjacent to the zone.

The absence of significant building sand suppliers in the Breede Valley Local Municipal district and forecasts predicting an increase in the construction industry in the Western Cape, a cost model was formulated to calculate the removal cost per 1 m^3 related to the different proportions that are to be mined out of the mapped sediment of zone B5. Three methods were investigated for removing the sediment in zone B5, namely dry excavation with the aid of sheet piling, dry excavation without sheet piling and dredging. The dry excavation methods use 20-ton excavator and tipper trucks with 16 m^3 carrying capacity whereas dredging rates were determined with an amphibian excavator attached to a cutter dredger pump and pontoons

From the cost models, it was calculated that each of the three methods can remove sediment feasibly from zone B5. For the methods of dry excavation without sheet piling and dredging the removal costs were considered feasible if any number from one to five sediment removal units were used to remove 20% to 100% of the poorly graded sand (SP) reserve in zone B5. However, the removal cost related to dry excavation with sheet piling will be considered unfeasible for the following scenarios:

- One excavator is used to remove less than 26% of the sediment reserve,
- Two excavators are used to remove less than 34% of the sediment reserve,
- Three excavators are used to remove less than 39% of the sediment reserve,
- Four excavators are used to remove less than 55% of the sediment reserve,
- Five excavators are used to remove less than 100% of the sediment reserve.

If the dam levels of the Greater Brandvlei Dam remain low, dry excavation can be commenced to remove sediments of zone B5 feasibly as fine-grained aggregates for construction purposes in and around the Worcester area. However, dredging these sediments will be a more feasible option (removal costs R15.46 to R25.94 per m^3) when the area is fully submerged compared to costs related to dry excavation with sheet piling (R112 to R540 per m^3) and without sheet piling (R55 to R250 per m^3).

Furthermore, the removal of the sediments from zone B5 will have a small impact on increasing the reservoir's capacity.

5.1.3 Waterzicht Dam

The sediment exposed at the smaller Waterzicht Dam consists mainly of clayey sands (CS) with silty sands (SM) also observed underlying these units. If the exposed sediment is removed, a storage increase of 2.47% will be achieved. Sample WZ2a (representing the clayey sands) passed the requirements to be used as clay liner in Class B and Class C landfills. In Microsoft Excel, it was calculated what it will cost to install CCLs from the clayey sands at different distances from the reservoir.

For the sediment to be feasible to be utilised as CCL, the calculated costs per m^2 of the CCL must be R53,00 or less (average cost for GCLs). The feasibility was estimated at different scenarios relating to hauling distances and the proportion of sediment to be mined. It was estimated that for the clayey sand reserve to be feasibly mined for the use of clay liner in Class B landfills, a maximum hauling distance from the reservoir to the landfill site is within 1 km from each other. Therefore, the utilisation of the clayey sand reserve for Class B landfill will only be feasible if the landfill is constructed on the Waterzicht farm or adjacent to the farm. In comparison, for the clayey sand reserve to be feasibly mined for the use of clay liners for Class C landfills, if transport distance from the dam to landfill site must be within 25 km of each other.

The removal of sediment from Waterzicht dam will have a more significant impact on the storage increase of the dam. In addition, the sediment can be easily removed with dry excavation methods if dam levels are low, with no expensive dredging methods required.

5.2 Recommendations

This study served as a good reference for the possibility of utilising sediment for construction materials. However, due to the limitations that occurred during this study, the findings attained by the study should serve as a basis for future studies on the utilisation of reservoir sediments. Recommendations for future studies based on the utilisation of reservoir sediments as construction materials to improve reservoir capacities include:

- Improving the accuracy of the mapping of exposed sediments by using drone technology and software.
- Estimating the true lateral and vertical extent of dam sediments and the actual storage increase upon removal of these sediments, through detailed investigations involving test pits spaced at close intervals in a grid-like pattern, together with penetration tests such as the standard penetration test (SPT) extending below the water table (retrieving samples to the required depth) should be undertaken.
- Calculating the total volume of sediment in reservoirs through different methods such as hydrography, mathematical and computer models, hydrometry, and remote sensing.
- Performing studies extensively focusing on farm dams where sediment is removed more economically and have a higher impact on increasing the capacity of dams. The private use of material by farmers will make the process less commercialised and thereby lessen the expensive legal fees.

This study concluded that removal costs of sediments out of reservoirs can be alleviated by using these sediments as construction materials. Nevertheless, it will be more beneficial and probably more economic if sediments are prohibited from entering reservoirs. It is recommended that future research should also focus on environmentally friendly methods that will prevent sediments from entering reservoirs.

References

Achour, R., Abriak, N.E., Zentar, R., Rivard, P. and Gregoire, P., 2014. Valorization of unauthorized sea disposal dredged sediments as a road foundation material. Environmental Technology, 35(16), pp.1997-2007.

Alexander, M., 2014. Aggregates and their properties in concrete. [ONLINE] Available at: https://concretesociety.co.za/images/stories/consem2014/presentations/Aggregates%20and%20t eir%20properties%20in%20concrete%20Presentation%20-%20Mark%20Alexander.pdf. [Accessed 11 December 2018].

Alexander, M. and Mindess, S., 2005. *Aggregates in Concrete*. Abingdon, Oxon, United Kingdom: Taylor & Francis.

American Society for Testing and Material (ASTM), 2006. *Standard Practice for Classification of Soils for Engineering Purposes (Unified Soil Classification System),* ASTM D2487–06, West Conshohocken, Pa.

American Society for Testing and Material (ASTM), 2010. *Standard Test Methods for Measurement of Hydraulic Conductivity of Saturated Porous Materials Using a Flexible Wall Permeameter,* ASTM D5084–10, West Conshohocken, Pa.

Annandale, G.W., Morris, G.L. and Karki, P., 2016. *Extending the life of reservoirs: sustainable sediment management for dams and run-of-river hydropower*. The World Bank.

Antipov, V.V., Antipov Yu, V., Brakker, I.I., Brenner, V.A., Naumov Yu, N., Pushkarev, A.E., Pushkarev, V.A., Podkolzin, A.A. and Zhabin, A.B., 2006. Channel dredging method involves cutting ground with working blades of mechanical cutting tools installed on rotary cutting head, which performs horizontal intermittent movement in both directions transversely to axis of rotation. RU122595.

Anupoju, S., 2019. *Soil Moisture Content-Dry Density Relationship*, The Constructor [ONLINE] Available at: https://theconstructor.org/geotechnical/soil-moisture-content-dry-density-relationship/6947/ [Accessed 26 March 2019].

Aras, T.U.C.E., 2009. Cost Analysis of sediment removal techniques from reservoir, Dept. of Civil Engineering, Hydromechanics Laboratory, Middle East Technical University, Ankara, Turkey.

Basson, G.R., 1996. *Hydraulics of reservoir sedimentation* (Doctoral dissertation, Stellenbosch: Stellenbosch University).

Beck, J.S. and Basson, G.R., 2002. Morphological impacts and mitigation measures: control of reservoir sedimentation and environmental flood releases. *Short course, Department of Civil Engineering, University of Stellenbosch*.

Benzerzour, M., Maherzi, W., Amar, M.A., Abriak, N.E. and Damidot, D., 2018. Formulation of mortars based on thermally treated sediments. *Journal of Material Cycles and Waste Management*, *20*(1), pp.592-603.

Boucot, A.J., Brunton, C.H.C. and Theron, J.N., 1983. Implications for the age of South African Devonian rocks in which Tropidoleptus (Brachiopoda) has been found. *Geological Magazine*, *120*(1), pp.51-58. Brink, A.B.A., 1981. Engineering geology of Southern Africa. V. 2.

Bovu Pumps. 2008. Bovu Pumps Ultatrex Machinery SDN. BHD.. [ONLINE] Available at: http://www.bovu-pumps.co.za/bovupump-ultratrex_brochure.pdf. [Accessed 15 February 2019].

Bowen, P., Pearl, R. and Akintoye, A., 2007. Professional ethics in the South African construction industry. *Building Research and Information*, *35*(2), pp.189-205.

Braune, E. and Looser, U., 1989. Cost impacts of sediments in South African rivers. Sediment and the Environment, (184), pp.131-143.

Budget Review 2018, Infrastructure Allocations and the Impact on Construction. Industry Insight Focus Forum, 14 March 2018.

Brink, A.B.A., 1984. *Engineering geology of Southern Africa V.4*, Pretoria: Building Publications

Burton Jr, G.A, 2002. Sediment quality criteria in use around the world. *Limnology*, *3*(2), pp.65-76.

Cape Winelands Professional Practices in Association. 2016. Heritage inventory of, and management plan for, the tangible resources in the Stellenbosch municipality project: Phase 2b report. [ONLINE] Available at: http://www.stellenboschheritage.co.za/wp-content/uploads/Stellenbosch-Heritage-Inventory-Report_Phase-2b_March-2018.pdf. [Accessed 15 January 2019].

COLTO, 1998. *Standard Specifications for Road and Bridge Works for State Road Authorities*, South African Institute of Civil Engineering (SAICE), Pretoria.

Cho, S.W., 2013. Effect of silt fines on the durability properties of concrete. *Journal of Applied Science and Engineering 16*(4), pp.425-430.

City of Cape Town. 2018. Dam levels report. [ONLINE] Available at: https://resource.capetown.gov.za/documentcentre/Documents/City%20research%20reports%20and%20review/damlevels.pdf. [Accessed 1 February 2018].

Chen, H.J., Yang, M.D., Tang, C.W. and Wang, S.Y., 2011. Producing synthetic lightweight aggregates from reservoir sediments. *Construction and Building Materials*, *28*(1), pp.387-394.

Cheng, Y.L., Wee, H.M., Chen, P.S., Kuo, Y.Y. and Chen, G.J., 2014. Innovative reservoir sediments reuse and design for sustainability of hydroelectric power plants. *Renewable and Sustainable Energy Reviews*, *36*, pp.212-219.

Chun, S.H., Hwang, H.J. and Byun, Y.H., 2015. Green supply chain management in the construction industry: Case of Korean construction companies. *Procedia-Social and Behavioural Sciences*, *186*, pp.507-512.

Clay Brick Association of South Africa. 2016. Survey of Informal Clay Brick Making | Clay Brick Association of South Africa. [ONLINE] Available at: http://www.claybrick.org/survey-informal-clay-brick-making. [Accessed 17 December 2018].

Climate-Data. 2019. *Paarl climate: Average Temperature, weather by month, Paarl weather averages - Climate-Data.org*. [ONLINE] Available at: https://en.climate-data.org/africa/south-africa/western-cape/paarl-9597/. [Accessed 17 January 2019].

Climate-Data. 2019. *Villiersdorp climate: Average Temperature, weather by month, Villiersdorp weather averages - Climate-Data.org*. [ONLINE] Available at: https://en.climate-data.org/africa/south-africa/western-cape/villiersdorp-21924/. [Accessed 17 January 2019].

Climate-Data. 2019. *Worcester climate: Average Temperature, weather by month, Worcester weather averages - Climate-Data.org*. [ONLINE] Available at: https://en.climate-data.org/africa/south-africa/western-cape/worcester-9598/. [Accessed 17 January 2019].

Cole, D.I. and Viljoen, J.H.A., 2001. *Building sand potential of the greater Cape Town area*, Pretoria, South Africa: Council for Geoscience.

Cole, D.I., 2003. The metallogeny of the Cape Town area. Explanation of metallogenic map sheet 3318 (scale: 1: 250 000). *Publication, Council for Geoscience, South Africa*.

Cole, D.I., 2013. The metallogeny of the Calvinia area: Explanation and metallogenic map of sheet 3118 (scale 1: 250 000).

Cole, D.I., Ngcofe, L. and Halenyane, K., 2014. Mineral Commodities in the Western Cape Province, South Africa. *Council for Geoscience, Western Cape Regional Office, Report*, *12*, pp.90.

Construction Industry Development Board, 2018, Construction monitor: Supply and demand. [ONLINE] Available at: http://www.cidb.org.za/publications/Documents/Construction%20Monitor%20-%20April%202018.pdf [Accessed 14 December 2018].

Corrosionpedia. 2019. What is Sediment? - Definition from Corrosionpedia. [ONLINE] Available at: https://www.corrosionpedia.com/definition/1014/sediment [Accessed 07 January 2019]

Council of Geosciences. 1997. Geological map of Sheet 3319 Worcester (scale 1:250 000). Publication, Council for Geosciences, South Africa.

De Nobili, M., Francaviglia, R. and Sequi, P., 2002. Retention and mobility of chemicals in soil. In Developments in Soil Science (Vol. 28, pp. 171-196). Elsevier.

Department of Mineral Resources. 2018. Western Cape | Department of Mineral Resources. [ONLINE] Available at: http://www.dmr.gov.za/mineral-policy-promotion/operating-mines/western-cape?search=ZIMCO. [Accessed 12 December 2018].

Department of Water Affairs and Forestry. 1998. Minimum requirements for waste disposal by landfill. [ONLINE] Available at: http://sawic.environment.gov.za/documents/266.PDF. [Accessed 22 February 2019].

Department of Water Affairs and Forestry. 2009. Western Cape Water Reconciliation Strategy. [ONLINE] Available at: http://www.dwaf.gov.za/Documents/Other/WMA/19/WCWRSNewsletterMarch09.pdf. [Accessed 31 January 2018].

Department of Water and Sanitation. 2018. Weekly State of the Reservoirs on 2018-01-29. [ONLINE] Available at: http://www.dwa.gov.za/Hydrology/Weekly/Weekly.pdf. [Accessed 29 January 2018].

Department of Water and Sanitation. 2018. List of DWS Dams, Available at: www.dwa.gov.za/Documents/DWS_DAMS%20LIST%20INTERNET.pdf [Accessed 16 Aug. 2018].

Du, Y. and Li, H., 2010. Mechanical technology for dyke reinforcement by sediment discharge in the lower reaches of the Yellow River. Yellow River Conservancy Press, *Chengdong Lu, Zhengzhou, Henan,* 450004.

Diop, S., Stapelberg, F., Tegegn, K., Ngubelanga, S. and Heath, L., 2011. A review on problem soils in South Africa. *Council for Geoscience*, *6*, pp.1-48.

Elzinga, L., 2017. Dredging of Reservoirs. MSc Thesis. Delft University of Technology, Delft.

Fan, J. and Morris, G.L., 1992. Reservoir sedimentation. I: Delta and density current deposits. *Journal of Hydraulic Engineering*, *118*(3), pp.354-369.

Frimmel, H.E., 2000. New U-Pb zircon ages for the Kuboos pluton in the Pan-African Gariep belt, South Africa: Cambrian mantle plume or far field collision effect? *South African Journal of Geology*, *103*(3-4), pp.207-214.

Fujimoto, T. and Tadasu, O., 1998. The development of underwater dredging system for rocky sea bottom at narrow channel. In Underwater Technology, 1998. Proceedings of the 1998 International Symposium on (pp. 340-345). IEEE.

Government Gazette, 2013. Republic of South Africa Regulation Gazette. Opengazettes. Available at: https://archive.opengazettes.org.za/archive/ZA/2013/government-gazette-ZA-vol-578-no-36784-dated-2013-08-23.pdf [Accessed 3 Apr. 2019].

GeoForm International. 2019. What is Dredging? | Benefits of Dredging, How Dredging Works, & More. [ONLINE] Available at: https://geoforminternational.com/sediment-removal-101/. [Accessed 08 January 2019]

Gunatilake, H.M. and Gopalakrishnan, C., 1999. The economics of reservoir sedimentation: a case study of Mahaweli reservoirs in Sri Lanka. International Journal of Water Resources Development, 15(4), pp.511-526.

Gresse, P.G., Von Veh, M.W., and Frimmel, H.E., 2006. Namibian (Neoproterozoic) to early Cambrian successions. *The Geology of South Africa.* Geological Society of South Africa, Johannesburg/Council of Geoscience, Pretoria, pp.395-406.

Hälbich, I.W., Fitch, F.J. and Miller, J.A., 1983. Dating the Cape orogeny. In *Geodynamics of the Cape Fold Belt*. Special Publication 12. Geological Society of South Africa, pp. 75–100.

Hamer, K. and Karius, V., 2002. Brick production with dredged harbour sediments. An industrial-scale experiment. *Waste Management*, *22*(5), pp.521-530.

Heath, A., Walker, P., Fourie, C. and Lawrence, M., 2009. Compressive strength of extruded unfired clay masonry units. *Construction Materials*, *162*, pp.105-12.

Hill, R.S., Theron, J.N., Cole, D.I., Roberts, D.L. and Mulholland, B.J., 1992. The geology and mineral resources of the Greater Cape Town region. Report, Geological Survey of South Africa, pp.-28.

Heckroodt, R.O., 1980. The brickmaking clays of the Western Cape. *Annals, Geological Survey of South Africa*, *13*, pp.1-8.

Howard, C.D.D., 2000. Operations, monitoring and decommissioning of dams. *Thematic Review IV*, *5*.

Hung, M.F. and Hwang, C.L., 2007. Study of fine sediments for making lightweight aggregate. *Waste Management & Research*, *25*(5), pp.449-456.

Hwang, C.L., Bui, L.A.T., Lin, K.L. and Lo, C.T., 2012. Manufacture and performance of lightweight aggregate from municipal solid waste incinerator fly ash and reservoir sediment for self-consolidating lightweight concrete. *Cement and Concrete Composites*, *34*(10), pp.1159-1166.

IADC Dredging. 2013. Water Injection Dredging. *Facts About*, (01).

Available at: https://www.iadc-dredging.com/ul/cms/fck-uploaded/documents/PDF%20Facts%20About/facts-about-water-injection-dredging.pdf [Accessed 13 October 2018]

IADC Dredging. 2014. Backhoe Dredgers. *Facts About*, (03),

Available at: http://www.iadc-dredging.com/ul/cms/fck-uploaded/documents/PDF Facts About/facts-about-backhoe-dredgers.pdf [Accessed 13 October 2018].

IADC Dredging. 2014. Cutter Suction Dredgers. *Facts About*, (02).

Available at: http://www.iadc-dredging.com/ul/cms/fck-uploaded/documents/PDF Facts About/facts-about-cutter-suction-dredgers.pdf [Accessed 13 October 2018].

IADC Dredging. 2014. Trailing Suction Hopper Dredger. *Facts About*, (01),

Available at: https://www.iadc-dredging.com/ul/cms/fck-uploaded/documents/PDF%20Facts%20About/facts-about-trailing-suction-hopper-dredgers.pdf [Accessed 13 2018].

Jennings, J.E., Brink, A.B.A. and Williams, A.A., 1973. *Revised guide to soil profiling for civil engineering projects in Southern Africa*. Civil Engineering= Siviele Ingenieurswese, 15(9), pp.251-252.

Junakova, N., Junak, J. and Balintova, M., 2015. Reservoir sediment as a secondary raw material in concrete production. *Clean Technologies and Environmental Policy*, *17*(5), pp.1161-1169.

Leschohier, J., 2007. How do compact tractor-loader-backhoes add up to other compact construction equipment? For Construction Pros [ONLINE] Available at: https://www.forconstructionpros.com/equipment/earthmoving-compact/tractor-loader-backhoes/article/10117628/how-do-compact-tractorloaderbackhoes-add-up-to-other-compact-construction-equipment. [Accessed 30 July 2019].

Kleyn, E.G., 1984. Aspects of pavement evaluation and design as determined with the Dynamic Cone Penetrometer. *MEng thesis (in Afrikaans), Faculty of Engineering, University of Pretoria, Pretoria*.

Koś, K. and Zawisza, E., 2016. Landfill liners from dam reservoir sediments. *Annals of Warsaw University of Life Sciences–SGGW. Land Reclamation*, *48*(1), pp.41-52.

Krishnappan, B.G., 1975. Dispersion of dredged spoil when dumped as a slug in deep water. First International Symposium on Dredging Technology.

Krizek, R.J., Giger, M.W. and Jin, J.S., 1975. Dewatering of dredged materials by evaporation. *[No source information available]*.

Mahdy, M., 2016. Structural Lightweight Concrete Using Cured LECA. [ONLINE] Available at: http://www.ijeit.com/Vol%205/Issue%209/IJEIT1412201603_05.pdf. [Accessed 14 December 2018].

Maher, A., Douglas, W.S., Jafari, F. and Pecchioli, J., 2013. The processing and beneficial use of fine-grained dredged material. A manual for engineers, Rutgers Center for Advanced Infrastructure and Transportation.

Maherzi, W., Benzerzour, M., Mamindy-Pajany, Y., Van Veen, E., Boutouil, M. and Abriak, N.E., 2018. Beneficial reuse of Brest-Harbor (France)-dredged sediment as alternative material in road building: laboratory investigations. *Environmental technology*, *39*(5), pp.566-580.

Manap, N. and Voulvoulis, N., 2015. Environmental management for dredging sediments–The requirement of developing nations. *Journal of Environmental Management*, *147*, pp.338-348.

Methvin. 2012. Bulk Excavation. [ONLINE] Available at: https://www.methvin.org/construction-production-rates/excavation/bulk-excavation. [Accessed 31 July 2019].

Mezencevova, A., Yeboah, N.N., Burns, S.E., Kahn, L.F. and Kurtis, K.E., 2012. Utilization of Savannah Harbor river sediment as the primary raw material in production of fired brick. *Journal of Environmental Management*, *113*, pp.128-136.

Millrath, K., Kozlova, S., Shimanovich, S. and Meyer, C., 2001. Beneficial use of dredged material 2. *Progress report prepared for Echo Environmental, Inc., Columbia University, New York, NY*.

Mineral Products Association, 2019. Lightweight concrete. [ONLINE] Available at: https://www.concretecentre.com/Performance-Sustainability-(1)/Special-Concrete/lightweight-concrete.aspx. [Accessed 10 January 2019].

Miraoui, M., Zentar, R. and Abriak, N.E., 2012. Road material basis in dredged sediment and basic oxygen furnace steel slag. *Construction and Building Materials*, *30*, pp.309-319.

Morris, G.L. and Fan, J., 1998. Reservoir sediment handbook. McGraw-Hill Book Co., New York

Morris, G.L., Annandale, G. and Hotchkiss, H., 2008. Reservoir Sedimentation. In García M.H, *Sedimentation Engineering - Processes, Measurements, Modelling, and Practice*. American Society of Civil Engineers (ASCE), pp. 1

Mueller, A., Sokolova, S.N. and Vereshagin, V.I., 2008. Characteristics of lightweight aggregates from primary and recycled raw materials. *Construction and Building Materials*, *22*(4), pp.703-712.

Mulligan, C.N., Yong, R.N. and Gibbs, B.F., 2001. An evaluation of technologies for the heavy metal remediation of dredged sediments. *Journal of Hazardous Materials*, *85*(1-2), pp.145-163.

Najafi, F., Chegenizadeh, A. and Nikraz, H., 2012. A Review on GCL Performance in Geotechnical Engineering. *International Journal of Biological, Ecological and Environmental Sciences*, *1*(3), pp.104-107.

Netterberg, F., 1998. Road-construction materials *in* The Mineral Resources of South Africa (M.G.C. Wilson and C.R. Anhaeusser, editors): *Handbook, Council for Geoscience, 16, pp. 575-583*.

Ngcofe, L. and Cole, D.I., 2014. The distribution of the economic mineral resource potential in the Western Cape Province. *South African Journal of Science*, *110*(1-2), pp.1-4.

One Stop Rental, 2019. What's the Difference Between an Excavator and Backhoe [ONLINE] Available at: https://www.onestoprent.com/whats-the-difference-between-an-excavator-and-backhoe/. [Accessed 30 July 2019].

Oxford Dictionaries | English. 2019. dredge | Definition of dredge in English by Oxford Dictionaries. [ONLINE] Available at: https://en.oxforddictionaries.com/definition/dredge [Accessed 08 January 2019].

Paipai, E., 2003. Beneficial uses of dredged material: Yesterday, today and tomorrow. Terra et aqua, pp.3-12.

Palm, J., 2017. Landfill Site Status Summary Table.

Pienaar, N.,2017, *The aggregate and sand industry in South Africa*.[ONLINE] Available at: http://www.aspasa.co.za/PDFs/THE-AGGREGATE-AND-SAND-INDUSTRY-IN-SA.pdf. [Accessed 14 December 2018].

Pillay, P. and Mafini, C., 2017. Supply chain bottlenecks in the South African construction industry: Qualitative insights. *Journal of Transport and Supply Chain Management*, *11*(1), pp.1-12.

Prajapati, S. and Maity, S., 2010. Vertical Shaft Brick Kiln- Operation Manual. [ONLINE] Available:https://www.researchgate.net/publication/272475622_Vertical_Shaft_Brick_Kiln_VSBK_Technologyfor_small_and_medium_Brick_Entrepreneur_and_Operational_Manual [Accessed 8 February 2019].

PricewaterhouseCoopers, 2017. *SA's emerging companies face a multitude of challenges-but there is room for improvement: PwC report* [ONLINE] Available at: https://www.pwc.co.za/en/assets/pdf/sa-construction-december-2013.pdf [Accessed 14 December 2018].

Quantec Research. 2018. Regional service. [Online] Available at: https://www.easydata.co.za [Accessed 17 December 2018].

Orris, G.J., 1998. *Additional descriptive models of industrial mineral deposits*. US Department of the Interior, US Geological Survey.

Rattanachan, S. and Lorprayoon, C., 2005. *Korat clays as raw materials for lightweight aggregates*. Science Asia, 31, pp.277-281.

Resource Management Services. 2015. Proposed waste recovery, beneficiation and energy project, Drakenstein Municipality, Western Cape. [ONLINE] Available at:

http://www.drakenstein.gov.za/docs/Documents/Annexure A Public%20Participation%20Report.pdf [Accessed 16 January 2019].

Riley, C.M., 1951. Relation of chemical properties to the bloating of clays. *Journal of the American Ceramic Society*, *34*(4), pp.121-128.

RME, 2017.Backhoes and Excavators-What's the Difference? [ONLINE] Available at: http://www.rmewa.com.au/backhoes-and-excavators-whats-the-difference/: [Accessed 30 July 2019].

Roberts, D.L., 2001. The geology of Melkbosstrand and environs. Explanation and Geological Map of Sheet 3318CB (1:50 000). Council for Geoscience, 50p.

Roberts, D.L., Botha, G.A., Maud, R.R., Pether, J. and Johnson, M.R., 2006. Coastal Cenozoic deposits. *The geology of South Africa. Johannesburg/Pretoria: Geological Society of South Africa/Council for Geoscience*, pp.605-628.

Roberts, D.L., Viljoen, J.H.A., Macey, P., Nhleko, L., Cole, D.I., Chevallier, L., Gibson, L. and Stapelberg, F., 2008. The geology of George and environs. *Explanation and geological map of sheets 3322CD and 3422AB (1: 50 000). Pretoria: Council for Geoscience*.

Saussaye, L., Van Veen, E., Rollinson, G., Boutouil, M., Andersen, J. and Coggan, J., 2017. Geotechnical and mineralogical characterisations of marine-dredged sediments before and after stabilisation to optimise their use as a road material. *EnvironmentalTechnology*, *38*(23), pp.3034-3046.

Schantz, S.L., Gasior, D.M., Polverejan, E., McCaffrey, R.J., Sweeney, A.M., Humphrey, H.E. and Gardiner, J.C., 2001. Impairments of memory and learning in older adults exposed to polychlorinated biphenyls via consumption of Great Lakes fish. *Environmental Health Perspectives*, *109*(6), p.605.

Scheepers, R. and Schoch, A.E., 2006. The Cape Granite Suite. *The geology of South Africa*, pp 421-430.

Scholtz D.L., 1946. On the younger Pre-Cambrian granite plutons in the Cape Granites. *Proc. Geological Society of South Africa.* pp 35-82.

Siegfried, H.P., 1993. *The Malmesbury Batholith and its relationship to granitic plutons in the Swartland tectonic domain*.

Shankar, M.U. and Muthukumar, M., 2017. Comprehensive review of geosynthetic clay liner and compacted clay liner. In *IOP Conference Series: Materials Science and Engineering* (Vol. 263, No. 3, p. 032026). IOP Publishing.

South African National Standard, 2006. *Chloride content of aggregates,* SANS202:2006, SABS Standards Division, Pretoria.

South African National Standard, 2006. *Mortar tests - Initial drying shrinkage and wetting expansion of mortar,* SANS 6254:2006, SABS Standards Division, Pretoria.

South African National Standard, 2006. *Soluble deleterious impurities in fine aggregates (limit test)*, SANS 5834:2006, SABS Standards Division, Pretoria.

South African National Standard, 2007. *Burnt clay masonry units,* SANS227:2007, SABS Standards Division, Pretoria.

South African National Standard, 2008. *Deleterious clay content of the fines in aggregate (methylene blue adsorption indicator test),* SANS 6243:2008, SABS Standards Division, Pretoria.

South African National Standard, 2009. *Aggregates from natural sources – Fine aggregates for plaster and mortar,* SANS 1090:2009, SABS Standards Division, Pretoria.

South African National Standard, 2011. *Computation of soil-mortar percentages, coarse sand ratio, grading modulus and fineness modulus.* SANS3001 Part PR5, SABS Standards Division, Pretoria.

South African National Standard, 2011. *Organic impurities in fine aggregates (limit test),* SANS 5832:2006*,* SABS Standards Division, Pretoria.

South African National Standard, 2011. *Part PR5: Computation of soil-mortar percentages, coarse sand ratio, grading modulus and fineness modulus,* SANS 3001-PR5:2011*,* SABS Standards Division, Pretoria.

South African National Standard, 2014. *Particle size analysis of aggregates by sieving,* SANS 3001-AG1:2014, SABS Standards Division, Pretoria.

South African National Standard, 2017. *Aggregates from natural sources-Aggregates for concrete,* SANS 1083:2017, SABS Standards Division, Pretoria.

Subramani, T. and Suresh, B., 2015. Experimental Investigation of Using Ceramic Waste As A Coarse Aggregate Making A Light Weight Concrete. *International Journal of Application or Innovation in Engineering & Management (IJAIEM)*, *4*(5), pp.153-162.

Sutton, A., Black, D. and Walker, P., 2011. *Unfired clay masonry: An introduction to low-impact building materials*. IHS BRE Press.

Technical Methods for Highways (TMH), 1984. *Measurement of the in situ strength of soils by dynamic cone penetrometer (DCP),* THM6-ST6:1984, State Road Authorities (CSRA), Pretoria.

Technical Methods for Highways (TMH), 1986. *Standard Methods of Testing Road Construction Materials,* TMH1*,* [ONLINE] Available at http://asphalt.csir.co.za/tmh/tmh1.htm [Accessed 22 February 2019].

Thamm, A.G., Johnson, M.R., Anhaeusser, C.R. and Thomas, R.J., 2006. The Cape Supergroup. *The geology of South Africa*, pp.443-459.

Thorn, M.F.C., 1975. Loading and consolidation of dredged silt in a trailer suction hopper dredger.

The Concrete Institute, 2018. Product Information-Lightweight Aggregate. [ONLINE] Available at: https://docs.wixstatic.com/ugd/5586b6_101fe6f775bf4b87901d092e1dba95ff.pdf. [Accessed 14 December 2018].

The Constructor, 2007. Types of Soil Excavation Tools and Machines in Construction. [ONLINE] Available at: https://theconstructor.org/construction/types-of-soil-excavation-tools-machines/12307/. [Accessed 30 July 2019].

Theron, J.N. 1972. *The stratigraphy and sedimentation of the Bokkeveld Group.* D.Sc. thesis (unplub.) Univ. Stellenbosch, 175 pp.

Technical Recommendations for Highways (TRH), 1985. Guidelines for road construction materials, TRH-14:1985, [ONLINE] Available at: http://www.gauteng.gov.za/Document%20Library/Roads%20and%20Transport/TRH14-%20Guidelines%20for%20Road%20Construction%20Materials.pdf. [Accessed 22 February 2019].

Tribout, C., Husson, B. and Nzihou, A., 2011. Use of treated dredged sediments as road base materials: Environmental assessment. *Waste and Biomass Valorization*, *2*(3), pp.337-346.

United States Environmental Protection Agency (US EPA), 2005. Contaminated sediment remediation guidance for hazardous waste sites.

Van Rijn, L.C., 2013. Sedimentation of Sand and Mud in Reservoirs in Rivers. Available at: https://www.leovanrijn-sediment.com Accessed 30 July 2018].

Veh, V. and Wolter, M., 1982. *Aspects of the structure, tectonic evolution and sedimentation of the Tygerberg Terrane, southwestern Cape Province* (Doctoral dissertation, University of Cape Town).

Vlasblom, W.J., 2004. Dredging Equipment and Technology, Ch. 6-Bucket (Ladder) Dredger. *Delft University of Technology*.

Vorosmarty, C. J., Meybeck, M., Fekete B., Sharma K., Green, P., and Syvitski, J. P. M., 2003. Anthropogenic sediment retention: Major global impact from registered river impoundments, Global Planet. Change, 39, 169–190.

Walling, D.E., 1999. Linking land use, erosion and sediment yields in river basins. In *Man and River Systems* (pp. 223-240). Springer, Dordrecht.

Wang, H.Y., Sheen, Y.N. and Hung, M.F., 2010. Performance characteristics of dredged silt and high-performance lightweight aggregate concrete. *Computers and Concrete*, *7*(1), pp.53-62.

Welte, A., 1975. New processes of unloading trailing suction hopper dredgers. First International Symposium on Dredging Technology.

Western Cape Government Provincial Treasury. 2018. Provincial Economic Review and Outlook 2018. [ONLINE] Available at: https://www.westerncape.gov.za/assets/departments/treasury/Documents/Research-and-Report/2018/2018_mero_revised.pdf. [Accessed 17 December 2018].

White, R., 2001. *Evacuation of sediments from reservoirs. Thomas Telford, London*

Zentar, R., Abriak, N.E., Dubois, V. and Miraoui, M., 2009. Beneficial use of dredged sediments in public works. *Environmental technology*, *30*(8), pp.841-847.

Appendix A: Rates used in cost models for sediment removal

Table A- 1: Rates used in the cost models for sediment removal

Information cost required for determining project costs				
Machinery	Wet rates per hour	Establishment costs	Total cost	Description for use
Excavator with 0,5 m3 bucket (20 ton)	R695,40	R5 600,00	Dependant on the number of days required to work	For the use of dry excavation of sediment
Tipper trucks (16m3)	R798,00	R3 192,00		The excavator loads excavated sediment directly onto tipper truck which transport it dumping site.
120 Grader	R7 592,40	R30 369,60		For road construction
Water truck (600 lite)	R240,00	R960,00		Required for wetting of liner material and road material before compaction
TLB (Tractor-Loader-Backhoe)	R350,00	R4 800,00		Required in assisting geotechnical engineer with determining the depth of sediment. Stockpile management.
Amphibious Excavator (8 ton)	R1 333,33			Excavator that may become semi-submerged
Amphibious Excavator (8 ton) + hydraulic cutter suction pump with 200 m long pipe	R2 188,89			Addition of hydraulic cutter suction pump in place of bucket. The pipe that connects to cutter suction pump and the ear were sediment is deposited
Amphibious Excavator (8 ton) + hydraulic cutter suction pump with 200 m long pipe pontoons	R3 022,22	R8 625,00		Addition of side pontoons required if water is 2 to 3 meters deep
Legal costs				
Mining rights			R1 000 000,00	Rough estimate based mining right, which is required for area over 5 ha is to be mined. These cost include application fees, environment assessments studies, social and labour plans studies etc.
Mining permit			R235 000,00	Rough estimate based mining permit, which is required for area under 5 ha that is to be mined. These cost include environment assessments studies, application fees and rehabilitation fees.
Addition costs				
Pilling :		R355 000,00		
Installation costs			R12 600 000,00	The installation cost for sheet piles over a length of 1200 m. The sheet pile serves as barrier to dam level as well as water increase. This installation is only used for the option of dry excavation
Extraction costs			R16 200 000,00	
Construction costs of a 200m road to Waterzicht Dam			R95 000,00	The cost related to stripping of vegetation and constructing a path consisting only out of subbase. This road will allow access for excavator and tipper trucks to the Waterzicht Dam
Additional cost related to dredging			R100 000,00	Cost related to sieving and dehydrating sediments, construction of depositing site for saturated sediments
Geotechnical studies at zone B5	R1 000,00		Dependant on the number of days required to work	Required for determining the depths of dam surface and bearing capacities at zone B5
Maintenance			5 % Equipment cost	Maintenance costs related to breakdowns and machine services
Infrastructure				
Portable Toilets			R3 000,00	Required infrastructure for labour
Storage container			R25 000,00	Required infrastructure to store equipment
Office container			R25 000,00	Required infrastructure for labour
Screens			R10 000,00	Infrastructure required to ensure the applicable particle size distribution is retained
Personal				
Site manager	R714,29		Dependant on the number of days required to work	Supervision of mining activities
Health and Safety officer	R990,00			Responsible for health and safety on mine location
Additional labour	R120,00			General workers
Geotechnical studies at zone B5	R1 000,00			Required for determining the depths of dam surface and bearing capacities at zone B5

Table A- 2 Additional costs related to dry excavation

Dry excavation of B5- Additional costs		
Site preparation costs		
Geotechnical engineer		
Rate per hour	R1 000,00	
Rate per day		**R9 000,00**
TLB hire		
Rate per hour (wet)	R350,00	
Rate per day (wet)		**R3 150,00**
Establishment cost		**R4 800,00**
Road construction with G5 material		
Water truck		
Rate per hour (wet)	R250,00	
Rate per day (wet)	R2 250,00	
Days	5,00	
Establishment cost		**R1 000,00**
Water truck total		**R11 250,00**
Compactor		
Rate per hour (wet)	R364,80	
Rate per day (wet)	R3 283,20	
Days	**5,00**	
Establishment cost		**R4 800,00**
Compactor total		**R1 824,00**
Cost of G5 material required		**R243 000,00**
Excavator		
Rate per hour (wet)	R695,40	
Rate per day (wet)	R6 258,60	
Days	**5,00**	
Total cost related to excavator		**R31 293,00**
Total		**R278 824,00**
Sheet pilling (9m in height)		
Installation Cost per linear 1 m	R10 500,00	
Total Installation Cost		**R12 600 000,00**
Establishment cost		**355 000**
Extraction of Sheet Piles per m2	1500	
Total Extraction Cost		**16200000**
Total piling		**R29 155 000,00**
Total additional cost for dry excavation		R29 433 824,00

Appendix B: Soil profiles

Table B- 1 Soil profiles of subzones RF1 and RF2.

Zone RF1	
Test hole ID	RF1.1
Distance from shoreline (m)	27
Description	**Depth (m)**
Slightly moist, dark brown, loose, intact, medium-grained (0.4-0.6mm in grain size) sand of alluvial origin.	0 -0.5
Water table preventing the measuring of full depth of sediment layer.	<0.5
Test hole ID	RF1.2
Distance from shoreline (m)	64
Description	**Depth (m)**
Slightly moist, dark brown, loose, intact, medium-grained (0.4-0.6mm in grain size) sand of alluvial origin.	0-0.5
Shale bedrock	<0.5
Test hole ID	RF1.3
Distance from shoreline (m)	117
Description	**Depth (m)**
Slightly moist, dark brown, loose, intact, medium-grained (0.4-0.6mm in grain size) sand of alluvial origin.	0-0.3
Slightly moist, grey, very stiff, mottled with red strips residual soil (weathered bedrock)	<0.3
Test hole ID	RF1.4
Distance from shoreline (m)	165
Description	**Depth (m)**
Slightly moist, dark brown, loose, intact, medium-grained (0.4-0.6mm in grain size) sand of alluvial origin.	0-0.5
Loose material detected with DCP testing.	0.5-1.4
Bedrock reached with DCP testing	<1.4

Zone RF2	
Test hole ID	RF2.1
Distance from shoreline (m)	100
Description	**Depth (m)**
Slightly moist, dark brown, loose, intact, medium-grained (0.4-0.6mm in grain size) sand of alluvial origin.	0-0.5
Pebble-rich bedrock	<0.5
Test hole ID	RF2.2
Distance from shoreline (m)	217
Description	**Depth (m)**
Slightly moist, dark brown, loose, intact, medium-grained (0.4-0.6mm in grain size) sand of alluvial origin.	0-0.5
Loose material detected with DCP testing.	0.5-1.25
Bedrock reached with DCP testing	<1.25

Zone RF1	
Test hole ID	RF4.1
Distance from shoreline (m)	52
Description	**Depth (m)**
Slightly moist, dark brown, loose, intact, medium-grained (0.4-0.6mm in grain size) sand of alluvial origin.	0 -0.4
Slightly moist, brownish yellow, loose, intact, medium-grained (0.4-0.6mm in grain size) sand of alluvial origin.	0.4-0.5
Loose material detected with DCP testing.	0.5-0.95
Bedrock reached with DCP testing	<0.95
Test hole ID	RF4.2
Distance from shoreline (m)	140
Description	**Depth (m)**
Slightly moist, dark brown, loose, intact, medium-grained (0.4-0.6mm in grain size) sand of alluvial origin.	0-0.5
Slightly moist, grey, very stiff, mottled with red strips residual soil (weathered bedrock)	<0.5
Test hole ID	RF4.3
Distance from shoreline (m)	270
Description	**Depth (m)**
Slightly moist, dark brown, loose, intact, medium-grained (0.4-0.6mm in grain size) sand of alluvial origin.	0-0.3
	<0.3
Test hole ID	RF4.4
Distance from shoreline (m)	70
Description	**Depth (m)**
Slightly moist, dark brown, loose, intact, medium-grained (0.4-0.6mm in grain size) sand of alluvial origin.	0-15
Slightly moist, grey, very stiff, mottled with red strips residual soil (weathered bedrock)	<0.15

Table B- 2 Soil profiles of zone QA.

Zone QA	
Test hole ID	QA2.1
Distance from shoreline (m)	40
Description	**Depth (m)**
Slightly moist, light brown, firm, intact silt (chalky feel on teeth) of alluvial origin.	0-0.1
Slightly moist, dark brown medium-grained, loose, intact (0.4-0.6mm in grain size) sand rich in organic matter was observed. At lower depth sand become saturated and colour change from dark brown to light grey was observed.	0-0.6
Water table preventing the measuring of full depth of sediment layer.	<0.6
Test hole ID	QA2.2
Distance from shoreline (m)	100
Description	**Depth (m)**
Slightly moist, light brown, firm, intact silt (chalky feel on teeth) of alluvial origin.	0-0.13
Dark brown, slightly moist, medium-grained (0.4-0.6mm in grain size) sand rich in organic matter was observed. At lower depth sand become saturated and change colour from dark brown to light grey was observed.	0.13-1.2
Water table preventing the measuring of full depth of sediment layer.	<1.2
Test hole ID	QA2.3
Distance from shoreline (m)	200
Description	**Depth (m)**
Slightly moist, light brown, firm, intact silt (chalky feel on teeth) of alluvial origin.	0-0.16
Slightly moist, dark brown medium-grained, very loose, intact (0.4-0.6mm in grain size) sand rich in organic matter was observed. At lower depth sand become saturated and colour change from dark brown to light grey was observed.	0.16-1.00
Water table preventing the measuring of full depth of sediment layer.	<1.00

Table B- 3 Soil profiles of zone TT.

Zone TT	
Test hole ID	T1.1
Distance from shoreline (m)	23
Description	**Depth (m)**
Slightly moist, light brown, loose, intact, medium-grained (0.4-0.6mm in grain size) sand of alluvial origin.	0-0.45
Stiff, weathered bedrock	<0.45
Test hole ID	TT1.2
Distance from shoreline (m)	57
Description	**Depth (m)**
Slightly moist, light brown, loose, intact, medium-grained (0.4-0.6mm in grain size) sand of alluvial origin.	0-0.15
Stiff, weathered bedrock	<0.15
Test hole ID	TT1.3
Distance from shoreline (m)	114
Description	**Depth (m)**
Slightly moist, light brown, loose, intact, medium-grained (0.4-0.6mm in grain size) sand of alluvial origin.	0-0.2
Stiff, weathered bedrock	<0.2

Table B- 4 Soil profiles of zone GF.

Zone GF	
Test hole ID	GF1.1
Distance from shoreline (m)	10
Description	**Depth (m)**
Slightly moist, light brown, loose, intact, medium-grained (0.4-0.6mm in grain size) sand of alluvial origin.	0-0.7
Water table preventing the measuring of full depth of sediment layer	<0.7
Test hole ID	GF1.2
Distance from shoreline (m)	33
Description	**Depth (m)**
Slightly moist, light brown, loose, intact, medium-grained (0.4-0.6mm in grain size) sand of alluvial origin.	0-0.15
Stiff, weathered bedrock	<0.15
Test hole ID	GF1.3
Distance from shoreline (m)	45
Description	**Depth (m)**
Slightly moist, light brown, loose, intact, medium-grained (0.4-0.6mm in grain size) sand of alluvial origin.	0-0.2
Stiff, weathered bedrock	<0.2

Table B- 5 Soil profiles of zone TSC.

Zone TSC	
Test hole ID	TSC2.1
Distance from shoreline (m)	45
Description	**Depth (m)**
Slightly moist, dark brown, loose, intact, medium-grained (0.4-0.6mm in grain size) sand of alluvial origin.	0-0.2
Slightly moist, yellowish brown, loose, intact, medium-grained (0.4-0.6mm in grain size) sand of alluvial origin.	0.2-0.65
Stiff, weathered bedrock	<0.65
Test hole ID	TSC2.2
Distance from shoreline (m)	190
Description	**Depth (m)**
Dark Brown, slightly moist, medium-grained (0.4-0.6mm in grain size) sand of alluvial origin.	0-0.3
Cobble rich bedrock	<0.3
Test hole ID	TSC2.3
Distance from shoreline (m)	279
Description	**Depth (m)**
Slightly moist, dark brown, loose, intact, medium-grained (0.4-0.6mm in grain size) sand of alluvial origin.	0-0.5
Slightly moist, yellowish brown, loose, intact, medium-grained (0.4-0.6mm in grain size) sand of alluvial origin.	0.5-0.9
Loose material detected with DCP testing.	0.9-1.2
Bedrock reached with DCP testing	<1.2

Table B- 6 Soil profiles of zone ADO.

Zone ADO	
Test hole ID	ADO1.1
Distance from shoreline (m)	180
Description	**Depth (m)**
Slightly moist, dark brown, loose, intact, medium-grained (0.4-0.6mm in grain size) sand of alluvial origin.	0-0.4
Water table preventing the measuring of full depth of sediment layer	<0.4
Test hole ID	ADO1.1
Distance from shoreline (m)	245
Description	**Depth (m)**
Slightly moist, dark brown, loose, intact, medium-grained (0.4-0.6mm in grain size) sand of alluvial origin.	0-1,4
Water table preventing the measuring of full depth of sediment layer	<1.4
Test hole ID	ADO1.1
Distance from shoreline (m)	323
Description	**Depth (m)**
Slightly moist, dark brown, loose, intact, medium-grained (0.4-0.6mm in grain size) sand of alluvial origin.	0-1.55
Water table preventing the measuring of full depth of sediment layer.	<1.55

Table B- 7 Soil profiles of zone TF.

Zone TF	
Test hole ID	TF2.1
Distance from shoreline (m)	20
Description	**Depth (m)**
Slightly moist, dark brown , firm, intact, silt (chalky feel on teeth) of alluvial origin	0-0.15
Moist, dark brown-orgainic rich, very loose, intact, medium-grained (0.4-0.6mm in grain size) sand of alluvial origin.	0.15 -1.28
Water table preventing the measuring of full depth of sediment layer.	<1.28

Table B- 8 Soil profiles of zone LL.

Zone LL	
Test hole ID	LL1.1
Distance from shore line (m)	20
Description	**Depth (m)**
Slightly moist, light brown, very loose, intact, fine-grained (0.06 to 0.2 mm) sand of alluvial origin.	0-0.1
Slightly moist, light brown, very loose, intact, medium-grained (0.4-0.6mm in grain size) sand of alluvial origin.	0.2-0.25
Slightly moist, light yellow, very loose, intact, medium-grained (0.4-0.6mm in grain size) sand of alluvial origin.	0.25-0.35
Stiff, weathered bedrock	<0,35
Test hole ID	LL1.3
Distance from shore line (m)	112
Description	**Depth (m)**
Yellow weathered wacke with dark subangular grains (3-5mm)	0-0.1
Slightly moist, red to yellowish, loose, intact, medium to coarse grained(5-15 mm) gravel with minor amounts of silt (gritty feel on teeth) which is derived from weathered conglomerate	0.1 -0.32
Soft weathered shale	<0.32

Table B- 9 Soil profiles of zone HF.

Zone HF	
Test hole ID	HF2.1
Distance from shoreline (m)	174
Description	**Depth (m)**
Slightly moist, dark brown, loose, intact, medium-grained (0.4-0.6mm in grain size) sand of alluvial origin.	0-0.15
Slightly moist, light brown, loose, intact, medium-grained (0.4-0.6mm in grain size) sand of alluvial origin.	0.15-0.5
Loose material detected with DCP testing.	0.5-1.03
Bedrock reached with DCP testing	<1.03
Zone HF	
Test hole ID	HF2.2
Distance from shoreline (m)	130
Description	**Depth (m)**
Slightly moist, dark brown, loose, intact, medium-grained (0.4-0.6mm in grain size) sand of alluvial origin.	0-0.5
Loose material detected with DCP testing.	0.5-1.3
Bedrock reached with DCP testing	< 1.3

Table B- 10 Soil profiles of zone B1.

Zone B1	
Test hole ID	B1.2
Distance from shore line (m)	130
Description	**Depth (m)**
Slightly moist, reddish-brown, very loose, intact, coarse-grained sand to fine-grained gravel (0.7-5mm) of alluvial origin	0-0.14
Moist, light brown, very loose, intact, fine-grained sand (0.06 to 0.2 mm) of alluvial origin	0.14 - 0.15
Slightly moist, reddish-brown, very loose, intact, coarse-grained sand to fine-grained gravel (0.7-5mm) of alluvial origin	0.15 - 0.56
Water table preventing the measuring of full depth of sediment layer.	< 0.56
Test hole ID	B1.3
Distance from shore line (m)	147
Description	**Depth (m)**
Slightly moist, reddish-brown, very loose, intact, coarse-grained sand to fine-grained gravel (0.7-5mm) of alluvial origin	0-0.2
Moist, light brown, very loose, intact, fine-grained sand (0.06 to 0.2 mm) of alluvial origin	0.2-0.3
Slightly moist, reddish-brown, very loose, cross-laminated, coarse-grained sand to fine-grained gravel (0.7-5mm) of alluvial origin	0.3-0.9
Water table preventing the measuring of full depth of sediment layer.	<0.9
Zone B1	
Test hole ID	B1.4
Distance from shore line (m)	160
Description	**Depth (m)**
Slightly moist, reddish-brown, very loose, intact, coarse-grained sand to fine-grained gravel (0.7-5mm) of alluvial origin	0-0.6
Water table preventing the measuring of full depth of sediment layer.	< 0.6

Table B- 11 Soil profiles of zone B5.

Zone B5	
Test hole ID	B5.1
Distance from shore line (m)	85
Description	**Depth (m)**
Slightly mois, light brown, slightly moist, very loose, intact fine to medium to coarse-grained sand (1-2 mm) and fine gravel (2.5-5mm) of an alluvial origin	0-0.36
Water table preventing the measuring of full depth of sediment layer.	<0.36
Test hole ID	B5.2
Distance from shore line (m)	111
Description	**Depth (m)**
Slightly mois, light brown, slightly moist, very loose, intact fine to medium to coarse-grained sand (1-2 mm) and fine gravel (2.5-5mm) of an alluvial origin	0-0.43
Water table preventing the measuring of full depth of sediment layer.	<0.43
Test hole ID	B5.3
Distance from shore line (m)	209
Description	**Depth (m)**
Slightly mois, light brown, slightly moist, very loose, intact fine to medium to coarse-grained sand (1-2 mm) and fine gravel (2.5-5mm) of an alluvial origin	0-0.6
Water table preventing the measuring of full depth of sediment layer.	<0.6
Test hole ID	B5.4
Distance from shore line (m)	339
Description	**Depth (m)**
Slightly mois, light brown, slightly moist, very loose, intact fine to medium to coarse-grained sand (1-2 mm) and fine gravel (2.5-5mm) of an alluvial origin	0-0.55
Water table preventing the measuring of full depth of sediment layer.	<0.55

Table B- 12 Soil profiles of subzones WZ1 and WZ2.

Zone WZ1		Zone WZ2	
Test hole ID	WZ1.1	**Test hole ID**	WZ2.1
Distance from shoreline (m)	12	**Distance from shoreline (m)**	12
Description	**Depth (m)**	**Description**	**Depth (m)**
Slightly moist, brown, loose, medium-grained (0.3-0.6mm) sand of alluvial origin	0.00-0.05	Moist, grey, soft, intact, very fine-grained (chalky feel on teeth), silt of alluvial origin. Isolated coarser grains (0.5-1.5mm) also present within sediment	0-0.25
Slightly moist, grey with orange mottled textures, stiff, very fine-grained (grains felt on nails) , silt of alluvial origin with intact structure. Isolated coarser grains (0.5-1.5mm) also present within sediment	0.05-0.3	Moist, dark grey (change to light grey at lower depths), very loose, medium-grained (0.3-0.6mm) sand and of alluvial origin.	0.25-0.4
Slightly moist, grey with orange mottled textures, very stiff (prohibitting further excavation), intact, very fine-grained (grains felt on nails) , silt of alluvial origin with intact structure. Isolated coarser grains (0.5-1.5mm) also present within sediment	<0.3	Water table preventing the measuring of full depth of sediment layer.	<0.4
Test hole ID	WZ1.2		
Distance from shoreline (m)	30		
Description	**Depth (m)**		
Slightly moist, brown, loose, medium-grained (0.3-0.6mm) sand of alluvial origin	0.00-0.15		
Grey, slightly moist, with orange mottled textures, stiff, very fine-grained (chalky feel on teeth) , silt of alluvial origin with intact structure. Isolated coarser grains (0.5-1.5mm) also present within sediment	0.15-0.25		
Slightly moist, grey with orange mottled textures, very stiff (prohibitting further excavation), intact, very fine-grained (grains felt on nails) , silt of alluvial origin with intact structure. Isolated coarser grains (0.5-1.5mm) also present within sediment	<0.25		
Test hole ID	WZ1.3		
Distance from shoreline (m)	50		
Description	**Depth (m)**		
Slightly moist, brown, loose, medium-grained (0.3-0.6mm) sand of alluvial origin	0.00-0.15		
Grey, slightly moist, with orange mottled textures, stiff, very fine-grained (chalky feel on teeth) , silt of alluvial origin with intact structure. Isolated coarser grains (0.5-1.5mm) also present within sediment	0.15-0.35		
Slightly moist, grey with orange mottled textures, very stiff (prohibitting further excavation), intact, very fine-grained (grains felt on nails) , silt of alluvial origin with intact structure. Isolated coarser grains (0.5-1.5mm) also present within sediment	<0.35		

Appendix C: DCP number (DN) against depth graphs

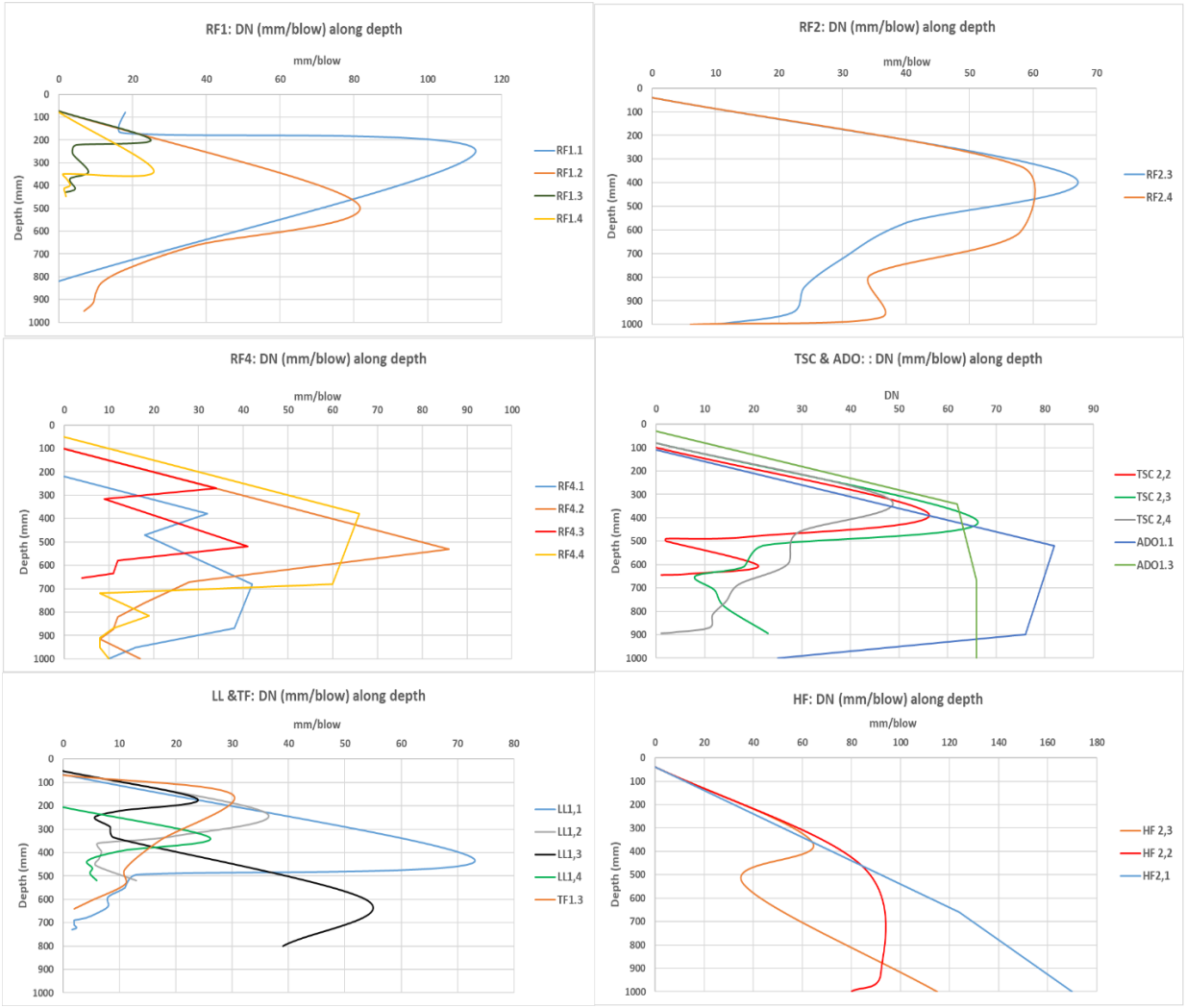

Figure C - 1 DCP number (DN) against depth graphs for zones demarcated in the Theewaterskloof Dam.

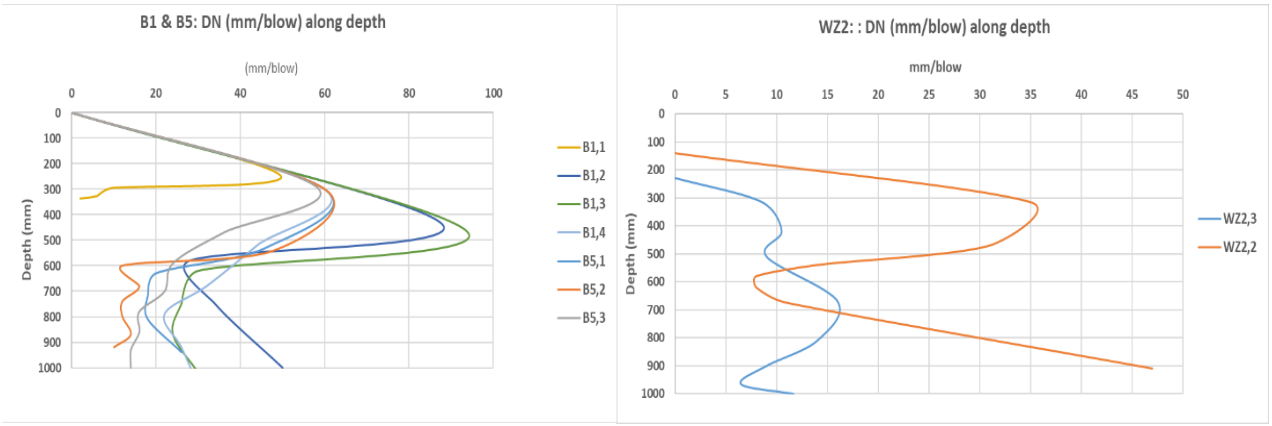

Figure C - 2 DCP number (DN) against depth graphs for zones demarcated in the Greater Brandvlei and Waterzicht Dams.

Appendix D: CBR against dry density graphs for the samples tested for road materials

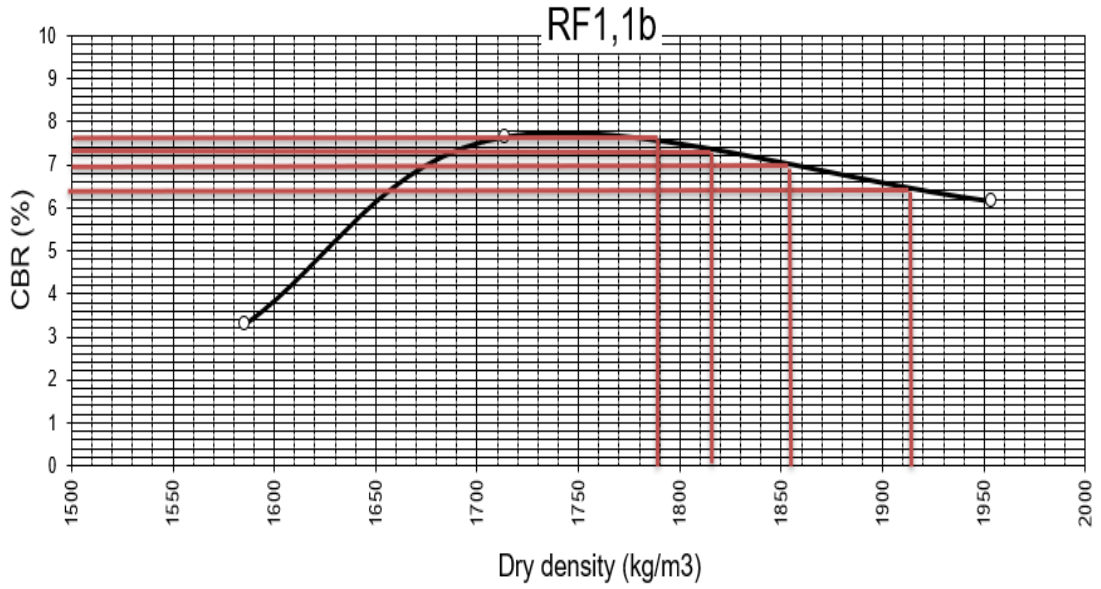

Figure C- 1: CBR against dry density curves indicating the CBR values related to 93%,95% and 98% of MDD value for sample RF1.1b

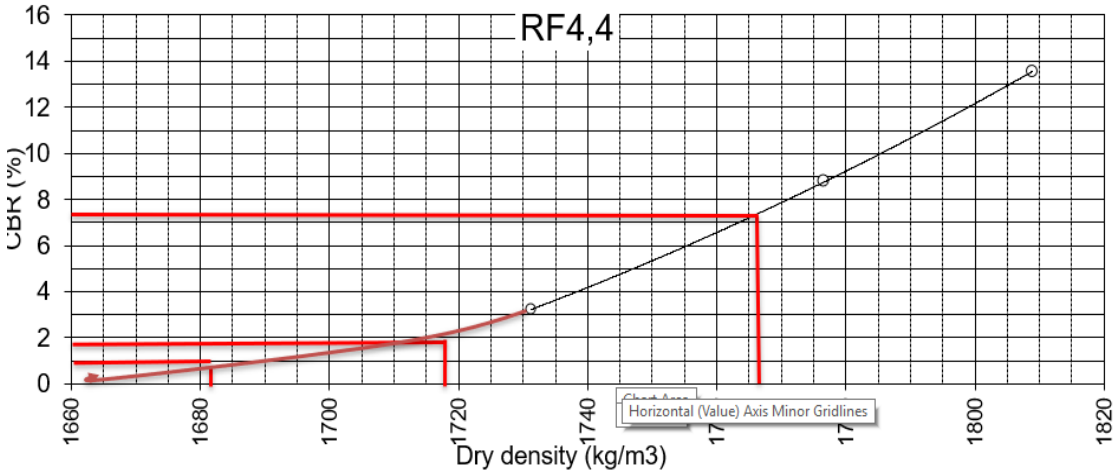

Figure C- 2: CBR against dry density curves indicating the CBR values related to 93%,95% and 98% of MDD value for sample RF4.4

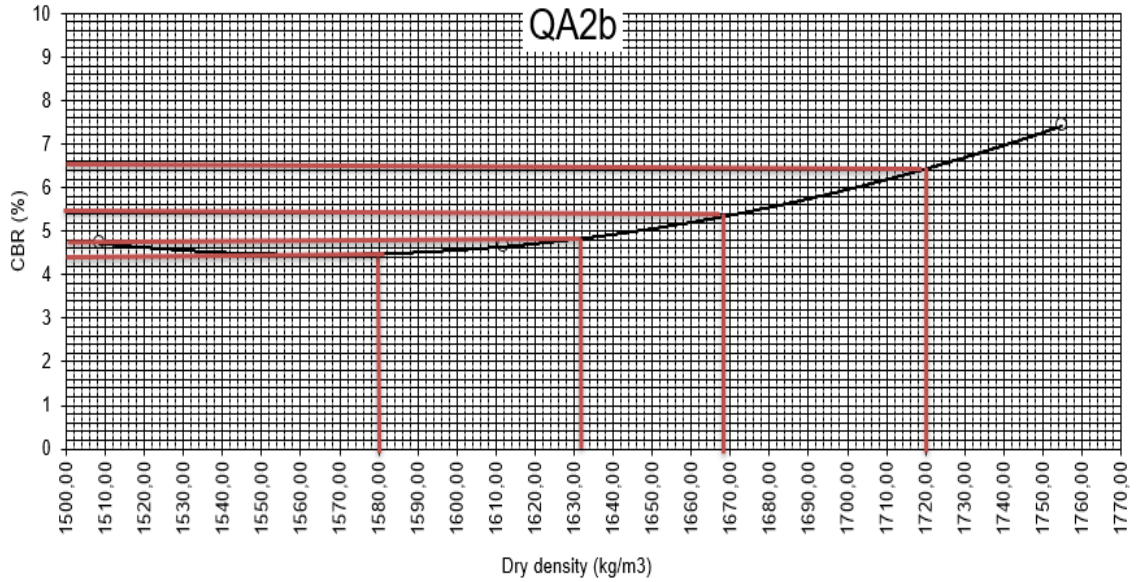

Figure B- 3: CBR against dry density curves indicating the CBR values related to 93%,95% and 98% of MDD value for sample QA2b

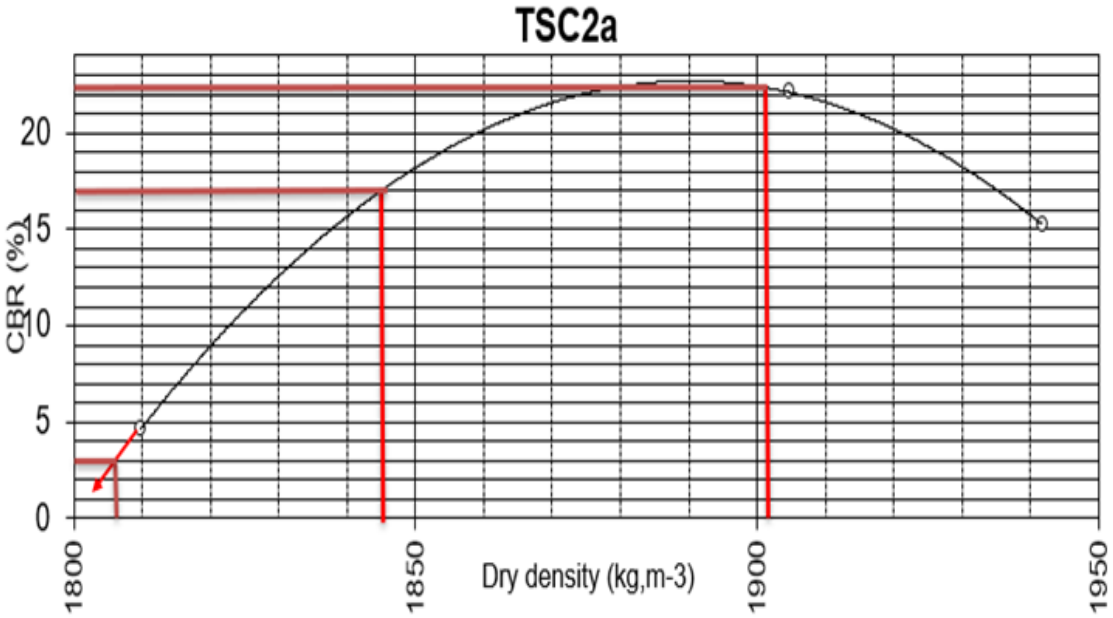

Figure B- 4: CBR against dry density curves indicating the CBR values related to 93%,95% and 98% of MDD value for sample TSC2a

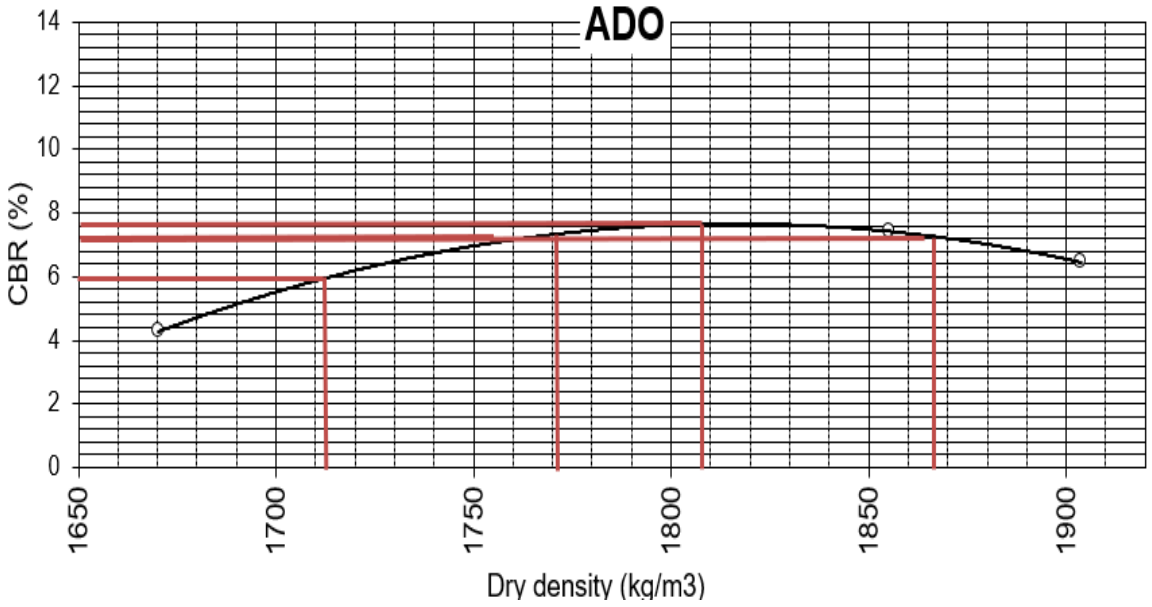

Figure B- 5: CBR against dry density curves indicating the CBR values related to 93%,95% and 98% of MDD value for sample ADO

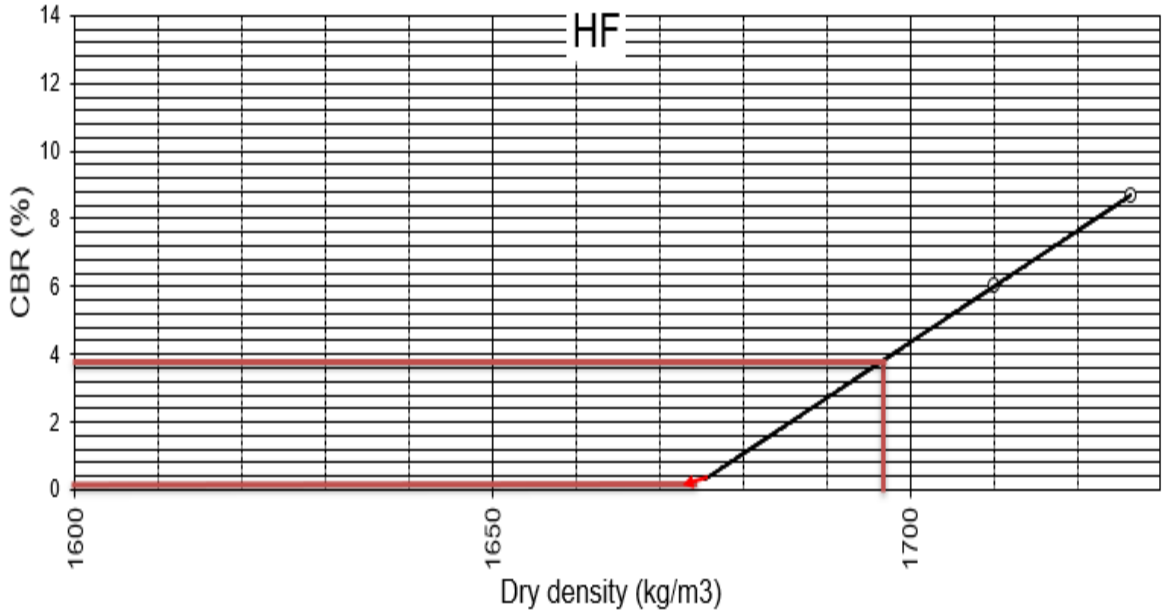

Figure B- 6: CBR against dry density curves indicating the CBR values related to 93%,95% and 98% of MDD value for sample HF

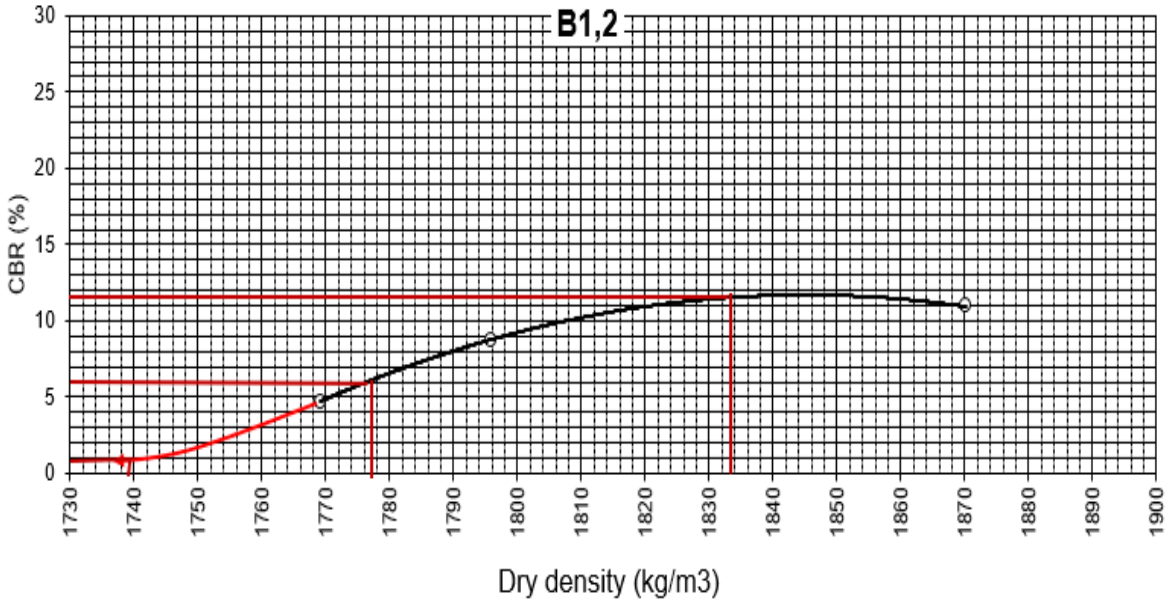

Figure B- 7: CBR against dry density curves indicating the CBR values related to 93%,95% and 98% of MDD value for sample B1.2

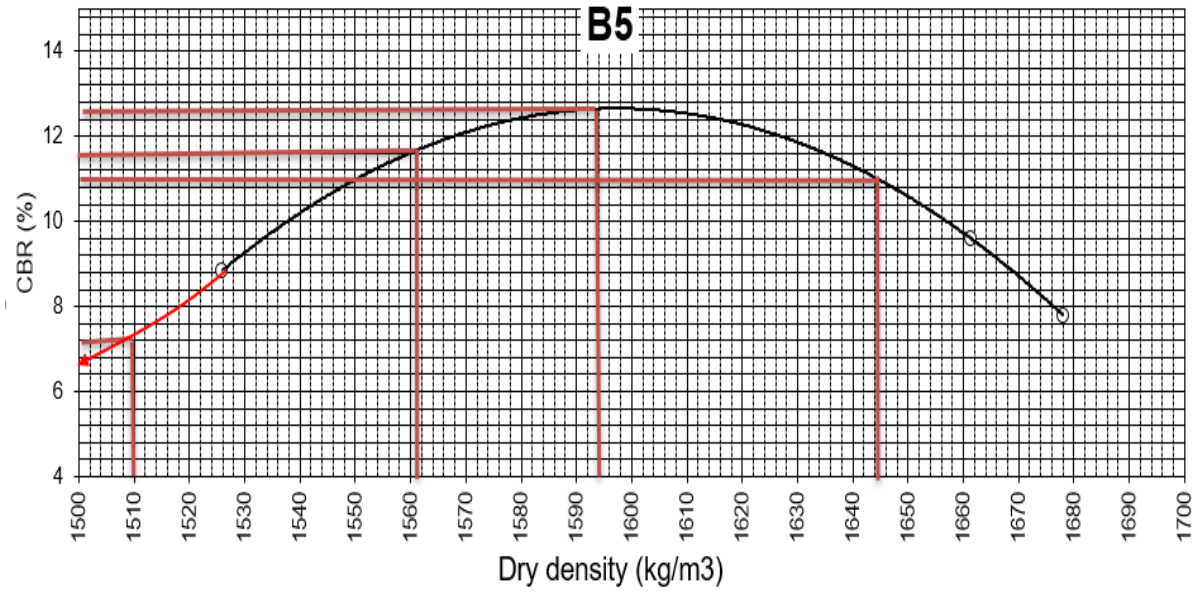

Figure B- 8: CBR against dry density curves indicating the CBR values related to 93%,95% and 98% of MDD value for sample B5

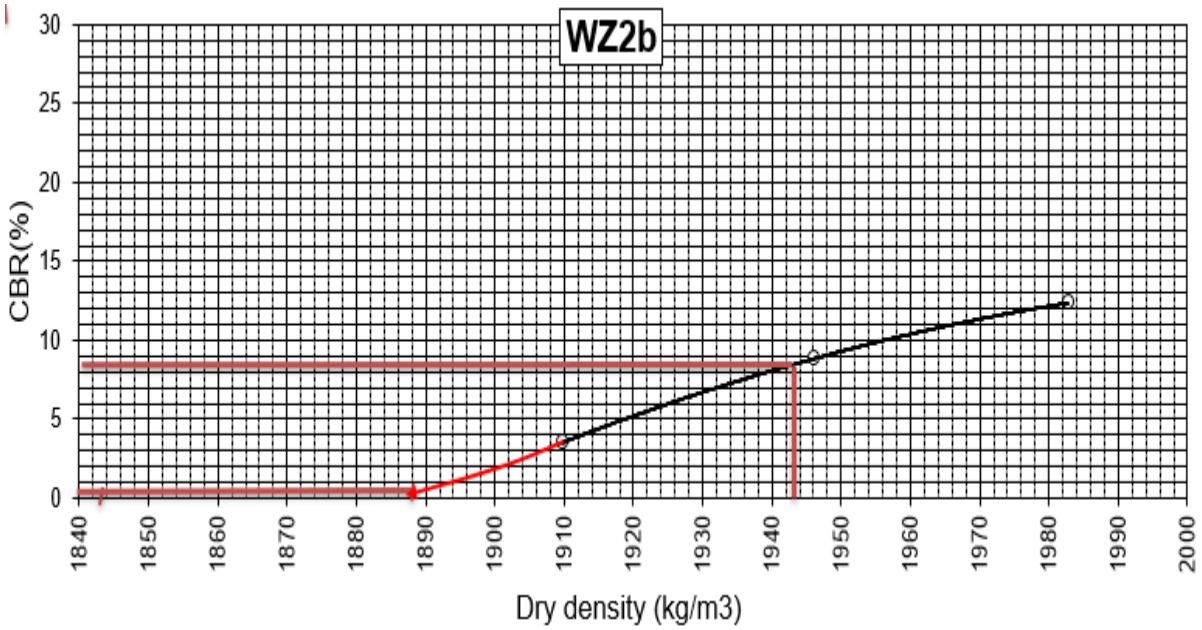

Figure B- 9: CBR against dry density curves indicating the CBR values related to 93%,95% and 98% of MDD value for sample WZ2B

Appendix E: Grading results based on sieve analyses according to SANS 3001 AG1 (2014)

Table C- 1 Particle size distribution according to SANS 3001 AG1 (2014). Red values indicating samples that failed criteria

	QA2b			RF1,1b			RF4,4			TSC2a			ADO		
Sieve size(mm)	Remaining mass (g)	% on sieve	% pass	Remaining mass (g)	% on sieve	% pass	Remaining mass (g)	% on sieve	% pass	Remaining mass (g)	% on sieve	% pass	Remaining mass (g)	% on sieve	% pass
4.75	0	0.0	100.0	0.6	0.1	99.9	1.8	0.4	99.6	4.7	0.9	99.1	1.9	0.4	99.6
2.36	0.4	0.1	99.9	0.5	0.1	99.8	2	0.4	99.2	7.8	1.6	97.5	0.6	0.1	99.5
1.18	1.5	0.3	99.6	1	0.2	99.6	6.2	1.2	98.0	13.7	2.7	94.8	4.6	0.9	98.6
0.6	3.3	0.7	99.0	4.8	1.0	98.6	64.8	13.0	85.0	13.6	2.7	92.0	57.1	11.4	87.2
0.3	68.6	13.7	85.2	30	0.0	98.6	146.7	29.3	55.7	75.5	15.1	76.9	96.7	19.3	67.8
150	241.6	48.3	36.9	159.7	31.9	66.7	156.1	31.2	24.5	141.5	28.3	48.6	139.8	28.0	39.9
0.75	95.2	19.0	17.9	137.4	27.5	39.2	63.4	12.7	11.8	87.7	17.5	31.1	96.4	19.3	20.6
	LL1,3c			HF			WZ2b			B1,2			B5		
	Remaining mass (g)	% on sieve	% pass	Remaining mass (g)	% on sieve	% pass	Remaining mass (g)	% on sieve	% pass	Remaining mass (g)	% on sieve	% pass	Remaining mass (g)	% on sieve	% pass
4.75	143.7	28.7	71.3	1.7	0.3	99.7	0.2	0.0	100.0	45.2	9.0	91.0	0	0.0	100.0
2.36	71	14.2	57.1	5.6	1.1	98.5	9.9	2.0	98.0	86.5	17.3	73.7	0.4	0.1	99.9
1.18	29.1	5.8	51.2	20.3	4.1	94.5	46	9.2	88.8	125.2	25.0	48.6	3.2	0.6	99.3
0.6	68.5	13.7	37.5	80.5	16.1	78.4	66	13.2	75.6	141.5	28.3	20.3	152	30.4	68.9
0.3	72.6	14.5	23.0	97.3	19.5	58.9	91.4	0.0	75.6	51.6	10.3	10.0	188.9	37.8	31.1
150	49.3	9.9	13.2	157.3	31.5	27.5	78.7	15.7	59.8	31.5	6.3	3.7	113.1	22.6	8.5
0.75	17.2	3.4	9.7	76	15.2	12.3	69.5	13.9	45.9	11.4	2.3	1.4	21.6	4.3	4.2

Appendix D: Cost model results for sediment removal of zone B5

Table D- 1 Cost model results for dry excavation (with and without sheet piling) and dredging at different proportion (%) of the sediment reserve to be removed if one to five sediment removal units are used.

	Removal costs per m3: one unit (excavator of amph. excavator) is used		
Proportion of sediment to be removed	Dry excavation with sheet piling	Dry excavation without sheet piling	Dredging
100%	R112,19	R55,60	R15,95
80%	R126,99	R56,26	R16,58
60%	R151,67	R57,36	R17,53
40%	R201,01	R59,55	R19,43
20%	R349,04	R66,11	R25,13

	Removal costs per m3: two units (excavator of amph. excavator) are used		
Proportion of sediment to be removed	Dry excavation with sheet piling	Dry excavation without sheet piling	Dredging
100%	R157,99	R101,41	R15,54
80%	R172,72	R101,98	R16,12
60%	R197,54	R103,23	R17,08
40%	R246,76	R105,30	R19,00
20%	R395,28	R112,35	R24,76

	Removal costs per m3: three units (excavator of amph. excavator) are used		
Proportion of sediment to be removed	Dry excavation with sheet piling	Dry excavation without sheet piling	Dredging
100%	R205,37	R148,78	R15,46
80%	R220,37	R149,64	R16,13
60%	R244,75	R150,44	R16,95
40%	R294,45	R152,98	R19,03
20%	R443,56	R160,63	R25,28

	Removal costs per m3: four units (excavators of amph. excavators) are used		
Proportion of sediment to be removed	Dry excavation with sheet piling	Dry excavation without sheet piling	Dredging
100%	R253,49	R196,90	R15,46
80%	R267,80	R197,07	R15,93
60%	R292,78	R198,47	R17,10
40%	R342,75	R201,29	R18,87
20%	R492,65	R209,72	R25,31

	Removal costs per m3: Five units (excavators of amph. excavators) are used		
Proportion of sediment to be removed	Dry excavation with sheet piling	Dry excavation without sheet piling	Dredging
100%	R300,88	R244,30	R15,32
80%	R316,76	R246,03	R15,98
60%	R341,47	R247,16	R17,09
40%	R390,90	R249,43	R19,30
20%	R539,16	R256,23	R25,94